Genetic analysis of signalling components of PAMP-triggered immunity (PTI) in plants

Benjamin Schweβinger

Thesis submitted to the University of East Anglia for the Degree of Doctor of Philosophy

September 2010

Abstract

The first and most conserved layer of plant innate immunity constitutes the perception of pathogen-associated molecular patterns (PAMPs) by pattern recognition receptors (PRRs). This type of immunity confers broad-spectrum disease resistance to a wide range of pathogens and is referred to as PAMP-triggered immunity (PTI). In *Arabidopsis* the leucin-rich repeat receptor kinases (LRR-RKs) FLS2 and EFR are the PRRs for the bacterial PAMPs flagellin and EF-Tu, respectively. Both form heteromeric complexes with the regulatory receptor- like kinase (RLK) BAK1. BAK1 is involved in brassinosteroide (BR) signalling via heteromerization with the BR receptor BRI1. In addition, BAK1 is also involved in cell death regulation. It is not known if BAK1 is able to differentially regulate these three pathways. In the case of BRI1 it was suggested that BAK1 plays a role as signal enhancer rather than being an intrinsic signalling component.

Here, I showed that BAK1 is principally able to differentially regulate these three signalling pathways. The novel allele *bak1-5* was strongly impaired in FLS2- and EFR-dependent PTI signalling pathways but displayed a wild-type-like signalling capacity in BR-signalling and BAK1-dependent cell death control. *Bak1-5* plants expressed a full-length mutant protein with a single missense substitution located close to the active site of the intracellular kinase domain. This mutant variant of BAK1 showed an increased interaction with the three ligand-binding RKs FLS2, EFR, and BRI1. Intriguingly, BAK1-5 displayed a reduced kinase activity *in vitro*. Nevertheless, the kinase activity of BAK1-5 was required to suppress EFR-dependent PTI-signalling *in planta*. These results strongly indicate a phosphorylation-dependent differential role of the regulatory RLK BAK1 in BR signalling, innate immunity and cell death control.

Furthermore, I showed that BAK1 and its closest homolog BKK1 play a partially redundant role in PTI signalling. The strong impairment of PTI signalling in the double mutant *bak1-5 bkk1-1* lead to compromised immunity against several adapted and non-adapted bacterial pathogens as well as to weakly virulent races of the obligate oomycete *Hyaloperonospora arabidopsidis*.

TABLE OF CONTENTS

LIST OF TABLES

LIST OF FIGURES

Acknowledgements

The most important person in my life is my mum not only because she gave birth to me…….

I am tremendously grateful to my PhD supervisor Cyril Zipfel for all the guidance, freedom, advice, knowledge and more he had and has to offer. I hope we will continue to foster our fruitful interaction in future.

I also say a big thanks to my two supervisory committee members Jonathan Jones and Sophien Kamoun for their constant support, critical comments and suggestions for my work. This has been and always will be very much appreciated.

I loved to work at the Sainsbury Laboratory as it is a great place to do, think and live science. Science does not happen in isolation but through interactions and this is what the TSL stands for. Even as a PhD student everybody was really open and forthcoming making my PhD time there a real pleasure.

Special thanks go to all Zipfel lab members and fellow Bolleros for patience, guidance, discussion, ideas, corrections and/or forgivingness.

Awesome thanks to Milena Roux my PhD-mate and…… and Alexandre Robert-Seilaniantz my squash-mate and……

I also thank Ken Shirasu and Sacco de Vries for the splendid extraordinary time in there labs. It was great to interact with them and their lab members and also to see the contrast between the Sainsbury and other Institutes. These experiences shaped my idea of science and how I would like to pursue my own science in future.

Finally, I thank maybe the two most important people inspiring and teaching me how to do science very early on in my career: Lucio Conti and Jürgen Kröner. Without them I would not be as critical and careful maybe sometimes even paranoid about my own work as they taught me science.

Of course there are many more people in my life I am greatly……

“ “

Abbreviations

aa	amino acid
ABA	absicic acid
ABA3	ABA deficient 3
AHA	autoinhibited H+-ATPase isofrom
Avr	avirulence
Ax21	activator of Xa21-mediated immunity
BAK1	BRI1 associated kinase 1
BEE	BR enhanced expression
BFA	brefeldin A
BIN2	BR insensitive 2
BIR1	BAK1-interacting receptor like kinase 1
BKI1	BRI1 kinase inhibitor 1
BKK1	BAK1-like1
BR	brassinosteroid
BRI1	brassinosteroid insensitive 1
BSK	BR-signalling kinase
BSU1	BRI1 suppressor 1
CaMV	cauliflower mosaic virus
CBL	calicnerin B-like proteins
CC	coiled-coil
CDPK	calcium dependent protein kinases
CEBip	chitin elicitor-binding protein
CERK1	chitin elicitor receptor kinase 1
Cf	*Cladopsorium fulvum*
CHX	cyclohexamide
CIPK	CBL-interacting protein kinases
CNGC2	cyclic nucleotide gated channel
CPS	cold shock protein
CSD2	CuZn-superoxide dismutase 2
cyt	cytoplasmic
D	aspartate
DAMP	damage-associated pattern
dpi	days post infection
DSF	diffusible signal factor
EDS1	Enhanced disease susceptibility 1
EFR	EF-TU receptor
EF-TU	elongation factor TU

EH	Eps15 homology
EIL1	EIN3-like 1
EIN3	ethylene insensitive 3
EIX	ethylene-inducing xylanase
eLRR	extracellular LRR
EPS	extracellular polysaccharides
ER	endoplasmatic reticulum
ET	ethylene
ETI	effector-triggered immunity
ETS	effector-triggered susceptibility
EVR	evershed
EX	executer
FLS2	flagellin sensing 2
FOX	**F**ull-length cDNA **O**ver-e**X**pressing gene
GA	gibberllic acid
GBP	glucan binding protein
GPA1	G protein alpha subunit 1
GRP7	glycine rich protein 7
Hpa	*Hyaloperonospera arabidopsidis*
HR	hypersensitive response
HSP90	heat shock protein 90
JA	jasmonic acid
KAPP	kinase-associated protein phosphatase
LPS	lipopolysaccharides
LRR	leucin rich repeat
LysM	lysin motif
MAP	mitogen associated protein
MIN7	HopM interactor 1
MKP	MPK phosphatase
MKS1	MAP kinase substrate 1
MLA10	intracellular mildew A 10
NB	nucleotide binding
NDR1	non race-specific disease resistance
NOS	reactive nitrogen species
NPR1	nonexpresser of PR genses 1
OG	oligoglalacturonide
OST1	open stomata 1
PAD3	phytoalexin deficient 3

PAMP	pathogen associated molecular pattern
PBL	PBS1-like protein
PBS1	AvrPphB susceptible 1
Pep1	elicitor peptide 1
pep-13	peptide 13
PEPR	Pep1 receptor
PGN	peptidoglycans
PM	plasma membrane
PMR4	powdery mildew resistant
Pph	*Pseudomonas syringae pv phaseolicola*
PPT	phosphinotricine
PRR	pattern recognition receptor
PS II	photosystem II
Pss	*P.syringae pv. syringae*
Pta	*Pseudomonas syringae pv. tabaci*
PTI	PAMP-triggered immunity
Pto	*P. syringae pv. tomato*
PTP1	protein tyrosine phosphatase 1
PUB	plant U-box
pv	pathovars
R	resistance
RAR1	required for MLA12 resistance 1
Rboh	respiratory burst oxidase homolg
RIN4	RPM1 interacting protein 4
RK	receptor kinase
RLK	receptor-like kinases
RLP	receptor-like protein
ROS	reactive oxygen species
RPG1	barley stem rust resistance protein 1
rpm	rounds per min
RPS5	resistant to *Pto* 5
SA	salicylic acid
SAG101	senescence-associated gene 101
SAR	systemic acquired resistance
SERK	somatic embryogensis related kinase
SGI	seelding growth inhibition
SGT1	Skyp1-Cullin-F-box protein
SID2	SA induced deficient 2

siRNA	small interfering RNAs
SNC	suppressor of *npr1-1*, constitutive
SOBIR	suppressor of *bir1-1*
SRRLK	small RNA generating RLK
T3SS	type-three secretion system
TIR	Toll and human interleukin-1 receptor
TIR	human interleukin-1 receptor
TIR1	transport inhibitor response 1
WAK	wall-associated protein kinases
XB	XA21-binding partner
Xcc	*Xanthomonas campestris pv. campestris*
Xoo	*Xanthomonas oryzae pv. oryzae*

Chapter 1: General Introduction

1.1. Introduction

Plants are the principal energy source for almost all living organisms on earth. They are under constant pressure to defend themselves against pathogenic bacteria, fungi, oomycetes, insects and herbivores. In principle humans are in competition with plant pathogens for this energy source and need to protect crop plants against these pathogens. In the last centuries this has been mostly done by conventional breeding or applying pesticides to kill potential pathogens. However, in future these practices are not sustainable on their own as we will require a sustainable intensification of agriculture to manifest food security. On the one side pesticides lead to the loss of beneficial microbes and insects and are potentially harmful for human health. On the other side resistances has developed in many plant pathogens either to applied chemicals or genetically encoded defence mechanisms. In order to overcome these problems and to improve current crop species we need to gain a detailed understanding of plants as biological systems in general and plant defence mechanisms in particular. Only this will enable us to make knowledge-based decisions on how to improve crops either by targeted conventional breeding, by genetic-modification or a combination thereof.

Most plants are healthy most of the time or can at least minimize pathogen growth meaning that most pathogens are non-pathogenic on most plants (Thordal-Christensen, 2003). The simplest explanation for this fact is that the pathogen and the plant have different habitats. Second, the plant does not support the pathogen's life style and therefore, the pathogen cannot express its pathogenicity factors or develop infection structures due to constitutively present barriers such as the bark, waxy cuticles or rigid cell walls (Nurnberger et al., 2004). These barriers are referred to as ecological or constitutive defences. However some pathogens can breach this constitutive defence layer and are then subject to the recognition close to or at the plasma membrane either directly or indirectly. At this stage the plant is able to perceive the pathogen as such by recognizing pathogen-associated molecular

patterns (PAMPs) or the disruption of its integrity by the pathogen via danger-associated molecular patterns (DAMPs) (Boller and Felix, 2009). These extracellular molecules, collectively termed elicitors, are recognized by specific pattern-recognition receptors (PRRs) and initiate an intracellular signalling cascade leading to PAMP-triggered immunity (PTI). However some pathogens are pathogenic on some plant species by masking their identity, evading recognition and/or suppressing PTI signalling using so called effectors. In the case of bacteria these effectors are mostly secreted via the type-three secretion system (T3SS) directly into the cytoplasm (Nomura et al., 2005). In other cases they are secreted by the pathogen into the apoplastic space and recently shown to be up-taken in a pathogen independent manner (Kale et al., 2010; Rafiqi et al., 2010). This leads to effector-triggered susceptibility (ETS). Plants in turn developed another immune layer to recognize these effector molecules employing resistance (R) proteins. In this case the effector, which normally fosters the virulence of the pathogen betrays it, causing avirulence and leads to effector-triggered immunity (ETI) (Chisholm et al., 2006; Jones and Dangl, 2006). The recognition of effectors, which are avirulence (avr) factors in this case, by R-proteins can be direct or indirect. Some pathogens inject other effectors into the plant cytoplasm to suppress ETI and induce another cycle of ETS. This co-evolution of the recognition of the pathogen by the plant and the disturbance thereof by the pathogen is considered an “arms race”.

Plants have a two-layered immune system whereby the first layer (PTI) recognizes infectious non-self or infected self characteristic of the action of a class of pathogens. In contrast the second layer (ETI) recognizes the presence of a specific pathogen race. Both immune layers are encoded in the germline and therefore referred to as innate immunity. Innate immunity is the only immune system in all living organisms; except for jawed vertebrates that possess an adaptive immune system in addition (Janeway and Medzhitov, 2002). Even though it is so widespread across kingdoms and uses similar molecular building blocks and mechanisms innate immunity is believed to be a result of convergent evolution (Ausubel, 2005; Zipfel and Felix, 2005).

1.2. PAMPs, DAMPs and PRRs

It has been known for over 30 years that plants possess an excellent chemoperception system for (conserved) microbe-derived substances and to induce the production of anti-microbial compounds termed phytoalexins (Albersheim and Valent, 1978; Keen et al., 1972). Without knowing the molecular identity of these substances they were collectively referred to as general elicitors (Keen et al., 1972). The molecular identity of the first elicitor was proven to be heptaglucoside from cell wall preparations of the oomycete *Phytophthora megasperma pv. glycinea* (later renamed *P. sojae pv glycinae*) (Sharp et al., 1984a; Sharp et al., 1984b). In the following years, a range of elicitors from oligosaccharides, peptides to lipid moieties were shown to elicit a set of defence responses in plants (Boller, 1995). In recent years, a new concept has been adapted from the animal innate immunity field where it was suggested that the focus of the innate immune system is to discriminate between infectious non-self and non-infectious self (Medzhitov and Janeway, 1997). This discrimination takes place by recognizing PAMPs, which are defined as (i) being relatively invariant epitopes within molecules that are fundamental to the pathogens' fitness, (ii) widely distributed within a class of microbes and (iii) absent from the host. This idea was extended to include infected, modified or infectious self by recognizing DAMPs, which can be defined as molecules of the potential host that are released by lytic enzymes or non-enzymatic activities of the pathogen (Matzinger, 2002). Early examples of elicitors included DAMPs as oligogalacturonides that were thought to be released from the plant cell wall during pathogen attacks elicit host defence responses (Nothnagel et al., 1983). Overall, these elicitors (PAMPs and DAMPs) are recognized by plasma membrane- localized PRRs that in plants apart from two exceptions are transmembrane receptor kinases (RKs) or receptor-like proteins (RLPs) (Boller and Felix 2009).

1.2.1. Orphan elicitors

Even though some elicitor/PRR pairs have already been identified, many orphan elicitors are still missing their corresponding PRR.

1.2.1.1. Orphan fungal PAMPs

Fungal cell wall components, such as ergosterol elicit defence responses at picomolar concentrations in tomato, tobacco and grapevine (Granado et al., 1995; Boller and Felix, 2009). Small secreted proteins like Sm1 and members of the cearto-platanin family cause defence responses on variety of monocots and/or dicots (Pazzagli et al., 1999; Djonovic et al., 2006).

1.2.1.2. Orphan oomycete PAMPs

Pep13 was the first epitope to be clearly defined as a PAMP in relation to plant defence (Brunner et al., 2002). It is a short 13-amino acid peptide of a conserved surface-exposed fragment within a calcium-dependent cell wall transglutaminase from the oomycete *Phytophthora sojae* that elicits defence responses in *Solanaceae* (Brunner et al., 2002). Recently, the cellulose binding elicitor lectin from *Phytophthora parasitica* var. *nicotianae* was shown to trigger defence responses in *Arabidopsis* and tobacco (Gaulin et al. 2006). The two cellulose binding domains, which are probably important for cell adhesion during infection, are sufficient for defence induction. Other elicitors from oomycetes are the fatty acid arachidonic acid, are small secreted proteins such as INF1 and other elicitins recognized by tobacco and other *Solanaceae* (Yu, 1995; Kamoun et al., 1997; Boller and Felix, 2009).

1.2.1.3. Orphan bacterial PAMPs

Plants recognise many different bacterial PAMPs. Lipopolysaccharides (LPS) are perceived by a range of plant species (Newman et al., 2007). The main PAMP

within LPS is the widely conserved lipid A, and its elicitor strength depends on its acetylation and phosphorylation pattern (Silipo et al., 2008). However, the core oligosaccharide and O-antigen structure are also recognised, potentially by a different perception system than for lipid A in *Arabidopsis* (Newman et al., 2007). Peptidoglycans (PGN) are a major cell-wall component of Gram-positive bacteria. PGN sugar chains longer than the disaccharide, but not the protein moieties are recognised as a PAMP in *Arabidopsis* (Gust et al., 2007). In several recent reviews it was suggested that LysM (lysin motif) containing receptor proteins could be the functional PRRs for PGN (Boller and Felix, 2009; Nicaise et al., 2009). Rhamnolipids were recently shown to induce defence responses in grapevine (Varnier et al., 2009). Nucleic acids of pathogens have long been known as potent immune elicitors in animals (Kawai and Akira, 2010). Only recently it was shown that unmethylated CpG-DNA elicits typical defence responses in *Arabidopsis* (Yakushiji et al., 2009). Bacteria also harbour many proteinaceous PAMPs. For example the cold shock protein (CPS) was shown to elicit defence responses in tobacco but not *Arabidopsis* cells (Felix and Boller, 2003). It was elegantly shown that functional indispensable amino acid residues in the highly conserved RNA and DNA-binding domain (RNP-1) were also essential for response elicitation and the core 22-amino acid peptide of the RNP-1 domain was identified as the corresponding PAMP (Felix and Boller, 2003). Also the secreted superoxide dismutase, Nep1-like proteins and harpins induce defence responses in several plant species (Nicaise et al., 2009).

1.2.1.4. Orphan DAMPs

Cutin monomers are released from the plant cell wall after pathogen attack by the enzymatic activity of cutinases and are recognized in micromolar concentrations (Boller and Felix, 2009). Plants potentially possess a positive feedback/forward loop as they secrete small peptides which are also perceived by cells in the surrounding non-attacked tissue (Ryan et al., 2007). Some of these peptides are synthesized as precursors and need activation by a protease before becoming fully active as for

example for systemin (McGurl et al., 1992). Other small peptide DAMPs, such as RAFL and HypSys are omnipresent in plant cell walls and were recently suggested to become activated by microbial proteases or by endogenous proteases after cell wounding (Boller and Felix, 2009; Pearce and Ryan, 2003). A subtilisin-like protein was recently identified as a novel peptide DAMP specific to soybean (Pearce et al., 2010). As in the last case the production and recognition of most of these small peptide DAMPs seems to be limited to a small phylogenetic family and they may have evolved independently to fine-tune specific defence responses. These actively produced DAMPs that are produced in response to PAMP perception or wounding could be also seen as plant cytokines homologos to cytokines of the jawed vetebrate immune system.

1.2.2. Known elicitor/PRR pairs

It has been known nearly over 30 years that plants are able to respond to elicitors (Keen et al., 1972). In addition these elicitors were long known to be able to bind to high-affinity binding sites within the plant cell membrane (Nurnberger et al., 1994). However the first plant PRRs have been identified only in the last ten years.

1.2.2.1. flg22/FLS2, the paradigmatic model pair

Flagellin represents the best studied PAMP in plants. Flagellin is the building block of the eubacterial flagellum, which is essential for bacterial movement. The eliciting epitope flg22 was isolated from *Pseudomonas syringae pv. tabaci* (*Pta*) and corresponds to a highly conserved N-terminal domain (Felix et al., 1999). Flg22 elicits responses in a wide variety of plant species from angiosperm to gymnosperms, suggesting that the corresponding perception system has evolved early in evolution (Albert et al. 2010). However, the recognition specificity is not necessarily the same for all species. Tomato for example is able to recognize a shorter version of the same epitope (flg15) whereas *Arabidopsis* is not (Bauer et al., 2001; Robatzek et al., 2007). Similarly, rice is able to recognize flg22 but is more responsive to full length

flagellin protein (Takai et al., 2008). This difference in recognition specificity is intrinsic to the respective receptor. Interestingly, flagellins with the same primary amino acid sequence where differentially recognized in rice based on their specific glycosylation status (Che et al., 2000; Tanaka et al., 2003; Fujiwara et al., 2004). In addition several bacterial pathogens can evade flagellin recognition. For example, *Xanthomonas campestris* pv. *campestris* (*Xcc*) has within-species polymorphism in flg22, which leads to the inability of *Arabidopsis* to recognise the 'disguised' epitope (Sun et al., 2006). Although the biological relevance of this relative recognition on *Xcc* compatible host plants needs further investigation.

The leucin rich repeat (LRR) RK FLS2 (Flagellin Sensing 2) was isolated by map-based cloning as the corresponding PRR in *Arabidopsis* (Gomez-Gomez and Boller, 2000). Further studies showed that flg22 binds directly to FLS2 and that this high-affinity binding site is absent in *fls2* knock-out mutant demonstrating that FLS2 is a *bona fide* receptor (Chinchilla et al., 2006). In recent years orthologous receptors were cloned and partially characterized from tomato, *Nicotiana benthamiana* and rice (Hann and Rathjen, 2007; Robatzek et al., 2007; Takai et al., 2008). FLS2 binds flg22 via its extracellular LRR domain, which most likely forms a horseshoe-like tertiary structure based on known LRR structures (Padmanabhan et al., 2009). Mutational and phylogenetic approaches suggested different parts of the extracellular LRR to be involved in ligand binding (Albert et al., 2010a; Boller and Felix, 2009; Dunning et al., 2007). Only crystallographic studies of the LRR domain in complex with flg22 will enable to clarify this controversy.

The intracellular part of FLS2 has most of the characteristic structural elements of a Ser/Thr kinase and was shown to possess kinase activity (Gomez-Gomez et al., 2001).

1.2.2.2. elf18/EFR a *Brassicaceae* specifc pair

The recognition of the bacterial elongation factor TU (EF-TU) is restricted to *Brassicaceae* (Kunze et al., 2004). The elicitor epitope could be narrowed down to the first 18 amino acids and requires N-acetylation for activity (Kunze et al., 2004).

Using a combination of reverse genetics and biochemical binding studies it was univocally shown that the LRR-RLK EFR (EF-Tu receptor) is the corresponding PRR in *Arabidopsis* (Zipfel et al., 2006). No orthologs from other species have been cloned so far. Interestingly EFR is a member of receptor-like kinases (RLK) subfamily XII the same as FLS2 (Shiu and Bleecker, 2001). As FLS2, EFR is highly glycosylated, however, EFR is far more sensitive to genetic disturbances in the protein folding, glycosylation and ER (endoplasmatic reticulum) quality control machinery (Haweker et al., 2010; Li et al., 2009; Lu et al., 2009; Nekrasov et al., 2009; Saijo et al., 2009; von Numers et al., 2010). Recently it was shown that the extracellular LRR domain of EFR is the domain of elf18 perception (Albert et al., 2010b). The expression of chimeric constructs encoding fusion proteins of the extracellular LRR of EFR fused to the intracellular kinase domain of FLS2 confer elf18 responsiveness to normally unresponsive *N. benthamina* (Albert et al., 2010b). Interestingly, the glycosylation status of the LRR seems to be important for peptide binding as mutations of a single predicted glycosylation site disables elf18 binding despite correct localization of the mutated protein to the plasma membrane (Haweker et al., 2010).

1.2.2.3. axY^{s}22/Xa21 a rice specific pair

Xa21 (*Xanthomonas oryzae* pv. *oryzae 21*) resistant was isolated by positional cloning form the wild rice species *Oryza longistaminanta* because of the broad-spectrum resistance it confers to *Xanthomonas oryzae pv. oryzae* (*Xoo*) (Song et al., 1995). It is the first LRR-RLK identified as being involved in disease resistance however the cognate ligand was unknown until recently (Lee et al., 2009). This ligand was long thought to be an effector molecule (AVR protein). However, it became apparent that a small sulfated secreted protein potentially involved in quorum sensing might rather be the recognized entity (Lee et al., 2006). Indeed a small tyrosin sulphated 17 amino acid long peptide from the small type-I secreted protein Ax21 (activator of Xa21-mediated immunity) was identified as the long-missing ligand (Lee et al., 2009). *Xa21* is part of a multi-gene family in rice (Song et

al., 1997). One other gene family member called XA21D is able to confer partial-resistance to *Xoo* (Wang et al., 1998). It is not clear if XA21D, a predicted extracellular LRR domain containing protein without transmembrane domain, is able to bind Ax21. Interestingly, Xa21 is closely related to FLS2 and EFR displaying a similar modular structure. As EFR, XA21 is sensitive to genetic disturbance in the ER quality control machinery (Park et al., 2010).

1.2.2.4. Several PRRs for chitin?

Chitin is a major component of the fungal cell wall and was first shown to possess elicitor activity in tomato cells (Felix, 1993). The cognate receptor CEBiP (chitin elicitor-binding protein) in rice was identified by biochemical binding assays, peptide sequencing, concomitant cloning and silencing of the coding gene (Kaku et al., 2006). CEBiP is a RLP with two extracellular LysM motifs, a single transmembrane domain and a cytoplasmic C-terminal tail without any known domain. It is likely that CEBiP requires additional signalling partner(s) to form a functional receptor complex (Kaku et al., 2006). Indeed OsCERK1 (chitin elicitor receptor kinase 1), a LysM-ontaining RLK, is required for full chitin responsiveness and directly interacts with CEBiP forming ligand-induced heteromeric complexes *in vivo* (Shimizu et al., 2010). The *Arabidopsis* ortholog of OsCERK1 has three LysM motifs and was previously found to be required for chitin responses (Miya et al., 2007; Wan et al., 2008). CEBiP homologs are present in *Arabidopsis* and it was therefore hypothesized initially that AtCERK1 plays rather the role of a regulatory RLK then being the *bona fide* ligand-binding PRR (Zipfel, 2009). However, AtCERK1 was identified recently as a major chitin-binding protein in *Arabidopsis* and does not require any additional plant proteins for *in vitro* chitin binding (Iizasa et al., 2009; Petutschnig et al., 2010). In both studies AtCERK1 was able to bind not only chitin polymers but also oligomeric chitin with a degree of polymerization greater than five (Iizasa et al., 2009; Petutschnig et al., 2010). This is in good agreement with the previously observed recognition specificity of *Arabidopsis* (Wan et al., 2008). Importantly, *AtCERK1* is also required for bacterial resistance

conferred by the recognition of unknown bacterial PAMP(s) (Gimenez-Ibanez et al., 2009a; Gimenez-Ibanez et al., 2009b). These PAMP(s) might be structurally related to chitin and may bind to a similar site in the extracellular domain of AtCERK1. Alternatively, AtCERK1 could form heteromeric complexes whereby the complex composition would determine ligand specificity in a manner reminiscent of TLR heterocomplexes in the vertebrate innate immune system (Kawai and Akira, 2010). The latter hypothesis is supported by the fact that AtCEBiP is another chitin binding protein in *Arabidopsis* in addition to AtCERK1 (Petutschnig et al., 2010).

1.2.2.5. Xylanase/Eix1/2 pair

The fungal ethylene-inducing xylanase (EIX) is a strong elicitor of defence responses in many different plant species (Boller, 1995). A map-based cloning approach in tomato isolated two RLPs, LeEix1 and LeEix2, as potential EIX PRRs (Ron and Avni, 2004). Transient expression of both proteins confers EIX binding to *N. tabacum cv* BY2 but only Eix2 can confer EIX responsiveness (Ron and Avni, 2004). LeEix1 and LeEix2 form heteromeric complexes *in vivo* and the over-expression of LeEix1 dampens EIX-induced responses (Bar et al., 2010). This suggests that LeEix1 is a negative regulator of LeEix2-mediated responses or that LeEix1 is a ligand-scavenging receptor without signalling capacity.

1.2.2.6. GBP a soluble PRR ?!?

Heptaglucoside forms an integral part of oomycete cell walls and was the first characterized elicitor at the molecular level (Sharp et al., 1984a; Sharp et al., 1984b). Heptaglucans are only recognized by members of the *Fabacae* and biochemical studies in soybean identified a soluble high affinity glucan binding protein (GBP) as the potential PRR (Fliegmann et al., 2004). However, a genetic proof for the requirement of GBP for heptaglucan perception is still missing. Also how a soluble extracellular protein can induce intracellular signal cascades is still an open question. One hypothesis is that after ligand-binding GBP interacts with a RLK or RLP and

this interaction induces down-stream signalling. Clearly, more studies are needed clarify the mechanism of heptaglucan perception in plants.

1.2.2.7. AtPeps and AtPEPR1/2 the first identified DAMP/PRR pairs

The 23 amino acid long peptide AtPep1 (elicitor peptide 1) was isolated from untreated *Arabidopsis* leaves and shown to induce defence responses generally associated with PTI (Huffaker et al., 2006). It is part of a multi-gene family containing 6 potential paralogs. Several of them are induced by wounding, stress hormone and elicitor treatment (Huffaker et al., 2006; Huffaker and Ryan, 2007). All of them are produced as longer propeptides and require processing via an unknown mechanism before becoming elicitor active (Huffaker et al. 2006). The LRR-RLK AtPEPR1 (Pep1 receptor 1) was identified as an AtPep1 binding protein and *bona fide* PRR in *Arabidopsis*. *Atpepr1* mutant lines lost the high affinity AtPep1 binding site, and transient expression of AtPEPR1 made tobacco AtPep1-responsive (Yamaguchi et al., 2006). Careful phenotypic analysis showed that *atpepr1* single mutants were not totally unresponsive to AtPep1 and its closest paralog AtPEPR2 was identified as a partially redundant AtPep1 PRR (Krol et al., 2010; Yamaguchi et al., 2010).

1.2.2.8. OGs and WAK1

Plants sense disturbance of their self by the intruder. For example oligoglalacturonides (OG), representing lytic plant cell wall fragments, induce defence gene responses in soybean and many other plant species (Nothnagel et al., 1983; Boller, 1995). Cell wall-associated protein kinases (WAKs) were hypothesised to constitute the respective PRR. WAK1 is able to bind OGs *in vitro* (Cabrera et al., 2008). Furthermore, heterologously expressed WAK1 and WAK2 bind to de-esterized pectin oligomers *in vitro* and *wak2* mutant plants are impaired in pectin-induced MPK3 activation (Kohorn et al., 2009). Using a domain swap approach it was demonstrated that a chimeric protein between the WAK1

ectodomain and the EFR kinase domain is able to recognize OGs and induce EFR-specific responses after transient expression in *N. benthamina* (Brutus et al., 2010). By using reciprocal fusion proteins it was shown that elf18 treatment induces WAK1-specific responses. These experiments demonstrate that the WAK1 ectodomain is able to perceive OGs and that the cytoplasmic kinase domain of WAK1 encodes downstream signalling specificity making WAK1 a prime PRR candidate for OGs.

1.2.3. Potential PRRs

1.2.3.1. non-RD kinase domains: Hallmark of PRRs ?!?

Kinases, including RKs and RLKs, can be subdivided into RD and non-RD kinases depending on the conservation of the amino-acid residue preceding the core catalytic aspartate (D) residue in subdomain VIb of the kinase domain (Johnson et al., 1996; Nolen et al., 2004). Most RD kinases require auto-phosphorylation of the activation loop for full kinase activity. In contrast, non-RD kinases do not require phosphorylation of the activation loop to adopt an active confirmation (Nolen et al., 2004). They are regulated by different mechanisms such as relief of auto-inhibition by C-terminal extensions (Kobe et al. 1996), Tyr phosphorylation in the P+1 loop (Mayans et al. 1998), or are constitutively active kinases (Nolen et al. 2001). Interestingly, several PRRs belong to the non-RD kinase class and this might be a hallmark of PRRs. 15 out of 18 PRRs belong to the non-RD class of protein kises even though members of this class are relatively infrequent in the genoms of animals and plants (Dardick and Ronald, 2006).

1.2.3.2. Potential orphan PRRs

While for many PAMPs the corresponding PRRs are still unknown, several RLKs and RLPs have been associated with defence responses and may potentially be orphan PRRs. For example, the two tomato RLPs Ve1 and Ve2 have been shown to

confer resistance to *Verticillium dahliae* and *V. albo-atrum* race 1 when expressed in potato (Kawchuk et al., 2001). However, in tomato only Ve1 was required and sufficient to confer resistance (Fradin et al., 2009). In *Arabidopsis* three LRR-RLPs were shown to be required for disease resistance to non-adapted bacterial or fungal pathogen (Ramonell et al., 2005; Wang et al., 2008a). Knock-out mutants of *AtRLP30* and *AtRLP13* are slightly more susceptible to the non-adapted bacterial pathogen *Pseudomonas syringae pv phaseolicola* (*Pph*) 1448A and a AtRLP30 YFP fusion protein localizes to the plasma membrane (Wang et al., 2008a). Mutants of *AtRLP52* were shown to be more susceptible to the non-adapted fungal pathogen *Erysiphe cichoracearum* (Ramonell et al., 2005).

Several RLKs represent potential PRRs. Recently the non-RD LRR-RLK NgRLK1 from *Nicotiana glutinosa* was shown to interact with an elicitin from *P. capsici in vitro* and in a yeast-two hybrid assay (Kim et al., 2010). Surprisingly, not only the extracellular LRR-domain but also the intracellular kinase domain interacted with the elicitin. Therefore further studies are necessary to define NgRLK1 as a PRR *per se* such as testing its requirement for elicitin-induced responses and *in vivo* binding. In rice, map-based cloning identified the non-RD RLK *Xa26* as a major component of the defence response against several *Xoo* strains (Sun et al., 2004). Rice cultivars lacking *Xa26* were more susceptible to *Xoo,* and transgenic lines expressing *Xa26* gained broad spectrum resistance against several strains of *Xoo* (Cao et al., 2007; Sun et al., 2004). Interestingly, *Xa26* is part of a multi-gene family and ectopic expression of another family member confers resistance to *Xoo* (Cao et al., 2007).

This enumeration is far from being exhaustive as SNC2 (suppressor of npr1-1, constitutive 2), SNC4, RPG1 (barley stem rust resistance protein 1), Pi-d2 and many other RLPs and RLKs full fill similar criteria (Brueggeman et al., 2002; Chen et al., 2006; Bi et al., 2010; Zhang et al., 2010). More studies are needed to identify potential cognate PAMPs and to demonstrate that these RLPs and RLKs are *bona fide* PRRs.

1.3. The importance of PTI in plant defence

Early on it was shown that soybean seedlings pre-treated with elicitors from oomycete cell walls became resistant to a normally compatible race of *P. megasperma pv. glycinea* (Ayers et al., 1976). Several years later it was shown that a glucan preparation from the same pathogen was able to induce cross-kingdom resistance to several plant-viruses in different *Nicotiana* species (Kopp et al., 1989). Pre-treatment of tobacco with laminarin, a linear β-1,3 glucan isolated from brown algae but also part of land plant and fungal cell walls, was shown to induce resistance against the soft rot bacterial pathogen *Erwinia carotovota* (Klarzynski et al., 2000). As described above huge progress has been made in identifying the genetic and molecular bases of elicitor recognition. This enabled the detailed investigation of the contribution of elicitor recognition to plant defence. Using the paradigmatic PAMP/PRR pair flg22/FLS2 (see above) Boller and colleagues demonstrated that flg22 pre-treatment restricts the growth of the adapted pathogen *P. syringae* pv. *tomato* (*Pto*) DC3000 on *Arabidopsis* (Zipfel et al., 2004). Importantly, the authors were able to show that this induced resistance is dependent on the cognate PRR FLS2 defining a genetic basis for the observed phenomena (Zipfel et al., 2004). Furthermore, *fls2* mutant plants are more susceptible to *Pto* DC3000 when spray-inoculated suggesting a role of PTI in pre-invasive defence (Zipfel et al. 2004). In addition, PTI is involved in non-host resistance as *fls2* mutants are more susceptible to non-adapted bacterial pathogens such as *Pph* or *Pta* (de Torres et al., 2006; Li et al., 2005). Silencing of *NbFLS2* in *N. benthamiana* leads to increased resistance to several bacterial pathogens (Hann and Rathjen, 2007). Similarly, in *Arabidopsis efr* and *cerk1* mutants are more susceptible to virulent and weakly virulent strains of *Pto* DC3000 (Gimenez-Ibanez et al., 2009a; Nekrasov et al., 2009; Saijo et al., 2009). As CERK1 is also involved in chitin perception *cerk1* mutants are more susceptible to fungal pathogens such as *Alternaria brassicicola* and *Erysiphie cichoracearum* (Miya et al., 2007; Wan et al., 2008). In rice silencing of *CEBiP* increases the susceptibility to the fungal pathogen *Magnaporthie oryzae* (Kishimoto

et al. 2010). Recently it was demonstrated that PAMPs are able to induce systemic acquired resistance (SAR) also (Mishina and Zeier, 2007).

The relatively little contribution of elicitor recognition, using single PRR mutants, to the overall resistance reported in most of these studies led to the postulate that PTI is a quantitative weaker response than ETI (Jones and Dangl, 2006). However, this neglects the possibility that mutants in multiple PRRs, blind to most elicitors, might be hyper-susceptible to normally non-adapted pathogens (PTI). This increase in susceptibility might be as large as the one observed for *R*-gene mutants infected with otherwise avirulent pathogens (ETI). In addition *Xa21*, which was previously defined as an R-protein (Song et al., 1995), is indeed a PRR that totally restricts the growth of otherwise virulent *Xoo* strains, clearly revoking the notion of quantitative differences between PTI and ETI (Lee et al., 2009). Similarly, the heterologous expression of *EFR* in tomato makes it resistant to the otherwise fully adapted pathogen *Ralstonia solanacearum* (Lacombe et al., 2010).

1.4. Downstream events after ligand binding

It is well known from studies on animal transmembrane receptor that the first event after ligand binding is a ligand-induced conformational change (Lemmon and Schlessinger, 2010; Rahimi and Leof, 2007). This conformational change leads to homo- and heteromerization with downstream signalling components enabling signal transduction from the outside into the cell. Even though a ligand-induced conformational change has not been demonstrated for plant PRRs it is assumed that it constitutes the first downstream signalling event.

1.4.1. Oligomerization: BAK1 as a regulatory RLK

BAK1 (BRI1 associated kinase 1), an LRR-RLK belonging to the subfamily II and also a member of the multi-genic *SERK* (somatic embryogensis related kinase) family, was recently shown to form ligand-dependent heteromeric complexes with several PRRs such as FLS2 and EFR *in vivo* and with AtPEPR1/2 in the yeast two

hybrid system (Chinchilla et al., 2007; Heese et al., 2007; Postel and Kemmerling, 2009; Roux et al., *submitted*). BAK1 was initially identified as a positive regulator of brassinosteroid (BR) responses, forming a ligand-dependent complex *in vivo* with the LRR-RK BRI1 (brassinosteroid insensitive 1), the main BR receptor (Li et al., 2002; Nam and Li, 2002; Wang et al., 2005; Wang et al., 2008b). Over-expression of BAK1 suppresses weak *bri1* alleles, and *bak1* knock-out mutants are hypo-sensitive to BR and resemble weak *bri1* alleles (Li et al., 2002; Nam and Li, 2002; Wang et al., 2008b). BAK1 is also involved in cell death control as *bak1* knock-out mutants have a spreading lesion phenotype upon pathogen infection and display premature senescence phenotypes (He et al., 2007; Kemmerling et al., 2007). This loss of cell death control is aggravated in double-mutant combinations with its closest homolog *BKK1(BAK1-LIKE1)/SERK4*, and strong *bak1 bkk1* allele combinations are seedling lethal even in sterile conditions (He et al., 2007; Jeong et al., 2010;). Additionally, BAK1 interacts with BIR1 (BAK1-interacting receptor like kinase 1), another LRR-RLK, mutants of which also show constitutive un-controlled cell death (Gao et al., 2009). Intriguingly, also other *SERK*-family members share (partially) functional redundant roles with *BAK1* or amongst each other (Albrecht et al., 2008). In addition to BAK1, SERK1 and BKK1 also interact with BRI1 as positive regulators of BR responses (Karlova et al., 2006; He et al., 2007; Albrecht et al., 2008; Jeong et al., 2010). Furthermore, *SERK1* and *SERK2* have redundant roles in male sporogenesis (Albrecht et al., 2005; Colcombet et al., 2005; Albrecht et al., 2008) and SERK1 was recently shown to be involved in organ separation in flowers (Lewis et al., 2010). Therefore it would be of great interest to investigate the role of other *SERK*-family members in PTI signalling and plant defence especially in higher order multiple mutants.

Interestingly, *bak1* mutants are not only compromised in the response to flg22, elf18 and AtPep1 (Chinchilla et al., 2007; Heese et al., 2007; Krol et al., 2010) but also several other PAMPs such as HrpZ, lipopolysaccharides (LPS), and peptidoglycans (PGN) (Shan et al., 2008). Furthermore, *BAK1*-silenced *N. benthamiana* plants are less sensitive to the PAMPs INF1 and csp22 (Heese et al., 2007). This clearly suggests that BAK1 might form heteromeric complexes with other yet unknown

PRRs. However not all elicitor perception requires BAK1 as chitin responses are not compromised in *bak1* mutant plants (Shan et al., 2008).

Whereas it is clear genetically that *BAK1* is a signal enhancer for both BR and PTI signalling. It is unclear how BAK1 regulates the different pathways mechanistically. It was recently suggested that BAK1 functions as a biochemical signal enhancer for the RD-kinase BRI1 by primarily increasing the kinase activity of BRI1 (Wang et al., 2008). This conclusion is based on biochemical studies on the auto- and trans-phosphorylation events revolving around BRI1-BAK1 followed by phenotypic analysis of BAK1 phospho-mimetic and phospho-dead mutants. Interestingly none of the mutant BAK1 alleles has a strong differential effect on PTI and BR signalling (Wang et al., 2008). It is unclear whether the BRI1-BAK1 model can be generalized to other RD- or non-RD kinases. For example, a recent study showed striking differences between FLS2-BAK1 complex formation (Schulze et al., 2010) and pervious insights into the BRI1-BAK1 complex (Wang et al., 2008). It was shown that FLS2 and BAK1 oligomerize and are phosphorylated within seconds of ligand addition (Schulze et al. 2010). Importantly, in contrast to the BAK1-BRI1 interaction that requires the BRI1 kinase activity for full interaction (Wang et al., 2008), FLS2-BAK1 phosphorylation but not complex formation is inhibited by pre-treatment with the general kinase inhibitor K252a (Schulze et al., 2010). This demonstrates that complex formation between BAK1 and FLS2 is rather a requirement than a consequence of detectable phosphorylation.

SERK-homologes in other plant species are potentially also involved in PTI as their transcripts are regulated by pathogens and defence-related hormones (Song et al., 2008; Santos et al., 2009). Furthermore, the over-expression of *OsSERK1* confers increased resistance to *M. oryzae* in rice whereas the suppression of *LsSERK* expression in lettuce renders plants more susceptible to *Sclerotinia* (Hu et al., 2005; Santos et al., 2009). This clearly suggests the functional conservation of *SERK*-family members in plant defence.

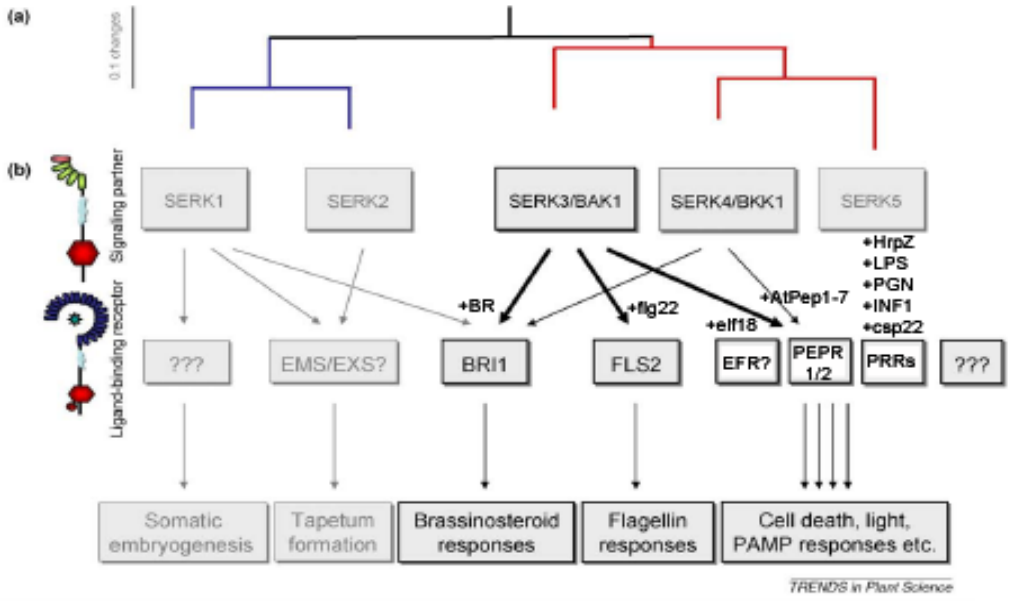

Figure 1.1: Multiple functions of BAK1 and other SERK family members

a) Phylogenetic tree of the SERK protein family. Blue indicates subgroup one containing SERK1 and 2, red indicates subgroup two with SERK3 to 5.

b) BAK1 regulates several important signaling pathways via the direct interaction with the ligand binding receptor BRI1, FLS2, EFR, PEPR1/2, and potentially unkown PRRs and other receptors (indicated by ???).

See 1.4.1. for more details also.

Figure adapted from Chinchilla et al. 2009

1.4.2. Ion fluxes

Seconds to minutes after elicitor treatment ion-fluxes occur across the plasma membrane that are easily recordable as growth medium alkalinisation and are often used as very early read-outs (Nurnberger et al., 2004). These ion fluxes coincide with a rise in cytoplasmic Ca^{2+} concentration (Jeworutzki et al., 2010). Interestingly, different elicitors give rise to different Ca^{2+}-signatures (Aslam et al., 2009), that might encode elicitor specific down-stream responses. In the case of LPS, this $[Ca^{2+}]_{cyt}$ rise is mediated by the cyclic nucleotide gated channel CNGC2 (Ali et al., 2007). Pathogen-induced $[Ca^{2+}]_{cyt}$ rise was recently shown to be blocked by adenylyl cyclase inhibitor alloxan suggesting a role of cNMPs signalling upstream of $[Ca^{2+}]_{cyt}$ alterations (Ma et al., 2009)

These different Ca^{2+} signatures are decoded by calcium binding proteins such as calcium dependent protein kinases (CDPKs), calmodulins, calicnerin B-like proteins (CBLs) and CBL-interacting protein kinases (CIPKs) (Dodd et al., 2010; Kudla et al., 2010). Recently, several of these proteins have been implicated in PTI signalling. For example OsCIPK14/15 were shown to be positive regulators of EIX induced PTI responses in rice and to interact with several CBLs in the yeast two hybrid system (Kurusu et al., 2010). *AtCPK1* is rapidly induced transcriptionally after fungal elicitor treatment and is a positive regulator of plant resistance to different fungal pathogens (Coca and Segundo, 2010). Another study, mainly based on transient over-expression studies in Arabidopsis protoplasts identified *AtCPK4/5/6/11* as major regulators of flg22-induceed ROS-burst and gene expression downstream of calcium and partially independent of MAPK signalling (Boudsocq et al., 2010). This clearly demonstrates that calcium is major regulator of PTI.

1.4.3. Phosphorylation and MAPK cascades

Phosphorylation is the earliest measurable response after ligand-induced oligomerization (Felix et al., 1991; Schulze et al., 2010). Recent studies identified over 2000 constitutively phosphorylated proteins in rice and *Arabidopsis* (Nakagami et al., 2010). Two quantitative studies identified over 70 differentially phosphorylated proteins after elicitor treatment (Benschop et al., 2007; Nuhse et al., 2007). In addition to transmembrane RLKs and calcium-regulated kinases (see above) the identity of several other kinases in PTI signalling is known.

1.4.3.1. Membrane-associated cytoplasmic RLKs regulate PTI signalling

Several membrane-associated cytoplasmic RLKs have been recently implicated in PTI signalling (Lu et al., 2010; Zhang et al., 2010). *BIK1 (Botrytis induced kinase 1)* was originally identified as being transcriptionally induced by *B. cineria* (Veronese et al., 2006). *Bik1* mutants are more susceptible to necotrophic fungi and more resistant to adapted bacterial pathogens *Pto* DC3000 due to elevated salicylic acid

(SA) levels. Interestingly, *bik1nahG* double mutants, without elevated SA levels, are slightly more susceptible to adapted *Pto* DC3000 than wild-type and *nahG* control plants (Veronese et al., 2006). Indeed, BIK1 was shown recently to be phosphorylated after elf18 and flg22 treatment, to interact constitutively with FLS2, EFR and potentially BAK1, and to dissociate from the receptor complex in a BAK1-dependent manner after PAMP treatment (Lu et al., 2010; Zhang et al., 2010). Interestingly, mutations of potential phosphorylation sites in the activation segment of BIK1, an RD-kinase, abolish not only *in vitro* kinase activity but also all PAMP-induced phosphorylation. These kinase dead BIK1 mutant proteins display a dominant negative effect on PTI signalling demonstrating the importance of BIK1 mediated phosphorylation. Notably BIK1 and paralogous cytoplasmic kinases such as PBS1 (AvrPphB susceptible 1) and PBS1-like proteins (PBLs) are required for PTI signalling downstream of FLS2, EFR and CERK1 (Zhang et al., 2010). Importantly, BIK1 and PBLs do not seem to be required for MPK activation in response to flg22 (Zhang and Zhou, 2010).

1.4.3.2. MAP kinase cascades in PTI signalling

MAP (mitogen associated protein) kinase cascades are common signalling modules in cell signalling pathways. A complete MAP kinase cascade AtMEKK1-AtMKK4/5-AtMPK3/6 leading to the activation of the transcription factors WRKY22/29 was suggested as a positive regulatory module of flg22 signalling mainly based on activation and expression studies of constitutively active kinases in protoplasts (Asai et al., 2002). However, recent reverse genetic studies demonstrated that AtMEKK1 is dispensable for the activation of AtMPK3/6, but is necessary for the activation of AtMPK4 (Ichimura et al., 2006; Nakagami et al., 2006; Suarez-Rodriguez et al., 2006). The MPKKK upstream of AtMKK4/5 is currently unknown. The two MAPKKs AtMKK1/2 act upstream of MPK4 (Meszaros et al., 2006; Qui et al. 2008). The activation of AtMPK4 after flg22 treatment leads to the phosphorylation of MKS1, the release of MKS1 (MAP kinase substrate 1) and WRKY33 from the complex and transcriptional activation of defence genes such as

PAD3 (phytoalexin deficient 3) (Qui et al., 2008). How these two MAP kinase cascades are connected to PRRs at the plasma membrane is one of the fundamental questions to be answered.

1.4.3.3. Phosphatases and other negative regulators

Kinases and their targets are under negative regulation by phosphatases to attenuate and fine tune signalling. Recently, several phosphatases have been shown to interact with and negatively regulate MAP kinases involved in PTI signalling (Bartels et al., 2010). The PP2C (protein phosphatase 2C)-type dual specific phosphatase AP2C1 negatively regulates MPK4 and MPK6 and mutants thereof are more resistant to mites, but more susceptible to necrotrophic pathogens due to changes in defence hormone homeostasis (Schweighofer et al., 2007). Similarly, the MAP kinase phosphatases MKP1 (MPK phosphatase 1) and PTP1 (protein tyrosine phosphatase 1) regulate MPK3/6 activity and double mutants are dwarf, resistant to *Pto* DC3000 and overproduce the defence hormone SA (Bartels et al., 2009). Lately, MKP2 was shown to dephosphorylate MPK3/6 *in vitro*, to interact with both MPKs *in vivo*, and to regulate disease resistance as *mpk2* mutants are more susceptible to necrotrophic fungus *B. cinerea* and more resistant to the soft rot bacteria *R. sonacearum* (Lee and Ellis 2007; Lumbreras et al., 2010). Whether, these phosphatases regulated PTI signalling still awaits further investigation. Importantly, phosphatases also regulate PRRs directly. The general kinase-associated protein phosphatase (KAPP) was shown to interact with FLS2 kinase domain in the yeast two-hybrid system and to negatively regulate FLS2 signalling (Gomez-Gomez et al., 1991). The rice PP2C XB15 (Xa21 binding partner 15) binds directly to the kinase domain of XA21, and negatively regulates XA21-mediated resistance by dephosphorylating XA21 (Park et al., 2008). Intriguingly, XA21 is also under negative regulations by phosphorylation as the ATPase XB24 leads to hyper-phosphorylation of XA21 *in vitro* and compromises *Xa21*-mediated resistance upon overexpression (Chen et al., 2010).

1.4.4. The oxidative burst

Many elicitors induce a rapid transient oxidative burst within a few minutes of treatment (Nicaise et al., 2009). This involves the production of reactive oxygen and reactive nitrogen species (ROS and NOS, respectively) (Ma and Berkowitz, 2007). In *Arabidopsis* the oxidative burst is mainly mediated by the NADPH oxidase *RbohD* (respiratory burst oxidase homolg D) (Meszaros et al., 2006; Zhang et al., 2007). The ROS-burst appears to be down-stream of the elicitor induced $[Ca^{2+}]_{cyt}$ elevations and down-stream of or parallel to MAPK activation (Zhang et al., 2007; Boudsocq et al., 2010). Interestingly, it was shown elegantly that the potato NADPH oxidates RbohB is phosphorylated on two N-terminal residues after treatment with INF1 (Kobayashi et al., 2007). This phosphorylation is mostly mediated by StCDPK4/5 and required for full functionality *in vivo*. Interestingly, it was reported that *Arabidopsis* RbohD is differentially phosphorylated after flg22 treatment (Nuhse et al. 2007). As the flg22-induced ROS-production is strongly impaired in *cpk4/5/6/11* quadruple mutant leaves, it is tempting to speculate that in *Arabidopsis* CPK4, 5, 6 and 11 play partially redundant roles in regulating RbohD via phosphorylation (Boudsocq et al., 2010).

Even though the oxidative burst is a long-described phenomenon its biological mechanism and significance in PTI signalling is hardly elucidated. Whereas *RbohB*-silenced *N. benthamiana* plants are more susceptible to fungal and oomycete pathogens (Asai et al., 2008), only minor disease resistance related phenotypes have been reported for Arabidopsis *rbohD* mutants (de Torres et al., 2006; Galletti et al., 2008; Mersmann et al., 2010).

1.4.5. Receptor endocytosis

In recent years the importance of endocytosis of transmembrane receptors in animals was shown to extend beyond signal attenuation by depleting ligand binding sites at the plasma membrane (Murphy et al., 2009). It became apparent that receptors are able to signal from endosomes and that endosomal signalling can trigger different

physiological responses due to differential complex composition and regulation in comparison to plasma-membrane localized signalling (Murphey et al., 2009). FLS2 was shown to be endocytosed in a ligand specific manner and FLS2 mutants with a reduced level of endocytosis display diminished flg22-responsivenes (Robatzek et al., 2006). However, it is not clear if FLS2 is able to signal from the endosomes as shown for BRI1 (Geldner et al., 2007). In the later case, treatment with the endocytosis inhibitor brefeldin A (BFA) leads to ligand-independent endosomal accumulation of BRI1 and contributes positively to BR-signalling (Geldner et al. 2007). Recently, LeEix2 was shown to undergo ligand-induced endocytosis after transient expression in *N. benthamiana* (Bar and Avni 2009). This endocytosis and downstream signalling is blocked by co-expression of the EH (Eps15 homology) domain containing protein AtEHD2. Interestingly, AtEHD2 over-expression also blocks responses mediated by other defence related RLPs, such as CF4 (*Cladopsorium fulvum* 4) and CF9 (Stergiopoulos and de Wit, 2009), but not responses mediated by the RK FLS2 (Bar and Avni, 2009a, b). This suggests the existence of different endocytitic routes for PRRs depending on there molecular identity e.g. RLKs or RLPs. Recently, stomatal cytokinesis defective 1 (SCD1) was identified as an *in vivo* interaction partner for FLS2 by mass spectrometry analysis (Korasick et al., 2010). SCD1 is coexpressed with coatomers, dynamins and adaptins (ATTED-II, http://atted.jp) suggesting a potential role in trafficking of FLS2. Unfortunatley the authors did not investigate FLS2 endocytosis in this mutant. Nevertheless SCD1 is important for PTI signaling as *scd1* mutants are less sensitive to PAMP application, manifested as reduced seedling growth inhibition and ROS production triggered by flg22 and elf18 (Korasick et al., 2010). *scd1* mutant plants are also impaired in proper SA signaling leading to enhanced accumulation of *PR1* transcripts and hydrogen peroxide. Consistenly, scd1 mutant plants are more resistant to infection with syringe-infiltrated *Pto* DC3000 (Korasick et al., 2010).

Clearly more detailed studies are required to explore the biological function and regulatory mechanisms of endosomal signalling in PTI.

1.4.6. Signaling from lipid microdomains !?!

Lipid rafts are comprised of membranes organized through interactions between sterols and sphingolipids, and are thought to spatially control signaling through dynamic association of protein partners. Proteomic studies of lipid raft-associated proteins are achieved through the isolation of detergent resistant membranes (DRMs), as the tight association of lipids in microdomains reduces the deterget solubility of the contained proteins (Borner et al., 2005; Kierszniowska et al., 2009). The lipid raft hypothesis remains controversial, though DRMs have been studied by several groups (Mongrand et al., 2004; Borner et al., 2005; Morel et al., 2006; Fujiwara et al., 2009; Kierszniowska et al., 2009). Proteomic studies of DRMs potentially provide knowledge of protein associations, which might be direct or indirect, and thus can provide insight into function. PTI signaling could be facilitated by close proximity and association of proteins that are contained in the same DRMs. A recent study used quantitative proteomics to investigate flg22-induced changes in Arabidopsis DRM-associated proteins (Keinath et al., 2010). 64 proteins were enriched in DRMs upon PAMP elicitation, including FLS2, though unexpectedly not BAK1 (Keinath et al., 2010). DRM-associated differentially identified proteins include LRR-RLKs FERONIA (FER), HERCULES (HERK1), remorins, H+-ATPases (AHA1, AHA2, AHA3, AHA4), Ca2+-ATPases (ACA8 and ACA10) and vacuolar ATPase subunit C DET3 (de-etiolated 3) (Keinath et al., 2010). AHA1, AHA2 and FER were previously 31 found to be phosphorylated in response to flg22 treatment (Benschop et al., 2007; Nühse et al., 2007). Mutants of FERONIA, DET3 and AHA1 were compromised for flg22-induced stomatal closure and concordantly had enhanced susceptibility to *Pto* DC3000 *ΔAvrPtoΔAvrPtoB* (Keinath et al., 2010). Interestingly, FER is involved in signaling for pollen tube reception (Escobar-Restrepo et al., 2007), as well as cell elongation, where it functions with related RLKs HERCULES1 (HERK1) and THESEUS1 (THE1) (Guo et al., 2009). Given the promiscuous nature of this protein in several signaling pathways, FER could be a signaling adaptor, however a specific FLS2-FER interaction has been proven yet. A similar quantitative study was carried out to identify proteins differentially DRM

associated in response to the elicitor cryptogein in tobacco BY-2 cells (Stanislas et al., 2009). In this study a 14-3-3 protein required for ROS burst was identified, as well as several dynamin-related proteins that play a role in trafficking (Stanislas et al., 2009).

1.4.7. Signalling regulation by E3 ligases

In animals receptor endocytosis, receptor degradation and down-stream signalling is often regulated by ubiquitination (Kawai and Akira, 2010; Lemmon and Schlessinger, 2010). Several E3 ligases have been implicated in plant defence in general, and a subset specifically in PTI signalling (Trujillo and Shriasu, 2010). The three *Arabidopsis* paralogous E3 ligases PUB22/23/24 (plant U-box 22/23/24) negatively regulate PTI signalling downstream of several PRRs, as triple mutants are hyper-responsive to flg22, elf18 and chitin treatment and more resistant to the adapted bacterial and oomycete pathogens (Trujillo et al., 2008). Interestingly, PTI is also under positive regulation by ubiquitination. In rice, the E3 ligase OsXB3 directly interacts with XA21 and is a specific phosphorylation target *in vitro* (Wang et al., 2006). Silencing of *OsXB3* leads to compromised XA21-mediated resistance and coincides with reduced amounts of XA21 protein (Wang et al. 2006). This suggests that OsXB3 is involved in Xa21 homeostasis.

1.4.8. Modulation of PTI signalling by small interfering RNAs

Small interfering RNAs siRNAs are major regulators of cell signalling and were first shown to be implicated in plant development and antiviral defences (Voinnet, 2005; Chuck and O'Connor, 2010; Katiyar-Agarwal and Jin, 2010). Recently, however they were shown to regulate host-microbe interactions and PTI signalling (Katiyar-Agarwal and Jin, 2010). Initial reports demonstrated that flg22 treatment downregulates auxin signalling via increased expression of the microRNA *miRNA393* targeting the mRNA of the main auxin receptor *TIR1* (transport inhibitor response 1) for degradation (Navarro et al. 2006). Also, mutants in the biogenesis

pathway of siRNAs, such as *ago1*, *ago4*, *dcl1* and *hen1,* are compromised in PTI signalling and are more susceptible to adapted and non-adapted bacterial pathogens (Agorio and Vera, 2007; Navarro et al., 2008; Li et al., 2010).

1.4.9. Transcriptional reprogramming

PTI signalling cumulates into a massive transcriptional reprogramming observable already after 30 min (Navarro et al., 2004; Zipfel et al., 2006). This reprogramming comprises up to 3% of the *Arabidopsis* genome and significantly overlaps with the ETI transcriptome (Sato et al., 2010). Elf18 and flg22 induce the same set of genes, and ~30% or ~50% of those are also regulated by PGN or chitin, respectively (Zipfel et al., 2006; Gust et al., 2007; Wan et al., 2008). This highly significant overlap in transcriptional regulation by different PAMPs clearly suggests signal convergence after PAMP recognition. Furthermore, comparison of *Arabidopsis* whole-genome transcriptional changes following infection with non-adapted, adapted and non-virulent bacteria identified over 800 PAMP-regulated genes (Thilmony et al., 2006; Truman et al., 2006). Ninety-six of them were up-regulated over a prolonged time period of 12 h post-infection by *Pto* DC3000 mutants defective in their type-III secretion system, as well as by four different PAMPs (flg22, elf18, LPS and HrpZ). Thus, these genes may represent the initial core PTI response (Truman et al., 2006).

1.4.10. Stomatal closure an important PTI response

Stomata are, in addition to natural wound sites, the major entry points for many plant pathogens. PAMP induced stomatal closure is therefore a very effective PTI responses to restrict pathogen growth (Melotto et al., 2008). LPS and flg22 treatment induce stomatal closure in *Arabidopsis* leaves and this relies on ABA (absicic acid) signalling components such as *OST1* (*open stomata 1*), *ABA3* (*ABA deficient 3*), *RbohD* and *GPA1* (*G protein alpha subunit 1*) (Melotto et al., 2006; Zeng and He, 2010; Mersmann et al., 2010). A recent study also suggests a predominant role of FLS2-dependent PTI signalling for growth restriction meditated by stomatal closure

during bacterial infection (Zeng and He, 2010). Stomatal opening is mostly driven by the uptake of anorganic cations and concomitant water influx. The two PM (plasma membrane) H^+-ATPases AHA1 (autoinhibited H^+-ATPase isofrom 1) and AHA2 are involved in generating the electrochemical gradient required (Merlot et al., 2002) and were found to be differentially phosphorylated after elicitor treatment (Nuhse et al., 2007). It was shown recently that the negative defence regulator and effector target RIN4 (RPM1 interacting protein 4) interacts with AHA1 and AHA2, thereby directly promoting H^+-ATPase activity and preventing stomatal closure (Lui et al. 2009). The finding that RIN4 interacts with MPK4 *in vivo* (Cui et al. 2010) makes it tempting to speculate that AHA1 and 2 are direct phosphorylation targets of MPK4 representing another layer of regulation.

1.4.11. Callose deposition

Callose deposition is the accumulation of β 1,3-glucans between the plasma membrane and the cell wall after elicitor treatment or attack by non-infectious pathogens (Nicaise et al. 2010). Callose deposition in *Arabidopsis* is mostly mediated by PMR4 (powdery mildew resistant 4), mutants thereof were originally identified as being more resistant to powdery mildew due to elevated SA levels (Nishimura et al., 2003). Surprisingly, the same mutant was later found to support more growth of T3SS deficient *Pto* DC3000 (Kim et al., 2005). Nevertheless, *pmr4 pad4* double mutants are slightly more susceptible to non-adapted bacterial *Pph* NPS3121 supporting the idea that callose deposition is important for pathogen growth restriction (Ham et al., 2007). Interestingly, callose deposition was linked to PAMP-induced glucosinolate production, secondary metabolites associated with microbial disease resistance (Clay et al., 2009; Bednarek et al., 2009).

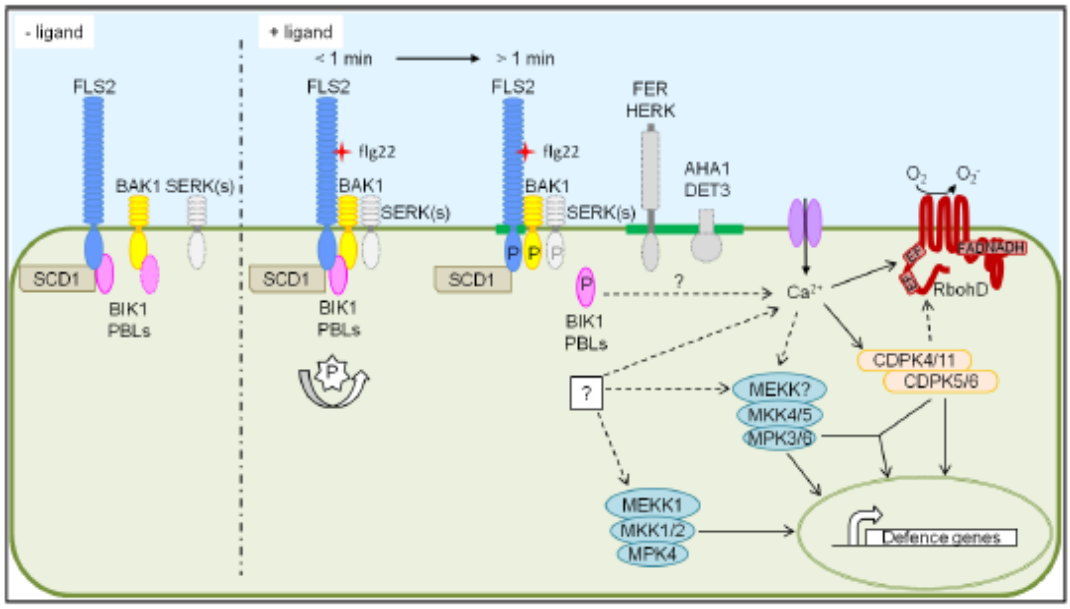

Figure 1.2. Current model of the FLS2 signaling pathway in Arabidopsis
FLS2 interacts constitutively with SCD1 and the RLCKs BIK1 and PBLs. BIK1 might also be associated with BAK1 in the resting state. Upon flg22 binding, a complex forms between FLS2, BAK1 and BIK1 almost instantaneously. Other SERKs, such as BKK1 might also be part of the FLS2 complex. The RLKs FER and HERK as well as the proton pumps AHA1 and DET3 are present in flg22-induced detergent-resistant membranes where FLS2 resides. Following flg22 binding, multiple phosphorylation events occur rapidly. Upon phosphorylation, BIK1 is released from the complex. Flg22 perception leads to the activation of at least two MAPK cascades, both involved in the induction of defence gene expression. Flg22 binding also triggers a Ca2+-burst that might activate Ca2+- dependent protein kinases (CDPKs) and the NADPH oxidase AtRbohD required for the ROS burst. Arabidopsis CDPK4, 5, 6 1 and 11 act synergistically and independently of the MAPKs to induce defence gene expression.
Figure and legend adapted from Segonzac et al. unpublished.

1.4.12. Hormone signalling in relation to PTI and general defence

SA, jasmonic acid (JA) and ethylene (ET) are the three major biotic stress hormones in plants. However, other hormones, *e.g.* auxin, ABA and gibberllic acid (GA), also influence disease-resistance outcomes (Robert-Seilaniantz et al., 2007). Traditionally, SA-dependent defences are implicated in the resistance against biotrophic and hemibiotrophic pathogens, whereas JA and ET signalling induces a different, sometimes antagonistic set of defence responses effective against necrotrophic pathogens, as well as herbivores (Glazebrook, 2005).

PAMP treatment or perception are able to increase SA levels and thereby promote local and systemic acquired resistance (Durrant and Dong, 2004; Mishina and Zeier, 2007; Tsuda et al., 2008). In addition expression profiling experiments using mini-arrays designed to analyse pathogen-responsive genes revealed the partial dependence of PTI-mediated gene induction on SA-signalling (Sato et al., 2007). Consequently, it was shown that mutations in the SA-signalling network reduce PTI induced defences (Tsuda et al., 2008). In a follow up study, Katagiri and co-workers recently used a network analysis approach to investigate the individual and combinatorial contributions to PTI signalling of four hormone signalling/biogenesis mutants *dde2, ein2, pad4* and *sid2* (Tsuda et al., 2009). It became apparent that SA, JA and ET contribute mostly synergistically to flg22 induced PTI responses (Tsuda et al., 2009). This "wipe out and reconstitute stepwise" approach, starting from a higher order multiple mutant and adding individual genes until the wild-type genetic background is reconstituted, applied in this study (Katagiri and Tsuda, 2010) is very helpful to elucidate complex genetic interactions. However, it neglects potential pleiotrophic effects on the signalling capacity of these mutants making a clear contribution to signalling *per se* difficult. This was nicely illustrated in a recent study demonstrating that FLS2 is under the direct transcriptional control of ethylene responsive transcription factors EIN3 (ethylene insensitive 3) and EIL1 (EIN3-like 1) even in the absence of elicitation (Boutrot et al., 2010). Mutants in the ethylene signaling pathways, such as *ein2* and *etr1-1*, display a constitutively reduced level of FLS2 leading to a reduced flg22-responsiveness (Boutrot et al., 2010). These results also suggest that elicitor induced ethylene synthesis (Paradies et al., 1980) might be part of a positive feedback loop downstream of flg22 perception by increasing *FLS2* transcription (Boutrot et al., 2010). Importantly, ethylene contributes positively to the resistance to *Pto* DC3000 early in the infection process (Mersmann et al., 2010). However, ET most likely interferes with SA-dependent defences at later time points via the repression of *SID2* (SA induced deficient 2) expression (Chen et al., 2009). These results add another layer of complexity, and warrants careful mutant phenotypic analysis combined with biochemical studies at different time-points during the infection process.

Auxin signalling is not only down-regulated by gene silencing (Navarro et al., 2006). SA also blocks auxin signalling by stabilizing auxin-response repressors (Wang et al., 2007; Kazan and Manners, 2009). Therefore auxin and SA possess antagonistic roles in defence signalling. Similarly, ABA behaves antagonistically to SA, as over-expression of ABA biogenesis genes leads to lowered SA levels after pathogen infection and increased susceptibility to several bacterial pathogens (Fan et al., 2009). In addition, bacterial pathogens actively promote ABA synthesis and signalling as a virulence mechanism (de Torres-Zabala et al., 2007). In contrast, GA and cytokinins seem to promote SA signalling (Navarro et al., 2008; Choi et al., 2010). It was elegantly shown that cytokinin enhances SA signalling via transcriptional co-activation mediated by physical interaction of SA- and cytokinin-regulated transcription factors (Choi et al., 2010). Overall, the interplay between PAMP-induced hormone production and initially hormone levels, *e.g*. influenced by environmental conditions and life history, significantly influences disease-resistance outcome.

1.5. Pathogens strike back: mechanisms to blur recognition and signalling

Successful pathogens need to avoid and/or suppress recognition by the plant. They can disguise their identity by either changing or hiding the epitopes that are recognized by the plant (see 1.2). Alternatively, they can disturb intracellular signalling downstream of the recognition event. Collectively, molecules that are secreted by the pathogen to suppress recognition or signalling are called virulence effectors.

1.5.1. Effectors preventing pathogen recognition before elicitor binding

Plants release lytic enzymes into the apoplastic space either as an active defence process or after cell collapse (Stergiopoulos and de Wit, 2009). These enzymes include chitinases that digest fungal cell wall chitin polymers releasing small chitin oligomers that are recognised as elicitors by the plant cell (Silipo et al., 2010).

Fungal pathogens have developed two independent strategies to avoid this recognition event. The effector Avr4 from *C. fulvum* binds chitin and protects it from basic plant chitinases (van Esse et al., 2007; Westerink et al., 2002). Plants constitutively expressing Avr4 are hyper-susceptible to a variety of fungal pathogens and *C. fulvum* silenced for Avr4 is less virulent on tomato (van Esse et al., 2007). These results clearly demonstrate the importance of Avr4 during the infection process. Intriguingly, *C. fulvum* employs another apoplastic effector, Ecp6, that is able to scavenge small chitin oligomers thereby preventing binding to the cognate PRR (de Jong et al., 2010). Interestingly, Ecp6 also employs LysM domains for chitin binding similar to plant PRRs, such as CEBiP and CERK1 (de Jong et al., 2010).

1.5.2. Bacterial polysaccharides suppressing pathogen recognition

Polysaccharides secreted by the bacteria fulfil different biological functions such as cell wall fortification, biofilm formation and cell-to-cell communication (Silipo et al., 2010). Recently, two different classes of bacterial polysaccharides have been implicated in the suppression of plant defence. Cyclic glucans have been reported to interfere with host defence responses locally and even to be able to suppress defence responses in distant leaves (Rigano et al., 2007). The molecular mode of action, however, is still unknown. In contrast extracellular polysaccharides (EPS) have been shown to directly bind and chelate divalent cations such as Mg^{2+} and Ca^{2+} (Aslam et al., 2008). Bacterial mutant strains unable to produce EPS are less virulent and induced stronger defence responses than wild-type bacteria. In addition, pure EPS suppress the Ca^{2+}-burst induced by several different PAMPs and purified EPS is able to bind Ca^{2+} directly (Aslam et al., 2008). This demonstrates that different types EPS have distinct function during the infections process. Some elicit defence responses whereas others are able to suppress those.

1.5.3. AvrPto and AvrPtoB the magic pair of T3SS effectors

AvrPto and AvrPtoB seem to be "all-rounder" amongst effectors being implicated in the suppression of multiple signalling pathways (Dodds and Rathjen, 2010). Initially, it was demonstrated that AvrPto and AvrPtoB block PTI signalling upstream of MAP-kinase activation early on in the signalling cascade and this PTI suppression is important as bacterial mutant strains missing either one or both effectors are compromised in their virulence (He et al., 2006). Later AvrPto was reported to interact with the kinase domains of FLS2 and EFR and thereby quelling kinase activity and signalling (Xiang et al., 2008). However, all interaction studies were based on transient over-expression in *Arabidopsis* protoplasts and a later report showed that functionally impaired variants of AvrPto are still able to bind FLS2 questioning the biological significance of the interaction (Shan et al., 2008). The authors showed instead that only functional AvrPto is able to interact with BAK1 after transient over-expression in protoplasts and in the yeast two-hybrid system. Furthermore, AvrPto and AvrPtoB blocked the ligand-induced interaction between BAK1 and FLS2 or BRI1 (Shan et al., 2008). Importantly, plants constitutively over-expressing AvrPto show a *bri1*-like morphology more severe than *bak1* null mutants and AvrPto also blocks BAK1-independent PTI pathways such as for chitin and NPP1 making it conceivable that AvrPto interferes with these pathways by interacting with other SERK-family members (Shan et al. 2008). In the case of AvrPtoB, an E3 ligase (Janjusevic et al., 2006), two additional targets were reported. AvrPtoB interacts with CERK1 *in vivo* and in the yeast two-hybrid system, mediates its poly-ubiquination *in vitro,* and induces its degradation via the vacuolar pathway *in planta* (Gimenez-Ibanez et al., 2009). Also, FLS2 was shown to interact with AvrPtoB and be poly-ubiquinated by it *in vitro* and *in vivo* (Gohre et al., 2008). This leads to the degradation of FLS2 via the 26S proteasome pathway. This finding was somehow surprising as the E3 ligase domain of AvrPtoB is not required for the suppression of FLS2-dependent responses (Gimenez-Ibanez et al. 2009).

1.5.4. MAP-kinases as effector virulence targets

Two bacterial effectors have been shown recently to interfere with PAMP-induced MAP kinase activation downstream of PRRs. HopF2, an ADP-ribosyltransferase, blocks the PAMP-induced activation of MPK4 after transient over-expression in *Arabidopsis* protoplasts (Wang et al., 2010). This inhibition was indirect as HopF2 interacts with several MAPKKs but not MAPKs *in vitro* and in protoplasts, including MKK5 an MAPKK previously not associated with MPK4 activation (Pitzschke et al., 2009a; Pitzschke et al., 2009b). Furthermore, HopF2 is able to ADP-ribosylate MKK5 *in vitro* and this enzymatic activity is required for the suppression of PTI responses by HopF2 (Wang et al., 2010). Interestingly, Desveaux and co-workers showed that the enzymatic activity of HopF2 and the *in planta* interaction partner RIN4 is required for its virulence function (Wilton et al., 2010). This suggests that either RIN4 is the major virulence target or that HopF2 targets MKK5 blocking MPK4 and thereby disturbing defence signalling via indirect manipulation of RIN4 (Cui et al., 2010; Wilton et al., 2010; Wang et al., 2010).
Another bacterial effector, HopAI1, was shown to block MPK3 and MPK6 directly (Zhang et al., 2007). HopAI1 is a member of an effector family conserved widely among animal and plant pathogens (Li et al., 2007). HopAI1 has a protein phosphothreonine lyase activity that constitutively deactivates MPK3 and MPK6 by dehydroxylating a phospho-threonine in the activation loop preventing potential re-phosphorylation (Zhang et al., 2007).

1.5.5 Tricking plants into re-open the gates

Plants close their stomata after elicitor recognition to prevent pathogen entry (Melotto et al., 2006; Melotto et al., 2008). However, some pathovars (pv) of *P. syringae* are able to trigger stomata re-opening using the non-protenaceous effector coronatine (Melotto et al., 2008; Melotto et al., 2006). Coronatine is a phytotoxin that structurally mimics the bioactive jasmonate JA-Ile. It binds directly to the corresponding JA receptor, the E3-ligase COI1 (Katsir et al., 2008). This most likely

leads to the degradation of transcriptional repressor proteins of the JAZ-family and activates the JA pathway (Chini et al., 2007; Thines et al., 2007; Katsir et al., 2008). Activation of the JA pathway inhibits SA signalling and further downstream NPR1 (Nonexpresser of PR genses 1)-dependent ABA mediated stomatal closure (Zeng and He, 2010). Interestingly, the function of coronatine is not restricted to re-opening stomata but extents to bacterial infection in the mesophylle space (Melotto et al., 2008).

Recently, *Xcc* was shown to be able to re-open stomata (Gudesblat et al., 2009b). *Xcc* cells are able to communicate with each other during the infection process using a diffusible signal factor (DSF) that induces pathogenicity related gene expression. One of these gene products induces stomata re-opening after elicitor recognition. In addition, *Xcc* extracts block ABA-induced stomata closure and can complement the virulence defects of *Pto* strains unable to produce coronatine (Gudesblat et al., 2009b). The molecular identity is unknown but is most likely distinct from coronatine (Gudesblat et al., 2009a).

1.5.6. AvrPphB, a cysteine protease targeting multiple cytoplasmic RLKs

AvrPphB was long known to target the cytoplasmic RLK PBS1 (Shao et al., 2003). PBS1 is guarded by RPS5 (Resistant to *Pto* 5) and the cleavage of PBS1 by AvrPphB induces ETI in a PBS1 kinase activity dependent manner (Shao et al., 2003). However, the virulence function of AvrPphB was unknown until recently. In addition to PBS1, AvrPphB cleaves several other cytoplasmic kinases, such as PBLs and BIK1 (Zhan et al., 2010), that are involved in PTI signalling immediately downstream of several PRRs (Zhan et al., 2010; Lu et al., 2010). Most likely, the AvrPphB-mediated disappearance of these cytoplasmic RLKs leads to reduced PTI signalling capacity as single and double mutants in these kinases are compromised in PTI responses and PAMP induced resistance (Zhang et al., 2010).

1.5.7. PTI-suppressing effectors with targets of unknown function in PTI signalling

The T3SS effector HopU1 is able to restrict flg22-induced callose deposition in transgenic *Arabidospsis* plants and ADP-ribosylates the RNA-binding protein GRP7 (glycine rich protein 7) *in vitro* and *in vivo* (Fu et al., 2007). Mutants of GRP7 are also compromised in flg22- induced callose deposition and are hyper-susceptible to disarmed bacterial pathogens supporting a functional role of GRP7 in PTI signalling (Fu et al., 2007).

The bacterial effector HopM1 targets the ARF GEF protein AtMIN7 (HopM interactor 1), a protein involved in vesicle trafficking, for ubiquination and proteasomal degradation (Nomura et al., 2006). AtMIN7 mutants are compromised in callose deposition triggered by a partially disarmed bacterial pathogen suggesting a role in vesicle trafficking leading to callose deposition (Nomura et al., 2006).

However, the detailed functional involvements of both effector targets in PTI are currently under investigation.

1.5.8. PTI-suppressing effectors without known targets

Several bacterial, fungal, and oomycete pathogen effectors have recently been shown to be able to suppress PAMP-triggered responses, such as ROS burst production or callose deposition (Underwood et al., 2007; Sohn et al., 2007; Guo et al., 2009; Bos et al., 2010). However, in many cases the molecular details and mechanisms of PTI-suppression and its biological significance are still not known.

1.6. From virulence to betrayal: ETI

The second layer of plant inate immunity is based on the recognition of specific pathogen effector molecules by plant resistance proteins (Dangl and Jones, 2006). In the case of ETI these effectors are historically referred to as avirulence proteins as they betray the pathogen to the host creating an incompatible interaction (Dangl and

Jones, 2006). In general, these Avr gene/R gene interactions (Flor, 1971) are rather restricted to the pathovar/cultivar level (Nurnberger and Kemmerling, 2006). The recognition of pathogen effectors can be directly or indirectly and takes place in some cases extracellular but mostly intracellular and is under laboratory conditions often associated with localized cell death at the infection site termed hypersensitive response (HR) (Dodds and Rathjen, 2010). As for most known AVR protein/R protein interactions no physical interaction could be observed it was speculated that instead of directly interacting with the AVR protein the corresponding R-protein would rather guard the biochemical target of AVR and perceive perturbations thereof (Jones and Dangl, 2001). In this model the guardee is the virulence target of the effector in the absence of the corresponding R-protein (Chisholm et al., 2006). This model was extended recently to include AVR protein targets whose sole function it is to detect the pathogen. These targets are guarded by an R-protein but do not have any other function in defence signalling in the absence of the corresponding R-protein (van der Hoorn and Kamoun, 2008). This "decoy" model is in evolutionary perspective an extension of the "guard" hypothesis as insomuch the guardee can evolve into a decoy reducing multiple structural constrains, being functional in signalling, functional in AVR protein recognition and/or to avoid effector-mediated perturbation. Importantly, both models rely on indirect effector recognition linked to its intrinsic virulence activity. This makes it conceivable that several structurally distinct effectors can be recognized by a single R-protein via a common guradee/decoy maximizing the recognition potential while reducing fitness costs.

1.6.1. R-proteins

R-proteins fall into two major structural classes namely intracellular nucleotide binding domain (NB)-LRR proteins or extracellular LRR (eLRR) proteins. In both cases the LRR domain is believed to determine effector recognition specificity (Collier and Moffet, 2009).

1.6.1.1. eLRR R-proteins

This class of R-proteins contains several tomato RLPs conferring resistance to specific *C. fulvum* races (Rivas and Thomas, 2005). For example *Cf-2, Cf-4, Cf-5* and *Cf-9* R genes confer resistance to races carrying *Avr2*, *Avr4, Avr5* and *Avr9*. These effectors are small poly-peptides secreted into the leaf apoplast during infection where they were shown to inhibit plant enzymes such as proteases and chitinases (Steriopoulos and de Wit, 2009). No direct interaction could be shown for any of these AVR proteins with their respective R-protein. In the case of Avr2 it was shown that its recognition event depends on the interaction with the cysteine protease Rcr3 but on its inhibition (Rooney et al., 2005). However, it is not clear if Rcr3 directly interacts with Cf-2 representing a *bona fide* guardee.

1.6.1.2. NB-LRR R-proteins

The largest class of R-proteins comprises NB-LRR R-proteins. The central nucleotide binding site is part of a larger NB-ARC domain which is also found in apoptosis related proteins from animals (Collier and Moffet, 2009). These domains are generally involved in ATP binding, hydrolysis and important for downstream signalling. In plants they can be divided in two subclasses that are correlated with the N-terminal characteristics of the R-protein and are speculated to be involved in down-stream signalling specificity (Lukasik and Takken, 2009). According to the identity of the N-terminal domain, NB-LRR proteins are subdivided into coiled-coil (CC-)-NB-LRR proteins or Toll and human interleukin-1 receptor (TIR) domain carrying NB-LRR proteins (Chisholm et al., 2006). The CC and TIR domains appear to function as homo- and hetero-dimerization regions, and also interact with upstream signalling parterns such as avirulence proteins, guardees or decoys (De Young and Innes, 2006; Lukasik and Takken, 2009). Therefore, in addition to the LRR-domain, the N-terminal domain also contributes to recognition specificity of AVR proteins (Dodds and Rajthen, 2010).

1.6.1.2.1. CC-NB-LRR proteins and their recognition events

CC-NB-LRR proteins are mostly membrane associated, and include *Arabidopsis* RPM1, RPS2, tomato Prf and barley MLA10 (Intracellular mildew A 10) (Dangl and Jones, 2006). The two distinct R-proteins RPM1 and RPS2 interact with the same guardee RIN4 that inhibits their activation (Mackey et al., 2002; Axtell and Staskawicz, 2003; Mackey et al., 2003). However, in response to AVR perception both R-proteins detect different post-translational modifications of RIN4. The bacterial effector AvrRpt2 degrades RIN4, thereby activating RPS2 which leads to ETI and restriction of bacterial growth (Axtell and Staskawicz 2003; Mackey et al., 2003). The two unrelated bacterial effectors AvrB and AvrRpm1 are recognized by RPM1 and this recognition event is associated with RIN4 phosphorylation (Mackey et al., 2002). This phosphorylation is an indirect effect of the effector function and in the case of AvrB potentially mediated by MPK4 (Cui et al., 2010).

The tomato CC-NB-LRR protein Prf recognizes two distinct bacterial effectors AvrPto and AvrPtoB indirectly by forming a constitutive complex with its guardee the Ser/Thr kinase Pto (Mucyn et al,. 2006; Dodds and Rathjen, 2010). AvrPto and AvrPtoB are unrelated structurally and functionally but both elicit ETI by interfering with an oligomeric Prf-Pto complex, which potentially contains other Pto-family members such as Fen (Gutierrez et al., 2010; Dodds and Rathjen, 2010). AvrPto does not have any known enzymatic activity and displays a three-helix bundle fold with a characteristic omega loop important for interaction with Pto (Wulf et al., 2004). AvrPto seems to stabilize the active kinase structure of Pto by interacting with an N-terminal loop and the P+1 loop (Xing et al., 2007). This induced conformational change was suggested to mediate Prf-dependent ETI. In the case of AvrPtoB the middle part of the protein folds into a four-helix bundle and interacts with Pto via two similar interfaces compared with AvrPto. However, the primary amino acid sequence employed by either effector is very different (Dong et al., 2009). AvrPtoB carries an E3 ligase domain in the C-terminus that is important for defence suppression as C-terminal deletion mutants are recognized in *pto*-tomato plants (Janjusevic et al., 2006). Interestingly, the recognition of this truncated

AvrPto was shown to be dependent on Prf and is mediated by direct interaction with Fen, a Pto homologe (Rosebrock et al., 2006). Fen is normally degraded by AvrPtoB via its E3 ligase activity and Pto is able to inactivate AvrPtoB by phosphorylation of a serine residue in the active site due to its stronger kinase activity (Ntoukakis et al., 2009). These studies clearly exemplify the so called "arms-race" between pathogens and its potential host.

Interestingly, the barley CC-NB-LRR MLA10 recognizes the fungal effector Avr10 (Ridout et al., 2006) and this recognition leads to the translocation of MLA10 into the nucleus where it interacts with two WRKY transcription factors (Shen et al., 2006). Notably, these transcription factors and their *Arabidopsis* homologs are negative regulators of basal immunity against bacterial and fungal pathogens, and are up-regulated transcriptionally after elicitor treatment (Shen et al., 2006). Thus the authors speculated that the interaction with the R-protein might lead to de-repression of PTI signalling (Shen et al., 2006). Intriguingly, several other R-proteins were shown to require a nuclear pool for ETI activation (Burch-Smith et al., 2007; Wirthmueller et al., 2007).

1.6.1.2.2. TIR-NB-LRR proteins and their recognition events

TIR-NB-LRRs are cytoplasmic-and nuclear-localized proteins including *Arabidopsis* RPS4, flax L proteins and tobacco N protein (Gassmann et al. 1999, Dodds et al. 2006, Whitham et al. 1994). RPS4 recognizes the bacterial effector AvrRPS4 via an unknown mechanism (Gassmann et al., 1999). In the case of the flax L R-proteins it was shown that different alleles of L proteins recognize different AvrL567 proteins via direct interactions at least partially mediated by the LRR domain (Dodds et al., 2006). The tobacco N protein recognizes the virus helicase domain p50 indirectly and forms a tertinary complex including the sulfurtransferase NRIP1 (Caplan et al. 2008). The normally chloroplastic localized NRIP1 relocalizes to the cytoplasm and nucleus in the presence of p50 and is required for N-dependent ETI. However, it is questionable whether NRIP1 is the real guardee of N or mediates downstream signalling after p50 recognition.

1.6.2. Genetic requirement for ETI signalling

Several *R* genes require *SGT1* (*Skyp1-Cullin-F-box protein*), *RAR1* (*Required for MLA12 resistance 1*) and *HSP90* (*Heat shock protein 90*) for protein stability and/or signalling (Shirasu, 2010). RAR1, a CHORD domain containing protein, was initially identified as being essential for MLA function in barley (Shirasu et al., 1999). SGT1 interacts with RAR1 *in vivo* and is required for signalling of several R-proteins in different plant species (Austin et al., 2002; Azevedo et al., 2002). The third protein in the complex was shown to be the chaperone HSP90 that is required for full RPS2-mediated resistance (Takahasi et al., 2003). The RAR1-SGT1-HSP90 chaperone complex functions in the stabilization, translocation and/or activation of NB-LRR proteins most likely in keeping them in a tight "signal-ready" confirmation before AVR protein recognition (Shirasu, 2009).

In general the two major classes of plant R-proteins CC-NB-LRR and TIR-NB-LRR have a differential genetic signal transduction requirement of either *NDR1* or *EDS1-PAD4-SAG101*, respectively (Aarts et al. 1998, Wiermer et al. 2005). *NDR1* (*Non race-specific disease resistance*) was initially identified as a locus in *Arabidopsis* required for the recognition of several bacterial avirulence proteins and resistance against incompatible *Hyaloperonospera arabidopsidis (Hpa)* races (Centruy et al. 1995). NDR1 posses several potential transmembrane domains (Century et al., 1997) and is localized to the plasma membrane via a GPI-anchor (Coppinger et al., 2004). Its exact molecular function is currently unknown. Similarly the molecular functions of EDS1 (Enhanced disease susceptibility 1), PAD4 and SAG101 (Senescence-associated gene 101) are unknown, however, all display structural similarities to lipases or lipid binding proteins (Wiermer et al. 2005). Furthermore, EDS1 was linked to reactive oxygen species and chloroplast related signalling (Wiermer et al., 2005; Straus et al., 2010). EDS1 and PAD4 were initially found to interact in the yeast two-hybrid system and *in vivo* (Feys et al., 2001). Mutant analysis suggested that EDS1 functions independently of PAD4 in the early events after AVR protein recognition, but later PAD4 and EDS1 function together in the amplification of defence responses (Feys et al., 2001). The structurally related protein SAG101 was

identified as an *in vivo* interaction partner of EDS1 and these interactions contribute to protein stability (Feys et al., 2005). Interestingly, EDS1, PAD4 and SAG101 not only contribute to ETI but play a partial redundant role in basal and non-host resistance to adapted and non-adapted bacterial, fungal and oomycete pathogens (Feys et al., 2005; Lipka et al., 2005).

1.7. Prologue

The following paragraph depicts literally the summary of my research project proposal written by myself at the beginning of my PhD.

Pathogen-associated nolecular pattern (PAMP)-triggered immunity (PTI) can be seen as the first layer of defense in plants. However the signalling events downstream of PAMP perception are poorly understood and no comprehensive genetic screen has been published. Previously, a screen has been performed by Cyril Zipfel to identify EF-Tu insensitive (*elfin*) mutants. Out of 167 elfin mutants, only one *elfin* mutant showed blocked or reduced responses to both flagellin and EF-Tu (the two most studied PAMPs in *Arabidopsis*). This was surprising as the current model of PTI (PAMP-triggered immunity) signalling suggests an early conversion of signalling after flagellin and EF-Tu perception by their respective receptors.

During the course of my PhD, I will first map-based clone and genetically confirm this exceptional *elfin* mutant, which appears to be defective in a positive regulator of PTI signaling. Furthermore, I will characterize the phenotype of the knockout and over-expression lines towards different PAMPs and a wide range of host and non-host pathogens. I will also study the molecular function and interaction of the gene product in further detail, which will depend on the gene's identity.

To complement the aforementioned analysis of a positive regulator of PTI, I will use the FOX- (**F**ull-length cDNA **O**ver-e**X**pressing gene) hunting system to screen for negative regulators in the laboratory of Dr. Ken Shirasu in Japan (Riken, Yokohama). I will use the previously developed seedling growth inhibition screen to identify lines insensitive either to EF-Tu or flagellin. Due to the fast identification of the genes involved, I will be able to select one or two interesting candidates which are

blocked in the response to both PAMPs. Those will be confirmed by re-transformation of *Arabidopsis thaliana* with an over-expression construct. Furthermore, I will identify single/multiple mutants of the gene/gene family. Those will be analyzed in the same respect as mention before for the positive regulator.
Finally, I will search for and analyze orthologs in other plant species and test their importance and evolutionary conservation in PTI signalling.

Chapter 2: Material and methods

2.1. Plant material and growth conditions

2.1.1. *Arabidopsis thaliana*

2.1.1.1. Growth conditions

The *Arabidopsis* plants were grown in controlled environment chambers on soil or MS salt medium (Duchefa), 1% sucrose and 1% agar with a 10 H or 16 H photoperiod at 20-22^{o}C and 65 % humidity. The third backcross of *bak1-5* with Col-0 was used for all experiments.

Table 2.1. List of *Arabidopsis thaliana* lines used in this study.

Lines	Description	Reference
Col-0	Columbia 0, wild-type reference line	
L*er*	Landsberg erecta ecotype, parental mapping line	
Ws-0	Wassilewskija 0	
Ws-eds1	EMS induced mutation in EDS1 in the Wassilewskija 0 ecotype	(Parker et al., 1996)
psb27-1	knock-out of the D1 repair protein Psb27	(Chen et al., 2006)
ex1	knock-out mutant of Executer1	(Lee et al., 2007)
ex2	knock-out mutant of Executer2	(Lee et al., 2007)
ex1/2	Double knock-out mutant of Executer1 and Executer2	(Lee et al., 2007)
CSD2 OE	Over-expression line of *Cu/Zn Dismutase 2*	(Myouga et al., 2008)
fls2	knock-out mutant of the PRR FLS2	(Zipfel et al., 2004)
efr	knock-out mutant of the PRR	(Zipfel et al., 2006)

	EFR	
fls2 efr	double knock-out mutant of FLS2 and EFR	(Nekrasov et al., 2009)
bak1-4	knock-out mutant of BAK1	(Chinchilla et al., 2007)
bak1-5	EMS-induced missense substitution mutant in *BAK1*, three times back-crossed to Col-0	(Schwessinger et al., *submitted*)
fls2 efr bak1-5	triple mutant generated by crossing *fls2 efr* with *bak1-5*	
bkk1-1	knock-out mutant of BKK1	(He et al., 2007)
bak1-4 bkk1-1	double mutant generated by crossing *bak1-4* with *bkk1-1*	(Schwessinger et al., *submitted*)
bak1-5 bkk1-1	double mutant generated by crossing *bak1-5* with *bkk1-1*	(Schwessinger et al., *submitted*)
bak1-4 pBAK1::BAK1	*bak1-4* expressing *BAK1* under its own regulatory sequence	(Schwessinger et al., *submitted*)
bak1-4 pBAK1::BAK1-5	*bak1-4* expressing *BAK1-5* under its own regulatory sequence	(Schwessinger et al., *submitted*)
*bak1-4 pBAK1::BAK1**	*bak1-4* expressing BAK1 (D418N) under its own regulatory sequence	(Schwessinger et al., *submitted*)
*bak1-4 pBAK1::BAK1-5**	*bak1-4* expressing BAK1-5 (D418N) under its own regulatory sequence	(Schwessinger et al., *submitted*)
bri1-301	missense mutation in *BRI1*	(Xu et al., 2008)
bri1-301 bak1-4	double mutant generated by crossing *bri1-301* with *bak1-4*	(Schwessinger et al., *submitted*)
bri1-301 bak1-5	double mutant generated by crossing *bri1-301* with *bak1-5*	(Schwessinger et al., *submitted*)
bak1-4 pBAK1::BAK1:Myc	*bak1-4* expressing *cBAK1:Myc* under its own regulatory sequence	(Chinchilla et al., 2007)
bak1-4 pBAK1::BAK1:HA$_3$	*bak1-4* expressing *BAK1:HA$_3$* under its own regulatory sequence	present study

bak1-4 pBAK1::BAK1-5:HA$_3$	*bak1-4* expressing *BAK1-5:HA$_3$* under its own regulatory sequence	present study
bak1-4 pBAK1::BAK1:GFP	*bak1-4* expressing *BAK1:GFP*under its own regulatory sequence	present study
bak1-4 pBAK1::BAK1-5:GFP	*bak1-4* expressing *BAK1-5:GFP* under its own regulatory sequence	present study

2.1.1.2. Stable transformation of *A. thaliana*

The transgenic *Arabidposis* plants were generated using floral dip method (Clough and Bent, 1998). Briefly, flowering *Arabidopsis* plants were dipped into suspension culture of *Agrobacterium tumefaciens* Agl1 carrying the indicated plasmid. Plants carrying a T-DNA insertion event were selected either on MS media containing the appropriate selection or as soil grown seedlings by the spray application of PPT (Phosphinotricine, Duchefa).

2.1.1.3. Generation of *Arabidopsis* F_1 and F_2 progeny

Fine tweezers were used to emasculate an individual flower. To prevent self-pollination, only flowers that had a well-developed stigma but immature stamen were used for crossing. Fresh pollen from three to four independent donor stamens was dabbed onto each single stigma. Mature siliques containing F_1 seed were harvested and allowed to dry. Approximately five F_1 seeds per cross were grown as described above and allowed to self pollinate. Produced F_2 seeds were collected and stored.

2.1.1.4. *Arabidopsis* seed sterilization

For *in vitro* growth of *Arabidopsis*, seeds were sterilized. Approximately 50 - 100 *Arabidopsis* seeds were put into a 1.5 mL tube. Tubes were put in a plastic rack. 100 ml of 12% Sodium-hypochloride solution (chlorine bleach) were poured into a

beaker and put together with the seed into a desiccator. 10 mL of 37% HCl was directly added into the hypochloride solution so that yellow-grenish vapours were forming and the solution was bubbling heavily. The lid of the desiccator was closed immediately. This was left for 4 – 8 H. After the sterilization period, the desiccator was slightly opened under a fume hood for 5 min to let out the gas.

2.1.2. *Nicotiana benthamiana*

2.1.2.1. Growth conditions

N. benthamiana plants were grown in controlled environment chambers at an average temperature of 24°C (range 18-26°C), with 45-65% relative humidity under long day conditions (16 H light).

2.1.2.2. Transient transformation

Agrobacteria cells from overnight cultures grown at 28°C in low-salt LB were harvested by centrifugation at 3500 rpm and resuspended in buffer containing 10 mM MgCl2 to a final OD_{600nm} of 0.3. The cultures were incubated at room temperature for 1 H and then hand-infiltrated on leaves of three to four week old *N. benthamiana* leaves using 1 mL needless syringe. All samples were taken 2 days post infiltration.

2.2. PAMP assays

2.2.1. PAMPs

The following elicitors were used in this study: crab shell chitin (Sigma, UK), flg22 peptide (CKANSFREDRNEDREV) (Peptron, South Korea), elf18 peptide (ac-SKEKFERTKPHVNVGTIG) (Peptron, South Korea), and AtPep1 peptide (ATKWKAKQRGKEKVSSGRPGQHN) (Peptron, South Korea).

2.2.2. Seedling growth inhibition

Fresh harvested seeds were surface sterilized, sown on MS media, stratified for 2 days at 4^{o}C in the dark and put in the light. Five-day-old seedlings were transferred into liquid MS with or without the indicated amount of peptide and incubated for eight further days. Dry weight of six replicates per treatment was measured using a precision scale (Sartorius) and blotted relative to untreated control.

2.2.3. ROS burst assay

Eight leaf discs (4 mm diameter) of at least four 3-4 week plants were sampled using a cork borer and floated over night on sterile water. The following day the water was replaced with a solution of 17 mg/mL (w/v) luminol (Sigma) and 10 mg/mL horseradish peroxidase (Sigma) containing 100 nM elf18 or 100 nM flg22. Luminescence was captured either using a Varioskan Flash (Thermo Scientific) multiplate reader or Photek camera (East Sussex, UK). The amount of relative light units might differ depending on the light capturing apparatus used.

2.2.4. MAP kinase assay

14-days-old seedlings were grown for five days on MS plates and than transferred to liquid MS. Triplicates of two seedlings each were treated with water, 100 nM elf18 or 100 nM flg22 for 0, 5 and 15 min before being pooled for harvest. Seedlings were ground to fine powder in liquid nitrogen and solubilised in better lacus buffer [50 mM Tris-HCl pH 7.5; 100 mM NaCl; 15 mM EGTA; 10 mM $MgCl_2$; 1 mM NaF; 1 mM $Na_2MoO_4.2H_2O$; 0.5 mM $NaVO_3$; 30 mM β-glycerophosphate; 0.1% IGEPAL CA 630; 100 nM calyculin A (CST); 0.5mM PMSF; 1 % protease inhibitor cocktail (Sigma)]. The extracts were centrifuged at 16,000 x *g*, the supernatant cleared by filtering through Miracloth and 4xLDS loading buffer (Invitrogen) added. 40 µg of total protein was separated by SDS-PAGE and blotted onto PVDF membrane (Biorad). Immunoblots were blocked in 5% (w/v) BSA (Sigma) in TBS-Tween

(0.1%) for 1-2 H. The activated MAP kinases were detected using anti-p42/44 MAPK primary antibodies (1:1000, Cell Signaling Technology) overnight, followed by anti-rabbit-HRP conjugated secondary antibodies (Sigma).

2.2.5. PAMP-induced defence gene induction

14-days-old seedlings grown for five days on MS plates and than transferred to liquid MS were used for all gene induction studies. RNA was extracted using RNeasy Plant Mini kit (Qiagen) followed by DNase-treatment using Turbo DNA-free (Ambion) and quantified with a Nanodrop spectrophotometer (Thermo scientific). cDNA was synthesized from 2.5 µg total RNA using SuperScript III reverse transcriptase (Invitrogen). SybrGreen master mix (Sigma) was used for qPCR reactions.

For defence gene induction analysis a triplicate of two seedlings each was treated either with water, 100 nM elf18 or 100 nM flg22 for 0, 30, 60 and 180 min and pooled before harvesting. Gene expression of *At2g17740* (*DC1-domain containing protein*), *At5g57220* (*CYP81F2*) and *At1g51890* (*LRR-RLK*) was monitored by qPCR analysis. The expression of each marker gene was normalized to the internal reference gene *At4g05320* (*UBQ10*) and plotted relative to the Col-0 steady-state expression level.

2.2.6. PAMP-induced ethylene production

Plants were grown for 6 weeks before sampling 2 mm leaf strips from 4 plants per genotype. Ethylene assays were performed as described by Felix et al. (1999) using 1 µM flg22, elf18 or AtPep1.

2.2.7. Crude elicitor extract preparation

Pta 6605 was grown O/N at 28^{o}C in Kings B medium supplemented with appropriate antibiotics. Spun down at 4,000 x *g* for 15 min, washed with 1 volume

sterile water and re-suspended in 1/10 volume sterile water. The extract was boiled for 10 min at 95°C, spun down and supernatant applied at a final concentration of 0.1 (v/v).

A. brassicicola was grown on V8 plates containing 0.8 % agarose for 14-days at RT in the dark. Biomaterial was harvested by scraping the plate, washed, filtered through Miracloth and re-suspended in sterile water. The extract was boiled for 10 min at 95°C, spun down and supernatant applied at a final concentration of 0.1 (v/v).

For *Hpa* crude elicitor extraction the following method was done. The aerial parts of 3-4 week old Ws-0 *eds1-1* infected (*Hpa* Emoy2, 7dpi) or non-infected plants were harvested and frozen in liquid nitrogen. 20 mL of cold sterile water was added and mixed vigorously by vortexing. The suspension was cleared of plant debris by filtering through Miracloth and enriched for heavier particles by centrifugation at 300 rpm for 15 min. The supernatant was removed, the pellet resuspended in 3 mL of sterile water and heated at 95°C for 10 min. These suspensions were used in a concentration of 1:100.

In the case of *Albugo laibachii Alem1* and *A. candida 20DD5* bio-samples were supplied by Eric Kemen (Sainsbury Laboratory, Norwich, UK). Crude elicitor extractions were performed as described for *Hpa*.

2.3. BR assays

2.3.1. Hypocotyl growth assay

Freshly harvested seeds were surface sterilized and stratified in sterile water at 4°C for 4-6 days in the dark. Individual seeds were put on ½ MS containing 0.8% pythoagar (Duchefa) without hormone, with 100 nM BL or with 100 nM BRZ and left up-right in the dark at 20-22°C. Hypocotyl length was measured after 5-day incubation.

2.3.2. Root growth assay

Freshly harvested seeds were surface sterilized and stratified in sterile water at 4^{o}C for 4-6 days in the dark. Individual seeds were put on ½ MS containing 0.8% pythoagar (Duchefa) without hormone, with 0.1, 1 or 10 nM BL and left up-right in long day conditions at 20-22^{o}C. Root length was measured after 7-day incubation.

2.3.3. BR-responsive gene expression analysis

14-days-old seedlings grown for five days on MS plates and than transferred to liquid MS were used for all gene induction studies. RNA was extracted using RNeasy Plant Mini kit (Qiagen) followed by DNase-treatment using Turbo DNA-free (Ambion) and quantified with a Nanodrop spectrophotometer (Thermo scientific). cDNA was synthesized from 2.5 µg total RNA using SuperScript III reverse transcriptase (Invitrogen). SybrGreen master mix (Sigma) was used for qPCR reactions.

For BR gene expression analysis a triplicate of two seedlings each was treated with either mock solvent control or 2.5 µM BRZ (Sigma) for 16 H over night. The next morning samples were further treated with mock solvent control or 200 nM brassinolide (SRICI) for another three hours before being pooled for harvesting. Gene expression of *At2g40610* (*EXP8*) and *At4g38850* (*SAUR-ACI*) was monitored by qPCR analysis. The expression of each gene was normalized to the internal reference gene *At5g15400* (U-box containing protein) and plotted relative to the Col-0 double mock treated expression level.

2.4. Pathogen assays

2.4.1. Bacterial spray-inoculation of *Arabidopsis*

The *Pto* DC3000 or *Pta* 6605 strains were grown in overnight culture in Kings B medium supplemented with appropriate antibiotics. Cells were harvested by

centrifugation and pellets resuspended in sterile water to appropriate OD_{600} (0.2 for *Pto* DC3000 *ΔAvrPto/ΔAvrPto* and *Pto* DC3000 *COR*$^-$; 0.02 for *Pto* DC3000). Immediately prior to spraying, Silwett L-77 was added to bacteria to 0.04 % (v/v). Bacteria were sprayed onto leaf surfaces until run-off and plants maintained at high humidity for 3 days. For syringe inoculation of *Pta* 6605, bacteria were similarly grown and harvested. Cell pellets were resuspended in sterile water to $O.D._{600}$ 0.002 and infiltrated using a needleless syringe into 2 leaves each of 4 plants per genotype. Samples were taken using a cork-borer (2 mm) to cut leaf discs from 2 leaves per plant and 4 plants per genotype. Leaf discs were ground in water, diluted and plated on TSA with appropriate selection. Plates were incubated at 28°C and colonies counted 2 days later.

2.4.2. *H. arabidopsidis* inoculation and scoring on *Arabidopsis*

Hpa infections were performed as described by Tör et al., 2002. Spores were harvested from infected Ws-*eds1* seedlings 7 days post-inoculation, suspended in cold water at a density of 5 x 10^4 spores/mL and spray-inoculated onto 7-day-old seedlings to the point of run-off. Inoculated seedlings were incubated at high humidity at 18°C for 7days then sporulation was assessed. The growth of the *Hpa* strains Cala2 and Emoy2 was assessed by counting the number of sporangiophores per cotyledon. The reproduction of the *Hpa* strain Emco5 infection was determined by vortexing sporulating seedlings in water and by quantifying spores using a haemocytometer.

2.4.3. Bacterial spray-inoculation of *N. benthamiana*

The *Pta* 11528 or *P.syringae pv. syringae* (*Pss*) B728a strains containing the broad host range vector construct pTD600 were grown in overnight culture in Kings B medium supplemented with appropriate antibiotics. Cells were harvested by centrifugation and pellets resuspended in sterile water to OD_{600} of 0.002. Immediately prior to spraying, Silwett L-77 was added to bacteria to 0.04 % (v/v).

Bacteria were sprayed onto leaves infiltrated the previous day with sterile water or *Agrobacterium* containing the indicated construct until run-off. Samples were taken using a cork-borer (2 mm) to cut leaf discs from 2 leaves per plant and 4 plants per genotype. Leaf discs were ground in water, diluted and plated on TSA with appropriate selection. Plates were incubated at 28°C and colonies counted 2 days later.

2.4.4. Pathogens used in this study

Table 2.2. Summary of pathogens used in this study.

Pathogen	Reference
***Pseudomonas* strains**	
Pta 11528	
Pta 6605	
Pss B728a	
Pto DC3000	
Pto DC3000 *ΔAvrPto/ΔAvrPto*	(Lin and Martin, 2005)
Pto DC3000 *COR*$^{-}$	(Melotto et al., 2006)
***Hyaloperonospora arabidopsidis* isolates**	
Cala2	(Holub, 2007)
Emco5	(Holub, 2007)
Emoy2	(Holub, 2007)
Other oomycete pathogens	
Albugo laibachii Alem1	Eric Kemen, unpublished
Albugo candida 20DD5	Eric Kemen, unpublished
Fungal pathogen	
Botrytis cinerea	
Alternaria brassiciola	

2.5. Molecular biological methods

2.5.1. DNA methods

2.5.1.1. Isolation of genomic DNA from *Arabidopsis*

The extraction DNA extraction method yields relatively poor quality DNA sufficient for standard PCR. Aliquots were stored at -20° C. Small leaf samples of an area of about 25 mm^2 was taken with a pair of tweezers and 400 µL of DNA extraction buffer were added. The tissue in the tube was crushed either using a grinder and blue pestles or by adding a small steel ball and shaking. The solution was centrifuged at maximum speed for 5 min in a microcentrifuge and 300 µL supernatant were transferred to a fresh tube. One volume of isopropanol was added to precipitate DNA and centrifuged at maximum speed for 5 min in a microcentrifuge. The supernatant was discarded carefully. The pellet was washed with 70% ethanol and dried. Finally the pellet was dissolved in 100 µL sterilized water and 1 µl of the DNA solution was used for a 20 µL PCR reaction mixture.

2.5.1.2. PCR methods

All PCR reactions were carried out in using a PTC-225 Peltier thermal cycler (MJ Research).

2.5.1.2.1. Standard PCR

This method was used when no sequence accuracy was required. Briefly; the PCR reaction mix contained 2 µL10 x reaction buffer, 0.6 µL 10 mM of each primer, 0.4 µL 2 mM dNTP mix, 0.1 µL Taq polymerase (NEB), 13.6 µL dH_2O and 1 µL of the DNA template solution. A typical Standard PCR thermal profile is shown below.

Table 2.3. Standard PCR thermal profile.

Stage	Temperature (^{o}C)	Time period	No. of cycle
Initial denaturation	94	3 min	1 x
Denaturation	94	15 sec	
Anealing	50-60	15 sec	25 – 40 x
Extension	72	1 min per kb	
Final extension	72	10 min	1 x

2.5.1.2.1. Colony PCR

The previously described PCR conditions were used with slight adjustments (2.5.1.2.1.). Instead of the DNA template a small pipette tip of colonies showing antibiotic resistance were added to each reaction and the volume was adjusted adding 1 µL of dH_2O. Additionally, the samples were heated for 10min at 94^{o}C before the first cycle. Each colony was streaked out onto a fresh LB plate containing the appropriate antibiotic selection

2.5.1.2.3. Hi-fidelity PCR

This method was used when sequence accuracy was required. Briefly; the reaction mix contained 2 µL 2 mM dNTP mix, 1 µL 2 mM of each primer, 4 µL 5 x hifidelity buffer, 0.6 µL DMSO, 1 µL of the template cDNA and, 11.2 µL dH_2O and 0.2 µL Phusion polymerase (Finzyme). The mix was kept on ice and put in the thermocycler when it reached 98^{o}C. A typical hi-fidelity PCR thermal profile is shown below.

Table 2.4. Hi-fidelity PCR thermal profile.

Stage	Temperature (^{o}C)	Time period	No. of cycle
Initial denaturation	98	1 min	1 x
Denaturation	98	10 sec	
Anealing	55-62	15 sec	20 – 30 x
Extension	72	20 sec per kb	
Final extension	72	5 min	1 x

2.5.1.2.4. Targeted mutagenesis PCR

This method was used to introduce a desired mutation within a DNA sequence. Briefly; the reaction mix contained 4 µL 2 mM dNTP mix, 2.5 µL 2 mM of each primer, 10 µL 5 x GC-rich buffer, 1.5 µL DMSO, 1 µL of the template plasmid (25 µg/ µl) and, 28.25 µL dH_2O and 0.75 µL Phusion polymerase (Finzyme). The mix was kept on ice and put in the thermocycler when it reached 98^oC. A typical targeted mutagenesis PCR thermal profile is shown below.

Table 2.5. Targeted mutagenesis PCR thermal profile.

Stage	Temperature (^oC)	Time period	No. of cycle
Initial denaturation	98	1 min	1 x
Denaturation	98	10 sec	
Anealing	55	15 sec	12 x
Extension	72	20 sec per kb	
Final extension	72	5 min	1 x

The PCR reactions were brought to room temperature and 1 µl DpnI per reaction was added. Reactions were incubated O/N at 37^oC and 5 µl used to transform *E. coli* DH5α.

2.5.1.2.5. DNA sequence verification

Dideoxy DNA sequencing reactions were carried out in a final volume of 10 µL containing 80-100 ng template DNA, 0.5 µL of 3.2 µM, 1.5 µL 5x buffer and 1 µL ABI Big Dye Terminator Ready Reaction Mix (Perkin Elmer, Massachusetts, USA). The PCR cycle conditions were: initial denaturation step at 96°C for 1 min, denaturation at 96°C for 10 sec, annealing at 50°C for 5 sec and elongation at 60°C for 4 min (35 cycles total). Sequencing was carried out on a 377 or 3700 ABI PRISMTM Dye-Deoxy Terminator Cycle Sequencer (Perkin Elmer, Massachusetts, USA) in the Genome centre (John Innes Centre). Sequences were analysed using the software package VNTI version 11 (Invitrogen).

2.5.1.2.6. Agarose gel electrophoresis

DNA fragments were separated by electrophoresis in horizontal agarose gels. The gels were prepared in 1 x TAE (40 mM Tris, 20 mM NAOAc, 1 mM EDTA, pH7.9) including 1 μg/ml ethidium bromide (Sigma) for visualization purposes. The concentration of agarose varied between 0.8-2% (w/v) depending on the sizes of the DNA fragments to be separated but 1% (w/v) gels were normally used for analytical purposes. DNA samples were prepared by adding 0.1 vol of 10 x loading buffer (50% (w/v) glycerol, 50 mM EDTA, 10 x TAE, 0.25% (w/v) 64 bromophenol blue, 0.25% (w/v) xylene cyanol) and were loaded into the wells of the gel submerged in 1 x TAE. Gels were run at 10-100 V until the desired separation was achieved. Analytical gels were photographed on a short wavelength UV transilluminator (gelDoc 1000, Biorad).

2.5.1.2.7. DNA purification from agarose gel pieces

DNA was visualised on a long wavelenght UV transilluminator (TM40, UVP) and the desired fragment was excised using a razor blade. Fragments were purified using QIAquick spin columns (Qiagen) following the manufacturer's instructions.

2.5.1.2.8. *bak1-5* marker design

For *bak1-5* homozygous mutant identification a dCAPS marker was designed using dCAPS Finder 2.0 (Neff et al., 2002). The genomic region around the *bak1-5* mutation was PCR amplified using Taq polymerase (Qiagen). The corresponding product was cut with RsaI (NEB) and *bak1-5* derived PCR products contained an additional RsaI site in addition to the internal restriction control site.

2.5.1.3. Cloning

The desired DNA sequences were amplified by hi-fidelity PCR (2.5.1.2.3) using the appropriate template and primers. All sequences were verified in the primary plasmid (2.5.1.3.1-3) by DNA sequencing analysis (2.5.1.2.5). Secondary plasmids (2.5.1.3.4-5) were verified by restriction analysis (2.5.1.3.8).

2.5.1.3.1. Blunt end cloning

The blunt end DNA fragment was ligated into the pCR-Blunt-II-TOPO (Invitrogen) primary vector combining 0.5 µL vector solution, 0.5 µL 6 x buffer salt solution, 0.5-2 µL of DNA fragment solution and making it up to 3 µL using sterile dH_2O. The reaction was left for 30 min at RT. The whole reaction volume was used to transform *E. coli* DH5α.

2.5.1.3.2. Gateway entry vector cloning

The DNA fragment containing a CACC at the 5'-end was ligated into the pENTRD-TOPO (Invitrogen) entry/primary vector combining 0.5 µL vector solution, 0.5 µL 6 x buffer salt solution, 0.5-2 µL of DNA fragment solution and making it up to 3 µL using sterile dH_2O. The reaction was left for 30 min at RT. The whole reaction volume was used to transform *E. coli* DH5α.

2.5.1.3.3. IN-Fusion cloning

The DNA fragments were amplified with primers carrying the following extension: 5'-AAGTTCTGTTTCAGGGCCCG- for the forward primer and 5'-ATGGTCT AGAAAGCTTTA- for the reverse primer. The destination vectors pOPINM and pOPINF were linearised previously using KpnI (NEB) and HindIII (NEB). 50 ng of purified insert and 100 ng of linearised destination vector were mixed in a total volume of 10 µl sterile dH_2O. The reaction mix was added to a well of dry-down In-

Fusion reaction powder and mixed by pipetting up and down. The reaction was incubated at 42oC for 30 min and terminated by adding 40 µL TE immediately afterwards. Up to 30 µL of the reaction volume was used to transform *E. coli* DH5α.

2.5.1.3.4. Classical "cut and paste" cloning

The DNA fragments of interest (inserts) were released from the primary vector (2.5.1.3.1**)** using appropriated restriction enzymes. The secondary vector was also pre-digest with appropriate restriction enzymes creating compatible ends. For DNA ligation 2 µL purified insert, 6 µL purified linearised vector, 1 µL ligase buffer and 1 µL of T4 DNA ligase were combined in one reaction tube, mixed and incubated at 16^{o}C O/N. The whole reaction volume was used to transform *E. coli* DH5α.

2.5.1.3.5. Gateway LR reaction

LR Gateway reaction was used to introduce the insertion of the entry vector into a destination vector that was either from the pGWB or pEarleygate series (Earley et al., 2006; Nakagawa et al., 2007). The reaction mix contained 50-150 ng of the entry vector (2.5.1.3.2), 200-250ng of the destination vector, TE buffer pH 8.0 up to a final volume of 4 µL, and 1 µL of the LR Clonase II mix (Invitrogen). The reaction was vortexed shortly and incubated for 4-6 H at RT. The reaction was stopped adding 1 µL of Proteinase K (Invitrogen) and incubating samples for 15min at 37^{o}C. Normally, 2 µL of the reaction volume was used to transform *E. coli* DH5α.

2.5.1.3.6. Vector map generation

Vector maps of primary and secondary plasmids were generated using VNTI version 11 (Invitrogen). *In silico* digests were performed to identify appropriated endonucleases for restriction analysis (2.5.1.3.8).

2.5.1.3.7. Transformation of bacteria by heat-shock

For transformation an aliquot of DH5α (Home made by Karen Morehouse) cells were mixed with indicated amount of ligation or plasmid solution and left on ice for 10-30 min. The cells were heat shocked at 42^{o}C for 1-2 min and immediately chilled on ice for another 5min. The cells were re-suspended in 750 µL of liquid LB and incubated while shaking at 300 rpm at 37^{o}C for 1-2 H. The solution was plated on LB-agar plates containing the appropriate antibiotic selection

2.5.1.3.8. Transformation of bacteria by electroporation

Prior to electroporation, electro-competent bacterial cells were thawed on ice for 5 - 10 min. The desired amount of desalted plasmid up to 5 µL was added to 20 µL of e electrocompetent cells. Cells were transformed in an electroporation cuvette with a width of 1 mm in a Bio-Rad electroporator (Bio-Rad, Hercules, CA, USA). The settings were 1800 V with a capacity of 25 µF, over 200 Ω resistance. Cells were recovered from the cuvette by adding 1 mL of liquid LB medium and transferring the suspension to a sterile Eppendorf tube. The bacteria were incubated while shaking at 300 rpm for 1-2 H in the case of *E. coli* at 37^{o}C and for *A. tumefaciens* at 28°C. The bacterial solution was plated on LB-agar plates containing the appropriate antibiotic selection.

2.5.1.3.9. Plasmid miniprep

Single colonies corresponding to positive colony PCR results were incubated O/N in 5 mL LB containing the appropriate antibiotics and spun down for 10 min at 4,000 rpm. Plasmids were extracted from the bacterial cell pellet using QIAprep spin miniprep kits (Qiagen) following the manufacturers protocol.

2.5.1.3.10. Restriction analysis

The reaction mix for the plasmid restriction contained 200-400 ng of the plasmid, 1 µL of 10 x reaction buffer, 0.5 µL of each of the cutting enzymes (NEB), and was incubated for 1.5 H at 37^{o}C. The product was analyzed by agarose gel electrophoresis.

2.5.1.3.11. Plasmids used in this study

Table 2.6. Summary of plasmids used in this study.

Name	Insert/Description	Backbone	Reference
Plant expression vectors			
p35S::GUS:YFP-HA	*GUS*	*pEarleygate103*	
p35S::cFoxR1	CDS *At5g15850*	*pEarleygate100*	
p35S::cFoxR2	CDS *At2g18300*	*pEarleygate100*	
p35S::cFoxR3	CDS *At2g12290*	*pEarleygate100*	
p35S::cFoxR4	CDS *At5g24660*	*pEarleygate100*	
p35S::cFoxR5	CDS *At1g68520*	*pEarleygate100*	
p35S::cFoxR6	CDS *At1g26920*	*pEarleygate100*	
p35S::cFoxR7	CDS *At3g59940*	*pEarleygate100*	
p35S::cFoxR8	CDS *At5g20790*	*pEarleygate100*	
p35S::cFoxR9	CDS *At5g03230*	*pEarleygate100*	
p35S::cFoxR10	CDS *At2g42280*	*pEarleygate100*	
p35S::cFoxR11	CDS *At2g41310*	*pEarleygate100*	
p35S::cFoxR1:YFP-HA	CDS *At5g15850*	*pEarleygate103*	
p35S::cFoxR2:YFP-HA	CDS *At2g18300*	*pEarleygate103*	
p35S::cFoxR3:YFP-HA	CDS *At2g12290*	*pEarleygate103*	
p35S::cFoxR4:YFP-HA	CDS *At5g24660*	*pEarleygate103*	
p35S::cFoxR5:YFP-HA	CDS *At1g68520*	*pEarleygate103*	
p35S::cFoxR6:YFP-HA	CDS *At1g26920*	*pEarleygate103*	
p35S::cFoxR7:YFP-HA	CDS *At3g59940*	*pEarleygate103*	
p35S::cFoxR8:YFP-HA	CDS *At5g20790*	*pEarleygate103*	

p35S::cFoxR9:YFP-HA	CDS *At5g03230*	*pEarleygate103*	
p35S::cFoxR10:YFP-HA	CDS *At2g42280*	*pEarleygate103*	
p35S::cFoxR11:YFP-HA	CDS *At2g41310*	*pEarleygate103*	
p35S::cFoxR9-H1	CDS *At5g60680*	*pEarleygate100*	
p35S::cFoxR9-H2	CDS *At2g28400*	*pEarleygate100*	
p35S::cFoxR9-H3	CDS *At3g45210*	*pEarleygate100*	
p35S::cFoxR9-H1:YFP-HA	CDS *At5g60680*	*pEarleygate103*	
p35S::cFoxR9-H2:YFP-HA	CDS *At2g28400*	*pEarleygate103*	
p35S::cFoxR9-H3:YFP-HA	CDS *At3g45210*	*pEarleygate103*	
pBAK1::BAK1	genomic region of *BAK1* including 1.5 kb upstream sequence	*pGWB2*	entry clone (Kemmerling et al., 2007)
pBAK1::BAK1-5	derivate of *pBAK1::BAK1*	*pGWB2*	
*pBAK1::BAK1**	derivate of *pBAK1::BAK1* expressing BAK1(D418N)	*pGWB2*	
*pBAK1::BAK1-5**	derivate of *pBAK1::BAK1-5* expressing BAK1-5(D418N)	*pGWB2*	
pBAK1::BAK1:HA$_3$	genomic region of *BAK1* including 1.5 kb upstream sequence	*pepiGreenB(HA)*	
pBAK1::BAK1-5:HA$_3$	derivate of *pBAK1::BAK1:HA$_3$*	*pepiGreenB(HA)*	
pBAK1::BAK1:GFP	genomic region of *BAK1* including 1.5 kb upstream sequence	*pepiGreenB(GFP)*	
pBAK1::BAK1-5:GFP	derivate of	*pepiGreenB(GFP)*	

	pBAK1::BAK1:GFP		
pBAK1::BAK1:Myc			(Chinchilla et al., 2007)
pFLS2::FLS2:Myc			(Robatzek et al., 2006)
pFLS2::EFR:HA$_3$			gift of Vladimir Nekrasov Sainsbury Laboratory UK
p35S::BRI1:HA$_3$			gift of Freddy Boutrot Sainsbury Laboratory UK
pCERK1::CERK1:HA$_3$			(Gimenez-Ibanez et al., 2009)
***E.coli* expression vector**			
pGST:BAK1	BAK1 CD (256-615aa)	*pGEX-4T1*	primary vector (Karlova et al., 2009)
pGST:BAK1-5	derivate of *pGST:BAK1*	*pGEX-4T1*	
*pGST:BAK1**	derivate of *pGST:BAK1* expressing BAK1 (D418N) CD	*pGEX-4T1*	
*pGST:BAK1-5**	derivate of *pGST:BAK1-5* expressing BAK1-5 (D418N) CD	*pGEX-4T1*	
pMBP:EFR	EFR CD (682-1031aa)	*pOPINF*	
*pMBP:EFR**	derivate of *pMBP:EFR* expressing EFR* (D849N) CD	*pOPINF*	
pMBP:FLS2	FLS2 CD (840-1173aa)	*pOPINF*	
*pMBP:FLS2**	derivate of *pMBP:FLS2* expressing FLS2*	*pOPINF*	

	(D977N) CD	
pMBP:BRI1	BRI1 CD (814-1196aa)	*pOPINF*
*pMBP:BRI1**	derivate of *pMBP:BRI1* expressing BRI1* (D977N) CD	*pOPINF*
pHis$_6$:FLS2	see above	*pOPINM*
*p His$_6$:FLS2**	see above	*pOPINM*
p His$_6$:BRI1	see above	*pOPINM*
*p His$_6$:BRI1**	see above	*pOPINM*

2.5.2. RNA methods

2.5.2.1. Isolation of total RNA from *Arabidopsis*

RNA was extracted using RNeasy Plant Mini kit (Qiagen) following the manufactures protocol. RNA quality was evaluated by agarose gel electrophoreses.

2.5.2.2. Reverse transcription PCR

This method was used to generate single stranded cDNA from total RNA. All reactions mixes were always kept on ice if not indicated otherwise. Briefly; the reaction mix contained 2.5 µg total RNA, 2 µL 2 mM oligo$(dT)_{15}$, 4 µL 2 mM dNTP and was made up with sterile dH_2O to a final volume of 13 µL. The reaction mix was heated for 5 min at 65^oC and put on ice immediately for 1-5 min. The contents of the tube were collected by brief centrifugation. 7 µL of the second reaction mix were added containing 4 µL First-Strand buffer, 1 µL 0.1 M DTT, 1 µL RNase OUT (Invitrogen) and 1 µL SuperScript III RT polymerase (Invitrogen). The reactions were vortexed briefly, spun down and incubated at 50^oC for 50 min. The reactions were terminated by heating at 70^oC for 15 min and kept at -20^oC for storage.

2.5.3. Protein methods

2.5.3.1. General protein methods

2.5.3.1.1. SDS-polyacrylamide gel electrophoresis

The reagents and SDS-polyacrylamide gel preparation methods were followed according to Laemmli, 1970. Gels were run in Mini PROTEAN III gel tanks (Bio-Rad) filled with Tris-glycine electrophoresis buffer (25 mM Tris, 250 mM glycine (electrophoresis grade, pH 8.3, 0.1% SDS). The gel electrophoresis was performed in a continuous buffer system at 2.1 - 3.4 mA cm/gel. All gels included a molecular size marker 10-250 K Bio-Rad Precision Plus Marker (Bio-Rad). Electrophoresis was continued until the loading dye band migrated out of the gel.

2.5.3.1.2. Western Blot

Two Watmann papers and sponges per gel were equilibrated for 5 min in pre-chilled transfer buffer (25 mM Tris, 192 mM glycin, 20% (v/v) methanol, pH 8.3). The PVDF membrane (BIO-RAD) was activated for 1 min in methanol. The sandwich and device were assembled according the manufacture's protocol (BIO-RAD). The membrane was facing the anode and the gel the cathode. The transfer took place at 4^{o}C overnight at 30 V or for 2 H at 95 V.

2.5.3.1.3. Coomassie stain

The proteins in the gel or on the membrane were visualized by coomassie staining. The gel was transferred to a tray containing coomassie stain solution (0.5% (w/v) bromophenol blue R-250, 50% (v/v) methanol, and 7.5% (v/v) glacial acetic acid), agitated at RT for 30 min, and de-stained three times under agitation for 30min with coomassie de-stain (20% (v/v) methanol, 5% (v/v) acetic acid).

2.5.3.1.4. Immunoblotting

PVDF transfer membrane containing immobilised, denatured proteins were blocked for one hour at room temperature with 0.1% TBST buffer (0.5 M NaCl, 200 mM Tris-HCl, 0.05% (v/v) Tween-20, 0.2% (v/v) Triton X-100, pH 7.5) containing 5% dried skimmed milk powder (w/v) with gentle agitation on a platform shaker. This step prevents nonspecific binding by blocking potential binding sites with irrelevant protein. After removal of the blocking solution, the membrane was washed for 2 min with TBS buffer. The membrane was then incubated with the primary antibodies directed against the target protein with 0.1% TBST buffer containing 5% dried skimmed milk powder (w/v) for 1 H at RT or O/N at 4^{o}C. The membrane was washed three times for 15 min each with 0.1% TBST buffer. The membrane was than incubated for 1 H at RT with 0.1% TBST buffer containing 5% dried skimmed milk powder (w/v) and secondary anti-bodies that are directed against the anti-immunoglobulin of the primary antibody and covalently coupled to horseradish peroxidase (HRP). The membrane was washed three times for 15 min each with 0.1% TBST buffer. Detection of the peroxidase signal of the secondary antibody-HRP conjugate was performed with ECL (Amersham Biosciences), or SuperSignal West Femto (Pierce) chemiluminescent detection reagent for Western blotting. The membrane was exposed onto ECL Hyperfilm (Amersham Biosciences). Film exposure ranged from 30 sec to 20 min. The film was aligned to the membrane and the protein standards were marked on the film to confirm the relative molecular weight of the signal.

Primary antibodies were diluted in 0.1% TBST buffer containing 5% dried skimmed milk powder (w/v) solution to the following concentration: anti-GFP (AMS Biotechnology) 1: 5000; anti-BAK1 1:500; anti-HA-HRP (Santa Cruz) 1: 2000; anti-FLS2 1:1000; anti-BRI1 1:1000.

Secondary antibodies were diluted in 0.1% TBST buffer containing 5% dried skimmed milk powder (w/v) solution to the following concentration: anti-rabbit-HRP (Sigma) 1:5000 or anti-rabbit-HRP (Ebioscience) 1:5000.

2.5.3.1.6. Antibodies

Polyclonal anti-BAK1 antibodies were generated by immunizing rabbits with a synthetic peptide [DSTSQIENEYPSGPR] derived from the C-terminus of BAK1 (Schulze et al., 2010).
Polyclonal anti-FLS2 antibodies were generated by immunizing rabbits with a synthetic peptide [KANSFREDRNEDREV] derived from the C-terminus of FLS2. (Chinchilla et al., 2006).
Polyclonal anti-BRI1 antibodies were generated by immunizing rabbits with a synthetic peptide [IDSQSTIRSIEDGGFS] derived from the C-terminus of BRI1.
Antibodies (final bleed) were affinity purified against the peptide (Eurogentec).

2.5.3.1.6. HPLC and Mass Spectrometry

Protein samples were prepared for the mass spectrometry analysis as described previously (Ntoukakis et al., 2009). LC-MS/MS analysis was performed using a LTQ-Orbitrap mass spectrometer (Thermo Scientific) and a nanoflow-HPLC system (nanoAcquity, Waters Corp.) as described previously (Ntoukakis et al., 2009). The entire TAIR9 database was searched (TAIR9 33596 sequences; 13487687 residues) (www.arabidopsis.org) using Mascot (with the inclusion of sequences of common contaminants such as keratins and trypsin). Parameters were set for ±5 ppm peptide mass tolerance and allowing for methionine oxidation and two missed tryptic cleavages. Carbiodomethylation of cysteine residues was specified as a fixed modification and oxidized methionine and phosphorylation of serine, threonine or tyrosine residues were allowed as variable modifications. Scaffold (v2_06_01, Proteome Software Inc., Portland, OR) was used to validate MS/MS based peptide and protein identifications. Peptide identifications were accepted if they could be established at greater than 95.0% probability as specified by the Peptide Prophet algorithm. Protein identifications were accepted if they could be established at greater than 95.0% probability and contained at least 2 identified peptides.

2.5.3.1.7. Quantificaiton of total protein concentration

In order to determine the total protein concentration of plant extracts, the Bio-Rad Protein Assay (Bio-Rad) was used. 10 µL of total 1:20 diluted total was added to the 990 µL of the 1:5 diluted Bio-Rad protein assay solution. The reaction was mixed thoroughly at room temperature. To determine the protein concentration of the sample, the OD_{595}nm was measured using a MBA2000 spectrophotometer (Perkin Elmer) and compared to a BSA (Sigma) standard curve.

2.5.3.2. *In vitro* protein analysis

2.5.3.2.1. Recombinant protein purification

Recombinant fusion proteins were produced in *E. coli* BL21 (Novagen), extracted using BugBuster reagent (Novagen) containing 1 µL/mL Benzoase (Novagen), 1 KU/mL Lysozyme (Novagen) and 150 µL/mL protease inhibitor cocktail set II (Novagen) and the soluble fraction was used to enrich for fusion proteins. GST-tagged fusion proteins (GST-BAK1, GST-BAK1*, GST-BAK1-5, GST-BAK1-5*) were enriched using Glutathione Sepharose Fast Flow (GE Healthcare) according to the manufactures protocol. MBP-tagged fusion proteins (MBP-BRI1, MBP-BRI1*, MBP-FLS2, MBP-FLS*, MBP-EFR, MBP-EFR*) were enriched using Amylose Resin (NEB) according to manufactures protocol. His-tag fusion proteins (His-BRI1, His-BRI1*, His-EFR, His-EFR*) were enriched using His-Bind Resin (Novagen) according to the manufactures protocol. After elusion fusion proteins were adjusted to the same concentration in 10% glycerol solution and stored at -20^{o}C until usage.

2.5.3.2.2. Radioactive *in vitro* kinase assays

The fusion proteins were incubated in 30 µL kinase buffer (50 mM Tris, pH 7.5, 10 mM $MgCl_2$, 10 mM $MnCl_2$, 1 mM DTT) in the presence of 1 µM unlabeled ATP and 183 kB of [^{32}P]-γ-ATP for 30 min at 30^{o}C with shaking at 900 rpm. The

reactions were stopped by adding 2xLDS loading buffer (Invitrogen). The phosphorylation status of fusion proteins was analyzed by audioradiography after separation of one-fourth of the *in vitro* kinase assay by SDS-PAGE followed by western blotting, if not indicated otherwise. Incorporated [^{32}P]-groups were visualised exposing the membrane onto ECL Hyperfilm over night (Amersham Biosciences). In autophosphorylation assays 1 µg fusion protein for MBP- and GST-tagged proteins and 5 µg for His-tagged proteins was incubated with 1 µg of MBP (Fluka). In transphosphorylation assays 1 µg of each fusion protein was used.

2.5.3.2.3. Non-radioactive *in vitro* kinase assays

The fusion proteins were incubated in 30 µL kinase buffer (50 mM Tris, pH 7.5, 10 mM $MgCl_2$, 10 mM $MnCl_2$, 1 mM DTT) in the presence of 3 mM unlabeled ATP for 30 min at 30^{o}C with shaking at 900 rpm. The reactions were stopped by adding 2xLDS loading buffer (Invitrogen). The phosphorylation status of fusion proteins was analyzed by immunoblot analysis or HPCL-MS/MS analysis.

2.5.3.2.4. Immunoblot phosphorylation site analysis

The indicated amount of fusion proteins (GST-BAK1, GST-BAK1*, GST-BAK1-5, GST-BAK1-5*) were separated by SDS-PAGE and blotted onto PVDF membrane (Biorad). The immunoblots were blocked in 5% (w/v) BSA (Sigma) in TBS-Tween (0.1 %) for 1-2 H. Phospho-Serine/Threonine sites were detected using anti-p-Thr (1:1000, Cell Signaling Technology) overnight, followed by anti-mouse-HRP conjugated secondary antibodies (1:5000, Sigma). Phospho-Tyrosine sites were detected using anti-p-Tyr (1:2000, Cell Signaling Technology) overnight, followed by anti-rabbit-HRP conjugated secondary antibodies (1:5000, Sigma).

2.5.3.3. *In vivo* protein analysis

2.5.3.3.1. Protein extraction and immunoprecipitation in *N. benthamiana*

Leaves were ground to fine powder in liquid nitrogen and 5 mL extraction buffer [50 mM Tris-HCl pH 7.5; 150 mM NaCl; 10 % glycerol; 10 mM DTT; 10 mM EDTA; 1 mM NaF; 1 mM $Na_2MoO_4.2H_2O$; 1% (w/v) PVPP; 1% (v/v) P9599 protease inhibitor cocktail (Sigma); 1% (v/v) IGEPAL CA-630 (Sigma)] added. Samples were cleared by centrifugation at 16.000 x *g* for 15 min at 4°C and adjusted to 2 mg/mL total protein concentration. Immunoprecipitation were performed on 1.5 mL total protein by adding 20 µL GFPTrap-A beads (Chromotek), 20 µL anti-HA sepharose beads (Roche), or 20 µL true-blot anti-rabbit Ig beads (Ebioscience) in combination with 15 µL antibody and incubation at 4°C for 3-4 H. Beads were washed 4 times with TBS containing 0.5% (v/v) IGEPAL CA-630, immunoprecipitates eluted with 30 µL 2xLDS (Invitrogen) and heating at 70°C for 10 min.

2.5.3.3.1. Protein extraction and immunoprecipitation in *A. thaliana*

Frozen tissue was ground to fine powder in liquid nitrogen and extraction buffer [50 mM Tris-HCl pH 7.5; 150 mM NaCl; 10 % glycerol; 5 mM DTT; 2mM EDTA; 1 mM NaF; 1 mM $Na_2MoO_4.2H_2O$; 1 mM PMSF (Sigma); 5 mM Na_3VO_4, 1 % (v/v) P9599 protease inhibitor cocktail (Sigma); 1 % (v/v) IGEPAL CA-630 (Sigma)] added. Samples were cleared by centrifugation at 16.000xg for 15 min at 4°C and adjusted to 2 mg/mL total protein concentration. Immunoprecipitations were performed on 1.5 ml total protein by adding 20 µL GFPTrap-A beads (Chromotek), 20 µl anti-HA sepharose beads (Roche), or 20 µL true-blot anti-rabbit Ig beads (Ebioscience) in combination with 15 µL antibody and incubation at 4°C for 3-4 H if not indicated otherwise. Beads were washed 4 times with TBS containing 0.5% (v/v) IGEPAL CA-630, immunoprecipitates eluted with 50 µL 2xLDS (Invitrogen) and heated at 70°C for 10 min.

2.6. Cellular biological methods

2.6.1. Confocal laser scanning microscopy

Nicotiana benthamiana leaf tissue transiently over-expressing the indicated proteins were analysed by CLSM employing the Leica SP5 Confocal Microscope (Leica Microsystems, Wetzlar, Germany). After excitation at 488 nm, eYFP emission and remaining autofluorescence were detected using the PI (>660 nm) filter set. All samples were imaged with the 40x objectives. Pictures were taken giving an average of four scans.

2.7. Antibiotics used in this study

Final concentrations of 50 μg/mL, 25 μg/mL, 100 μg/mL, 100 μg/mL and 50 μg/mL were used for kanamycin, gentamycin, carbenicillin, rifampicin and spectinomycin (all Duchefa) for bacterial cultures, respectively. For the selection of *Arabidopsis* transgenic lines, 50 μg/mL, 40 μg/mL or 10 μg/mL of kanamycin, hygromycin, or phosphinothricin (all Duchefa) respectively, were used. All antibiotic solutions were filtersterilized using 22 μm micro filter.

2.8. Media used in this study

All recipes are for the scale of 1 L.

LB

10 g tryptone, 5 g yeast extract, 10 g NaCl, pH 7.0. For solid Medium, 10g agar was included.

King's B

20 g Peptone, 1.5g Heptahydrated Magnesium Sulfate, 1.5g Potassium Hydrogen Phosphate, 10mL glycerol. pH7.0. For solid medium, 10 g

agar was included.

MS

4.3 g MS salts, 0.59 g MES, 0.1 g myo-inositol, 1 ml of 1000x MS vitamin stock, 10 g sucrose pH was adjusted to 5.7 with KOH . For solid medium, 8 g phyto-agar was included.

2.9. Primers used in this study

Table 2.7. Primers used in this study.

Primer name	5' to 3' sequence
BAK1_4_F_GT	CATGACATCATCATCATTCGC
BAK1_4_R_GT	ATTTTGCAGTTTTGCCAACAC
BKK1-1_F_GT	TGGCTCAGAAGAAAACCACAG
BKK1-1_R_GT	CTGCTCCACTTCTGTTTCCAC
BRI1-301_F_GT	CATCGAAATCTTGTGCCTCTT
BRI1-301_R_GT	GAACGTAACCCGGTGTACCA
BAK1_dCAPS_F_GT	AAGAGGGCTTGCGTATTTACATGATCAGT
BAK1_dCAPS_R_GT	GAGGCGAGCAAGATCAAAAG
EFR_KD_F	AAGTTCTGTTTCAGGGCCCGGCCAGTGATGGTAACCC ATC
EFR_KD_R	ATGGTCTAGAAAGCTTTACATAGTATGCATGTCCGTAT TTAACATC
FLS2_KD_F	AAGTTCTGTTTCAGGGCCCGGAAAATTCATCAGAGTC CTCATTACCG
FLS2_KD_R	ATGGTCTAGAAAGCTTTAAACTTCTCGATCCTCGTTAC GATC
BRI1_KD_F	AAGTTCTGTTTCAGGGCCCGGGTAGAGAGATGAGGAA GAGACG
BRI1_KD_R	ATGGTCTAGAAAGCTTTATAATTTTCCTTCAGGAACTT CTTTTATAC
BAK1_+1445_FBsmBI	CGTCTCGAATTCTGTCGTGAAAAGGGCACTAA
BAK1_nostop_R_Bam HI	GGATCCTCTTGGACCCGAGGGGTAT
BAK1_(C408Y)_F	GAGGGCTTGCGTATTTACATGATCATTACGACCCAAA GATTATTCATCGAGATGTG
BAK1_(C408Y)_R	CACATCTCGATGAATAATCTTTGGGTCGTAATGATCAT GTAAATACGCAAGCCCTC
BAK1_(D416N)_F	CCCAAAGATTATTCATCGAAATGTGAAAGCTGCAAAT ATTTTGTTG

BAK1_(D416N)_R	CAACAAAATATTTGCAGCTTTCACATTTCGATGAATAA TCTTTGGG
EFR_(D848N)_F	GACCCTGTAGCTCACTGTAATATTAAGCCAAGCAACA
EFR_(D848N)_R	TGTTGCTTGGCTTAATATTACAGTGAGCTACAGGGTC
FLS2_(D997N)_F	GGTTTTCCCATCGTTCATTGTAATCTGAAGCCAGCTAA TATACTC
FLS2_(D997N)_R	GAGTATATTAGCTGGCTTCAGATTACAATGAACGATG GGAAAACC
BRI1_(D1009N)_F	GTCCGCATATCATCCACAGAAACATGAAATCCAGTAA TGTGTTG
BRI1_(D1009N)_R	CAACACATTACTGGATTTCATGTTTCTGTGGATGATAT GCGGAC
FoxR1_Fstart	CACCATGTTGAAAGTAGAGAGTAACTGGG
FoxR1_Fstop	TCAGAATGATGGAACAATTCCATATC
FoxR1_Fnostop	GAATGATGGAACAATTCCATATC
FoxR2_Fstart	CACCATGTTGGAAGGTCTTGTCTCTCA
FoxR2_Rstop	TTAGTAATGAAAACCGAGGCTAG
FoxR2_Rnostop	GTAATGAAAACCGAGGCTAGATG
FoxR3_Fstart	CACCATGTAACAATCAGCGAGAGTTTG
FoxR3_Rstop	TCAACACCATTCGTAATGTGAA
FoxR3_Rnostop	TTTCTTCACATTACGAATGGTGT
FoxR4_Fstart	CACCATGGGGAAAGGAGGAAACTATG
FoxR4_Rstop	CTACGGAGAGGCAGAGGCA
FoxR4_nostop	CGGAGAGGCAGAGGCAG
FoxR5_Fstart	CACCATGATGAAAAGTTTGGCTAGTGC
FoxR5_Rstop	TTAGTGAGCAACACCAATTGAAG
FoxR5_Rnostop	GTGAGCAACACCAATTGAAGA
FoxR6_Fstart	CACCATGGCTGAAACATCTGATGTATCG
FoxR6_Rstop	CTACATGAACAGCTCAGACTGCAG
FoxR6_Rnostop	CATGAACAGCTCAGACTGCAGC
FoxR7_Fstart	CACCATGGGAGTGTCAAAGAAGAAATC
FoxR7_Rstop	TCAAACGTAGATTGAAGAACACG
FoxR7_Rnostop	AACGTAGATTGAAGAACACGAGA
FoxR8_Fstart	CACCATGTCGACTTTGGAATCTCCAT
FoxR8_Rstop	TTAGACACATGCCGCCGTTA
FoxR8_Rnostop	GACACATGCCGCCGTTACTAG
FoxR9_Fstart	CACCATGGCGTCAAGGAAGCTTTT
FoxR9_Rstop	CTAATCCTGAAACCCAATCTTCTC
FoxR9_Rnostop	ATCCTGAAACCCAATCTTCTCC
FoxR10_Fstart	CACCATGGATTCAAATAATCATCTCTACG
FoxR10_Rstop	CTATATTGACTTCTTCTCCTTGTTCATA
FoxR10_Fnostop	TATTGACTTCTTCTCCTTGTTCATACA

FoxR11_Fstart	CACCATGGTAATGGAAACAGAGTCAAAGT
FoxR11_Rstop	TCAGACCGAGGTTGTGATATCA
qFRK1_F	ATCTTCGCTTGGAGCTTCTC
qFRK1_R	TGCAGCGCAAGGACTAGAG
qAt1g51890_F	CCAGTTTGTTCTGTAATACTCAGG
qAt1g51890_R	CTAGCCGACTTTGGGCTATC
qAt2g17740_F	TGCTCCATCTCTCTTTGTGC
qAt2g17740_R	ATGCGTTGCTGAAGAAGAGG
qAt5g57220_F	AATGGAGAGAGCAACACAATG
qAt5g57220_R	ATACTGAGCATGAGCCCTTTG
qAt2g46400_F	TCAACCAAGACAAGAACAT
qAt2g46400_R	GTTCTCAATCTCATGGTTAG
qUBQ10_F	AGATCCAGGACAAGGAGGTATTC
qUBQ10_R	CGCAGGACCAAGTGAAGAGTAG
qAt1g80460_F	GCTGCTCCTAATGCTGTTGTC
qAt1g80460_R	GATTCAGGCTGATCTGATGG
qAT5G15400_R	TGCGCTGCCAGATAATACACTATT
qAT5G15400_R	TGCTGCCCAACATCAGGTT
qSAUR-ACI_F	GAGGATTCATGGCGGTCTATG
qSAUR-ACI_R	GTTAAGCCGCCCATTGGAT
qEXP8_F	CAACCATCACCGTCACAGCTA
qEXP8_R	TGAAGAGGAGGATTGCACCAA

Chapter 3: FOX-hunting for novel regulators of PTI signalling

3.1. Objectives

Several lines of evidence suggest the presence of a negative regulatory signalling network controlling plant defence. Firstly, treatment of tomato suspension cell cultures with the broad spectrum phosphatase inhibitor calyculin A mimics the medium alkalinisation and change in phosphorylation pattern induced by xylanase (Felix et al., 1994), leading to the hypothesis that PTI signalling is under constant negative regulation by phosphatases. Secondly, treatment with the protein synthesis inhibitor cyclohexamide (CHX) elicits similar gene expression as seedlings treated with flg22 (Navarro et al., 2004), suggesting the presence of unstable negative regulators, which are rapidly degraded after defence elicitation. Thirdly, PAMP treatment induces the expression of several transcription factors that have been shown to negatively regulate PTI signalling (Shen et al., 2006; Xu et al., 2006; Journot-Catalino et al., 2006). Lastly, it became a paradigm that plant hormones de-repress signalling pathways that are normally constitutively suppressed (Berleth et al., 2004; Vert et al., 2005; Raghavendra et al., 2010). At the beginning of this study only few negative regulators of PTI signalling were known in *Arabidopsis*. One is the kinase-associated protein phosphatase (KAPP), which negatively regulates many different RLKs (Gomez-Gomez et al., 2001; Ding et al., 2007). However its specific role in PTI signalling is unclear. Further downstream several WRKY transcription factors negatively regulate basal resistance against biotrophic and hemibiotrophic pathogens (Shen et al., 2006; Xu et al., 2006; Journot-Catalino et al., 2006). Comparatively, in animal innate immunity many negative regulators are known ranging from Toll-like receptor homologs, inactive signalling molecule mimetics, phosphatases, to ubiquitin ligases and lyases (Liew et al., 2005). I therefore hypothesized the existence of additional unknown negative regulators of PTI signalling in *Arabidopsis*. In order to identify such negative regulators I followed two independent approaches. Both are based on the assumption that the constitutive over-expression of a negative regulator leads to insensitivity to the applied stimulus.

This approach was previously successfully used to identify negative/positive regulators of ABA signalling or salt stress/tolerance such as *AtPP2CA* or *OST1/2*, respectively (Kuhn et al., 2006; Conti et al., 2008).

For the forward genetic approach I went to RIKEN Plant Science Centre Yokohama (Japan) to screen the **F**ull-length cDNA **O**ver-e**X**pressing gene (FOX) hunting system library (Ichikawa et al., 2006) for lines that lost elf18 or flg22-induced seedling growth inhibition (SGI). In this FOX system, a normalized full-length *Arabidopsis* cDNA library containing initially over 15,000 independent cDNAs under the control of the constitutive CaMV (cauliflower mosaic virus) 35S promoter was transformed into *Arabidopsis* plants. On average 2.6 cDNA clones are integrated in each individual plant representing 1.2 independent cDNAs (Ichikawa et al., 2006). This library was chosen due to several potential advantages; (i) the identity of the over-expressed gene(s) can be obtained easily by PCR sequencing using vector-specific primers and (ii) lines showing intermediate phenotypes can be re-screened easily within the same generation.

The reverse genetic approach was based on the hypothesis that genes commonly down-regulated by several PAMPs are potential negative regulators of PTI signalling. Transcription profile analyses identified 15 genes down-regulated after elf18, flg22, and chitin treatment of *Arabidopsis* seedlings (Zipfel et al., 2004; Wan et al., 2007). Eleven of those were screened for loss of flg22-triggered ROS-burst after transient over-expression in *N. benthamiana*.

These two independent approaches identified eleven candidate genes with potential regulatory function in PTI signalling. Interestingly, several of these candidates are implicated in chloroplastic ROS homeostasis or signalling. However, no clear link between previously published chloroplastic ROS homeostasis signalling mutants and PTI signalling could be observed.

3.2. Results and Discussion

3.2.1. Identification of potential regulators of PTI signalling in a forward genetic screen using the FOX-hunting system library

I performed the forward genetic screen using the FOX-hunting system (Ichikawa et al., 2006) during a short-term stay at the RIKEN Plant Science Centre, Yokohama

FOX line	ATG number	Description of encoded protein
FOXF1	*At2g28190*	chloroplastic copper/zinc superoxide dismutase CSD2
FOXF2	*unknown*	n.a.
FOXF3	*unknown*	n.a.
FOXF4	*At1g09310*	protein of unknown function
FOXF5	*unknown*	n.a.
FOXF6	*At3g53950*	glyoxal oxidase-related protein
FOXF7	*At3g03630*	O-acetylserine (thiol-) lyase
FOXF8	*At1g03600*	Psb27
FOXF9	*unknown*	n.a.
FOXF10	*At4g38620*	MYB4
FOXF12	*unknown*	n.a.
FOXF13	*At1g53840*	encodes a pectin methylesterase
FOXF14	*At3g23920*	BMY7
FOXF16	*unknown*	n.a.
FOXF17	*unknown*	n.a.
FOXF18	*At1g18260*	suppressor of lin-12-like protein-related / sel-1 protein-related
FOXF19	*At1g73190*	alpha-tonoplast intrinsic protein
FOXF20	*At2g22240*	inositol-3-phosphate synthase isozyme 2
FOXF21	*At2g30750*	CYP71A12
FOXF22	*unknown*	n.a.
FOXF23	*At4g02620*	vacuolar-type H+-ATPase subunit F
FOXF24	*unknown*	n.a.
FOXF25	*At4g00030*	plastid-lipid associated protein PAP
FOXF26	*At5g24430*	CRK4
FOXF27	*At3g08860*	alanine--glyoxylate aminotransferase
FOXF28	*At5g01970*	protein of unknown function
FOXF29	*At5g13520*	peptidase M1 family protein
FOXF30	*At1g04630*	MEE4
FOXF31	*At2g19810*	putative CCCH-type zinc finger protein
FOXF34	*At3g07390*	AIR12
FOXF35	*unknown*	n.a.
FOXF36	*unknown*	n.a.
FOXF37	*At1g27690*	protein of unknown function
FOXF38	*At3g53180*	glutamate-ammonia ligase
FOXF39	*At1g06890*	transporter-related protein
FOXF40	*unknown*	n.a.
FOXF41	*At1g10200*	putative transcription factor
FOXF42	*At1g07890*	cytosolic ascorbate peroxidase
FOXF43	*At1g74920*	aldehyde dehydrogenase

Table 3.1. 39 FoxF candidate lines after two successive rounds of screening.
Uncoloured, yellow, and blue underlined rows indicate *FoxF* lines identified in the flg22-induced SGI assay, elf18-induced SGI assay or in both, respectively. n.a. not available

(Japan). I screened approximately 12,000 individual T2 lines for reduced sensitivity to elf18- or flg22-induced SGI. In the first round the SGI of 12-14 day-old seedlings in the presence of 50 nM elf18 or 65 nM flg22 was compared qualitatively with wild-type or respective receptor mutant control. Three replicates per treatment and line were used. In this initial screen I identified 150 potential candidates. All candidate lines were re-screened in the same generation (T2) using eight replicates per treatment confirming 39 lines (Table 3.1). None of these lines showed a total PAMP insensitivity. The inserted gene was initially identified by database searches and later confirmed by PCR and sequence analysis of genomic DNA using vector-specific primers (Table 3.1). This was clearly an advantage of the Fox-hunting system and the corresponding candidates are called *FoxF* (F for forward). We requested these 39 T2 lines from RIKEN, Yokohama, in order to re-screen them more quantitatively upon my return to The Sainsbury Laboratory. Unfortunately, I did not obtain many T2 seeds for these 39 candidates and had to progress one generation for seed amplification. I therefore isolated individual antibiotic resistant T2 transformants. For every candidate identified in the T2 generation (Table 3.1) I measured the responsiveness of three independent T3 progeny lines in the flg22- or

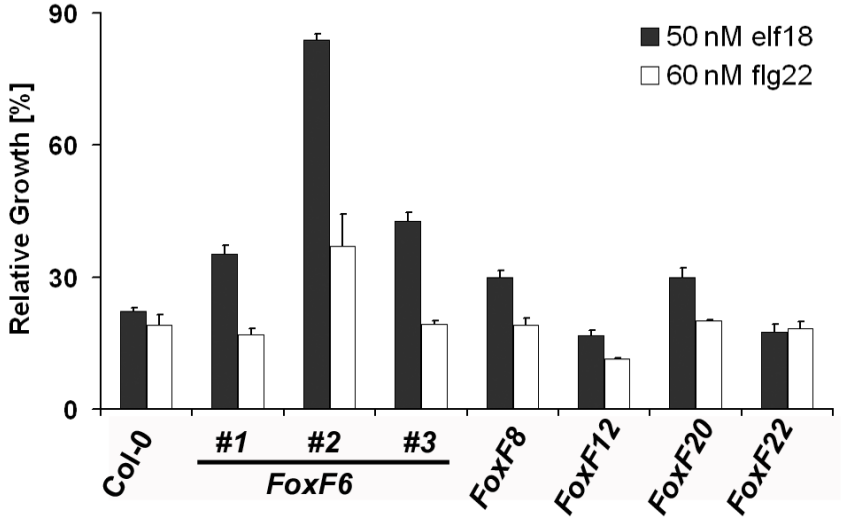

Figure 3.1. Three *FoxF6* T3 lines are partially insensitive to PAMP-induced SGIA.
SGI of Col-0, *FoxF6* #1-3, *FoxF8*, *FoxF12*, *Fox20* and *FoxF22* in the presence of either 50 nM elf18 or 65 nM flg22. Fresh weight is represented relative to untreated control. Results are average ± s.e (n=6).
This is a representative graph for the T3 re-screening process of all 39 *FoxF* candidate lines. For candidates with responsiveness similar to Col-0 the result of only one T3 line is shown.

elf18-induced SGI assay. An illustration thereof is shown in Figure 3.1. The candidate line *FoxF6*, but not *FoxF8*, *FoxF12*, *FoxF20* and *FoxF22,* was confirmed in the T3 generation (Figure 3.1). Using this approach I could confirm seven candidates in the T3 generation (Table 3.2). In addition I included *FoxF1* and *FoxF8* for further characterization as they showed the strongest phenotype in the T2 but loss thereof in the T3 generation (Figure 3.1 and data not shown). Interestingly, relative high genomic instability through generations was reported for this FOX-hunting system library (Minami Matsui, personal communication). It is therefore conceivable that the expression of the corresponding gene was silenced in the T3 generation leading to the loss of the previous observed phenotype. To demonstrate the causative role of the *FoxF* candidate, optimally, I should have performed expression analysis of the inserted gene in combination with linkage analysis using a backcross to Col-0 or segregation analysis in subsequent generations. However, I did not work further with the original Fox lines due to several known disadvantages such as multiple insertions and gene-silencing over generations. Alternatively, I intended to test all candidates by independent re-transformation and phenotyping of independent over-expression lines. For this purpose I amplified the full-length coding sequence of all identified *FoxF* genes (Table 3.2) and cloned them under the *35S* promoter in a binary vector. I created one clone without epitope tag and one

FOX line	Atg number	Description
FOXF1	*At2g28190*	CSD2 copper zinc dismutase
FOXF6	*At3g53950*	glyoxal oxidase-related protein
FOXF8	*At1g03600*	Psb27, repair cycle of the D1
FOXF13	*At1g53840*	pectin methylesterase
FOXF18	*At1g18260*	suppressor of lin-12-like protein-related / sel-1 protein-related
FOXF25	*At4g00030*	plastid-lipid associated protein PAP
FOXF31	*At2g19810*	putative CCCH-type zinc finger protein
FOXF37	*At1g27690*	protein of unknown function
FOXF38	*At3g53180*	glutamate-ammonia ligase

Table 3.2. Table of final nine *FoxF* lines identified after three rounds of screening.
Green underlined rows indicate *FoxF* lines carrying gene insertions coding for proteins with shown or predicted chloroplastic localization

clone with C-terminal *YFP-HA* tag for future localization studies. In parallel I ordered publicly available T-DNA insertion lines for all candidates and of up to three closest homologs from stock centres. I genotyped individual plants by PCR to identify homozygous insertion mutants and started to investigate the transcript level

of the corresponding genes by RT-PCR (data not shown). However, due to time limitation I was not able to progress beyond this stage in the project.

3.2.2. Initial phenotypic analysis of a small mutant collection in genes related to plastidic ROS signalling and homeostasis

Interestingly, the cDNA within the T-DNA insertion fragments of five out of these eight candidates encoded for proteins that are known or predicted to localize to the chloroplasts (Table 3.2). Most of those are related to ROS signalling or homeostasis. For example, *Psb27* (*FoxF8*) was previously shown to be involved in the repair cycle of the D1 the major subunit of the photosystem II (PS II) reaction centre (Chen et al., 2006; Nowaczyk et al., 2006). It is believed that singlet-oxygen is generated through energy transfer from excited chlorophyll to oxygen at the reaction centre of PS II (Kim et al., 2008). As D1 is one of the most highly turned-over proteins in plants, inhibition of the repair mechanism could lead to the generation of excessive energy, photo-inhibition and generation of increased amounts of singlet oxygen (Apel and Hirt, 2004). We therefore requested mutants impaired in singlet oxygen signalling such as *ex1 (executer 1), ex2* and *ex1/2* (Lee et al., 2007). *CSD2* (*CuZn-superoxide dismutase 2*) (*FoxF1*) is involved in the dissipitation of excessive energy promoted by the water-water cycle in the chloroplasts (Asada, 1999). It catalyzes the conversion of superoxide anions to hydrogen peroxide and is required for normal plant development as *csd2* null mutants are lethal (Rizhsky et al., 2003). It is also noteworthy that CSD2 is upregulated post-transcriptionally by compatible pathogens (Navarro et al., 2008) and chloroplastic hydrogen peroxide antagonizes singlet oxygen signalling (Laloi et al., 2006). We therefore requested *CSD2* over-expression lines (Myouga et al., 2008).

First, I performed flg22- and elf18-induced SGI assays, but no difference was observed for any of the mutant or over-expression lines (Figure 3.2 A-B). Similarly, no difference was observed for ROS-burst either induced by flg22 or chitin (Figure 3.2 C-D). Finally, I performed spray-infection assays with *Pto* DC3000 and *Pto* DC3000 *Cor*$^{-}$, that is not able to produce coronatine (Melotto et al., 2006). I

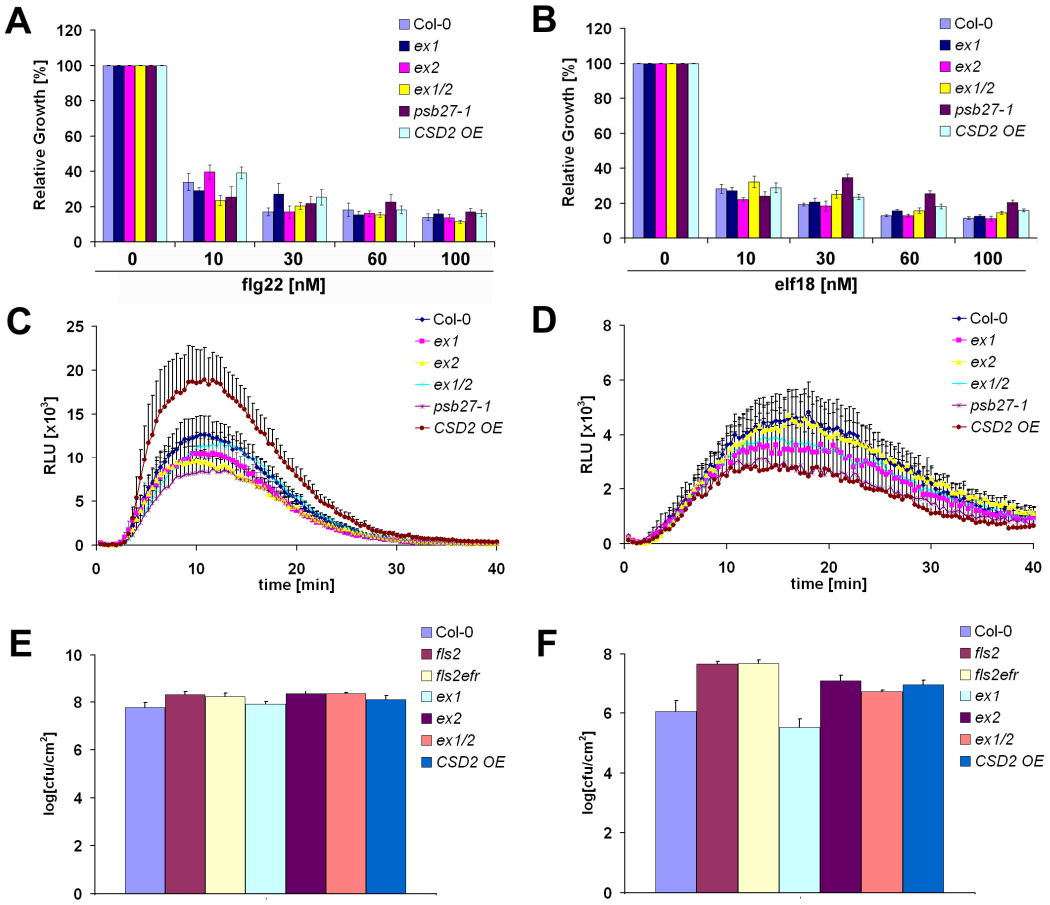

Figure 3.2. Mutants in chloroplastic ROS-production or signalling are not impaired in PTI-signalling but compromised in defence to bacterial pathogens.

A. SGI of Col-0, *ex1*, *ex2*, *ex1/2*, *psb27-1* and *CSD2* OE in the presence of the indicated concentration of flg22. Fresh weight is represented relative to untreated control. Results are average ± s.e (n=6).

B. SGI of Col-0, *ex1*, *ex2*, *ex1/2*, *psb27-1* and *CSD2* OE in the presence of the indicated concentration of elf18. Fresh weight is represented relative to untreated control. Results are average ± s.e (n=6).

C. ROS burst in leaves of Col-0, *ex1*, *ex2*, *ex1/2*, *psb27-1* and *CSD2* OE induced by 100 nM flg22. Fresh weight is represented relative to untreated control. Results are average ± s.e (n=6).

D. ROS burst in leaves of Col-0, *ex1*, *ex2*, *ex1/2*, *psb27-1* and *CSD2* OE induced by 500 µg/ml chitin. Fresh weight is represented relative to untreated control. Results are average ± s.e (n=6).

E. Four-week-old plants (Col-0, *fls2, fls2 efr, fls2 ex1*, *ex2*, *ex1/2* and *CSD2* OE) were spray-inoculated with *Pto* DC3000 (OD_{600}= 0.02).

F. Four-week-old plants (Col-0, *fls2, fls2 efr, fls2 ex1*, *ex2*, *ex1/2* and *CSD2* OE) were spray-inoculated with *Pto* DC3000 *Cor*$^-$ (OD_{600}= 0.2).

Bacterial counts were carried out at 3 days post-inoculation (3 dpi). Results are average ± s.e. (*n*=4).

performed up to six independent infections for each strain and the results between experiments were variable to a certain degree. A description of the general tendency observed for each mutant is given.

The *psb27-1* and *ex1/2* mutant plants were as susceptible as WT (Figure 3.2 E-F and data not shown). *Ex2* mutants were more susceptible to *Pto* DC3000 in 4 out of 6 independent experiments and more strikingly to *Pto* DC3000 *Cor*$^-$ in 3 out of 3 experiments (Figure 3.2 E- F). *CSD2* over-expression lines were more susceptible in 2 out of 4 experiments (*Pto* DC3000) and 2 out of 3 experiments (*Pto* DC3000 *Cor*$^-$). On the contrary *ex1* was more resistant especially to *Pto* DC3000 in 3 out of 6 experiments (Figure 3.2 E-F). This suggests that these genes are implicated in the defence response as such, even though these mutants or over-expression lines are not impaired in PTI-signalling measured as PAMP-induced ROS-burst or SGI. Interestingly, singlet oxygen was previously shown to rapidly induce SA production and to partially require EDS1 for signalling (Ochsenbein et al., 2006). In addition, in tobacco chloroplastic-generated ROS plays an important role in cell-death induced by over-expression of the constitutive active *NtMEK2*^{DD} or by the non-host pathogen *Xanthomonas campestris pv. vesicatoria* (Liu et al., 2007; Zurbriggen et al., 2009). The change in disease resistance observed in *ex1, ex2* and *CSD2* OE lines could therefore, be potentially explained by differential activation of ETI responses triggered by weakly recognized effectors.

3.2.3. Reverse genetic approach to identify potential PTI-signalling regulators using transient over-expression in *N. benthamiana*

I hypothesised that genes down-regulated by several PAMPs could represent negative regulators of PTI-signalling. Analysis of publicly available micro-array data identified 15 genes down-regulated at either 30 or 60 min after treatment with flg22, elf18 or chitin (Zipfel et al., 2006; Wan et al., 2008). We focused our efforts on genes that were not implicated in auxin signalling as the research group of Prof. Jonathan Jones (The Sainsbury Laboratory) was working on the hormonal aspect of plant defence signalling (Navarro et al., 2006; Robert-Seilaniantz et al., 2007). The

FOX line	ATG number	Description of encoded protein
FoxR1	*At5g15850*	COL1 (CONSTANS-LIKE 1)
FoxR2	*At2g18300*	basic helix-loop-helix (bHLH) family protein
FoxR3	*At2g12290*	similar to protein binding / zinc ion binding
FoxR4	*At5g24660*	protein of unknown function
FoxR5	*At1g68520*	zinc finger (B-box type) family protein
FoxR6	*At1g26920*	protein of unknown function
FoxR7	*At3g59940*	kelch repeat-containing F-box family protein
FoxR8	*At5g20790*	protein of unknown function
FoxR9	*At5g03230*	protein of unknown function
FoxR10	*At2g42280*	basic helix-loop-helix (bHLH) family protein
FoxR11	*At2g41310*	ATRR3 (RESPONSE REGULATOR 3)

Table 3.3. The eleven *FoxR* genes commonly down-regulated by efl18, flg22 and chitin.

resulting eleven genes were called *FoxR1* to *11* (R for reverse) (Table 3.3). I amplified the full length coding sequence of each *FoxR* gene and cloned it under the *35S* promoter. I created one clone without epitope tag and one clone with C-terminal *YFP-HA* tag for potential localization studies. To test their possible involvement in PTI signalling I transiently over-expressed all eleven genes with and without C-terminal fusion tag in *N. benthamiana.* I investigated the impact of the over-expressed gene on PAMP-induced ROS-burst production 3 dpi (days-post infiltration). The expression of the tagged variants were verified by Western-blot analysis (data not shown). After several rounds of screening I could identify three genes that influenced PAMP-induced ROS-burst consistently in several independent experiments. The over-expression of the two bHLH transcription factors *FoxR2* and *FoxR10* increased the flg22-induced ROS-burst production compared with the negative control *GUS:YFP-HA* as shown for *FoxR10* in Figure 3.3 A. In contrast, over-expression of *FoxR9* lead to a dramatic reduction in flg22-induced ROS-production (Figure 3.3 B). Interestingly, *FoxR2* is closely related to three paralogous transcription factors, *BEE* (*BR enhanced expression*) 1-3, that together positively regulated BR responses (Friedrichsen et al., 2002). Additionally, plants over-expressing *BEE1* are not only BR hypersensitive but also show a reduced responsiveness to exogenous ABA application (Friedrichsen et al., 2002). *FoxR2* might be potentially involved in hormone signalling and thereby influence PTI signalling.

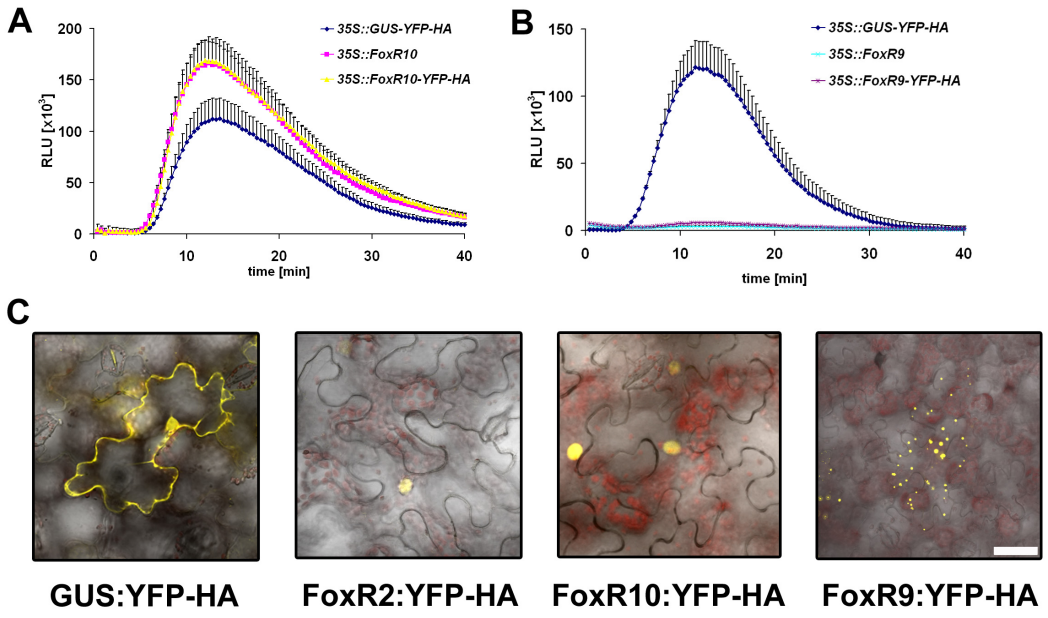

Figure 3.3. Three *FoxR* genes influence flg22-induced ROS burst and localize to distinct sub-cellular locations after transient over-expression in *N. benthamiana*.

A. The over-expression of *FoxR10* leads to enhanced flg22-induced ROS-burst in *N. benthamiana*. ROS burst in leaves of *N. benthamiana* transiently over-expressing *GUS:YFP-HA*, *FoxR10* or *FoxR10:YFP-HA* induced by 100 nM flg22 at 3 dpi. Results are average ± s.e. (n=8).

B. The over-expression of *FoxR9* leads to the abolishment of flg22-induced ROS-burst in *N. benthamiana*. ROS burst in leaves of *N. benthamiana* transiently over-expressing *GUS:YFP-HA*, *FoxR9* or *FoxR9:YFP-HA* induced by 100 nM flg22 at 3 dpi. Results are average ± s.e. (n=8).

C. FoxR2:YFP-HA and FoxR10:YFP-HA localized to the nucleus whereas FoxR9:YFP-HA aggregates in "vesicle-like" structures after transient over-expression. Confocal images of *N. benthamiana* leaves 2 dpi transiently over-expressing *GUS:YFP-HA*, *FoxR2:YFP-HA*, *FoxR10:YFP-HA* or *FoxR9:YFP-HA*, respectively. Scale bar represents 50 µm.

I also investigated the localization of the C-terminal YFP-HA fusion proteins after transient over-expression in *N. benthamiana* (Figure 3.3 C). As expected FoxR2:YFP-HA and FoxR10:YFP-HA localized to the nucleus whereas the GUS:YFP-HA control was distributed between nucleus and cytoplasm. Surprisingly, FoxR9:YFP-HA seemed to localize to "vesicle-like" structures forming aggregates (Figure 3.3 C). The expression of full length fusion protein was confirmed by Western blot analysis (data not shown) indicating that the protein was not degraded. For further analysis I created stable transgenic over-expressing lines. In addition, I ordered publicly available T-DNA insertion lines for all three candidates and up-to three closest homologs from stock centres. I genotyped by PCR individual plants to

identify homozygous insertion mutants and started to investigate the transcript level of the corresponding gene by RT-PCR (data not shown). However, due to time limitation I was not able to progress beyond this stage in the project.

3.1.4. Initial phenotypic characterization of *FoxR9* and its three closest homologs using the transient over-expression system *N. benthamiana*

FoxR9 is part of a plant-specific 13-member gene family in Arabidopsis, which is characterized by the Pfam protein domain DUF584. FoxR9 forms an out-group with its three closest homologs FoxR9-H1 (At5g60680.1), FoxR9-H2 (At2g28400.1) and FoxR9-H3 (At3g45210.1) (Figure 3.4 A). They are highly conserved showing up to 60% identity at the amino acid level (Figure 3.4 B). I therefore tested if transient over-expression of any of these close homologs could interfere with flg22-induced ROS-burst in *N. benthamiana*. Indeed the over-expression of any of the three homologs was able to suppress the flg22-induced ROS-burst (Figure 3.4 C). Similar to FoxR9:YFP-HA also the C-terminal YFP-HA fusion proteins of its three closest homologs accumulated in "vesicle-like" aggregates (Figure 3.4 D). The expression of full length fusion protein was confirmed by Western blot analysis (data not shown) indicating that the protein is not degraded. Finally, I tested if the abolished ROS-burst after transient over-expression of *FoxR9* correlates with compromised resistance of *N. benthamiana* to bacteria. To this end I syringe-infiltrated water or *Agrobacterium*-suspensions carrying plasmids coding for *FoxR9:YFP-HA* or as negative control *GUS:YFP-HA*. The following day, leaves were spray-infected with either *P. syringae pv. tabaci* 11528 or *P.syringae pv. syringae* B728a. Interestingly, the pre-infiltration with *Agrobacterium* on its own seemed to induce defence responses leading to enhanced resistance as leaves expressing *GUS:YFP-HA* were more resistant to both compatible pathogens at 2 dpi (day-post infection) (Figure 3.4 E). Nevertheless, both bacterial strains were more virulent on leaves expressing *FoxR9:YFP-HA* compared to leaves expressing *GUS:YFP-HA* control (Figure 3.4 E).

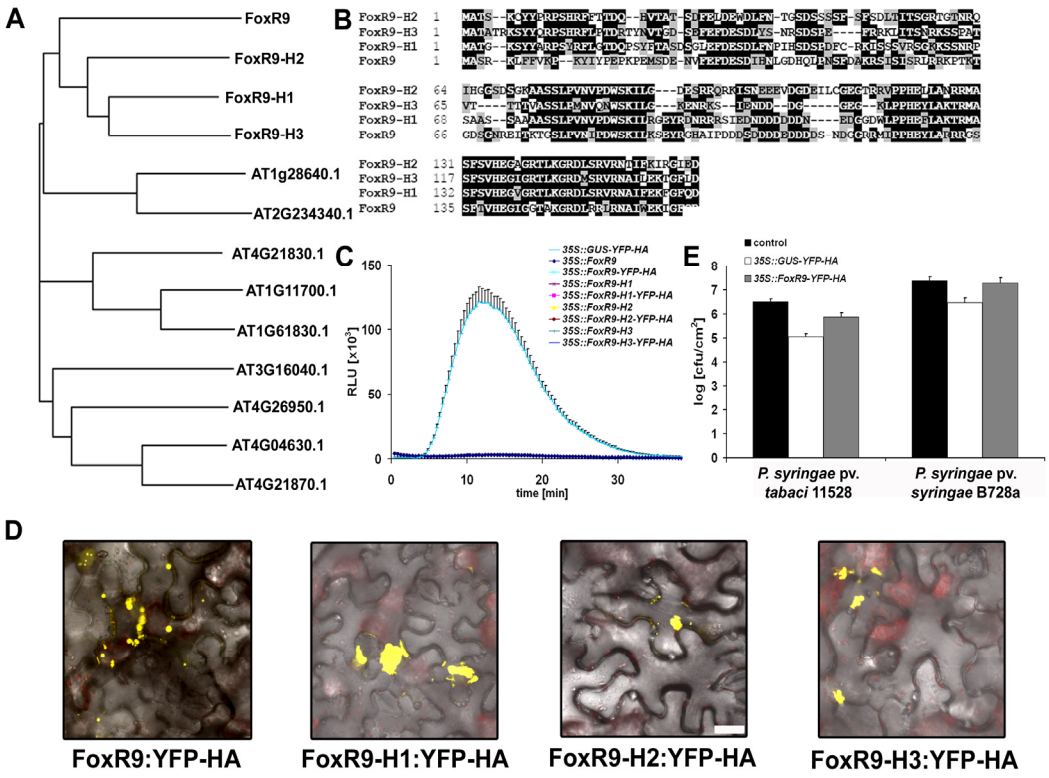

Figure 3.4. *FoxR9* and its closest homologs suppress plant defences after transient over-expression in *N. benthamiana.*

A. FoxR9 forms an out-group with its three closest homologs. Phylogenetic tree of FoxR9 and its twelve homologs in Arabidopsis.

B. FoxR9 and its three closest homologs are highly conserved especially in the C-terminus part. Alignment of FoxR9 and its three closest homologs.

C. FoxR9 and its closest homologs suppress PAMP-induced ROS-burst after transient over-expression in *N. benthamiana*. ROS burst in leaves of *N. benthamiana* transiently over-expressing *GUS:YFP-HA*, *FoxR9* or *FoxR9:YFP-HA, FoxR9-H1*, *FoxR9-H1:YFP-HA, FoxR9-H2*, *FoxR9-H2:YFP-HA, FoxR9-H3* or *FoxR9-H3:YFP-HA* induced by 100 nM flg22 at 3 dpi. Results are average ± s.e. (n=8).

D. FoxR9:YFP-HA FoxR9-H1:YFP-HA, FoxR9-H2:YFP-HA and FoxR9-H3:YFP-HA aggregate in "vesicle-like" structures after transient over-expression. Confocal images of *N. benthamiana* leaves 2 dpi transiently over-expressing *FoxR9:YFP-HA, FoxR9-H1:YFP-HA*, *FoxR9-H2-YFP-HA* or *FoxR9-H3-YFP-HA*, respectively. Scale bar represents 25 µm

E. Over-expression of *FoxR9:YFP-HA* leads to increased susceptibility of *N. benthamiana* to two adapted bacterial pathogens. Leaves expressing the indicated construct were spray-infected with either *P. syringae pv. tabaci* 11528 or *P. syringae pv. syringae* B728a and sampled 2 dpi. See text for experimental details.

Bacterial counts were carried out at 3 days post-inoculation (3 dpi). Results are average ± s.e. (*n*=4).

This shows that the over-expression of *FoxR9* in *N. benthamiana* blocks defence signalling and leads to an enhanced susceptibility to two adapted bacterial pathogen. As the effect of three FoxR9 homologs on ROS production was similar to that of FoxR9, it is tempting to speculate that some of these proteins fulfil a similar and partial redundant role in PTI-signalling. However, all conclusions are based on results obtained after transient over-expression of Arabidopsis genes in *N. benthamiana*. Therefore further studies in *Arabidopsis* are needed to investigate the potential role of *FoxR9* and its close homologs in PTI signalling.

Chapter 4: *bak1-5*, a novel *BAK1* allele, strongly impaired in PTI signalling and plant defence

4.1. Objectives

PAMP-triggered immunity is often described as the first layer of plant defence. In recent years some progress has been made in the elucidation and characterization of molecular events immediately downstream of ligand-binding to the corresponding PRR (Boller and Felix, 2009). However when I started my PhD only very few PRRs and even less immediate downstream signalling components were known (Schwessinger and Zipfel, 2008). In *Arabidopsis*, the only three known PRRs were FLS2, EFR and potentially CERK1 (Zipfel, 2008). It was recently shown that BAK1 interacts with FLS2 in a ligand-dependent manner and that it is required for late and early flg22-triggered responses (Heese et al, 2007; Chinchilla et al., 2007). Furthermore, *bak1* T-DNA insertion mutant alleles were known to be impaired in early but not late elf18-triggered responses, such as elf18-induced SGI (Chinchilla et al., 2007). A MAP-kinase cascade including MPK 3, 4 and 6 was known to be downstream of elf18, flg22 and chitin perception regulating a common core set of PTI-induced and -repressed genes (Schwessinger and Zipfel, 2008). In addition, several WRKY transcription factors were shown to be implicated in this transcriptional reprogramming. In order to elucidate novel signalling components or regulators we performed a forward genetic screen using the well described elf18-induced SGI (Nekrasov et al., 2009). Within this screen we identified a unique mutant being strongly impaired in both flg22 and elf18-triggered SGI.

Here, I show that *elfin 27-6* is a novel allele of *BAK1* harbouring a single mis-sense substitution in the 10th exon. First I demonstrate that the mutation within the coding region of *BAK1* is causative for the observed SGI phenotypes using a combined approach of reconstitution in the null mutant background and allelism tests. In a detailed phenotypic characterization using the back-crossed mutant I show that *bak1-5* is compromised in all early and late responses triggered by elf18 and flg22 tested. This strong impairment in PTI signalling leads to enhanced susceptibility to

bacterial pathogens. Next, I demonstrate the importance of *BKK1*, the closest homologe of *BAK1*, in PTI signalling. The novel *bak1-5 bkk1-1* double mutant is more strongly impaired in flg22- and elf18-triggered PTI signalling then either single mutant. This strong impairment in PTI signalling leads to enhanced susceptibility to bacterial pathogens and biotrophic oomycetes. Overall, my results suggest that *BAK1* and *BKK1* play a partially redundant role in PTI signalling of known and yet unknown PRRs.

4.2. Results

4.2.1. Identification of *elfin27-6*, an elf18- and flg22-insensitive mutant

In order to discover new PTI signalling components, in collaboration with several other lab members I performed a forward genetic screen using a Col-0 EMS (ethyl-methanesulfonate) mutagenised population. On wild-type seedlings elf18 normally triggers severe growth retardation (Zipfel et al., 2006). However, mutants of the corresponding receptor EFR, of the protein folding and maturation machinery (Haweker et al., 2010; Li et al., 2009; Lu et al., 2009; Nekrasov et al., 2009; Saijo et al., 2009; von Numers et al., 2010) or of signalling components are impaired in this inhibition and identified as bigger seedlings. After three reiterative rounds of screening and identification of *EFR* mutant alleles by sequence analysis, I identified a single mutant allele out of 103 non-*efr elfin* mutants that was not only impaired in elf18-triggered SGI but also totally insensitive to flg22 (Figure 4.1 A). Importantly, this mutation was not specific to the SGI assay as both elf18- and flg22-triggered ROS burst was also strongly impaired in *elfin27-6* (Figure 4.1 B). Next, we went on to determine if the observed phenotype was due to a single mutation event. For this purpose we analysed the F2 segregating population of a Col-0 x *elfin27-6* cross using SGI triggered by concomitantly application of 50 nM elf18 and 50 nM flg22. At these peptide concentrations, 24 out of 98 seedlings displayed an enhanced growth phenotype suggesting a single recessive causative mutational event.

Furthermore, this suggests a mutation in an important component shared between both EFR- and FLS2- dependent signalling pathways.

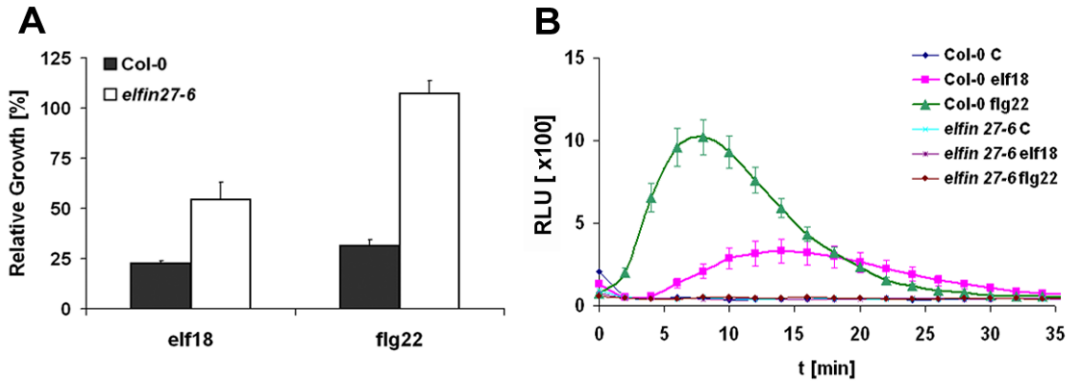

Figure 4.1. *elfin27-6* is strongly impaired in FLS2- and EFR-dependent PTI signalling.

A. *elfin27-6* is impaired in seedling growth inhibition triggered by 60 nM elf18 or flg22. Fresh weight is represented relative to untreated control. Results are average ± s.e (n=6).

B. *elfin27-6* is strongly impaired in the ROS-burst triggered by 100 nM elf18 or 100 nM flg22. Results are average ± s.e (n=8). [c = water control]

4.2.2. Map-based cloning of *elfin 27-6*

I chose a map-base cloning approach to identify the causative mutation in *elfin27-6*. Therefore, I generated a mapping population by crossing *elfin 27-6* with L*er*-0. I screened a segregating F2 population in SGI assay using 100 nM elf18, a concentration at which both Col-0 and L*er*-0 displayed severe growth retardations compared to *elfin27-6*. At this high peptide concentration *elfin27-6* segregated as a single recessive locus. Rough-mapping on 20 elf18-insensitive individuals combined with bulk segregant analysis linked the mutation to the molecular marker CER451534 on the lower arm of Chromosome IV. I generated a bigger mapping population for high resolution mapping, which confirmed initial results and located the mutation 4.2 cM south of CER451534 (Figure 4.2 A). *BAK1* (*At4g33430*) is located in close proximity to the identified location and bak1 mutants were known to be impaired in flg22-, but not elf18-induced SGI (Chinchilla et al., 2007). Therefore *BAK1* was a prime candidate for targeted sequence analysis. Indeed sequencing of the whole genomic locus of *BAK1* identified a single mis-sense substitution in the

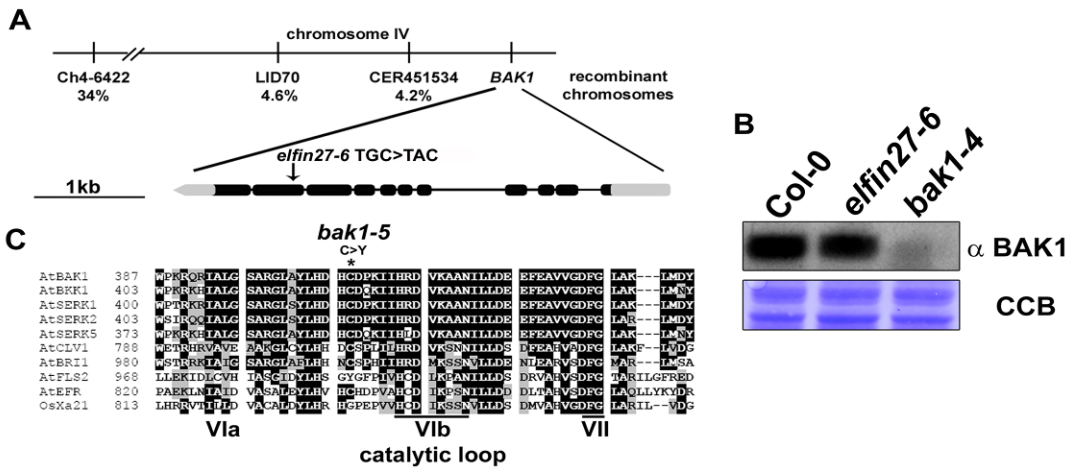

Figure 4.2. *elfin27-6* is *bak1-5*, a novel allele of BAK1.

A. *elfin27-6* carries a single mis-sense mutation in the 10th exon of *BAK1*. Schematic representation of relative marker positions and observed recombination rates in a L*er*-0 x *elfin27-6* F2 mapping population.

B. BAK1-5 accumulates to wild-type levels. Immunoblot of total protein from Col-0, *elfin27-6* and *bak1-4* using anti-BAK1 antibody. Immunoblot, upper panel; Coomassie colloidal blue stained membrane, lower panel.

C. The Cys408 residue mutated in BAK1-5 mutated is conserved in all AtSERK family members but not in all RLKs. Alignment of kinase subdomains VIa, VIb and VII of AtSERKs, AtBRI1, AtCLV1, AtFLS2, AtEFR and OsXA21. The star indicates the Cys to Tyr change in BAK1-5.

10th exon. The guanine at position 1223 of the coding sequence was exchanged with an adenine (Figure 4.2 A), which represents the most commonly observed substitution for EMS mutagenesis (Kohalmi and Kunz, 1988). Next we tested whether this missense mutation affected the accumulation of the BAK1 protein in *elfin27-6* plants. To this end, we performed immunoblot analysis using anti-BAK1 antibodies on total protein extracts from Col-0, *elfin27-6* and *bak1-4*, a previously described T-DNA insertion null allele (Chinchilla et al., 2007). Full length mutant BAK1 protein accumulated in *elfin 27-6* to similar level as the wild-type protein (Figure 4.2 B). In contrast the corresponding band was almost completely missing in *bak1-4* null mutant (Figure 4.2 B). Therefore the strong impairment of *elfin27-6* in elf18- and flg22-induced SGI is most likely due to expression of the mutated BAK1-5 protein. I therefore renamed *elfin27-6* as *bak1-5*.

Interestingly, the mis-sense substitution in *bak1-5* leads to the single amino acid change C408Y in subdomain VIa of the cytoplasmic kinase just preceding the catalytic triad (Figure 4.2 C). The corresponding Cys residue is conserved in all

SERK family members and in ~17% of all RLKs in *Arabidopsis thaliana* (Figure 4.2 C, data not shown).

4.2.3. *bak1-5* a novel semi-dominat allele of *BAK1*

To confirm that the C408Y mutation in BAK1-5 is causative for the observed strong impairment in elf18- and flg22-triggered responses, I first transformed the null mutant *bak1-4* with the genomic locus of *BAK1* or *bak1-5* under the control of its own regulatory sequence. In the T2 generation I selected transgenic lines with similar expression levels compared to wild-type (Figure 4.3 A) and tested their responsiveness to elf18 and flg22 as measured by PAMP-triggered ROS production. As expected, the wild-type transgene was able to complement the compromised flg22- and elf18-induced oxidative burst of *bak1-4* (Figure 4.3 B-C). Consistently, transgenic plants expressing bak1-5 were strongly impaired in flg22- and elf18-induced oxidative burst, and thus phenocopied the *bak1-5* mutant (Figure 4.3 B-C). This clearly demonstrates that not any mutations closely linked to the genetic locus of *BAK1* but actually the mutation in *BAK1* is causative for the observed phenotypes of *bak1-5*.

Initial experiments with high concentrations of flg22 and elf18 in the SGI assay suggested that *bak1-5* was a recessive mutation. However, I wanted to test for potential subtle semi-dominant effects of the mutant bak1-5 protein on the wild-type protein using heterozygous plants. For this purpose we performed an allelism analysis using Col-0, *bak1-4* and *bak1-5*. Initially, I tested the effect of the *bak1-5* mutation on the flg22-triggered ROS burst. Confirming previous results *bak1-5* and importantly *bak1-5* x *bak1-4* heterozygous F1 plants displayed a near abolishment of the ROS-burst (Figure 4.4 A).

In the case of *bak1-5* x Col-0 heterozygous F1 plants only a slight delay in the onset of the flg22-induced ROS-burst could be observed but no clear reduction in the amplitude (Figure 4.4 A). We obtained similar results for the flg22-induced SGI. Heterozygous F1 *bak1-5* x Col-0 plants displayed an intermediate phenotype between *bak1-5* and Col-0 seedlings (Figure 4.4 B). Next we tested the contribution

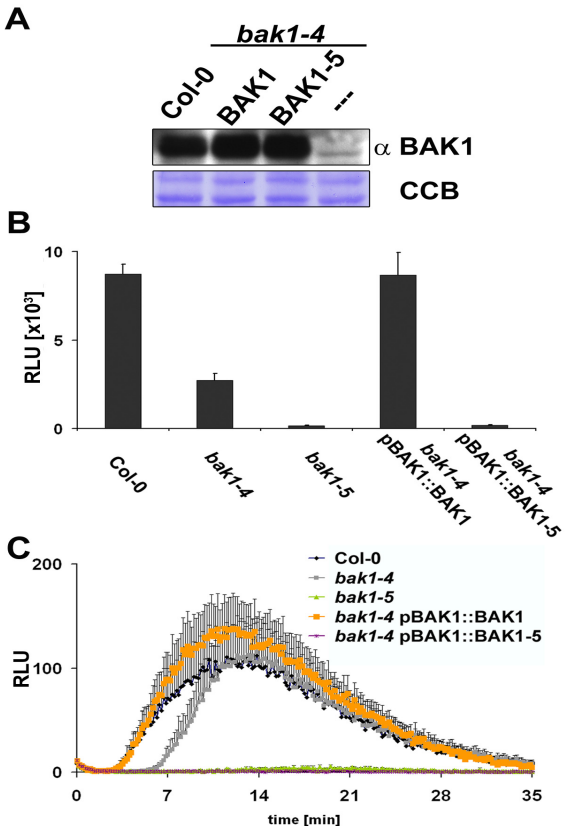

Figure 4.3. BAK1-5 is causative for the *bak1-5* phenotype.

A. Expression of BAK1 and BAK1-5 in transgenic plants in the *bak1-4* background. Immunoblot of total protein from Col-0, *bak1-4 pBAK1::BAK1*, *bak1-4 pBAK1::BAK1-5* and *bak1-4* using anti-BAK1 antibody. Immunoblot, upper panel; Coomassie colloidal blue stained membrane, lower panel.

B. The *bak1-5* mutation is causative for the reduced flg22-induced ROS burst. Total ROS production after 35 min in leaves of Col-0, *bak1-4*, *bak1-5*, *bak1-4 pBAK1::BAK1*, and *bak1-4 pBAK1::BAK1-5* after treatment with 100 nM flg22. Results are average ± s.e. (n=8).

C. The *bak1-5* mutation is causative for the compromised elf18-induced ROS burst. ROS burst in leaves of Col-0, *bak1-4*, *bak1-5*, *bak1-4 pBAK1::BAK1* and *bak1-4 pBAK1::BAK1-5* plants treated with 100 nM elf18. Results are average ± s.e. (n=8).

of BAK1-5 to elf18-triggered responses. Consistently with all previous observations, *bak1-5* x *bak1-4* heterozygous F1 plants phenocopied *bak1-5* mutants in both elf18-induced ROS-production and SGI (Figure 4.4 C-D). More importantly, *bak1-5* x Col-0 heterozygous F1 plants were markedly compromised in their elf18 induced ROS-burst. Furthermore, these plants were partially insensitive to low concentration of elf18 (10 nM) in the SGI, growing more than Col-0 or *bak1-4* seedlings. This careful investigation clearly demonstrates the semi-dominant nature of the *bak1-5*

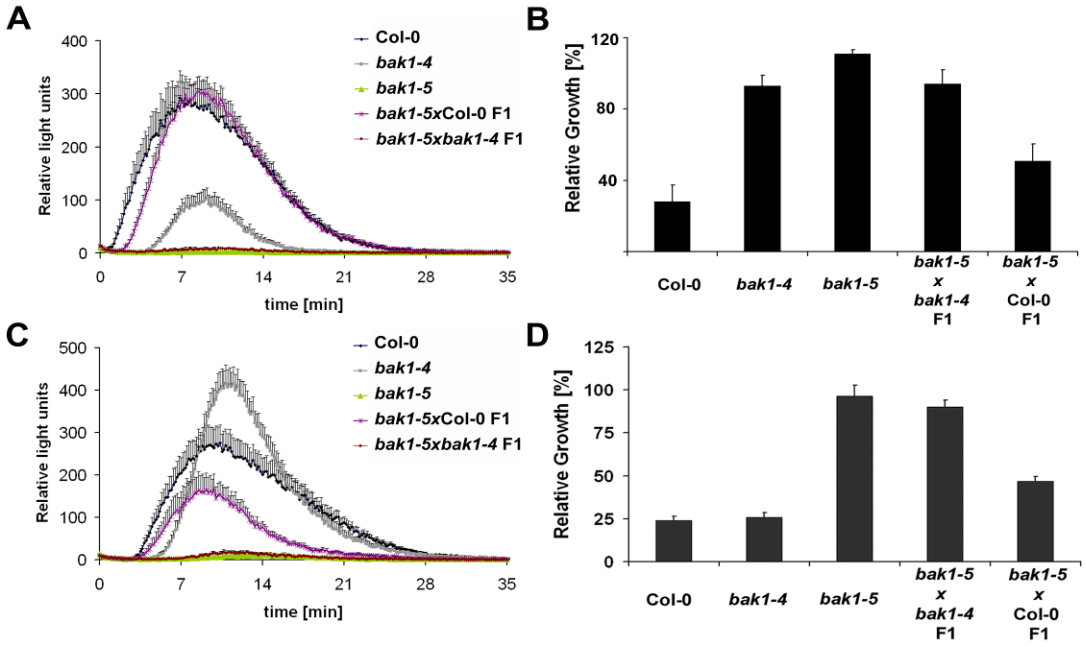

Figure 4.4. *bak1-5* is a semi-dominant allele.

A. The flg22-induced ROS burst is delayed but not reduced in *bak1-5* x Col-0 F1 plants. ROS burst in leaves of Col-0, *bak1-4*, *bak1-5*, *bak1-5* x Col-0 F1 and *bak1-5* x *bak1-4* F1 plants treated with 100 nM flg22. Results are average ± s.e. (n=8).

B. *bak1-5 x* Col-0 F1 seedlings are slightly impaired in the flg22-triggered SGI. SGI of Col-0, *bak1-4*, *bak1-5*, *bak1-5* x *bak1-4* F1 and *bak1-5* x Col-0 F1 in the presence of 40 nM flg22. Fresh weight is represented relative to untreated control. Results are average ± s.e (n=6).

C. The elf18-induced ROS burst is significantly compromised in *bak1-5* x Col-0 F1 plants. ROS burst in leaves of Col-0, *bak1-4*, *bak1-5*, *bak1-5* x Col-0 F1 and *bak1-5* x *bak1-4* F1 plants treated with 100 nM elf18. Results are average ± s.e. (n=8).

D. *bak1-5* x Col-0 F1 seedlings are slightly impaired in the elf18-triggered SGI. SGI of Col-0, *bak1-4*, *bak1-5*, *bak1-5* x *bak1-4* F1 and *bak1-5* x Col-0 F1 in the presence of 10 nM elf18. Fresh weight is represented relative to untreated control. Results are average ± s.e (n=6).

mutation. This also suggests that bak1-5 has a semi-dominant negative effect on the endogenous wild-type BAK1 most likely in a dose-dependent manner interfereing with the function of the wild-type protein via protein-protein interaction. Intriguingly, the semi-dominant effect of bak1-5 was more pronounced in the case of EFR-dependent signalling pathway.

4.2.4. *bak1-5* is strongly impaired in PTI signalling

The initial phenotypic characterization of *bak1-5* suggested a strong impairment in all elf18- and flg22-triggered responses. In order to obtain a precise overview of the impairment in PTI signalling and to illustrate potential differences to the previous described *bak1-4* null allele (Chinchilla et al., 2007; Heese et al. 2007), I performed a detailed comparative phenotypic analysis using Col-0, *bak1-4* and *bak1-5* mutant plants.

Previous reports showed that *bak1-4* was not impaired in elf18-triggered SGI (Chinchilla et al., 2007). I was able to recapitulate these results as only *bak1-5* seedlings were impaired in the elf18-triggered SGI (Figure 4.5 A). Interestingly, *bak1-5* was also more strongly impaired in flg22-induced SGI at high peptide concentrations of 1μM compared to *bak1-4* (Figure 4.5 A). Similarly, I found that the ROS-burst induced by flg22 and elf18 treatment was strongly reduced in *bak1-5* leaves (Figure 4.5 B), whereas leaves of the null mutant *bak1-4* showed only a delayed and slightly reduced oxidative burst (Figure 4.5 B), as previously reported (Chinchilla et al., 2007; Heese et al., 2007).

Next, I analysed the impact of *bak1-5* on the activation of MAP kinases by flg22 and elf18. Consistent with previous observations, the activation of MPK3, 4 and 6 after flg22 and elf18 treatment was delayed and reduced in *bak1-4* seedlings (Figure 4.5 C). Surprisingly, the activation of these MPKs by flg22 and elf18 was differentially regulated in *bak1-5* seedlings. The activation of MPK3 and 6 by flg22 and elf18 was also delayed, but the level of activation ultimately reached levels similar to that observed in wild-type seedlings at 15 min. Notably, MPK4 was not activated at all during the time-course of the experiment (Figure 4.5 C).

Since MPK activation is linked to PAMP-induced transcriptional reprogramming (Fiil et al., 2009; Boudsocq et al., 2010), I then assessed whether PAMP-induced gene expression was also affected in *bak1-5* seedlings using three different PTI marker genes (He et al., 2006) over a 3 hours time course experiment. The induction of the three genes by flg22 and elf18 was partially impaired in *bak1-4* over the time-course although this effect was minor or absent at certain time-points (Figure 4.5 D).

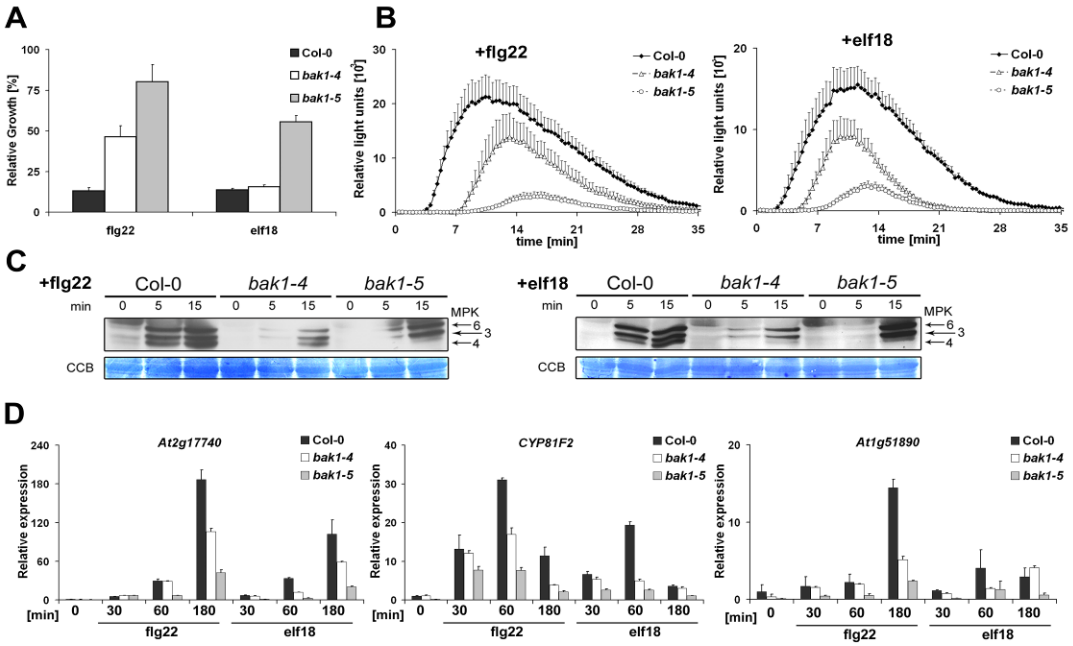

Figure 4.5. *bak1-5* is strongly impaired in EFR- and FLS2-dependent PTI signalling.

A. *bak1-5* is strongly impaired in flg22- and elf18 induced SGI even at high peptide concentrations. SGI of Col-0, *bak1-4* and *bak1-5* in the presence of 1µM flg22 or 1µM elf18. Fresh weight is represented relative to untreated control. Results are average ± s.e (n=6).

B. *bak1-5* is strongly impaired in flg22- and elf18-induced ROS burst. ROS burst in leaves of Col-0, *bak1-4, bak1-5* after treatment with 100 nM flg22 (left) or elf18 (right). Results are average ± s.e. (n=8).

C. Differential MPK activation in *bak1-5* after flg22 and elf18 treatment. The kinetics of kinase activation in seedlings of Col-0, *bak1-4* and *bak1-5* treated with either 100 nM flg22 (left) or elf18 (right) as shown by immunoblot analysis using an anti-p44/42-ERK antibody. Individual MPKs are identified by molecular mass and indicated by arrows. Immunoblot, upper panel; Coomassie colloidal blue stained membrane, lower panel.

D. Defence gene induction by flg22 and elf18 is strongly impaired in *bak1-5*. Gene expression of *At2g17740* (left), *CYP81F2* (*At5g57220*) (middle) and *At1g51890* (right) in seedlings of Col-0, *bak1-4* and *bak1-5* treated with 100 nM flg22 or 100 nM elf18 was measured by qPCR analysis. Results are average ± s.e. (n=3).

In contrast, after flg22 or elf18 treatment the transcript levels of all three PTI-marker genes were drastically reduced in *bak1-5* over the time-course (Figure 4.5 D). Interestingly, the steady-state expression of the marker genes was already lower in *bak1-5* when compared to wild-type (Figure 4.5 D, Figure 4.6).

My results clearly demonstrate that *bak1-5* plants were strongly affected in all flg22 and elf18 responses measured. Strikingly, the new allele *bak1-5* was more strongly impaired in PTI signalling than the null allele *bak1-4* suggesting a mis-regulation of

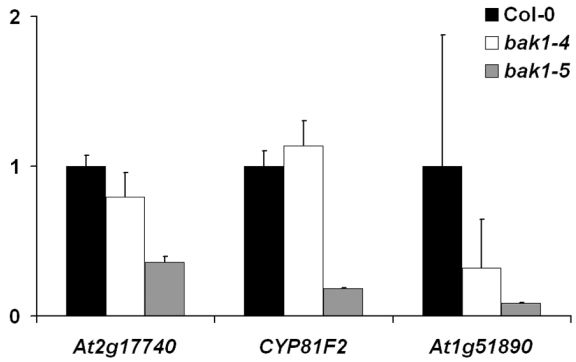

Figure 4.6. Reduced steady-state defence genes expression in *bak1-5*.
Gene expression of *At2g17740* (left), *CYP81F2* (middle) and *At1g51890* (right) in seedlings of Col-0, *bak1-4* and *bak1-5* was measured by qPCR analysis. Results are average ± s.e. (n=3).

PTI signalling. This effect was particularly apparent with EFR-dependent responses, as *bak1-4* null mutants were not affected in elf18-triggered late responses, whereas *bak1-5* mutants were.

4.2.5. The absence of BKK1 in *bak1-5 bkk1-1* double mutant drastically enhances the impairment in PTI signalling

Next, in collaboration with Milena Roux I wanted to test if *BKK1*, the closest homolog of *BAK1*, is also implicated in PTI signalling. *bkk1* single mutant plants were previously reported not to be impaired in PTI signalling (Albrecht et al., 2008; Heese et al., 2007). However, the investigation of more subtle or redundant roles was precluded by the seedling lethality of the *bak1-4 bkk1-1* double mutant due to uncontrolled cell death (He et al., 2007). Fortunately, we were able to overcome this technical limitation using *bak1-5 bkk1-1* double mutant, which is fully viable (see Chapter 5). This allowed us to perform a detailed analysis of the role of BKK1 in FLS2- and EFR-dependent signalling pathways.

The double mutant *bak1-5 bkk1-1* showed strikingly reduced responses to both flg22 and elf18 in all assays conducted. Remarkably, only a negligible ROS-burst was triggered in leaves of *bak1-5 bkk1-1* double mutants by either flg22 or elf18

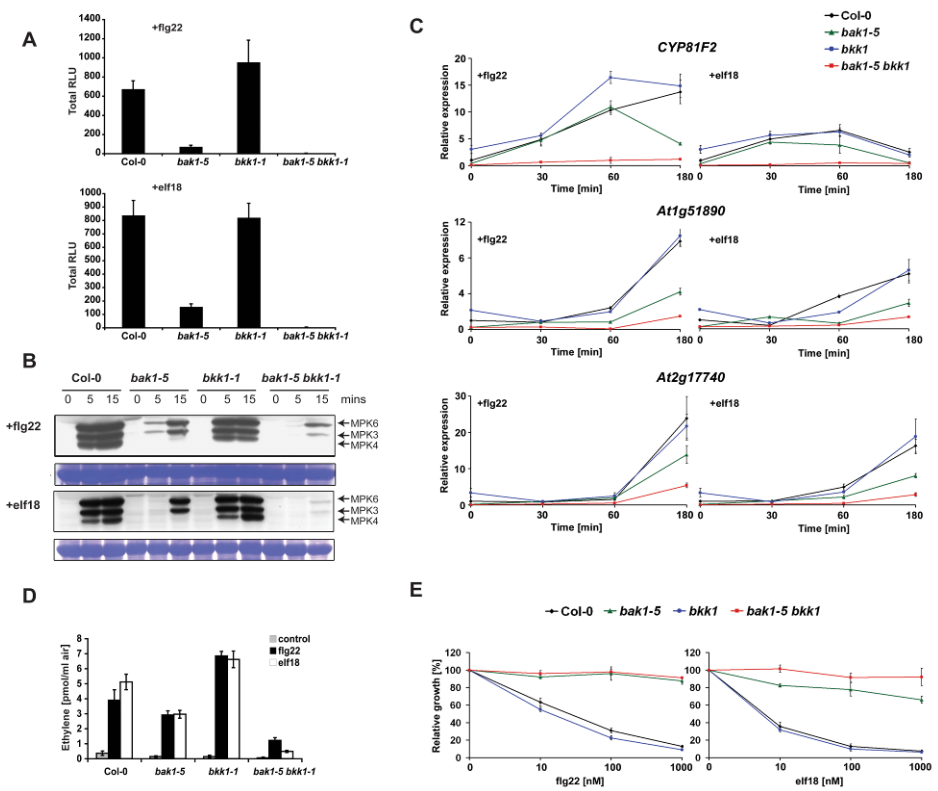

Figure 4.7. BAK1 and BKK1 are required for EFR- and FLS2-dependent PTI signalling.

A. *bak1-5 bkk1-1* plants are totally impaired in flg22- and elf18- induced ROS burst. Total ROS production after 35 min in leaves of Col-0, *bak1-5, bkk1-1,* and *bak1-5 bkk1-1* after treatment with 100 nM flg22 (upper panel) or 100 nM elf18 (lower panel). Results are average ± s.e. (n=8).

B. MAPK activation is nearly totally abolished in *bak1-5 bkk1-1* seedlings after flg22- or elf18-treatment. The kinetics of kinase activation in seedlings of Col-0, *bak1-5, bkk1-1,* and *bak1-5 bkk1-1* treated with either 100 nM flg22 (upper panel) or 100 nM elf18 (lower panel) as shown by immunoblot analysis using an anti-p44/42-ERK antibody. Individual MPKs are identified by molecular mass and indicated by arrows. Immunoblot, upper panel; Coomassie colloidal blue stained membrane, lower panel.

C. Near total abolishment of flg22- or elf18-induced defense gene expression in *bak1-5 bkk1-1* seedlings. Gene expression of *CYP81F2* (upper panel), *At1g51890* (middle panel) and *At2g17740* (lower panel) in seedlings of Col-0, *bak1-5, bkk1-1,* and *bak1-5 bkk1-1* treated with 100 nM flg22 or 100 nM elf18 was measured by qPCR analysis. Results are average ± s.e. (n=3).

D. *bak1-5 bkk1-1* plants are strongly impaired in flg22- and elf18-induced ethylene production. Ethylene production in Col-0, *bak1-5*, *bkk1-1* and *bak1-5 bkk1-1* leaves after mock, 100 nM flg22, 100 nM or elf18 treatments. Results are average ± s.e. (n=6). Ethylene assays were performed by Delphine Chinchilla (University of Basel).

E. *bak1-5 bkk1-1* seedlings are totally insensitive to flg22- and elf18-triggered SGI even at high peptide concentrations. SGI triggered by elf18 or flg22 in Col-0, *bak1-5*, *bkk1-1* and *bak1-5 bkk1-1* seedlings. Fresh weight is represented relative to untreated control. Results are average ± s.e (n=6).

treatment (Figure 4.7 A). This was even lower than in *bak1-5* mutant leaves. *bkk1-1* single mutant displayed no impairment in the ROS-burst triggered by either PAMP (Figure 4.7 A). We then tested the sensitivity of *bak1-5 bkk1-1* double mutant in other PTI signalling responses, which show a different temporal behaviour. First, we tested MAP kinase activation after flg22 and elf18 treatment. As previously shown the activation of MPK3 and 6 was reduced and delayed in *bak1-5* seedlings in comparison to wild-type and *bkk1-1* (Figure 4.7 B). Intriguingly, only residual MAPK activation in response to flg22 and elf18 could be detected in *bak1-5 bkk1-1* seedlings over the time course assayed (Figure 4.7 B).

Next we tested if this near total impairment in early PTI signalling extended to PAMP-triggered gene induction of three independent marker genes (He et al., 2006) over a 3 hours time course. Indeed in *bak1-5 bkk1-1* double mutant seedlings the expression levels were hardly changed by either flg22 or elf18 treatment and even lower than in *bak1-5* single mutant (Figure 4.7 C). In contrast in *bkk1-1* seedlings the expression level of all three marker genes was nearly indistinguishable from wild type (Figure 4.7 C).

An increase in ethylene biosynthesis can be measured within 2 hours of treatment with flg22 or elf18 (Felix et al., 1999; Kunze et al., 2004). We were able to recapitulate these results and measured a clear flg22- or elf18-induced production of ethylene in Col-0 and *bkk1-1* plants (Figure 4.7 D). In contrast, this was significantly reduced in *bak1-5* leaves; and only marginal ethylene production could be measured in *bak1-5 bkk1-1* in response to flg22 or elf18 (Figure 4.7 D). Interestingly, the ROS burst and ethylene production triggered by flg22 and elf18 was sometimes higher in *bkk1-1* leaves than in Col-0 leaves, which may be explained by the weak constitutive cell death and early senescence of this mutant (He et al., 2007; Jeong et al., 2010).

Finally we tested SGI as a late PTI signalling response. As shown in Figure 4.7 E, elf18- and flg22-triggered SGI in *bkk1-1* seedlings was comparable to wild-type at all concentrations tested (Figure 4.7 E). In contrast *bak1-5* and *bak1-5 bkk1-1* seedlings were totally impaired in the SGI triggered by flg22. Notably, the only partial impairment in elf18-triggered SGI of *bak1-5* seedlings was even further decreased in *bak1-5 bkk1-1* seedlings (Figure 4.7 E).

In summary, we showed that loss of *BKK1* further decreased early and late responses of *bak1-5* to elf18 and flg22 unravelling a partially redundant role of *BKK1* in PTI signalling.

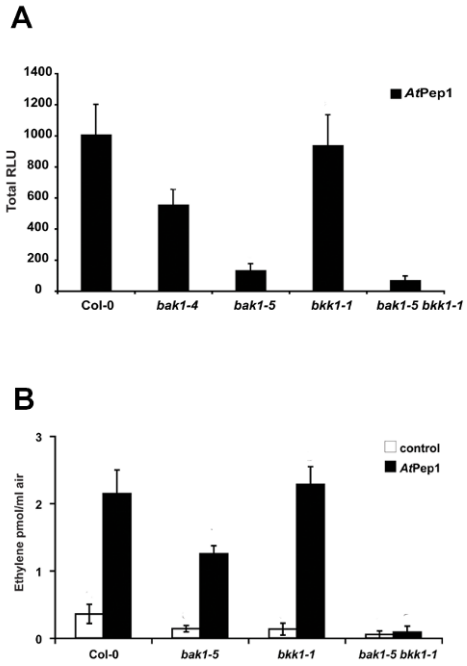

Figure 4.8. BAK1 and BKK1 are partially redundant in AtPep1-triggered DTI-signalling.

A. *bak1-5 bkk1-1* leaves nearly totally impaired in AtPep1-induced ROS burst. Total ROS production after 35 min in leaves of Col-0, *bak1-5, bkk1-1,* and *bak1-5 bkk1-1* after treatment with 100 nM AtPep1. Results are average ± s.e. (n=8).

B. Total impairment of AtPep1-triggered ethylene production in *bak1-5 bkk1-1* plants. Total Ethylene production after 3 hours in Col-0, *bak1-5*, *bkk1-1* and *bak1-5 bkk1-1* leaves after mock or 100 nM AtPep1 treatments. Results are average ± s.e. (n=6). Ethylene assays were performed by Delphine Chinchilla (University of Basel).

4.2.6. BAK1 and BKK1 play partially redundant roles in DAMP-induced PTI signalling

It was recently shown that BAK1 is also involved in PTI induced by AtPep1 (Krol et al. 2010). *bak1-4* null mutant shows a reduced sensitivity to AtPep1 and BAK1 interacts with the two corresponding ligand-binding receptors AtPEPR1/2 in a targeted yeast-two hybrid approach (Postel et al. 2009). Therefore, in collaboration

with Milena Roux I tested if AtPEPR1/2-dependent signalling was also compromised in *bak1-5* and if *BKK1* plays a similar role as in PTI signalling. We were able to reproduce the attenuated AtPep1-induced ROS burst in *bak1-4* (Figure 4.8 A). Consistently with observations made for flg22 or elf18-induced PTI-signalling, the AtPep1-triggered ROS burst was further decreased in *bak1-5* leaves, and almost completely abolished in *bak1-5 bkk1-1* (Figure 4.8 A). The partially redundant role of *BKK1* was even more evident in AtPep1-induced ethylene production as *bak1-5* leaves still generated reduced but measurable amounts of ethylene whereas *bak1-5 bkk1-1* double mutant leaves were totally unresponsive (Figure 4.8 B). *bkk1-1* plants were not affected in their responsiveness to AtPep1 (Figure 4.8 A-B). These experiments demonstrate that *BAK1* and *BKK1* play partially redundant roles in AtPep1-induced PTI-signalling.

4.2.7 *BAK1* and *BKK1* are required for disease resistance against bacterial pathogens

After having clearly demonstrated the importance of *BAK1* and *BKK1* for PTI signalling and shown the strong impairment of it in *bak1-5* single and *bak1-5 bkk1-1* double mutants in collaboration with Milena Roux I tested how this impairment in PTI signalling would impact general disease resistance.

We first spray-inoculated plants with the highly virulent hemibiotrophic bacterium *Pto* DC3000. As reported previously (Zipfel et al., 2004; Nekrasov et al., 2009), *fls2* and *fls2 efr* plants were hyper-susceptible to this strain upon spray-inoculation (Figure 4.9 A). The *bak1-4* and *bkk1-1* mutants however exhibited wild-type susceptibility levels (Figure 4.9 A). In contrast, leaves of *bak1-5, fls2 efr bak1-5* and *bak1-5 bkk1-1* allowed higher growth of *Pto* DC3000, comparably to *fls2 efr* (Figure 4.9 A).

PTI defects can be detected more sensitively with weakly virulent bacterial strains lacking effector molecules, such as AvrPto and AvrPtoB, or the phytotoxin coronatine, that are involved in PTI suppression (Melotto et al., 2006; Xiang et al., 2008; Goehre et al., 2008; Shan et al., 2008; Nekrasov et al., 2009). As shown in

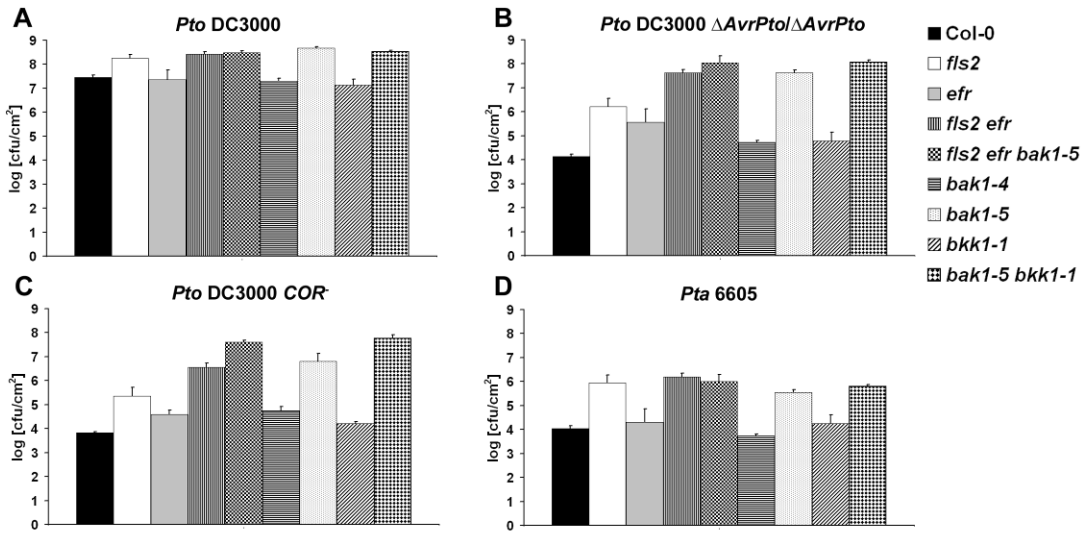

Figure 4.9. *BAK1* and *BKK1* are required for resistance to adapted and non-adapted bacterial pathogens.

A. Four-week-old plants (Col-0, *fls2, efr, fls2 efr, fls2 efr bak1-5, bak1-4, bak1-5, bkk1-1 and bak1-5 bkk1-1*) were spray-inoculated with *Pto* DC3000 (OD_{600}= 0.02).

B. Four-week-old plants (Col-0, *fls2, efr, fls2 efr, fls2 efr bak1-5, bak1-4, bak1-5, bkk1-1 and bak1-5 bkk1-1*) were spray-inoculated with *Pto* DC3000 ΔAvrPto/ΔAvrPto (OD_{600}= 0.2).

C. Four-week-old plants (Col Col-0, *fls2, efr, fls2 efr, fls2 efr bak1-5, bak1-4, bak1-5, bkk1-1 and bak1-5 bkk1-1)* were spray-inoculated with *Pto* DC3000 *COR*$^-$ (C) (OD_{600}=0.2).

D. Four-week-old plants (Col-0, *fls2, efr, fls2 efr, fls2 efr bak1-5, bak1-4, bak1-5, bkk1-1 and bak1-5 bkk1-1)* were syringe-inoculated with *P. syringae* pv. *tabaci* 6605 (OD_{600}=0.002)

Bacterial counts were carried out at 3 days post-inoculation (3 dpi). Results are average ± s.e. (*n*=4).

Figure 4.9 B, *efr* and *fls2* single mutants where already more susceptible to spray-inoculation with *Pto* DC3000 Δ*AvrPto/*Δ*AvrPtoB* while *bak1-4* and *bkk1-1* plants were not. This increased susceptibility was even more pronounced in *fls2 efr* double mutant plants and importantly in *bak1-5* single mutants. Interestingly, *bak1-5 bkk1-1* double and *fls2 efr1 bak1-5* triple mutant leaves supported even slightly more growth of *Pto* DC3000 Δ*AvrPto/*Δ*AvrPtoB* (Figure 4.9 B). Indeed, *Pto* DC3000 Δ*AvrPto/*Δ*AvrPtoB* grew to similar levels in *bak1-5 bkk1-1* and *fls2 efr1 bak1-5* as the isogenic wild-type *Pto* DC3000 in Col-0 plants, showing that the these mutations almost completely restored the virulence defect associated with the loss of AvrPto and AvrPtoB. This pattern was even more pronounced when infecting with the *Pto* DC3000 *COR*$^-$ strain. This strain grew already to much higher numbers in *fls2 efr*

when compared to Col-0, *bak1-4* or *bkk1-1* (Figure 4.9 C). *bak1-5* plants were similarly hyper-susceptible as *fls2 efr*, while this strain reproducibly colonized *bak1-5 bkk1-1* and *fls2 efr1 bak1-5* leaves to an about 10-fold higher level (Figure 4.9 C), reaching again levels comparable to the ones observed with isogenic wild-type *Pto* DC3000 in Col-0 leaves (Figure 4.9 C). Thus, BAK1 and BKK1 both contribute to the basal resistance to *Pto* DC3000 mediated by FLS2, EFR and other yet unknown PRRs.

We then tested if BAK1 and BKK1 play a role in the non-host resistance against the non-adapted bacterium *P. syringae* pv. *tabaci* 6605 (*Pta* 6605) , which partially depends on *FLS2* (Li et al., 2005) (Figure 4.9 D). Growth in *bak1-4* and *bkk1-1* reached similar low levels as wild-type Col-0, while the *fls2* and *fls2 efr* mutant were significantly more susceptible, supporting up to 2 logs more bacterial growth than Col-0 (Figure 4.9 D). The *bak1-5, bak1-5 bkk1-1* and *fls2 efr1 bak1-5* mutants were as susceptible to this non-adapted strain as the *fls2* single and *fls2 efr* double mutant (Figure 4.9 D). This suggests that the contribution of PTI to the non-host resistance to *Pta* 6605 is mostly mediated by FLS2 and is therefore also compromised in the absence of functional BAK1 and BKK1.

4.2.8. BAK1 and BKK1 are required for disease resistance against oomycete pathogens

Next we wanted to know if this strong impairment of basal and non-host resistance in *bak1-5 bkk1-1* is also applicable to biotrophic pathogens. Therefore Nick Holten (HRI, Warwick, UK) assessed the role of *BAK1* and *BKK1* in resistance to the obligate biotrophic oomycete pathogen *Hpa*. We first performed infections with the virulent isolate Emco5 that causes abundant sporangiophores and spore formation within 7 days after inoculation (dai) on Arabidopsis Col-0 seedlings (McDowell et al., 2005). In comparison to Col-0, we observed a decreased sporulation on *bak1-4* seedlings (Figure 4.10 A), probably due to their increased cell death phenotype upon infection (Kemmerling et al., 2007). In contrast, no decrease in the number of spores could be observed in *bak1-5, bkk1-1* or *bak1-5 bkk1-1* (Figure 4.10 A). The absence

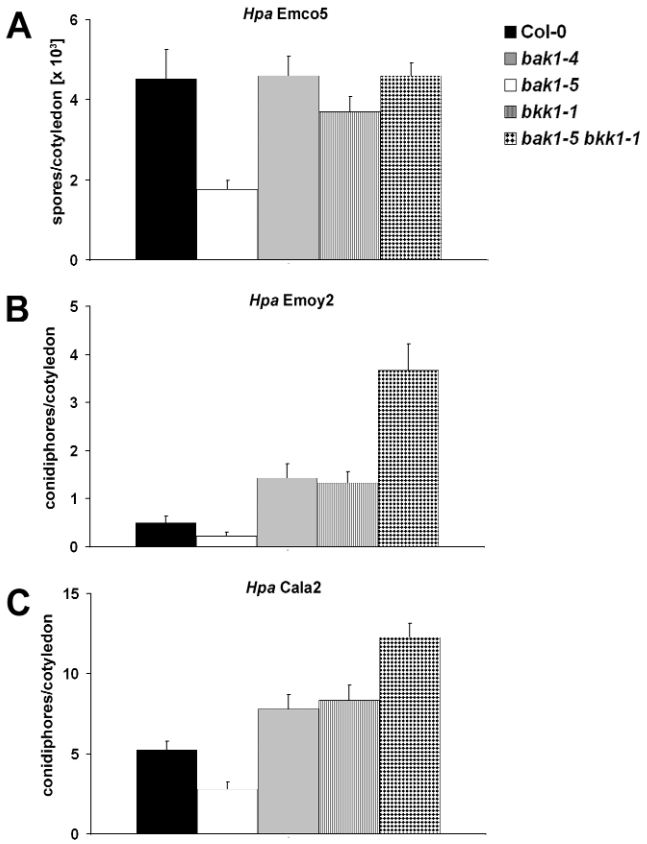

Figure 4.10. BAK1 and BKK1 are required for resistance to the obligate biotrophic oomycete pathogen *Hyaloperonospora arabidopsidis*.

A. Infection of Col-0, *bak1-4, bak1-5, bkk1-1* and *bak1-5 bkk1-1* seedlings with *H. arabidopsidis* Emco5. Spores were counted at 7 days post-inoculation (7 dpi). Results are average ± s.e. (*n*=12).
B. Infection of Col-0, *bak1-4, bak1-5, bkk1-1* and *bak1-5 bkk1-1* seedlings with *H. arabidopsidis* Cala2. Conidiophores were counted at 7 dpi. Results are average ±s.e. (*n*=40).
C. Infection of Col-0, *bak1-4, bak1-5, bkk1-1* and *bak1-5 bkk1-1* seedlings with *H. arabidopsidis* Emoy2. Conidiophores were counted at 7 dpi. Results are average ± s.e. (*n*=40).

All infections and disease scoring was performed by Nick Holten (HRI, Warwick, UK).

of noticeable phenotype of *bak1-5 bkk1-1* seedlings could be due to the already high susceptibility of Col-0 to *Hpa* Emco5 that may mask a contribution of PTI. We thus decided to perform infections with *Hpa* isolates that are only moderately virulent on Col-0 seedlings. Sporulation of the *Hpa* isolate Cala2 on Col-0 seedlings is rare due to RPP2-based resistance (Holub et al., 1994). Indeed, we observed only occasional conidiophore formation on Col-0 seedlings inoculated with *Hpa* Cala2 that never resulted in sporulation (Figure 4.10 B). In contrast, *bak1-5* and *bkk1-1* seedlings

appeared reproducibly more susceptible to this isolate and this enhanced susceptibility was even more pronounced in *bak1-5 bkk1-1* seedlings (Figure 4.10 B). Additionally, infection with another weakly virulent isolate, *Hpa* Emoy2, where resistance in Col-0 is provided by RPP4 (Holub et al., 2008), revealed a similar pattern. Consistently, *bak1-5 bkk1-1* seedlings support the growth of about double the number of conidiophores than Col-0 (Figure 4.10 C). As observed with the highly virulent isolate Emco5, *bak1-4* seedlings were less susceptible to the *Hpa* isolates Cala2 and Emoy2 (Figure 4.10 B-C), as expected due to their deregulated cell death upon infection.

These results revealed a redundant role for BAK1 and BKK1 in resistance to the obligate biotrophic oomycete *Hpa*.

4.3. Discussion

4.3.1. *bak1-5* a novel semi-dominant allele of BAK1 leads to a strong impairment in FLS2- and EFR-dependent PTI signalling

bak1-5 was isolated in a screen designed to identify regulators of EFR-dependent PTI signalling based on their reduced elf18-sensitivity in an SGI assay (Nekrasov et al., 2009). It came as a surprise to identify a novel *BAK1*-allele within such a screen as previously described null *bak1* mutant alleles were not impaired in elf18-induced SGI (Chinchilla et al., 2007; Hesse et al., 2007). However, several lines of evidence univocally demonstrate that the *bak1-5* mutation causes the observed phenotypes: (i) *bak1-5* plants need to express a full-length or truncated version of BAK1 in order to exert an elf18-insensitivity in the SGI assay as the expression of no BAK1 protein in the null allele does not confer elf18-insensitivity. Indeed full length bak1-5 mutant protein is expressed in *bak1-5* plants (Figure 4.2 B). (ii) Expression of the bak1-5 mutant protein in the *bak1-4* null mutant background phenocopied *bak1-5* plants (Figure 4.3 and 4.4). And (iii) BAK1-5 has a dose-dependent dominant-negative effect on the endogenous wild-type BAK1 as plants heterozygous for the *bak1-5*

mutation are partially compromised in their flg22- and elf18-responsiveness (Figure 4.4).

It has been previously reported that *bak1* null alleles in *Arabidopsis* are compromised in early and late responses to flg22 but only in early responses to elf18 (Chinchilla et al., 2007). In contrast *bak1-5* mutant plants were compromised in elf18-induced SGI, a late response (Figure 4.1). This observation prompted me to perform a comprehensive comparative phenotypic analysis between *bak1-4* and *bak1-5* mutant plants in respect to their elf18- and flg22-responsiveness (Figure 4.5). *Bak1-5* mutants were more strongly compromised in flg22- and elf18-induced ROS-burst, defence gene expression and SGI (Figure 4.5). The differential and stronger effect of *bak1-5* compared to *bak1-4* was more apparent for EFR-dependent responses. This might be due to the relatively small impairment of EFR-dependent responses in *bak1-4* and the concomitant greater ability to observe a differential behaviour. Alternatively, it could be that bak1-5 has *per se* a greater impact on EFR- compared to FLS2-dependent signalling. Interestingly, heterozygous *BAK1*/*bak1-5* plants show more consistent and stronger impairment in elf18-triggered responses than flg22-triggered responses supporting the later hypothesis (Figure 4.4.). This and several additional observations suggest that PTI signalling is differentially mis-regulated in *bak1-5* plants.

The flg22- and elf18-induced activation of MPK3, 4 and 6 was reduced and delayed in *bak1-4* seedlings (Figure 4.5 C). In contrast, in *bak1-5* seedlings the activation of MPK3 and 6 was only delayed but after 15 min reached similar activation levels as observed for Col-0 (Figure 4.5 C). Importantly, MPK4 was not activated at all in *bak1-5* seedlings during the time-course of the experiment. This might suggest that proper MPK4 activation is required for full PTI signalling challenging its previously ascertained role as a negative regulator of defence signalling (Petersen et al., 2000; Qui et al., 2008a). Interestingly, *bir1-1* mutants also display a strong impairment of flg22-induced MPK4 but not MPK3 and MPK6 activation (Gao et al., 2008). This specific impairment of MPK4 in *bir1-1* was only observed under non-permissive temperature and was fully reverted at 27^{o}C, a temperature at which *bir1-1* mutant

plants are fully viable (Gao et al., 2008). This might suggest a differential regulation of BIR1 in the *bak1-5* mutant background.

Intriguingly, the basal transcript levels of three unrelated PTI marker genes was markedly reduced in *bak1-5* plants (Figure 4.6). Therefore, the activity of negative regulators of PTI signalling might be constitutively higher in *bak1-5* plants leading to repression of defence genes. Alternatively, assuming that MPK4 is a negative regulator of PTI signalling another hypothesis is also conceivable. In *bak1-5* plants, defence signalling might be weakly constitutive leading to the activation of a postulated negative feedback loop (Schwessinger and Zipfel, 2008) thereby down-regulating basal defence gene expression. Both hypotheses require bak1-5 to actively manipulate PTI signalling.

4.3.2. BAK1 and BKK1 have a partially redundant role in FLS-, EFR- and AtPEPR1/2-dependent PTI signalling

The transcripts of *SERK1-4* are up-regulated in response to PAMP or pathogen treatments (Postel et al., 2009), supporting a potential role for these SERKs in plant immunity. Yet, no other *serk* single mutant apart from *bak1* is affected in flg22- or elf18-triggered responses (Chinchilla et al., 2007; Heese et al., 2007). However, several SERK-family members share (partially) redundant roles in different signalling pathways with *BAK1* or amongst each other (Chinchilla et al., 2009). For example, BKK1, the closest homolog of BAK1, has a partially redundant role in cell death control (He et al., 2007; de Jonge et al., 2010). Strong *bak1 bkk1* double mutant alleles are seedling lethal under sterile conditions (He et al., 2007). Even weak allele combinations have strong developmental phenotypes, such as early senescence making them unamenable for PTI signalling analysis. So in order to test if BKK1 has a partially redundant role with BAK1 in PTI signalling I took advantage of the fact that *bak1-5 bkk1-1* mutants are not impaired in cell death control (see Chapter 5). *Bak1-5 bkk1-1* mutants were more strongly impaired in all flg22- and elf18-induced responses tested than either single mutant (Figure 4.7). In some assays such as flg22- and elf18-induced ROS production *bak1-5 bkk1-1* plants

even phenocopied receptor mutant plants (Figure 4.7 A). This demonstrates that BAK1 and BKK1 function in a partially redundant manner in FLS2- and EFR-dependent signalling. Additionally, BAK1 and BKK1 are also involved in DAMP-signalling as *bak1-5 bkk1-1* mutants are nearly totally impaired in AtPep1-induced ROS-burst and ethylene production (Figure 4.8). Therefore, BAK1 and BKK1 might be the most important SERK family members for FLS2-, EFR- and AtPEPR1/2-dependent signalling. Though, additional analysis of *serk1 bak1-5*, *serk2 bak1-5* and higher order mutants might reveal subtle roles of other SERK-family members in PTI signalling.

4.3.3. BAK1 and BKK1 are required for immunity to hemi-biotrophic and obligate biotrophic pathogens

The role of BAK1 and to a larger extent BKK1 in plant disease resistance is unclear. An unambiguous analysis of the role of BAK1 and BKK1 in *Arabidopsis* disease resistance is hindered by the constitutive and pathogen-induced cell death phenotype of *bak1* and *bkk1* single and double null mutants (He et al., 2007; Kemmerling et al., 2007; Jeong et al., 2010). Accordingly, *bak1-4* plants exhibited pronounced chlorotic lesions upon infection with the hemibiotrophic bacterium *Pto* DC3000, but were not more susceptible to this bacterium (Kemmerling et al., 2007). Concomitantly, the same mutant plants were more resistant to the obligate biotrophic oomycete *Hpa*, but more susceptible to the necrotrophic fungi *B. cinerea* and *A. brassicicola* (Kemmerling et al., 2007).

Intriguingly, silencing of *NbSERK3*/*BAK1* in *N. benthamiana* resulted in a clear hyper-susceptibility to the adapted bacterium *Pta* 11528 and the non-adapted bacterium *Pto* DC3000 (Heese et al., 2007). In addition, *SERK3/BAK1* silencing in tomato led to loss of *Verticillium* resistance mediated by the LRR-RLP Ve1 (Fradin et al., 2009). Several non-mutually-exclusive hypotheses could explain the strong impact of *SERK3/BAK1* silencing on disease resistance in *N. benthamiana* and tomato without an apparent impact on cell death control as observed in *Arabidopsis*. First, the silenced gene may not correspond to the true functional ortholog of

AtBAK1 and therefore not be involved in cell death control. Second, the silencing fragment may affect the expression of additional *SERK* paralogs those function and/or identity is currently unknown. Thirdly, the hypothetical R protein guarding the BAK1-BKK1 complex integrity and/or activity may not be present in *N. benthamiana* and tomato. Thus, silencing of *SERK3/BAK1* in these plants does not result in observable cell death phenotypes.

Another issue in interpreting the role of BAK1 and BKK1 in disease resistance is that the impact of BR signalling in defence is still unclear (Divi et al., 2010). Consequently, conclusions on disease susceptibility of *bak1* mutants always need to be carefully weighed as these lines exhibit defects in hormone signalling, innate immunity and cell death.

As *bak1-5* mutant plants are strongly impaired in PTI but not BR signalling, and *bak1-5 bkk1-1* mutants are fully viable not showing any cell-death related phenotypes (see Chapter 5) I used these mutant lines to test the role of BAK1 and BKK1 in defence signalling. *Bak1-5* and *bak1-5 bkk1-1* mutants were as susceptible as *fls2 efr* double receptor mutants to the highly virulent bacterial pathogen *Pto* DC3000 and the non-adapted strain *Pta 6605* (Figure 4.9 A and D). Intriguingly, *bak1-5* single mutant leaves supported nearly as much growth of two weakly virulent bacterial strains *Pto* DC3000 Δ*AvrPto/*Δ*AvrPtoB* and *Pto* DC3000 *COR*$^-$ as observed with the isogenic *Pto* DC3000 strain in Col-0 leaves (Figure 4.9 C-D). This super-susceptibility of plants carrying a single mutation in a central regulator of PTI signalling underscores the tremendous contribution of PTI to general plant defences. Importantly, *bak1-5 fls2 efr* and *bak1-5 bkk1-1* mutants were more susceptible than *bak1-5* and *fls2 efr* mutants to the weakly virulent strain *Pto* DC3000 *COR*$^-$ (Figure 4.9 C). This suggests a partial redundant role of BAK1 and BKK1 in FLS2- and EFR-independent plant defence signalling pathways. It is therefore tempting to speculate that BAK1 and BKK1 are involved in the perception of other bacterial PAMP(s). This hypothesis may be extended to include oomycete PAMP(s) as *bak1-5 bkk1-1* double mutants support some growth of two *Hpa* isolates Cala2 and Emoy2 that are normally resisted by the R proteins RPP2 and RPP4, respectively (Holub, 2007). However, an alternative explanation might be that BAK1 and BKK1 are

involved in effector-triggered immunity (ETI). Yet, results presented in Chapter 7 showing that *bak1-5 bkk1-1* plants display a reduced responsiveness to a crude elicitor extract from *Hpa*-infected *Arabidopsis* plants rather supports the initial hypothesis. Therefore it is tempting to speculate that BAK1 and BKK1 are involved in the perception of multiple unknown PAMP(s) via the interaction with yet unidentified PRR(s).

Overall, I was able to demonstrate the importance of BAK1 and BKK1 in basal and non-host resistance in *Arabidopsis* to hemibiotrophic bacteria and the obligate biotrophic oomycete *Hpa*.

Chapter 5: *bak1-5* is not impaired in cell death control or brassinosteroid signalling

Excursion: Brassinosteroid: perception, signalling and action

The main plant steroid hormones are collectively called brassinosteroids (BR) and are a class of structurally related molecules that are produced via the mevalonate and isoprenoid pathway (Clouse and Sasse, 1998). BRs are growth promoting hormones that are involved in nearly all aspects of plant development, such as cell expansion, vascular patterning, flowering time, photomorphogenesis, senescence and sterility (Mussig, 2006, Domagalska et al., 2007; Ibanes et al., 2009; Clouse, 2002).

Genetic screens in *Arabidopsis* isolated many dwarf BR insensitive mutants. The main locus *BRI1* encodes an RK belonging to subfamily Xa with 25 extracellular LRRs, a single transmembrane spanning domain and a functional intracellular dual-specific kinase domain (Li and Chory, 1997; Friedrichsen et al., 2000; Oh et al., 2009). The perception of BRs is mediated by the extracellular LRR domain of BRI1 (He et al., 2000). Brassinolide (BL), the most bioactive BR (Thompson et al., 1982), binds directly to the island domain of BRI1 situated between LRR21 and LRR22 (Kinoshita et al., 2005). BRI1 forms constitutive homodimers and is under negative regulation by its C-terminal domain (Wang et al., 2005; Russinova et al., 2004). BL binding to the extracellular domain of BRI1 leads the activation of the intracellular kinase domain presumably by releasing autoinhibition (Wang et al., 2005). The BRI1 activation triggers the dissociation of the BRI1 kinase inhibitor 1 (BKI1) from the plasma membrane (Wang et al., 2005). Furthermore, BRI1 forms hetero-complexes with BAK1 (Nam and Li, 2002; Li et al., 2002; Russinova et al., 2004). Also other members of the SERK-family such as SERK1 and BKK1 are able to interact with BRI1 *in vivo* (Karlova et al., 2006; He et al. 2007; Jeong et al., 2010). SERK1, BAK1 and BKK1 are positive regulators of BL-signalling and play partially redundant roles (He et al., 2007; Albrecht et al., 2008). The interaction of BRI1 and BAK1 is enhanced by BL application and this is dependent on BRI1 kinase activity (Wang et al., 2008). BAK1 and BRI1 undergo bidirectional phosphorylation

believed to be important for full BRI1 activation (Wang et al., 2008). BL application also leads to the phosphorylation of several homologous cytoplasmic RLKs (Tang et al., 2008). Three BR-signalling kinases (BSKs) interact directly and constitutively with BRI1 and are phosphorylated by BRI1 but not BAK1 (Tang et al.; 2008). This trans-phosphorylation by BRI1 is believed to lead to the activation and release of BSK family members from the complex. BSK1 interacts with BSU1 (BRI1 suppressor 1) and is hypothesised to activate BSU1 by phosphorylation (Kim et al., 2009). BSU1 is a kelch-repeat-containing phosphatase and a positive regulator of BR signalling (Mora-Garcia et al., 2004). BSU1 in turn is able to inactivate BIN2 (BR insensitive 2) by dephosphorylating a crucial tyrosine residue in BIN2 (Kim et al., 2009). This dephosphorylation leads most likely to the proteasome mediated degradation of BIN2 (Peng et al. 2008). BIN2 is a GSK3-like kinase and a negative regulator of BR signalling (Li and Nam, 2002). In the absence of BR, BIN2 normally phosphorylates the two transcription factors BZR1 (BRZ resistant 1) and BES1 (*bri1*-EMS-suppressor 1) (Wang et al., 2002; Yin et al., 2002; He et al., 2002). This phosphorylation leads to the inhibition of BZR1 and BES1 by degradation, cytoplasmic retention and/or reduced affinity to the target gene promoter sequences (Kim and Wang, 2010). Interestingly, BES1 and BZR1 regulate a different subset of BR-responsive genes whereby BES1 is a transcriptional activator (Yin et al., 2002) and BZR1 a transcriptional repressor (He et al., 2005). Overall, over 500 genes have been reported to be differentially expressed after exogenous BR application and a large set of them is co-regulated by auxin (Nemhauser et al., 2004). BR and auxin signalling display an intimate inter-dependency that is believed to occur mainly at the promoter level of common target genes (Nemhauser et al., 2004). This transcriptional reprogramming leads to cell expansion and growth as a final outcome of BR signalling.

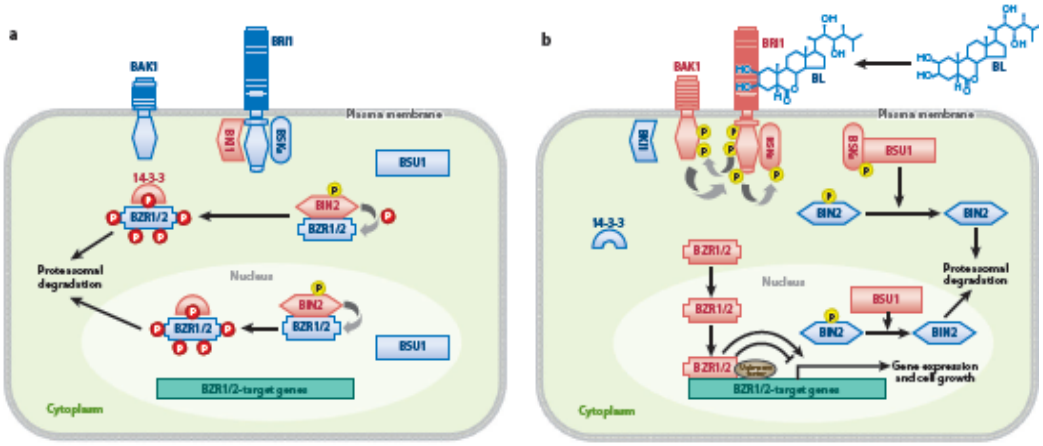

Figure 5.1.: Current model of the brassionsteriod signaling pathway in Arabidopsis
The signaling components in active and inactive status are shown in pink and blue, respectively. Phosphorylation confers positive effects (*yellow circles*) and negative effects (*red circles*).

a) In the absence of BR, BKI1 interacts with inactive forms of BRI1, leading to block of BRI1 binding to BAK1. BRI1-bound BSKs are kept in inactive status. Consequently, BSU1 is inactive. Active BIN2 constitutively phosphorylates BZR1 and BZR2/BES1, leading to nuclear exporting and cytoplasmic retention by the 14-3-3 proteins, loss of DNA-binding activity, and proteasomal degradation of BZR1 and BZR2/BES1.

b) In the presence of BR, BR binds to BRI1, which induces association with BAK1 and disassociation of BKI1. By sequential transphosphorylation between BRI1 and BAK1, BRI1 is fully activated and phosphorylates BSKs. Then the phosphorylated BSKs are released from the receptor complex and bind to BSU1, presumably to enhance BSU1 activity. Activated BSU1 inhibits BIN2 that in turn allows for accumulation of unphosphorylated BZR1 and BZR2/BES1 in the nucleus. Active BZR1 and BZR2/BES1 bind to genomic DNA to regulate BR-target gene expression, thereby modulating growth and development of plants.

Figure and legend adapted from Kim and Wang 2010.

5.1. Objectives

BAK1 is not only implicated in PTI signalling. Actually, BAK1 was originally indentified as an interacting protein of BRI1, the main BR receptor, in the yeast two hybrid system (Nam and Li, 2002), and as being able to suppress the phenotype of weak *bri1-5* mutant allele upon over-expression (Li et al., 2002). These initial studies showed that BAK1 is a positive regulator of BR signalling by interacting with BRI1 *in vivo* (Nam and Li, 2002; Li et al., 2002; Wang et al. 2005, 2008). *Bak1* null mutants are hypersensitive to BR synthesis inhibitor brassinazole (BRZ) (Nagata et al., 2000), BL hyposensitive and display morphological phenotypes

similar to weak *bri1* mutant alleles (Nam and Li, 2002; Li et al., 2002). Furthermore, the absence of BAK1 aggravates, while the over-expression of *BAK1* rescues the cabbage-like rosette phenotype of weak but not of strong *bri1* alleles (Nam and Li, 2002; Li et al., 2002). Kinase activity of BAK1 is required for its function in BR signalling as over-expression of a kinase-inactive variant dramatically enhances the growth retardation of weak *bri1* alleles (Wang et al., 2008; Li et al., 2002). This is mostly likely due to a dominant negative effect on endogenous BAK1 and other SERK-family members as some of them play redundant roles in BR-signalling (Albrecht et al., 2008). For example, SERK1 plays a partially redundant role in BL signalling as *serk1 bak1* double mutants are less sensitive to exogenous BL application and have shorter hypocotyls than *bak1* single mutants (Karlova et al., 2006; Albrecht et al., 2008).

Interestingly, BKK1/SERK4 plays a partially redundant role in BAK1-dependent cell death control. *Bak1* null mutants displayed a BR-independent spreading lesion phenotype after pathogen infection (Kemmerling et al., 2007). This logically leads to an enhanced susceptibility to nectrophic pathogens such as *A. brassicicola* and *B. cinerea* (Kemmerling et al., 2007). In contrast *bak1* null mutants were more resistant to the obligate biotrophic oomycete pathogen *Hpa* race Noco2 (Kemmerling et al., 2007). This inducible loss of cell death control of *bak1* single mutants is dramatically enhanced in strong *bak1 bkk1* double mutant alleles, which display constitutive cell death leading to seedling lethality under sterile conditions within 2 weeks of germination (He et al. 2007). Weak allele double mutant combinations are viable but display early senescence under non-stress conditions (He et al., 2007; Jeong et al., 2010). In addition, BIR1 seems to be implicated in BAK1-dependent cell death control (Gao et al., 2009). *bir1* mutants are lethal when grown at ambient temperature but fully viable at 27^{o}C. This constitutive cell death is partially reversed by a second site mutation in *SOBIR1* (*suppressor of bir1-1*) encoding a RLK belonging to subfamily XI (Gao et al., 2009). *SOBIR1* is also known as *SRRLK* (*small RNA generating RLK*) and *EVR* (*evershed*) as it is involved in the generation of bacterial-induced small RNAs and foral organ abscission, respectively (Katiyar-Agarwal et al., 2007; Leslie et al., 2010). Importantly, BIR1 interacts with SERK1-

4 *in vivo* but not with SOBIR1, suggesting that the effect of SOBIR1 on BIR1/BAK1-dependent cell death control might be indirect (Gao et al., 2009).
Here, I demonstrate that cell death control is not impaired in *bak1-5* or *bak1-5 bkk1-1* mutant plants. I also show that *bak1-5*, in contrast to previously published *bak1* null mutant alleles, is not generally impaired in BR signalling and is fully responsiveness to exogenous BL application.

5.2. Results

5.2.1. *bak1-5* is not impaired in cell death control

BAK1 was previously shown to be implicated in cell death control resulting in increased resistance to biotrophic pathogens of *bak1* mutants (Kemmerling et al., 2007). I made similar observations as *bak1-4* mutants were more resistant to three different isolates of the biotrophic oomycete pathogen *Hpa* (see Chapter 4). However, I did not observe this increased resistance in the case of *bak1-5* (see Chapter 4). In contrary, *bak1-5* mutant plants seemed to support more growth of this biotrophic pathogen, which suggests that cell death control is not compromised in this mutant. In order to test this initial observation more thoroughly I crossed *bak1-4* or *bak1-5* with the null mutant *bkk1-1* (He et al., 2007). Twenty out of seventy individuals (X^2=0.476, p=0.49) from a *bak1-4 x bkk1-1* F2 segregating population died after 2 weeks in sterile conditions (Figure 5.1 A), confirming previous observations of *bak1-4 bkk1-1* seedling lethality (He et al., 2007). In contrast, none of *bak1-5 x bkk1-1* F2 segregating seedlings (n=76) died under the same conditions, and I could isolate fully viable double mutants that completed their life cycle (Figure 5.1 A-B). To test for more subtle or development-regulated defects I grew plants in soil under non-sterile conditions. Weak allele combinations of *bak1 bkk1* show early senescence and spreading lesion phenotypes under these conditions (He et al., 2007; Jeong et al., 2010). Consistently with the growth under sterile conditions, soil-grown *bak1-5 bkk1-1* plants did not show any cell death or early senescence-related

phenotypes and looked similar to wild-type plants (Figure 5.1 B). The *bak1-5* allele is therefore not associated with loss of cell death control.

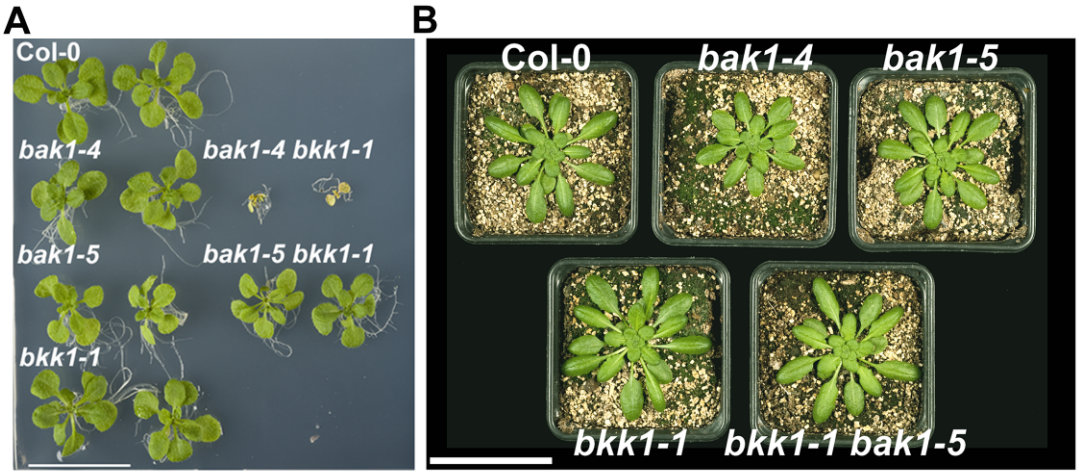

Figure 5.2. Cell death control is not compromised in *bak1-5*.

A. *bak1-5 bkk1-1* seedlings are fully viable. Picture of representative individuals of 2.5 week-old seedlings of Col-0, *bak1-4, bak1-5, bkk1-1, bak1-4 bkk1-1* and *bak1-5 bkk1-1*. Scale bar represents 2cm.

B. *bkk1-1 bak1-5* does not show any early senescence phenotypes. Picture of representative individuals of six-week-old Col-0, *bak1-4*, *bak1-5*, *bkk1-1* and *bak1-5 bkk1-1* plants grown under short-day conditions. Scale bar represents 5cm.

5.2.2. *bak1-5* is not impaired in brassinosteroid signalling

All *bak1* null mutants are compromised in BR signalling and are hyposensitive to exogenous BL application (Nam and Li, 2002; Li et al., 2002; Kemmerling et al., 2007). Therefore, I performed a detailed phenotypic analysis comparing the impact of the novel *bak1-5* allele on BR signalling with the impact of the strong *bak1-4* null allele. Classically, the *bak1-4* loss-of-function allele displayed a semi-dwarf cabbage-like rosette when grown under short-day conditions similar to weak *bri1* mutant plants (Figure 5.2 A). Surprisingly, *bak1-5* plants displayed a morphology comparable to wild-type despite being slightly smaller under these conditions (Figure 5.2 A). I made similar observations under long-day conditions; *bak1-4* plants displayed a slightly stunted growth when compared to Col-0 or *bak1-5* plants (Figure 5.2 B).

As morphology does not always correlate with defects in other BR responses (Wang et al., 2002; Albrecht et al., 2008), I compared the effect of exogenous treatments

with BL or BRZ on *bak1-4* and *bak1-5* plants. First, I tested the sensitivity of roots towards different BL concentration. As previously reported (Nam and Li, 2002; Li et al., 2002) *bak1-4* showed a reduced responsiveness to BL induced root growth inhibition (Figure 5.2 C). In contrast *bak1-5* roots were at least as inhibited as wild-type roots and even showed a slight tendency to being hypersensitive (Figure 5.2 C). Next, I quantitatively investigated the BR-responsiveness of etiolated seedlings grown under different BR regimes. As expected, *bak1-4* hypocotyls were much smaller than wild-type and were hypo-sensitive to the growth inhibition effect of BL (Figure 5.2 D). In contrast, although *bak1-5* hypocotyls were slightly smaller than wild-type, they displayed a wild-type-like responsiveness to BRZ and BL (Figure 5.2 D).

To test for subtle changes in BR sensitivity in the *bak1-4* and *bak1-5* seedlings, we performed BL marker gene analysis by quantitative real-time RT-PCR. For this purpose, I investigated the expression pattern of two well-characterised BL marker genes, *SAUR-AC1* (*At4g38850*) as an auxin co-regulated gene, and *EXP8* (*At2g40610*) as a BL-specific gene (Goda et al., 2004). In order to fully capture the signalling capability of either *bak1* allele, I included a pre-treatment with BRZ to reduce any hormone level adaptation within genotypes that may have altered BR signalling capacity as previously reported for *bzr1-1D* (Wang et al., 2002). BL treatment on its own did not reveal any significant differences between the genotypes for *EXP8* expression (Figure 5.2 E, left). However, the induction of *SAUR-AC1* by BL was clearly impaired in *bak1-4* but less so in *bak1-5* (Figure 5.2 E, right). Interestingly, BRZ pre-treatment prior to BL treatment revealed a clear impairment of *bak1-4* in BL-induced gene expression for both marker genes (Figure 5.2 E). On the contrary, *bak1-5* showed an induction of *SAUR-AC1* comparable to

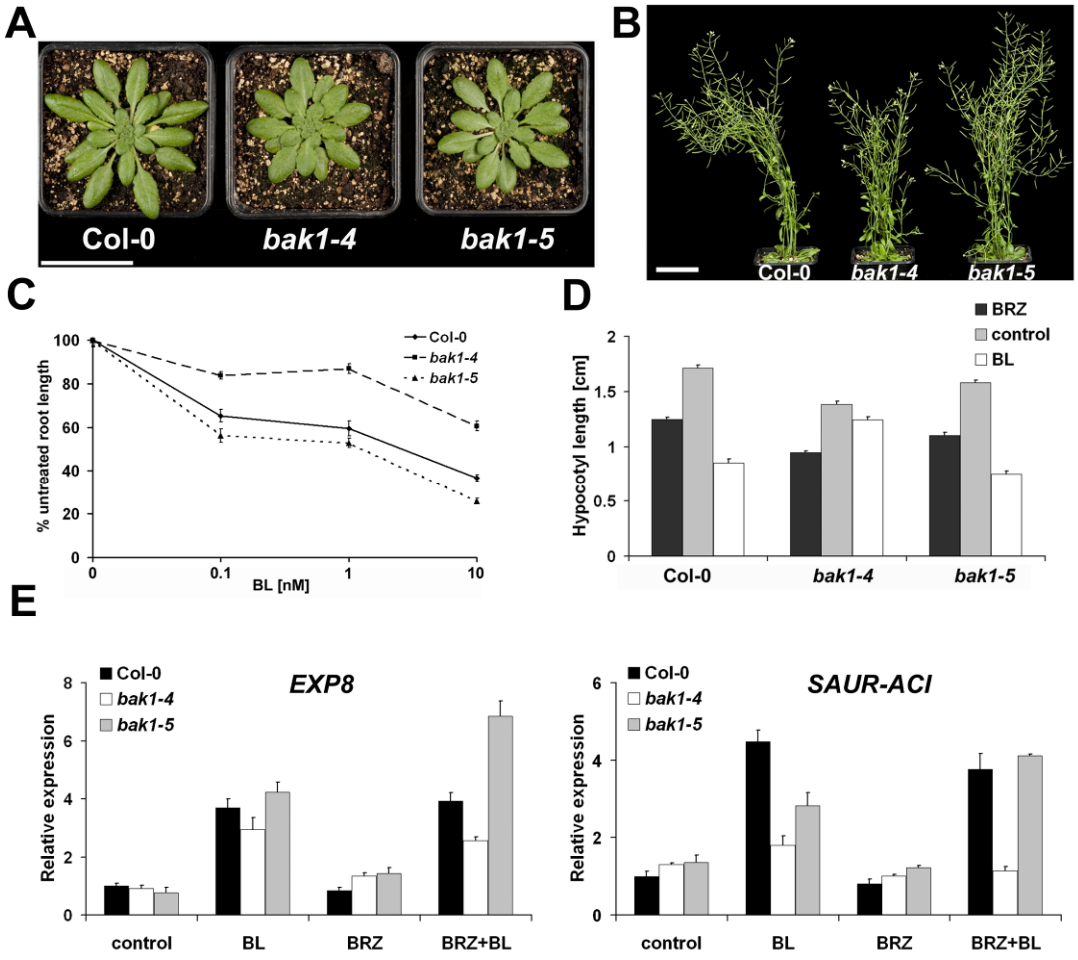

Figure 5.3. *bak1-5* is not impaired in brassinosteroid signalling.

A. *bak1-5* plants have a wild-type-like morphology under short day conditions. Picture of representative individuals of five-week-old Col-0, *bak1-4* and *bak1-5* plants grown under short-day conditions. Scale bar represents 5 cm.

B. *bak1-5* plants have a wild-type-like morphology under long-day conditions. Picture of representative individuals of six-week-old Col-0, *bak1-4*, *bak1-5* plants grown under long-day conditions. Scale bar represents 5 cm.

C. *bak1-5* is slightly hyper-sensitive in the BL-induced root growth inhibition. Relative root growth of 7-day-old Col-0, *bak1-4* and *bak1-5* seedlings grown without or with different concentration of BL. Root growth is represented relative to untreated control. Results are average ± s.e ($n \geq 10$).

D. *bak1-5* shows a wild-type-like BL-induced hypocotyl growth inhibition in etiolated seedlings. Hypocotyl length of 5-day-old etiolated Col-0, *bak1-4* and *bak1-5* seedlings grown without or with 100 nM BRZ or 100 nM BL. Results are average ± s.e. ($n \geq 30$).

E. *bak1-5* shows a wild-type-like BL marker gene induction. Col-0, *bak1-4* and *bak1-5* seedlings were pre-treated for 16 H with 2.5 µM BRZ or not before treatment with 100 nM BL or not for 3 H. Gene expression of *EXP8* (left) and *SAUR-ACI* (right) was measured by qPCR. Results are average ± S.E. (n=3).

wild-type (Figure 5.2 E, left), and the induction of *EXP8* appeared higher in *bak1-5* than wild-type under this treatment regime (Figure 5.2 E, right).

Defects in BR sensitivity are often revealed when mutations in potential BR signalling components or biosynthetic genes are combined with weak *bri1* alleles (Kim and Wang, 2010). To test if the *bak1-5* mutation affects BR sensitivity in such assays, I crossed *bak1-4* or *bak1-5* with *bri1-301* that carries a point mutation in the kinase domain of BRI1 (Xu et al., 2008). As previously reported (Nam and Li, 2002), the *bak1-4* mutation increased the cabbage-like rosette phenotype of *bri1-301* under short-day growth conditions and aggravated the stunted growth in long-day growth conditions (Figure 5.3 A-B). In contrast, the *bak1-5* mutation did not aggravate the *bri1-301* phenotype to the same extent in these conditions. The *bri1-301* rosette morphology was only slightly altered in *bri1-301 bak1-5* in short-day growth condition (Figure 5.3 A). Furthermore, *bri1-301 bak1-5* double mutant plants developed much bigger inflorescences compared to *bri1-301 bak1-4* mutants in long day growth conditions (Figure 5.3 B). Next I performed quantitative hypocotyl growth assays on BL- or BRZ-containing media. As expected, the *bak1-4* allele also severely enhanced the BRZ hypersensitivity and BL hyposensitivity of *bri1-301* in this assay (Figure 5.3 C). Surprisingly, but as noted before for BL-induced root growth inhibition and marker gene expression in *bak1-5* (Figure 5.2 C and E), etiolated *bri1-301 bak1-5* seedlings appeared slightly hyper-responsive to BL when compared to *bri1-301* (Figure 5.3 C).

Overall, my results clearly demonstrate that *bak1-5* is still fully sensitive to BR, and may display a slight increase in BL sensitivity under certain experimental conditions. This phenotype is in stark contrast with the hypo-sensitivity generally associated with *bak1* loss-of-function alleles.

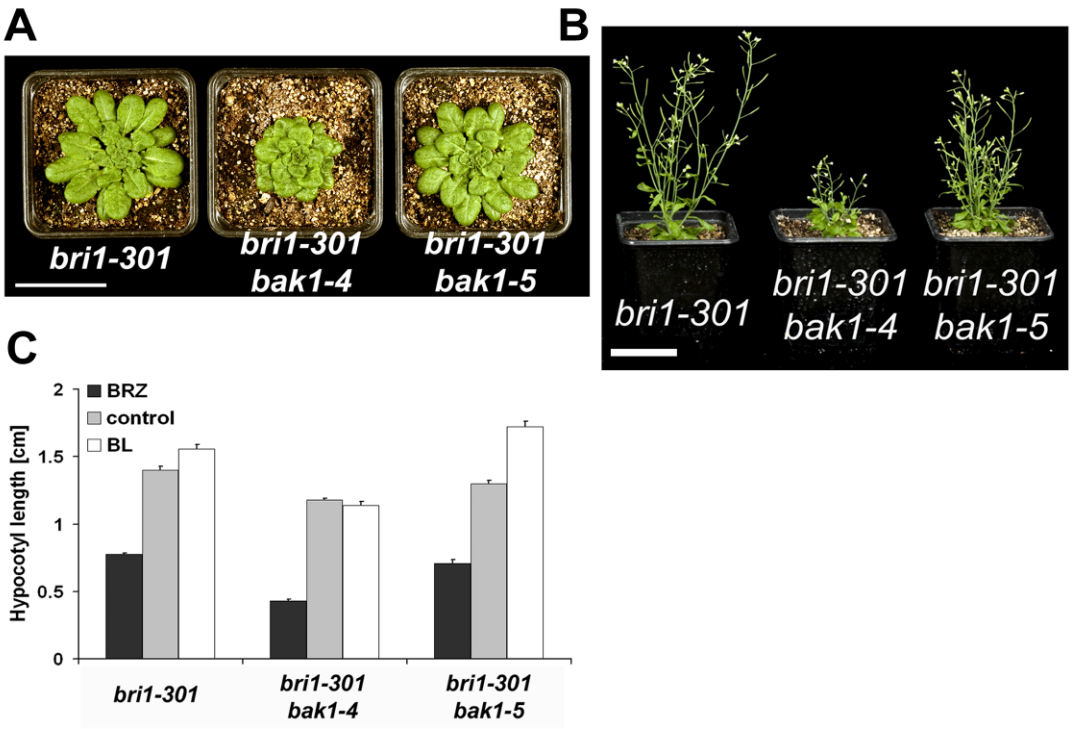

Figure 5.4. *bak1-5* does not aggravate *bri1-301* BL-related phenotypes.

A. *bak1-5* does not aggravate the *bri1-301* cabbage-like rosette under short-day conditions. Picture of representative individuals of six-week-old *bri1-301*, *bri1-301 bak1-4* and *bri1-301 bak1-5* plants grown under short-day conditions. Scale bar represents 5 cm.

B. *bak1-5* does not significantly enhance the *bri1-301* growth retardation under long-day conditions. Picture of representative individuals of six-week-old *bri1-301*, *bri1-301 bak1-4* and *bri1-301 bak1-5* plants grown under long-day conditions. Scale bar represents 5 cm.

C. *bri1-301 bak1-5* is slightly hyper-responsive to BL-induced hypocotyl elongation of etiolated seedlings. Hypocotyl length of 5-day-old *bri1-301*, *bri1-301 bak1-4* and *bri1-301 bak1-5* etiolated seedlings grown without or with 100 nM BRZ or 100 nM BL. Results are average ± s.e. ($n \geq 16$).

5.3. Discussion

5.3.1. *bak1-5* is not impaired in cell death control

In contrast to previously described *bak1* null alleles (Kemmerling et al., 2007; He et al., 2007) *bak1-5* is not compromised in cell death control (Figure 5.1). In addition, *bak1-5* mutants are hyper-susceptible to adapted and non-adapted bacterial

pathogens (see Chapter 4). Furthermore, *bak1-5 bkk1-1* double mutants are not only fully viable (Figure 5.1.), but are also more susceptible to the obligate biotrophic pathogen *Hpa* (see Chapter 4). This is in stark contrast with phenotypes observed for *bak1* and *bkk1* null alleles that do not express any full length BAK1 or BKK1 protein (Kemmerling et al., 2007; He et al., 2007). This loss of cell death control is hypothesised to be due to the constant de-repression of a RK controlling cell death that would be normally under the negative regulation of BAK1 and BKK1 (He et al., 2007; Kemmerling and Nurnberger, 2008). However, I would like to suggest an alternative model based on several observations. The constitutive cell death observed in *bak1-4 bkk1-1* is partial dependent on salicylic acid and is light-dependent (He et al., 2007; He et al., 2008). *Bir1-1* cell death phenotype is partially reverted by high temperatures and mutations in *PAD4* and *EDS1* (Gao et al., 2009). These components are classically associated with R protein-mediated HR (Dodds and Rathjen, 2010). It is therefore conceivable that the integrity and/or activity of a multimeric complex containing BAK1, BKK1 and BIR1 may be "guarded" by an R protein. The absence of BAK1 and BKK1, or BIR1 would trigger constitutive cell death and explain the mutant seedling lethality even in sterile conditions. Interestingly though, the kinase activity of BAK1 seems to be important for cell death control, as kinase-dead variants of BAK1 cannot rescue the *bak1-4 bkk1-1* lethality (Wang et al., 2008). Following this line of thought, it is not surprising that *bak1-5* plants are not compromised in cell death control as they are still expressing full length BAK1 protein variant. In addition, BAK1-5 kinase activity cannot be impaired *per se* as *bak1-5* plants are not compromised in BR signalling (Figure 5.2, 5.3) a phenotypic characteristic generally associated with the expression of kinase dead BAK1 variants (Nam and Li, 2002; Li et al., Wang et al., 2008).

5.3.2. *bak1-5* is not impaired in BR signalling

My detailed phenotypic analysis clearly demonstrates that *bak1-5* is not impaired in BR signalling even though *bak1-5* mutants are slightly smaller than WT (Figure 5.2. and 5.3.). In contrast *bak1-5* mutants might be even hypersensitive to the

exogenously applied BR (Figure 5.2. C-E). This is somehow reminiscent of *bzr1D* mutants harbouring a missense substitution that stabilizes the transcription factor BRZ1 and thereby relieving it from its constitutive negative regulation (Wang et al. 2002: He et al., 2002). The stabilization of brz1D leads to constitutive BR signalling and triggers a negative feedback loop that down-regulates BR biosynthesis genes such as *CPD* (Wang et al., 2002). Consequently, soil-grown *bzr1D* plants display a reduced rosette size reminiscent of BR hyposensitive mutants (Wang et al., 2002). However, when *brz1D* mutants are treated with BRZ or crossed with mutants compromised in BR perception (*bri1*) or production (*det2*) its positive role in BR signalling becomes apparent (Wang et al., 2002). If *bak1-5* indeed renders plants BR hypersensitive, why does it not revert the *bri1-301* rosette phenotype? This could be explained by the current model that BAK1 is a signal enhancer of BR signalling rather than an integral signalling component (Wang et al. 2008). Therefore, in contrast to brz1D, bak1-5 requires a signalling-competent BRI1 to exert is function. In addition, the fact that it is not known if BAK1 is required for all or only a subset of BR responses makes it difficult to fully explain the impact of *bak1-5* on BR signalling. Nevertheless, I tried to test the possible BR hypersensitivity of *bak1-5* further measuring *CPD* expression levels. Unfortunately, I did not obtain any consistent results either for *bak1-4* or *bak1-5* seedlings (data not shown). I also crossed *bak1-5* to *det2* and I am currently waiting to obtain F2 seeds for segregation and phenotypic analysis (data not shown).

Based on the results presented in Chapters 4 and 5, I conclude that BAK1 is in principle able to differentially regulate PTI- and BR-signalling. *bak1-5* mutants are strongly impaired in PTI-signalling but display BR signalling capacity at least comparable to wild-type.

Chapter 6: BAK1-5 is a hypo-acitve kinase displaying an enhanced interaction with different ligand-binding receptors

Corrigendum: During the writing and the final analysis of this thesis chapter I identified a mutation in the expression clone of *BAK1* used for *in vitro* studies. This only influences results presented in 6.2.5. and 6.2.7. The corrected versions including newer results with a corrected clone are presented under 6.2.10 and discussed in 6.3. I decided to include previous results as they reflect the research process during my PhD and therefore should be reproduced within this research PhD thesis.

6.1. Objectives

BAK1 is known to interact with the ligand-binding receptors BRI1, FLS2, EFR and PEPR1/2 (Chinchilla et al. 2009, Postel et al. 2009, Roux et al. *submitted*). Initially BAK1 was identified as an interactor of BRI1, the BR receptor, in the yeast two-hybrid system (Nam and Li, 2002). The authors went on to show that BAK1 also interacts with BRI1 *in vivo* using either double tagged lines expressing *BAK1:MYC* under the control of the CaMV 35S promoter and *BRI1:GFP* under the control of its own regulator sequence or single transgenic lines expressing *BAK1:GFP* under the control of its own promoter in combination with an endogenous anti-BRI1 antibody (Nam and Li, 2002). Similarly, Li and colleagues also used wild-type double transgenic lines expressing both *BAK1:GFP* and *BRI1:FLAG* under the strong CaMV 35S promoter (Li et al. 2002). Using these double tagged lines it was later shown that the BRI1-BAK1 interaction is enhanced after ligand addition and this enhanced interaction is dependent on BRI1 but not BAK1 kinase activity (Wang et al., 2008). Furthermore, in these double transgenic lines the BRI1 and BAK1 phosphorylation status on Thr/Ser residues is enhanced after BL treatment in a mostly BRI1 kinase dependent manner (Wang et al., 2008). BAK1 and BRI1 undergo bidirectional phosphorylation *in vitro* whereby the phosphorylation of BRI1 by BAK1 increases its phosphorylation capacity of the artificial synthetic substrate

BR13 (Oh et al., 2000; Wang et al. 2008). Based on these results and phospho-mimetic mutant analysis of BAK1 and BRI1, it was suggested that BRI1 and BAK1 undergo bidirectional phosphorylation *in vivo* leading to an enhanced BR-signalling out-put *via* enhanced BRI1 kinase activity (Wang et al., 2005; Wang et al., 2008). In this model BAK1 plays a role as signal enhancer for BRI1 but has no intrinsic signalling specificity on its own. It is not known if this model can be extended to other RK interacting with BRI1.

The knowledge of molecular events surrounding the BAK1 FLS2 interaction is much less well defined. FLS2 was initially found to interact with BAK1 in a ligand-dependent manner in *bak1-4* transgenic plants expressing *BAK1:MYC* under the control of its own promoter or *BAK1:GFP* under the control of CaMV 35S promoter in combination with the use of anti-FLS2 antibodies (Chinchilla et al., 2007; Heese et al., 2007). BAK1 and FLS2 form heteromeric complexes and are phosphorylated immediately after ligand addition in Arabidopsis cell cultures (Schulze et al. 2010). Interestingly, the general kinase inhibitor K-252a did not block heteromerization suggesting that kinase activity is not required for complex formation. However, it is not known if the observed phosphorylation of either partner is due to the intrinsic predicted kinase activity of FLS2 and/or BAK1 or rather due to third party kinases. Furthermore, nothing is known about the directionality of the phosphorylation events in this system.

In the case of EFR and PEPR1/2 even less is known. BAK1 interacts with EFR in a ligand-dependent manner in *efr* transgenic lines expressing *EFR:GFP* under its own promoter and after transient over-expression of tagged proteins in *N. benthamiana* (Roux et al. *submitted*). In the case of PEPR1/2 the interaction with BAK1 was only shown in the yeast two-hybrid system (Postel et al., 2009).

As shown in Chapter 4 and 5 the *bak1-5* mutation has a differential impact on three *BAK1*-dependent signalling pathways. *bak1-5* is not impaired in cell death control (see Chapter 5). In addition, it displays a wild-type like morphology and is fully BR responsive (see Chapter 5). On the contrary EFR- and FLS2-dependent PTI signalling is strongly impaired in *bak1-5*. A simple hypothesis to explain the differential impact of *bak1-5* on the three signalling pathways would be that BAK1-

5 interacts differentially with the ligand-binding receptors. For example, bak1-5 would still be able to interact with BRI1, but would loss its ability to form ligand-dependent complex with FLS2 or EFR. However, here I show that bak1-5 is still able to interact with BRI1, FLS2 and EFR using three independent approaches. Interestingly, bak 1-5 shows an enhanced interaction with all three receptors when compared to the wild-type BAK1 protein. Next, I show that bak 1-5 is a hypo-active kinase *in vitro* that is able to trans-phosphorylate BRI1 and EFR. I also demonstrate that BAK1 performs an unidirectional trans-phosphorylation of EFR *in vitro* and that the two non-RD kinases FLS2 and EFR posses a reduced kinase activity when compared to the strong RD kinase BRI1. I also demonstrate that bak1-5 kinase activity is required for the suppression of EFR-dependent PTI signalling. Finally, I describe novel *in vitro* phosphorylation sites on BAK1/bak1-5 using MS/MS analysis.

6.2. Results

6.2.1. Currently available C-terminal tagged BAK1 transgenic lines are unable to complement *bak1-4* PTI phenotypes

At the start of this PhD project no anti-BAK1 antibodies were available. In order to confirm *bak1-5*-related phenotypes and to test the impact of the single amino acid change in bak1-5 on hetero-complex formation with the ligand-binding receptors I generated transgenic *bak1-4* lines expressing BAK1 or BAK1-5 C-terminally tagged with either GFP or 3xHA. Interestingly, previously published transgenic *bak1-4* lines expressing BAK1:GFP or BAK1:MYC were only used for BAK1-FLS2 interaction studies but were not shown to complement *bak1-4* related PTI signalling defects.

I tested if transgenic *bak1-4* T3 lines expressing *BAK1:HA$_3$* or *bak1-5:HA$_3$* under the control its own regulatory sequence (data not shown) could complement the delay and reduction in the flg22-induced ROS burst of *bak1-4* plants or phenocopy the strong impairment thereof in *bak1-5*, respectively (see Chapter 4). As shown for two

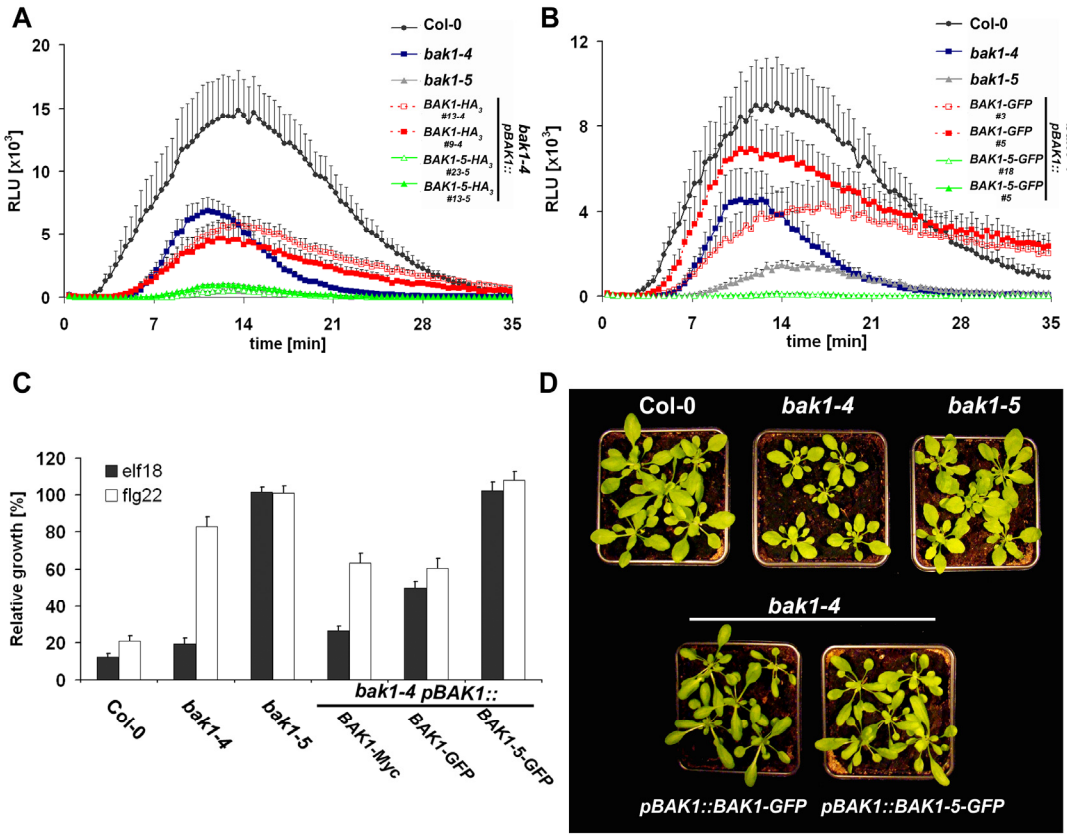

Figure 6.1. Currently available C-terminal tagged BAK1 transgenic lines are unable to complement *bak1-4* PTI phenotypes.

A. Expression of *BAK1:HA*$_3$ is not able to complement the impairment in flg22-triggered ROS-burst of *bak1-4* plants. ROS burst in leaves of Col-0, *bak1-4, bak1-5, bak1-4 pBAK1::BAK1:HA*$_3$ T3 line #13-4 and #9-4, *bak1-4 pBAK1::BAK1-5:HA*$_3$ T3 line #23-5 and #13-5 after treatment with 100 nM flg22. Results are average ± s.e. (n=8).

B. Expression of *BAK1:GFP* is not able to complement the impairment in flg22-triggered ROS-burst of *bak1-4* plants. ROS burst in leaves of Col-0, *bak1-4, bak1-5, bak1-4 pBAK1::BAK1:GFP* T3 line #3 and #5, *bak1-4 pBAK1::BAK1-5:GFP* T3 line #18 and #5 after treatment with 100 nM flg22. Results are average ± s.e. (n=8).

C. Neither the expression of *BAK1:Myc* nor *BAK1:GFP* is able to complement the impairment in flg22-triggered SGI of *bak1-4*. SGI of Col-0, *bak1-4*, *bak1-5*, *bak1-4 pBAK1::BAK1:Myc* T4, *bak1-4 pBAK1::BAK1:GFP* T3 and *bak1-4 pBAK1::BAK1-5:GFP* T3 in the presence of 60 nM flg22 or 60 nM elf18. Fresh weight is represented relative to untreated control. Results are average ± s.e (n=6).

D. Expression of *BAK1:GFP* and *BAK1-5:GFP* can rescue the *bak1-4* growth retardation. Picture of representative individuals of four-week-old Col-0, *bak1-4*, *bak1-5, bak1-4 pBAK1::BAK1:GFP* T3 and *bak1-4 pBAK1::BAK1-5:GFP* T3 plants grown under short-day conditions. Scale bar represents 5 cm.

independent lines the expression of BAK1:HA$_3$ in *bak1-4* was unable to complement the impairment of flg22-induced ROS burst of *bak1-4* (Figure 6.1 A). In contrast, the

expression of BAK1-5:HA_3 in *bak1-4* was able to further reduce the flg22-triggered ROS burst in leaves of two independent transgenic lines phenocopying *bak1-5* plants (Figure 6.1 A). Next, I tested transgenic *bak1-4* T2 lines expressing BAK1:GFP or BAK1-5:GFP (data not shown). As observed for *bak1-4* expressing BAK1-5:HA_3 the flg22-triggered ROS burst was nearly totally abolished in leaves of two independent *bak1-4* BAK1-5:GFP lines (Figure 6.1 B). In the case of BAK1:GFP a partial complementation of the *bak1-4* phenotype could be observed for one transgenic *bak1-4* BAK1:GFP line but not the other (Figure 6.1 B). I tested if this inability of complementing *bak1-4* related PTI phenotypes was specific to my constructs and/or to the bioassay used. Neither the expression of BAK1:GFP nor BAK1:MYC (Chinchilla et al., 2007) could complement the flg22-insensitivity of *bak1-4* seedlings in the SGI assay (Figure 6.1 C). Interestingly the expression of either BAK1 epitope fusion protein actually led to a partially insensitivity of *bak1-4* seedlings to elf18 (Figure 6.1 C). Consistently with previous results *bak1-4* BAK1-5:GFP seedlings phenocopied *bak1-5* seedlings and were insensitive to both flg22- and elf18-induced SGI (Figure 6.1 C).

Previous reports showed that the (over-) expression of BAK1:GFP leads to bigger plants with elongated petioles and leaves complementing the impairment of *bak1* null-mutant alleles in BR signalling (Li and Nam, 2002; Li et al., 2002). Therefore, I tested if our BAK1:GFP lines were able to complement the growth retardation of *bak1-4*. Indeed the expression of BAK1:GFP or BAK1-5:GFP in the *bak1-4* background gave rise to plants with elongated petioles, as well as with longer and narrower leaves (Figure 6.1 D). Overall, the expression of BAK1:GFP is able to rescue the partial BR insensitivity of *bak1-4* plants but not its impairment in FLS2- and EFR-dependent signalling.

6.2.2. BAK1-5 displays an increased affinity to the ligand-binding receptors FLS2, EFR and BRI1 after transient expression in *N.benthamiana*

While generating stable transgenic Arabidopsis lines I initially preformed interaction studies in the heterologous plant expression model system *N. benthamiana* after

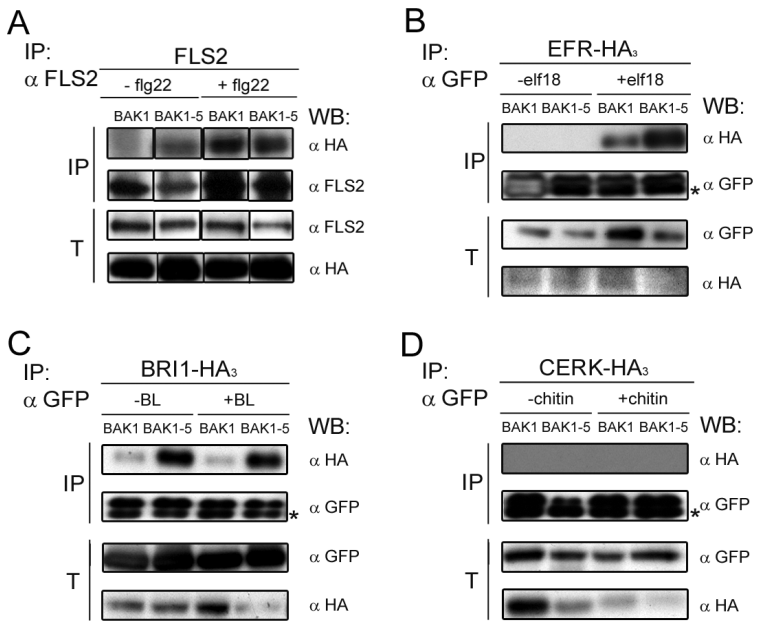

Figure 6.2. BAK1-5 shows an enhanced interaction with ligand-binding RKs FLS2, BRI1 and EFR after transient co-expression in *N. benthamiana.*

A. BAK1-5:HA_3 shows an enhanced interaction with FLS2:Myc in *N. benthamiana*. Co-immunoprecipitation of leaves expressing FLS2:Myc with either BAK1:HA_3 or BAK1-5:HA_3. Leaves were treated or not with 100 nM flg22 for 5 min. Total proteins (T) were subjected to immunoprecipitation (IP) with anti-FLS2 antibody and IgG beads followed by immunoblot analysis using either anti-FLS2 or anti-HA antibodies.

B. BAK1-5:GFP shows an enhanced interaction with EFR:HA_3 in *N. benthamiana*. Co-immunoprecipitation of leaves expressing EFR:HA_3 with either BAK1:GFP or BAK1-5:GFP. Leaves were treated or not with 100 nM elf18 for 5 min. Total proteins (T) were subjected to immunoprecipitation (IP) with GFP-Trap beads followed by immunoblot analysis using either anti-GFP or anti-HA antibodies. The asterisk indicates an unspecific background band.

C. BAK1-5:GFP shows an enhanced interaction with BRI1:HA_3 in *N. benthamiana*. Co-immunoprecipitation of leaves expressing BRI1:HA_3 with either BAK1:GFP or BAK1-5:GFP. Leaves were treated or not with 100 nM BL for 3 H. Total proteins (T) were subjected to immunoprecipitation (IP) with GFP-Trap beads followed by immunoblot analysis using either anti-GFP or anti-HA antibodies. The asterisk indicates an unspecific background band.

D. BAK1:GFP or BAK1-5:GFP does not interact with CERK1:HA_3 in *N. benthamiana.* Co-immunoprecipitation of CERK1:HA_3 with either BAK1:GFP or BAK1-5:GFP after transient expression in *N. benthamiana* leaves. Leaves were treated or not with 100 μg/mL chitin for 5 min. Total protein (T) was subjected to immunoprecipitation with GFP-Trap beads followed by immunoblot analysis using anti-GFP or anti-HA antibodies. The asterisk indicates an unspecific band.

Agrobacterium-mediated transient expression of epitope-tagged fusion proteins (Goodin et al., 2008). I started by the co-expression of FLS2:MYC with either BAK1:HA_3 or BAK1-5:HA_3. When I immunoprecipitated FLS2:MYC using anti-

FLS2 antibodies I was able to observe a slight interaction with BAK1-5:HA_3 even before ligand addition (Figure 6.2 A). Consistently with previous reports BAK1:HA_3 only interacted with FLS2 after flg22 treatment and to similar levels as BAK1-5:HA_3 (Figure 6.2 A). We recently reported that EFR interacts with BAK1 in a ligand-dependent manner (Roux et al., *submitted*). So we tested the interaction between EFR:HA_3 and BAK1:GFP or BAK1-5:GFP after co-expression in *N. benthamiana*. When I immunoprecipitated BAK1:GFP or BAK1-5:GFP I could observe an interaction with EFR:HA_3 only after elf18 treatment (Figure 6.2 B). While pulling-down similar amounts of BAK1:GFP and BAK1-5:GFP much more EFR:HA_3 co-immunoprecipitated with BAK1-5:HA_3 than with BAK1::GFP after elf18 treatment (Figure 6.2 B). Next I tested the interaction of BRI1:HA_3 with BAK1:GFP or BAK1-5:GFP. Interestingly, more BRI1:HA_3 co-immunoprecipitated with BAK1-5:GFP before and after ligand addition when pulling-down similar amounts of BAK1:GFP or BAK1-5:GFP using GFP-trap beads (Figure 6.2 C). The constitutive interaction between BAK1:GFP/BAK1-5:GFP and BRI1:HA_3 was most likely due to the presence of endogenous BR produced by *N. benthamiana*. Importantly, BAK1-5 still retained its interaction specificity as it did not interact with CERK1, a LysM-RLK involved in BAK1-independent chitin perception (Miya et al., 2007; Wan et al., 2008). When pulling-down either BAK1:GFP or BAK1-5:GFP using GFP-trap beads before or after chitin treatment neither of the two proteins co-immunoprecipitated with CERK1:HA_3 (Figure 6.2 D).

In conclusion transient over-expression in *N. benthamiana* epitope-tagged BAK1-5 shows an increased affinity to the ligand-binding receptors FLS2, BRI1 and EFR but not to the un-related RLK CERK1.

6.2.3. BAK1-5 displays a slightly increased affinity to the ligand-binding receptors FLS2 and BRI1 in stable transgenic *bak1-4* plants expressing C-terminally tagged BAK1 variants

I tested if the enhanced interaction of BAK1-5 with the ligand-binding receptors was also observable in stable *Arabidopsis* transgenic lines. At this point, I was unaware

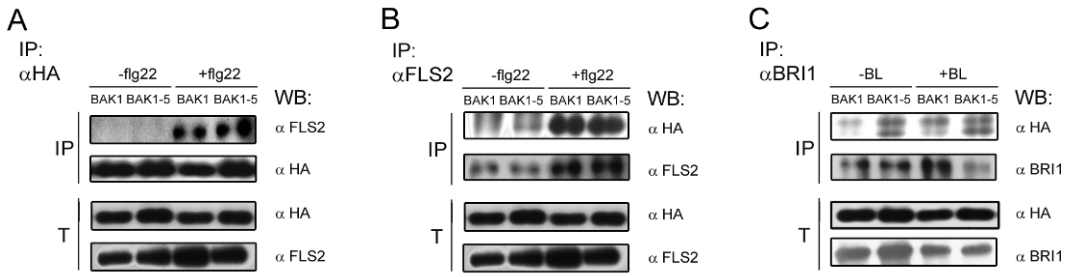

Figure 6.3. BAK1-5 shows a slight enhanced interaction with ligand-binding RK FLS2 and BRI1 in stable transgenic *bak1-4* plants expressing C-terminally tagged BAK1 variants.

A. FLS2 does hardly show an enhanced interaction with BAK1-5:HA_3 in stable transgenic *bak1-4* plants. Co-immunoprecipitation of FLS2 with either BAK1:HA_3 or BAK1-5:HA_3 in *bak1-4 pBAK1::BAK1:HA_3* T2 or *bak1-4 pBAK1::BAK1-5:HA_3* T2 plants treated with or not with 100 nM flg22 for 5min, respectively. Total proteins (T) were subjected to immunoprecipitation (IP) with anti-HA antibodies beads followed by immunoblot analysis using either anti-FLS2 or anti-HA antibodies.

B. BAK1-5:HA_3 shows a slight ligand-independent interaction with FLS2 in stable transgenic *bak1-4* plants. Co-immunoprecipitation of BAK1:HA_3 or BAK1-5:HA_3 with FLS2 in *bak1-4 pBAK1::BAK1:HA_3* T2 or *bak1-4 pBAK1::BAK1-5:HA_3* T2 plants treated with or not with 100 nM flg22 for 5min, respectively. Total proteins (T) were subjected to immunoprecipitation (IP) with anti-FLS2 antibodies and IgG beads followed by immunoblot analysis using either anti-FLS2 or anti-HA antibodies.

C. BAK1-5:HA_3 shows an enhanced interaction with BRI1 in stable transgenic *bak1-4* plants. Co-immunoprecipitation of BAK1:HA_3 or BAK1-5:HA_3 with BRI1 in *bak1-4 pBAK1::BAK1:HA_3* T2 or *bak1-4 pBAK1::BAK1-5:HA_3* T2 plants treated with or not with 100 nM BL for 3 H, respectively. Total proteins (T) were subjected to immunoprecipitation (IP) with anti-HA antibodies beads followed by immunoblot analysis using either anti-FLS2 or anti-HA antibodies.

that the expression of BAK1:HA_3, BAK1:GFP or BAK1:MYC in *bak1-4* was unable to complement the impairment in FLS2-dependent signalling.

I immunoprecipitated BAK1:HA_3 or BAK1-5:HA_3 from total protein extracts of previously described transgenic plants using anti-HA beads. Consistently with previous results I observed a ligand-dependent interaction of BAK1:HA_3 with FLS2 (Figure 6.3 A). I was unable to detect an increased interaction between BAK1-5:HA_3 and FLS2 when immunoprecipitating BAK1-5:HA_3 (Figure 6.3 A). Interestingly, when I performed the reciprocal IP using anti-FLS2 antibodies I was able to observe a slight interaction between FLS2 and BAK1-5:HA_3 but not BAK1:HA_3 without ligand addition (Figure 6.3 B). FLS2 interacted with BAK1:HA_3 only after ligand addition and this with similar strength when compared to BAK1-5:HA_3 (Figure 6.3

B). Finally, I also tested the interaction between BRI1 and BAK1:HA_3/BAK1-5:HA_3 by immunoprecipitating BRI1 with anti-BRI1 antibodies. The interaction between BRI1 and BAK1:HA_3 was constitutive and slightly enhanced by ligand addition (Figure 6.3 C). Consistently, the amount of BAK1-5:HA_3 interacting with BRI1 was much higher with and without BL treatment. Interestingly, co-immunoprecipitated BAK1-HA_3 and BAK1-5-HA_3 migrated as a doublet with the upper band migrating much slower than the corresponding protein in the total protein extract (Figure 6.3 C). This suggests the interaction of BAK1 with BRI1 leads to post-translational modification of BAK1, such as phosphoryaltion.

In summary, BAK1-5 displays a slightly enhanced interaction with FLS2 and BRI1 in transgenic *bak1-4* plants expressing epitope-tagged BAK1 or BAK1-5.

6.2.4. BAK1-5 displays an increased affinity to the ligand-binding receptors FLS2 and BRI1 in *Arabidopsis*

During the course of my PhD study a novel anti-BAK1 antibody became available (Schulze et al. 2010), which recognized an epitope outside of the region containing the BAK1-5 mutation. This enabled me to perform interaction studies between BAK1/BAK1-5 and FLS2 or BRI1 under native conditions using specific antibodies. First, I investigated the interaction with FLS2 by immunoprecipitating BAK1 or BAK1-5 using the newly available anti-BAK1 antibodies. As previously reported, BAK1 interacted with FLS2 in a ligand specific manner (Figure 6.4 A). FLS2 co-immunoprecipitated with BAK1-5 from non-elicited seedlings and the amount of BAK1-5 in complex with FLS2 after flg22 treatment was greater than in the case of BAK1 (Figure 6.4 A). I observed similar results when performing reciprocal immunoprecipitation experiments using specific anti-FLS2 antibodies (Figure 6.4 B). BAK1-5 formed a strong ligand independent complex with FLS2 and showed an enhanced interaction after flg22-treatment when compared with wild-type BAK1 protein (Figure 6.4 B). Finally, I tested the interaction of BRI1 with BAK1 or BAK1-5 using anti-BRI1 antibodies (Figure 6.4 C). I was able to confirm the *in*

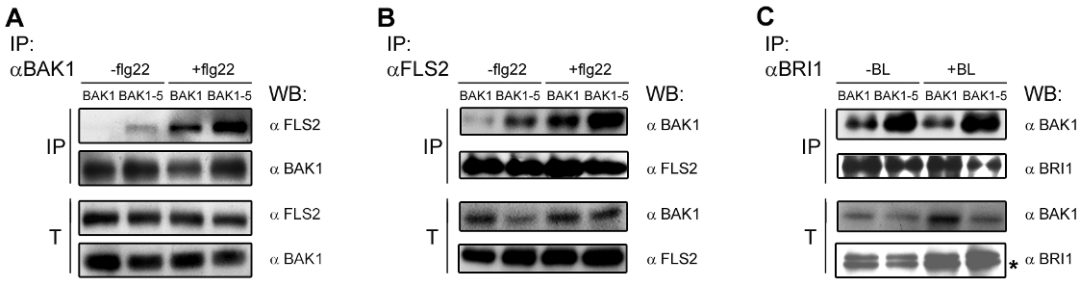

Figure 6.4. BAK1-5 shows an enhanced interaction with ligand-binding RK FLS2, and BRI1 in native conditions.

A. FLS2 shows a ligand-independent interaction with BAK1-5 in *A. thaliana*. Co-immunoprecipitation of BAK1 or BAK1-5 with FLS2 in Col-0 or *bak1-5* plants treated or not with 100 nM flg22 for 5 min, respectively. Total proteins (T) were subjected to immunoprecipitation (IP) with anti-BAK1 antibodies and IgG beads followed by immunoblot analysis using either anti-FLS2 or anti-BAK1 antibodies.

B. BAK1-5 shows a ligand-independent interaction with FLS2 in *A. thaliana*. Co-immunoprecipitation of BAK1 or BAK1-5 with FLS2 in Col-0 or *bak1-5* plants treated or not with 100 nM flg22 for 5 min, respectively. Total proteins (T) were subjected to immunoprecipitation (IP) with anti-FLS2 antibodies and IgG beads followed by immunoblot analysis using either anti-FLS2 or anti-BAK1 antibodies.

C. BAK1-5 shows an enhanced interaction with BRI1 in *A. thaliana*. Co-immunoprecipitation of BAK1 or BAK1-5 with BRI1 in Col-0 or *bak1-5* treated or not with 100 nM BL for 1.5 H, respectively. Total proteins (T) were subjected to immunoprecipitation with anti-BRI1 antibodies and IgG beads followed by immunoblot analysis using either anti-BRI1 or anti-BAK1 antibodies. The asterisk indicates an unspecific band.

planta BRI1-BAK1 interaction previously only reported using transgenic lines expressing epitope-tagged BRI1 and/or BAK1 proteins (Nam and Li, 2002; Li et al., 2002; Wang et al., 2008). As observed in *N. benthamiana* and in stable transgenic lines, BAK1-5 showed an enhanced interaction with BRI1 independent of BL-treatment (Figure 6.4 C).

In conclusion, BAK1-5 displays an enhanced interaction with the two ligand-binding RKs FLS2 and BRI1 in native conditions.

6.2.5. BAK1-5 is a hyper-active kinase

I demonstrated that BAK1-5 has an increased affinity with the three ligand- binding RKs BRI1, FLS2 and EFR. However, BAK1-5 does not show a preferential interaction for any of these three RKs. Therefore, this enhanced interaction of BAK1-5 *per se* cannot explain the differential regulation of three BAK1-dependent

signalling pathways observed in *bak1-5*. Since the *bak1-5* mutation corresponds to a C408Y amino acid change just before the catalytic loop of the kinase domain (see Chapter 4), the *bak1-5* phenotype could be due to altered kinase activity.

To test potential differences in BAK1-5 kinase activity, I expressed the cytoplasmic domains (CD: residues 256 to 615) of BAK1 and BAK1-5 in *Escherichia coli* (*E. coli*), as well as the respective kinase-dead mutant variants (D416N) (indicated as BAK1* and BAK1-5*, respectively) as N-terminally tagged glutathione-S-transferase (GST) -fusion proteins and purified them using glutathione beads. In agreement with previously published results (Li et al., 2002; Li and Nam, 2002;

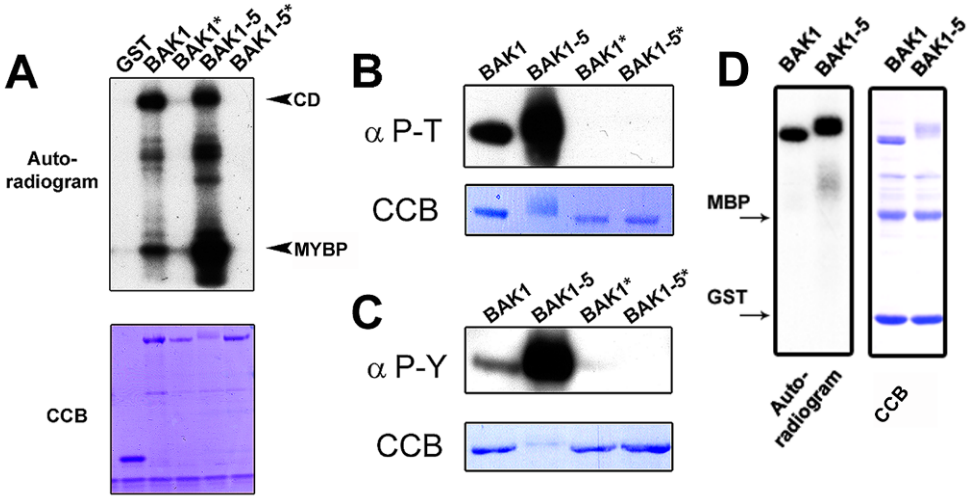

Figure 6.5. BAK1-5 is a hyperactive kinase *in vitro*.

A. BAK1-5 CD has an increased trans-phosphorylation capacity. *In vitro* kinase assay incubating equal amounts of GST control or N-terminal GST-tagged BAK1, BAK1-5, BAK1* and BAK1-5* CD with artificial substrate myelin basic protein (MYBP). Autoradiogram, upper panel; Coomassie colloidal blue stained membrane, lower panel.

B. BAK1-5 CD is a hyperactive kinase on Ser and Thr residues. 0.25 µg of heterologously-expressed N-terminal GST-tagged BAK1, BAK1-5, BAK1* and BAK1-5* CD were subjected to immunoblot analysis with anti-phosphoThr antibodies. Immunoblot, upper panel; Coomassie colloidal blue stained membrane, lower panel.

C. BAK1-5 CD is a hyperactive kinase on Tyr residues. 0.75 µg of heterologously-expressed N-terminal GST-tagged BAK1, BAK1-5, BAK1* and BAK1-5* CD were subjected to immunoblot analysis with anti-phospho-Tyr antibodies. Immunoblot, upper panel; Coomassie colloidal blue stained membrane, lower panel.

D. BAK1-5 CD does not trans-phosphorylate the epitope tag MBP or GST. *In vitro* kinase assay incubating equal amounts of N-terminal GST-tagged BAK1 or BAK1-5 with epitope tagges MBP or GST. Autoradiogram, right panel; Coomassie colloidal blue stained membrane, left panel.

Wang et al., 2008), I detected a strong auto-phosphorylation of BAK1-CD when incubated with radioactive [^{32}P]-γ-ATP *in vitro* (Figure 6.5 A). The kinase-dead BAK1*-CD had no auto-phosphorylation activity (Figure 6.5 A). Intriguingly, heterologously expressed BAK1-5 CD showed a mobility shift on SDS-PAGE compared to BAK1 CD or kinase dead BAK1-5*-CD (Figure 6.5 A-C), indicative of a potential hyper-phosphorylation in *E. coli* during recombinant protein production as previously observed in the case of hyper-active kinase variant BRI1(T872A) CD (Wang et al., 2005). Although I could not observe a significant increase in the auto-phosphorylation activity of BAK1-5 CD when compared to BAK1 CD *in vitro* using radio-active labelled [^{32}P]-γ-ATP, BAK1-5 CD hyper-phosphorylated the artificial substrate myelin basic protein (MYBP) in this assay (Figure 6.4 A). The absence of increased auto-phosphorylation activity in *in vitro* radioactive kinase assays was also previously observed with BRI1(T872A) CD (Wang et al. 2005). Therefore, I probed purified BAK1 CD and BAK1-5 CD in immunoblots with specific anti-phospho-threonine(Thr)/serine(Ser) antibodies (α P-T). Indeed, BAK1-5 CD showed a major increase in the auto-phosphorylation activity on Thr- and Ser-residues (Figure 6.4 B). Importantly, the kinase-dead variants BAK1* CD and BAK1-5* CD had no detectable Thr/Ser-phosphorylation signal demonstrating that the observed signal resulted exclusively from auto-phosphorylation (Figure 6.5 B).

I was interested whether this increased auto-phosphorylation activity was restricted to Thr/Ser residues, as BAK1 was recently shown to also auto-phosphorylate on Tyrosine (Tyr) residues *in vitro* (Oh et al. 2009). Interestingly, Tyr auto-phosphorylation was also increased in BAK1-5 CD as observed on immunoblots with anti-phospho-Tyr antibodies (α P-Y) (Figure 6.5 C).

Finally, I tested if any of the observed phosphorylation of BAK1 or BAK1-5 occurs on the epitope-tags used in this study. Neither BAK1 nor BAK1-5 CD trans-phophorylated the maltose binding protein (MBP) or GST-protein in radio active kinase assays using [^{32}P]-γ-ATP (Figure 6.5 D).

These results clearly indicated that BAK1-5 has increased kinase activity *in vitro*.

6.2.6. The RD kinase BRI1 and the two non-RD kinases EFR and FLS2 have different kinase activities *in vitro*

Ultimately, I wanted to study the trans-phophorylation events between BAK1/BAK1-5 CD and the CDs of the respective ligand-binding RKs. Therefore, I first analyzed FLS2 and EFR kinase activities and compared them with the kinase activity of BRI1 *in vitro*. For this purpose, I expressed in *E. coli* the CDs of EFR (residues 682 to 1031), FLS2 (residues 840 to 1173) and BRI1 (residue 814 to 1196) as fusion proteins with an N-terminal MBP tag. As controls, I also constructed the respective kinase-dead variants EFR* CD (D849N), FLS2* CD (D997N) and BRI1* CD (D1009N). Having all three kinases in the same expression system enabled us to directly compare their kinase activities *in vitro* using radioactive [^{32}P]-γ-ATP. As previously reported (Oh et al. 2000), BRI1 CD had a very strong auto- and trans-

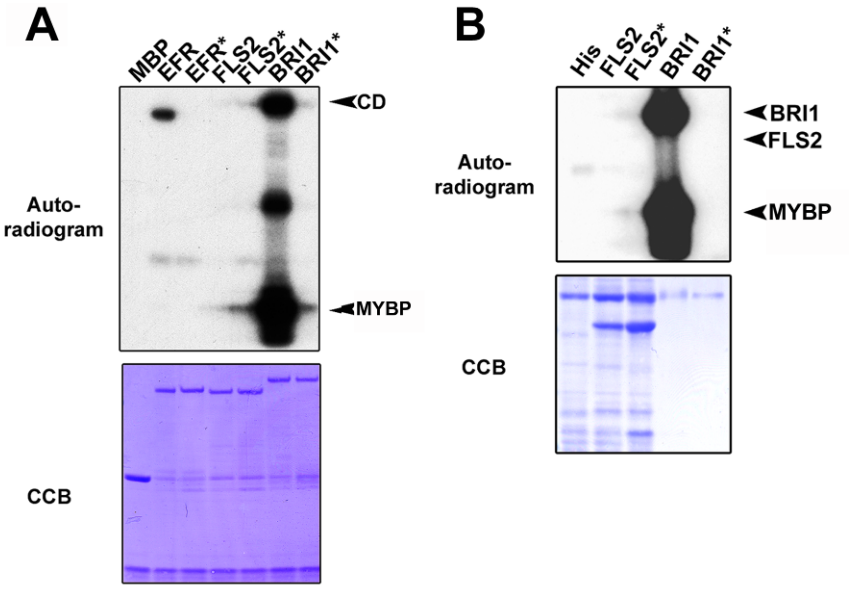

Figure 6.6. The RD kinase BRI1 and the two non-RD kinases EFR and FLS2 have different kinase activities *in vitro*.

A. Differential kinase activity of the RD kinase BRI1 and the non-RD kinases FLS2 and EFR. *In vitro* kinase assay incubating equal amounts of MBP control or N-terminal MBP-tagged EFR, EFR*, FLS2, FLS2*, BRI1 and BRI1* CD with artificial substrate myelin basic protein (MBP). Autoradiogram, upper panel; Coomassie colloidal blue stained membrane, lower panel.

B. FLS2 is an inactive kinase *in vitro*. *In vitro* kinase assay using His or N-terminal His-tagged FLS2, FLS2*, BRI1 and BRI1* CD. Note that ten times more FLS2 and FLS2* CD was loaded compared to BRI1 and BRI1* CD. Autoradiogram, upper panel; Coomassie colloidal blue stained membrane, lower panel

phosphorylation capacity using the artificial substrate MYBP (Figure 6.6 A). In contrast, EFR CD possessed only minor auto-phosphorylation capacity and negligible trans-phosphorylation ability on MYBP (Figure 6.6 A). Notably, these activities were abolished in BRI1* CD and EFR* CD (Figure 6.6 A), demonstrating that the observed phosphorylations are indeed due to the intrinsic kinase activities of these protein.

Surprisingly, I was unable to detect any FLS2 CD phosphorylation *in vitro* (Figure 6.6 A), indicating that FLS2 is an extremely weak kinase. The later result is in disagreement with previous reports that revealed phosphorylation activities *in vitro* for FLS2 (Gomez-Gomez et al., 2001; Lu et al., 2010; Xiang et al., 2008). As Zhou and colleagues (2008) used a N-terminally His tagged FLS2 fusion protein to report FLS2 kinase activity, I also generated His:FLS2 CD. Again, as observed with MBP:FLS2 CD, I was unable to observe any phosphorylation activity (Figure 6.6 B). Under the same conditions, His:BRI1 CD displayed a strong kinase activity (Figure 6.6 B).

Consequently, it appears that in comparison to BRI1 that is an extremely strong kinase, EFR is a moderately good kinase, while FLS2 is almost kinase-inactive *in vitro*.

6.2.7. Differential trans-phosphorylation capacities of BAK1, BAK1-5, BRI1 and EFR

As FLS2 CD did not posseses any detectable phosphorylation capacity *in vitro*, I focused my trans-phosphorylation studies with BAK1 and BAK1-5 on the comparison between the non-RD kinase EFR and the RD kinase BRI1.

I first confirmed in our experimental conditions that BAK1 CD was able to trans-phosphorylate BRI1* CD, and reciprocally that BRI1 CD was able to trans-phosphorylate BAK1* CD (Figure 6.7 A). Next, I asked if the increased auto- and trans-phosphorylation capacities of BAK1-5 CD (Figure 6.5) would translate into an increased trans-phosphorylation of the biologically relevant substrate BRI1* CD.

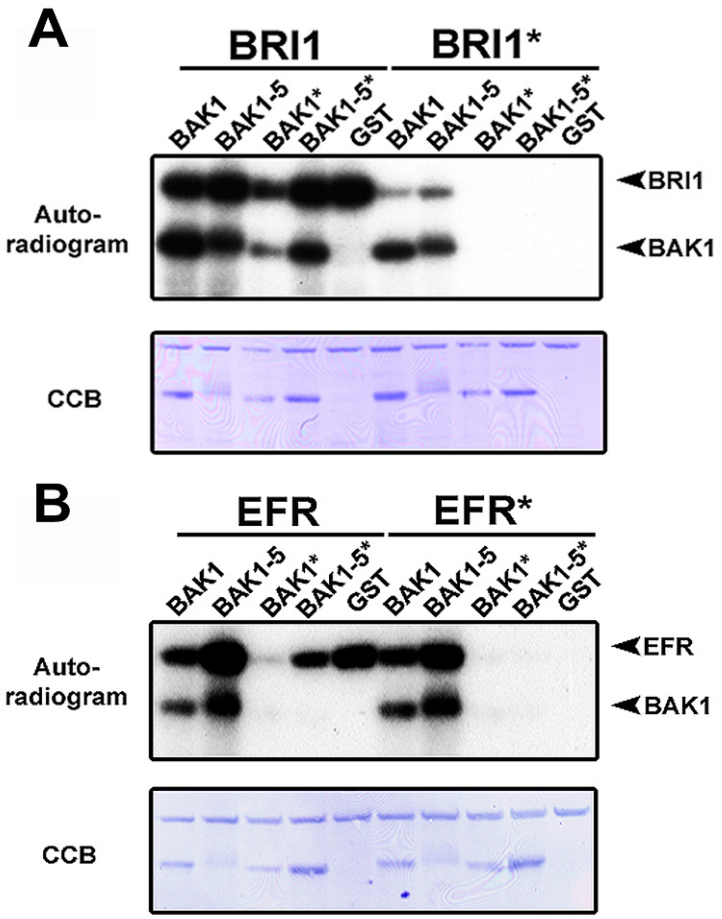

Figure 6.7. Differential transphosphorylation capacities of BAK1, BAK1-5, BRI1 and EFR.

A. BRI1 and BAK1 undergo bi-directional trans-phosphorylation *in vitro*. *In vitro* kinase assay incubating equal amounts of N-terminal MBP-tagged BRI1 or BRI1* CD with N-terminal GST-tagged BAK1, BAK1*, BAK1-5, BAK1-5* CD or GST control, respectively. Autoradiogram, upper panel; Coomassie colloidal blue stained membrane, lower panel.

B. Uni-directional trans-phosphorylation of EFR by BAK1 *in vitro*. *In vitro* kinase assay incubating equal amounts of N-terminal MBP-tagged EFR or EFR* CD with N-terminal GST-tagged BAK1, BAK1*, BAK1-5, BAK1-5* CD or GST control, respectively. Autoradiogram, upper panel; Coomassie colloidal blue stained membrane, lower panel.

Indeed, BAK1-5 CD hyper trans-phosphorylated BRI1* CD (Figure 6.7 A). Interestingly, BAK1* CD slightly inhibited BRI1 CD auto-phosphorylation, when compared to the empty vector control GST (Figure 6.7 A). In contrast, BAK1-5* CD hardly influenced BRI1 CD auto-phosphorylation activity and therefore was still strongly trans-phosphorylated by BRI1 CD (Figure 6.7 A).

Next, I investigated the *in vitro* trans-phosphorylation events surrounding EFR CD. I found that BAK1 CD was able to trans-phosphorylate EFR* CD to a level comparable to the EFR CD auto-phosphorylation (Figure 6.7 B). This is in contrast to the BAK1-BRI1 trans-phosphorylation events in which BAK1 CD trans-phosphorylation of BRI1* CD is minimal in comparison to BRI1 CD auto-phosphorylation (Figure 6.7 B). Another striking difference was the inability of EFR CD to trans-phosphorylate BAK1* CD (Figure 6.7 B). This could be due to the inhibition of EFR CD (auto)-phosphorylation by BAK1* CD. However, EFR CD was still unable to trans-phosphorylate BAK1-5* CD, which hardly influenced EFR CD auto-phosphorylation (Figure 6.7 B). Importantly, BAK1-5 CD was able to hyper trans-phosphorylate EFR* CD and significantly enhanced the phosphorylation status of EFR CD (Figure 6.7 B).

6.2.8. The kinase activity of BAK1-5 is required for the *bak1-5* phenotype

I tested if the kinase activity of BAK1-5 is required for the *bak1-5* phenotype. As *bak1-5* has the strongest differential phenotype with elf18 response when compared to *bak1-4*, I concentrated on EFR-dependent responses to address this question.
I created stable transgenic lines in the *bak1-4* background expressing *BAK1*, *BAK1**, *BAK1-5* and *BAK1-5** under the native regulatory sequence of *BAK1* (Figure 6.8 A). The wild-type allele of *BAK1* was able to rescue the reduced and delayed elf18-induced ROS burst of *bak1-4* (Figure 6.8 B). As previously shown (see Chapter 4), expression of *BAK1-5* in *bak1-4* recapitulated the *bak1-5* phenotype (Figure 6.8 B). Interestingly, the expression of the kinase inactive *BAK1** in *bak1-4* led to a further decrease in elf18-induced ROS burst (Figure 6.8 B), revealing a dominant-negative effect of *BAK1** and demonstrating the importance of BAK1 kinase activity for downstream signalling. Strikingly, the expression of *BAK1-5** in *bak1-4* led to a similar dominant-negative effect as *BAK1** but did not fully suppress elf18-induced ROS burst as observed in *bak1-5* or when *BAK1-5* was expressed in *bak1-4* (Figure 6.8 B).

These two observations demonstrate that BAK1-5 requires its kinase activity to quench EFR-dependent signalling. More importantly, it strongly suggests that the differential impact of the *bak1-5* mutation on different signalling pathways is linked to phosphorylation.

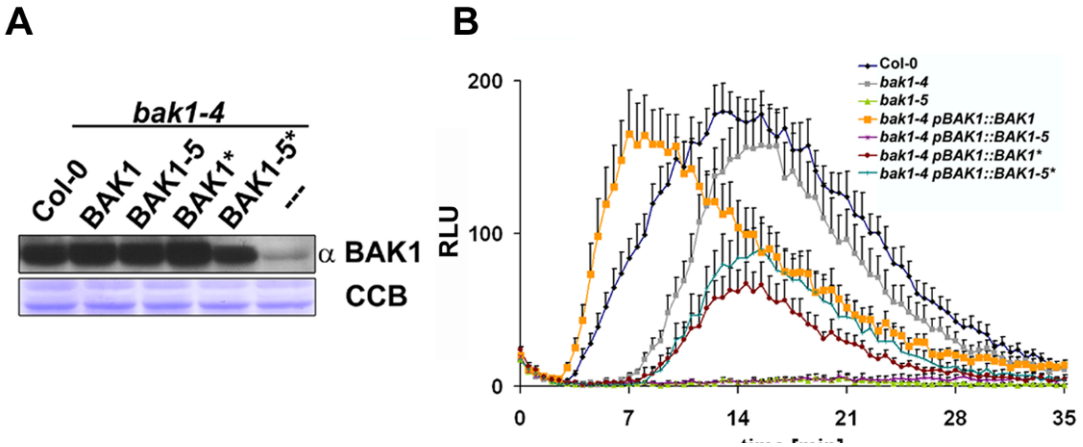

Figure 6.8. BAK1-5 requires its kinase activity for surpression of elf18-induced ROS burst.

A. Expression of BAK1, BAK1-5, BAK1* and BAK1-5* in transgenic plants in the *bak1-4* background. Immunoblot of total proteins from Col-0, *bak1-4 pBAK1::BAK1*, *bak1-4 pBAK1::BAK1**, *bak1-4 pBAK1::BAK1-5, pBAK1::BAK1-5** and *bak1-4* using anti-BAK1 antibodies. Immunoblot, upper panel; Coomassie colloidal blue stained membrane, lower panel.

B. The kinase activity of BAK1-5 is required for the suppression of elf18-induced ROS burst. ROS burst in leaves of Col-0, *bak1-4*, *bak1-5*, *bak1-4 pBAK1::BAK1*, *bak1-4 pBAK1::BAK1-5 bak1-4, pBAK1::BAK1** and *bak1-4 pBAK1::BAK1-5** treated with 100 nM elf18. Results are average ± s.e. (n=8).

6.2.9. Mapping of *in vitro* phosphorylation sites on BAK1 and BAK1-5

I demonstrated that BAK1-5 is a hyper-active kinase *in vitro* and its kinase activity is required for full suppression of elf18-induced ROS burst (Figure 6.8 B). In order to obtain a more qualitative insight in the change of the phosphorylation status of BAK1-5 compared to BAK1 I in collaboration with Jan Seklar and Alex Jones performed exhaustive phosphorylation site mapping by tandem mass-spectrometry (MS/MS). The CDs of BAK1, BAK1-5, BAK1* and BAK1-5* were used in nonradioactive autophosphorylation assays and subjected to in gel digestion using one or a combination of the following proteases: trypsin, AspN and elastase. The use of different proteases clearly increased the sequence coverage and the amount of

identified phosphorylation sites, especially in the C-terminus which is deprived of Arg and Lys usually defining trypsin protease specificity. We obtained near total sequence coverage of ≥ 97% for both kinase dead mutant cytoplasmic domains missing only a single 4 aa long-peptide. In the case of BAK1-5 an additional 17 aa long-peptide was missing containing three potential phosphorylation sites. Surprisingly, in the case of BAK1 we were unable to obtain any peptides with good quality scores covering the activation loop. Less stringent database search algorithms consistently suggested that the Thr at position 449 in the activation loop is mutated to an Ala (Figure 6.9 A). This was totally unexpected as previous DNA sequence analysis of the corresponding expression vector did not

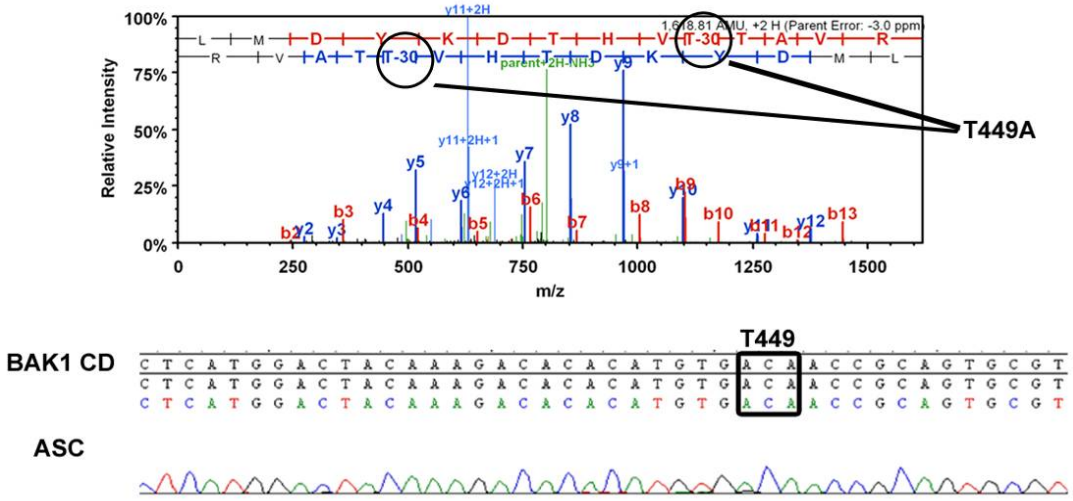

Figure 6.9. The BAK1 CD carries a previously un-identified mutation at position T449 creating an Alanine substitution.

A. Fragmentation spectra identified the threonin at position 449 to substituted by an alanin. The depicted spectrum was obtained using error tolerant search parameters and has an Mascot Ion Score of ≥ 93. The highlighted T-30 indicates a mass loss of 30 Dalton corresponding to a T to A substitution.

B. Absence of T449A corresponding base-pair change in the sequence of the BAK1 CD expression vector. The obtained assigned sequence chromatogram (ASC) corresponding to the peptide sequence depicted in A is shown. The codon corresponding to T449 is boxed.

reveal any point mutation of the corresponding codon (Figure 6.9 B). Nevertheless, the evidence clearly suggested that the analysed BAK1 protein is a mutant variant BAK1(T449A) which has been previously shown to posses reduced kinase activity (Wang et al., 2008). This fact impeded a comprehensive comparative analysis of the phosphorylation status in a qualitative and quantitative manner. However, a

summary of the identified phosphorylation sites is shown in Table 6.1 and the corresponding spectra can be found in the Appendix V.II. Phosphorylation sites were assigned initially using SEQUEST (Eng et al., 1994), Mascot (Perkins et al., 1999) and/or X! Tandem scores. In addition the MS/MS fragmentation spectra of all phosphopeptides were inspected visually to confirm predicted phosphosite assignment.

We were able to identify all previously published *in vitro* and *in vivo* phosphorylation sites (Wang et al., 2008; Karlova et al., 2009) except for the ambiguously identified site T589/S595 (Table 6.1). In addition we obtained good evidence for several previously unpublished sites including two Tyr-phosphorylation sites confirming previous result obtained by immunoblot analysis using anti-phospho-Tyr anti-bodies (Figure 6.5 C). We found two sites in the N-terminal lobe (T355, T357), three in the P+1 loop (Y463, S465, T466) and three additional sites in the C-terminus (S602, T603, Y610) (Table 6.1). In the case of the two neighbouring sites S602 and T603 we cannot exclude that these two predicted sites are actually only one phosphosite. In addition, we found weak evidence for Y443, which was only identified on doubly phosphorylated peptides (Table 6.1).

Interestingly, three of the previously published phosphosites (S286, T312, T455) were also identified as being phosphorylated in BAK1* or BAK1-5* making them potential targets of *E. coli* kinases (Table 6.1).

Identified Site[a]	Domain	BAK1(T449A) CD					BAK1-5 CD				
		Peptide sequence[b]	Sequest Xcorr	delta Cn	Mascot score	X! Tandem	Peptide sequence[b]	Sequest Xcorr	delta Cn	Mascot score	X! Tandem
from single phosphorylated peptides											
S286*	JM	R.ELQVApSDNFSNK.N	2.76	0.434	31.9	2.62	R.ELQVApSDNFSNKNILGR.G	3.17	0.507	66.4	2.36
S290	JM	R.ELQVASDNFpSNKNILGR.G	3.82	0.466	75.6	2.32	R.ELQVASDNFpSNKNILGR.G	3.33	0.508	77.7	2.85
T312*	NT-lope(β3 sheet)	R.LADGpTLVAVKR.L	4.57	0.446	72.7	3.05	R.LADGpTLVAVKR.L	3.69	0.483	92.8	2.89
T355	NT-lope(β4-β5 turn)						R.LRGFcCMpTPTER.L	3.16	0.425	50.2	0.959
T357	NT-lope(β4-β5 turn)						R.LRGFcCMTPpTER.L	3.06	0.397	36.5	2.54
T449	activation loop						K.LMDYKDpTHVTTAVR.G	3.74	0.597	46.9	3.21
T455*	activation loop	R.GpTIGHIAPEYLSTGK.S	4.05	0.503	55.9	5.04	R.GpTIGHIAPEYLSTGK.S	3.89	0.548	82	6.96
Y463	P+1 loop/αEF	R.GTIGHIAPEpYLSTGK.S	3.61	0.511	51.5	4.33	R.GTIGHIAPEpYLSTGK.S	4.02	0.532	69.5	4.04
S465	P+1 loop/αEF						R.GTIGHIAPEYLpSTGK.S	5.25	0.457	68.9	4.55
T466	P+1 loop/αEF	R.GTIGHIAPEYLSpTGK.S	3.05	0.337	34.7	3.6	R.GTIGHIAPEYLSpTGK.S	4.47	0.421	70.5	5.08
S602	CT	G.DpSTSQIENEYPSGPR.-	n.d.	n.d.	94	n.d.	G.DpSTSQIENEYPSGPR.-	n.d.	n.d.	66.1	n.d.
T603	CT	G.DSpTSQIENEYPSGPR.-	n.d.	n.d.	42.8	n.d.	G.DSpTSQIENEYPSGPR.-	n.d.	n.d.	57.5	n.d.
S604	CT	G.DSTpSQIENEYPSGPR.-	n.d.	n.d.	86.8	n.d.					
Y610	CT	G.DSTSQIENEpYPSGPR.-	n.d.	n.d.	45.4	n.d.					
S612	CT	G.DSTSQIENEYPpSGPR.-	n.d.	n.d.	66	n.d.	G.DSTSQIENEYPpSGPR.-	n.d.	n.d.	76.1	n.d.
from doubly phosphorylated peptides											
S286/S290	JM						R.ELQVApSDNFpSNKNILGR.G	2.85	0.487	55.1	2.46
Y443/T449	activation loop						K.LMDpYKDTHVpTTAVR.G	3.14	0.329	37.3	1.89
Y443/T450	activation loop						K.LMDpYKDTHVTpTAVR.G	2.64	0.304	30.7	-0.477
T446/T449	activation loop						K.DpTHVpTTAVR.G	3.86	0.313	40.7	0.854
T455/S465	activation loop/P+1 loop						R.GpTIGHIAPEYLpSTGK.S	4.89	0.523	54.8	1.48
T455/T466	activation loop/P+1 loop						R.GpTIGHIAPEYLSpTGK.S	4.46	0.524	56.3	1.74
T455/Y463	activation loop/P+1 loop						R.GpTIGHIAPEpYLSTGK.S	3.6	0.492	27.9	2.26

Table 6.1. Identification of *in vitro* phosphorylation sites of BAK1(T449A) or BAK1-5 by MS/MS analysis.

[a] underlined residues have been identified previously as *in vitro* and/or *in vivo* phoshporylation sites (Karlova et al. 2009, Wang et al. 2008). The "*" indicates residues which were found to be phosphorylated in the kinase dead variants BAK1* or BAK1-5* CD.

[b] identified peptide sequence including amino acid residues before and after, respectively the corresponding residues in the primary protein sequence. Carbamylation of cystein residues is indicated by a preceding "c", phosphorylation of serine, threonine or tryosin residues in denoted by a preceding "p"

Corrigendum:

6.2.10. BAK1-5 is a hypo-active kinase able to trans-phosphorylate BRI1 and EFR *in vitro*

As soon as I identified the missense substitution of the *in vitro* expression clone of BAK1 CD, I in collaboration with Yasuhiro Kadota re-transformed the expression vector and confirmed the presence of the wild-type plasmid in individual *E. coli* BL21 clones (data not shown). We re-purified all four proteins, BAK1, BAK1-5, BAK1* and BAK1-5* after heterologous expression in *E.coli*. To test for the overall phosphorylation status we performed cold kinases assays in combination with immunoblot analysis using anti-phospho-Thr/Ser or anti-phospho-Tyr antibodies (Figure 6.10. A-B). BAK1 CD displayed an even more dramatic mobility shift on SDS-PAGE than BAK1-5 CD suggesting a compromised kinase activity of BAK1-5 CD *in vitro*. This was indeed confirmed by immunoblot analysis as the signal corresponding to BAK1-5 CD was considerably lower than this of BAK1 CD for either phospho-Thr/Ser (α P-T) or phospho-Tyr (α P-Y) sites, respectively (Figure 6.10. A-B). We than tested if BAK1-5 CD was still able to trans-phosphorylate BRI1 or EFR CD *in vitro*. Therefore, we performed radioactive kinase assays using [^{32}P]-γ-ATP. When we incubated BAK1 with BRI1* CD we could see a clear trans-phosphorylation of BRI1* CD (Figure 6.10. C). Similarly, BAK1-5 CD was able to trans-phosphorylate BRI1* CD albeit to a lower level. Both BAK1* and BAK1-5* CD were trans-phorylated by BRI1 CD to similar degree (Figure 6.10 C). Therefore, BAK1/BAK1-5 CD undergo a bi-directional trans-phosphorylation with BRI1 CD *in vitro*. Next, we investigated the trans-phosphorylation events between EFR CD and BAK1/BAK1-5 CD. Both BAK1 and BAK1-5 CD were able to trans-phosphorylate EFR* CD (Figure 6.10 D). However, the trans-phosphorylation activity of BAK1-5 CD on EFR* CD was considerably lower when compared to BAK1 CD. Interestingly, the trans-phosphorylation of EFR* CD by BAK1 CD was much stronger than the auto-phosphorylation of EFR CD (Figure 6.10. D). This relatively low activity of EFR CD was also reflected by its inability to trans-phosphorylate

BAK1* or BAK1-5* CD (Figure 6.10. D). Therefore, BAK1/BAK1-5 CD undergo unidirectional phosphorylation with EFR CD *in vitro*.

These results confirm previous observations on the difference in phosphorylation directionality between BAK1/BRI1 and BAK1/EFR shown in 6.7. In addition, they illustrate that BAK1-5 has a reduced kinase activity and is able to trans-phosphorylate either ligand-binding receptor *in vitro*.

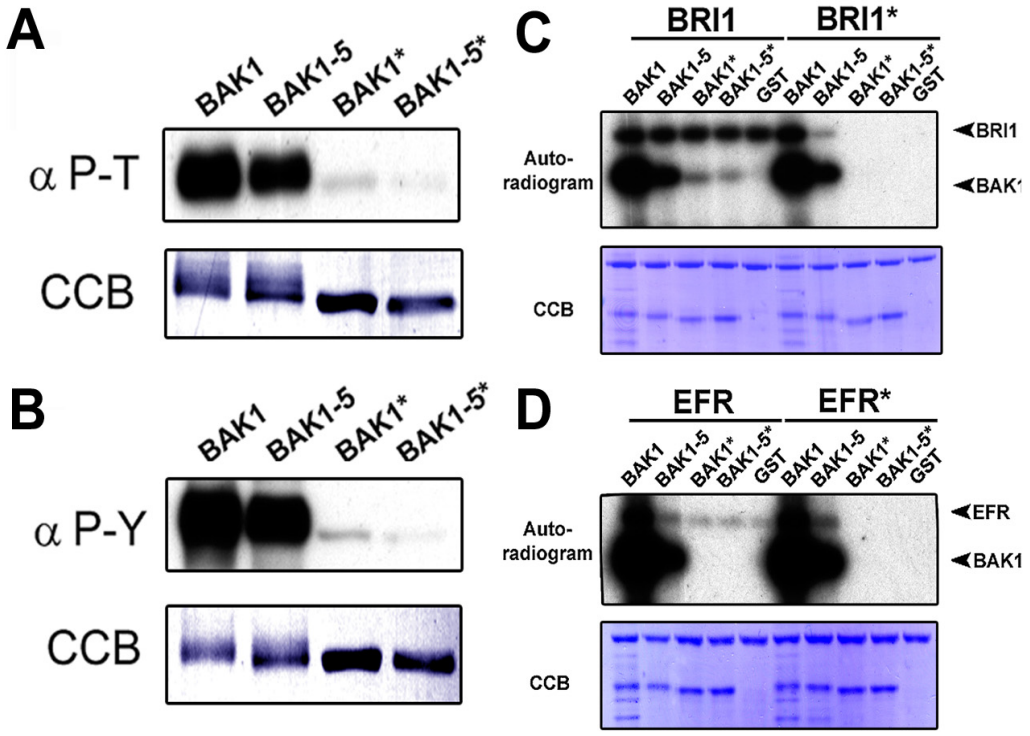

Figure 6.10. BAK1-5 is a hypo-active kinase able to transphosphorylate BRI1 and EFR *in vitro*.

A. BAK1-5 CD is a hypo-active kinase on Ser and Thr residues. 0.25 µg of heterologously-expressed N-terminal GST-tagged BAK1, BAK1-5, BAK1* and BAK1-5* CD were subjected to immunoblot analysis with anti-phosphoThr antibodies. Immunoblot, upper panel; Coomassie colloidal blue stained membrane, lower panel.

B. BAK1-5 CD is a hypo-active kinase on Tyr residues. 0.75 µg of heterologously-expressed N-terminal GST-tagged BAK1, BAK1-5, BAK1* and BAK1-5* CD were subjected to immunoblot analysis with anti-phospho-Tyr antibodies. Immunoblot, upper panel; Coomassie colloidal blue stained membrane, lower panel.

C. BRI1 and BAK1 undergo bi-directional trans-phosphorylation *in vitro*. *In vitro* kinase assay incubating equal amounts of N-terminal MBP-tagged BRI1 or BRI1* CD with N-terminal GST-tagged BAK1, BAK1*, BAK1-5, BAK1-5* CD or GST control, respectively. Autoradiogram, upper panel; Coomassie colloidal blue stained membrane, lower panel.

D. Uni-directional trans-phosphorylation of EFR by BAK1 *in vitro*. *In vitro* kinase assay incubating equal amounts of N-terminal MBP-tagged EFR or EFR* CD with N-terminal GST-tagged BAK1, BAK1*, BAK1-5, BAK1-5* CD or GST control, respectively. Autoradiogram, upper panel; Coomassie colloidal blue stained membrane, lower panel.

6.3. Discussion

In recent years, the importance of the regulatory RLK BAK1 became apparent, as it is involved in several independent signalling pathways, namely BR responses, innate immunity, and cell death control (Chinchilla et al., 2009). It was however unclear whether the regulatory role and the importance of BAK1 in these different biological processes is similar. The results presented in Chapters 4 and 5 clearly suggest that BAK1 is able to differentially regulate these different signalling pathways as *bak1-5* mutant plants are strongly impaired in PTI-signalling but display a wild-type-like behaviour in respect to BAK1-dependent cell death control and BR-signalling. In this chapter I explored the underlying biochemical mechanisms of this observed phenomenon. Intriguingly, BAK1-5 displayed an enhanced interaction with the three different ligand-binding RKs FLS2, EFR and BRI1 (Figure 6.2-6.4). Interestingly, BAK1-5 is a hypo-active kinase *in vitro* that is able to trans-phosphorylate the two ligand-binding RKs EFR and BRI1 (Figure 6.10). Importantly, BAK1-5 requires its kinase activity to suppress EFR-dependent PTI-signalling as *bak1-4* plants expressing kinase dead BAK1-5* were only partially able to suppress elf18-triggered ROS burst (Figure 6.8). Therefore, BAK1-5 differentially regulates PTI- and BR-signalling in a phosphorylation dependent manner.

In addition, I was able to show a significant difference in the kinase activities of the two RD-kinases BRI1 and BAK1 compared with the two non-RD kinases FLS2 and EFR *in vitro* (Figure 6.6 and 6.10). Furthermore, whereas BRI1 and BAK1 underwent a bidirectional phosphorylation, only a unidirectional phosphorylation originating from BAK1 could be observed in the case of EFR and BAK1 (Figures 6.8 and 6.10).

6.3.1. Phosphorylation-dependent differential regulation of BAK1-dependent signalling pathways

My initial (clearly) over simplified working hypothesis for the differential regulation of PTI- and BR-signalling in *bak1-5* was based on a potential differential interaction

of BAK1-5 with the different ligand-binding RKs. However, this hypothesis did not hold true as BAK1-5 displays an enhanced interaction with all three ligand-binding RKs tested, namely FLS2, EFR and BRI1 (Figure 6.2-4). Surprisingly, I found that BAK1-5 is a hypo-active kinase *in vitro* (Figures 6.10). This reduced kinase activity of BAK1-5 might be sufficient to support BR-signalling but not PTI-signalling. Yet, several observations do not support this hypothesis: (i) There is no direct correlation between the *in vitro* kinase activity of BAK1 mutant variants and their ability to complement either the compromised flg22-triggered SGI of *bak1-4 bkk1-1* or the growth retardation phenotype of *bri1-5* (Wang et al., 2008). BAK1(T449A) is able to complement both phenotypes but has a reduced kinase activity compared to BAK1(T450A) that is not able to complement either phenotype (Wang et al., 2008). Interestingly, BAK1-5 posses a stronger kinase activity than BAK1(T449A) (data not shown) further substantiating this observation. (ii) Plants expressing the hypo-active kinase variant BAK1(Y610F) are blocked only in BR signalling but not flg22-triggered SGI (Oh et al. 2010) thereby displaying an opposite phenotype to *bak1-5* plants even though both BAK1 variants are compromised in their overall kinase activity. Therefore, the quantitative kinase output of BAK1 is not the determining factor *per se* that enables BAK1 to function in PTI- or BR-signalling (Table 6.2). (iii) In *bak1-5* plants PTI signalling is not simply more strongly impaired than in *bak1-4* loss of function mutants but rather differentially regulated. This is exemplified in the differential MPK activation in *bak1-5* plants whereby MPK3 and 6 but not MPK4 are fully activated 15 mins after ligand-treatment (Figure 6.5). (iv) BAK1-5 requires its kinase activity to fully suppress efl18-triggered ROS-burst *in vivo* (Figure 6.8). Altogether, this leads to the new hypothesis that BAK1-5 differentially regulates PTI- and BR-signalling pathways by discriminative auto-phosphorylation and/or trans-phosphorylation of the main-ligand binding receptors. Therefore, the qualitative kinase output of BAK1 defines its signal competence in respect to PTI- or BR- signalling pathways.

	BAK1	BAK1-5 (C408Y)	BAK1 (Y610F)[2]	BAK1 (T450A)[1]	BAK1 (T449A)[1]	BAK1* (D418N)[3]
PTI	**WT**	**---**	**WT[b]**	**-[b]**	**WT[b]**	**--**
BR	**WT**	**WT**	**--**	**-**	**WT**	**---**
Cell-death	**WT**	**WT**	**WT**	**WT**	**WT**	**-**
kinase activity[a]	**WT**	**-**	**-/--**	**--**	**---**	**----**

Table 6.2.: The quantitative kinase out-put of BAK1 is not correlated with its ability to full-fill its function in PTI or BR signaling pathways.
The number of "- " indicates the severity of impairment of BAK1's specific function
[a] *in vitro* kinase activity of BAK1 variants, relative impairment partially approximated
[b] Impairment in PTI signaling was only measured as the respective BAK1 variant's ability to rescue bak1-4 bkk1-1 impairment in flg22-triggered SGI
[1] ref. Wang et al. 2008
[2] ref. Oh et al. 2010
[3] ref. Li et al. 2002, Wang et al. 2008 and present study

6.3.2. The differential regulation of BAK1-dependet signalling pathways

The current paradigmatic model based on BRI1 and BAK1, implies that BAK1 is a mere signalling enhancer required for optimal activity of BRI1 and subsequent signalling (Gendron and Wang 2007; Wang et al., 2008). Upon BR binding, trans-phosphorylation of BRI1 in the preformed homodimer induces BRI1 kinase activity, a prerequisite for heteromerization with BAK1. Trans-phosphorylation of BAK1 on residues in the kinase domain activates BAK1, which then trans-phosphorylates BRI1 on residues within the intracellular juxta-membrane and C-terminal regions increasing BRI1 kinase activity (Wang et al., 2008). Ligand-activated BRI1 can signal without BAK1, but its signalling output is increased by BAK1. In contrast little is known about the molecular events surrounding the BAK1 and FLS2/EFR interactions. It is known that the heterocomplex formations are ligand-inducible (Chinchilla et al. 2007; Heese et al., 2007; Roux et al., *submitted*) and that at least in the case of FLS2 happens *quasi* instantaneously with ligand addition (Schulze et al., 2010). Another important difference between the interaction of BRI1-BAK1 and FLS2/EFR-BAK1 is that the former requires BRI1 but not BAK1 kinase activity for

full interaction *in vivo* (Wang et al., 2008) whereas the later is totally kinase independent (Milena Roux, unpublished). In both cases BAK1 kinase activity does not influence the interaction status. So, for me it was intitially counterintuitive that BAK1-5, having a reduced kinase activity *in vitro*, displays an enhanced interaction with the ligand binding RKs in co-immunoprecipitation experiments even without ligand addition (Figure 6.2-4). These initially counterintuitive observations might be unified in the following hypotheses. BAK1-5 might be a de-regulated kinase *in vivo* and thereby be constitutively active albeit with a *sensus stricto* lower activity than wild-type BAK1. The position of the BAK1-5 muatation (C408Y) clusters with potentially orthologous mutations in the mammalian RKs ALK1 (F1245C) and EGFR (L833V) (George et al., 2008; Mosse et al., 2008) at the interface between the β6 and β9 strands in the active kinase conformation structure (Kannan and Neuwald, 2005). Interestingly, the interface between the β6 and β9 strands is involved in the correct positioning of the activation segment and of residues in the catalytic loop and is a hotspot for oncogenic mutations (Dibb et al., 2004). Therefore, the C408Y mutation might interfere with the proper positioning of the core catalytic residues leading to reduced kinase activity *in vitro* as observed for BAK1-5 (Figure 6.10). However, residues in the β6 strand are also known to be involved in kinase auto-inhibition either by its C-terminal tail or in case of several mammalian RTKs by its juxta-membrane region (Kobe et al., 1996; Hubbard 2004; Dibb et al., 2004; Bose and Zhang, 2009). The C408Y mutation potentially not only reduces kinase activity *sensus stricto* but in addition might interfere with auto-inhibition *in vivo*. FLS2 and BAK1 are assumed to assemble in preformed complex in close proximity in the plasma membrane as their interaction occurs *quasi* instantaneously with ligand addition (Schulze et al., 2010). A deregulated but still active BAK1-5 might stabilize these preformed complexes leading to the enhanced interaction *in vivo* observed in co-immunoprecipitation experiments (Figure 6.2-4). Similarly, a deregulated BAK1-5 might stabilize a complex with BRI1 leading to a more frequent interaction *in vivo* and thereby to an increased immunoblot signal in co-immunoprecipitation experiments (Figure 6.2-4). This would also explain the slight BR hypersensitivity of *bak1-5* observed in some bioassays (see Chapter 5).

Alternatively, the hypo-active kinase BAK1-5 might form a dead-locked and thereby stabilized complex with the ligand-binding receptors. In the case of PRRs this could quell the kinase activity of the receptor and down-stream signalling activation.

In order to test these different hypotheses I attempted to investigate the kinase acitivty or phosphorylation status of BAK1, BAK1-5 and the respective ligand-binding receptors BRI1 and FLS2 *in vivo*. I combined immunoprecipitation of the protein of interested using endogenous antibodies against the native proteins with immunoblot analysis with anti-phospho-Thr/Ser antibodies. Unfortunately, no signal specific to the immunoprecipitated protein could be observed (data not shown). Similarly, I did not succeed in performing isoelectric focusing in combination with immunoblot analysis using antibodies against the protein of interest (data not shown). Finally, I also tried to combine immunoprecipitation of the protein of interest with *in vitro* kinase assays using MYBP as artificial substrate. This was unsuccessful most likely due to precipitation of proteins due to high salt concentrations (data not shown). In future studies I will try to adapt the protocols accordingly.

Intriguingly, the expression of BAK1:GFP and BAK1:HA_3 was able to rescue the BR-related growth phenotype of *bak1-4* but not the compromised flg22-triggered ROS burst and SGI (Figure 6.1, data not shown). On the contrary BAK1:GFP and BAK1:HA_3 seemed to have a slight dominant negative effect on the responsiveness of *bak1-4* to elf18 in SGI assay (Figure 6.1, data not shown). This suggests that the C-terminal tag on BAK1 does not block BRI1-specific responses but interfers with FLS2-and EFR-dependent signalling. This is not due to a compromised interaction of BAK1:GFP and BAK1:HA_3 with FLS2 or EFR (Figure 6.2-3, 7.1, data not shown), but might be due to imposed structural changes on the C-terminal tail of BAK1. This differential complementation of *bak1-4* phenotypes by C-terminally tagged BAK1 variants is in accordance with the differential regulation of PTI- and BR-signalling in *bak1-5* mutant plants (see Chapter 4 and 5). The enhanced interaction of BAK1-5 with FLS2 and EFR (Figure 6.2-4) does not explain *per se* the inhibition of PTI signalling observed in *bak1-5*. However this inhibition requires the kinase activity of BAK1-5 (Figure 6.9). Therefore, I would like to suggest that in contrast to BR-signalling, in which BAK1 is potentially only a signal enhancer

(Wang et al., 2008), BAK1 might be an intrinsic component of PTI-signalling. The differential auto-phosphorylation of BAK1-5 could theoretically already lead to a differential interaction surface for potential downstream signalling components. Alternatively or concomitantly, BAK1-5 could trans-phosphorylate specific residues on EFR and FLS2 that would affect interactions with positive and/or negative regulators such as BIK1 and related proteins (Zhang et al., 2010; Lu et. al. 2010). Phosphorylation of specific phosphosites in the juxta-membrane region and C-terminal tail of mammalian RTKs and Ser/Thr RKs are known to regulate signal complex composition, sub-cellular localization, receptor degradation, and therefore the initiation, amplitude, complexity and/or duration of the signal (Birchmeier et al., 2003; Lemmon and Schlessinger, 2010). Importantly, neither FLS2 nor BAK1-5 protein levels were reduced in *bak1-5* (Figure 6.4) showing that BAK1-5 does not affect its own or the expression level of FLS2. Similarly, BAK1:GFP and BAK1:HA_3 might be unable to phosphorylate specific residues in their C-terminal tail and/or bind to specific PTI down-stream signalling partners.

In this respect it is also noteworthy that BAK1 was recently shown to be a dual specificity kinase that also auto-phosphorylates on Tyr residues *in vitro* (Oh et al., 2009) (Figure 6.10). As in mammals, these phosphorylated Tyr residues could represent docking sites in the C-terminal tail and recruit specific interaction partners (*eg.* SH2 domain-containing proteins) dictating signalling specificity (Pawson, Cell 2004; Bae et al., Cell 2009; de la Fuente van Bentem and Hirt, 2009; Lemmon and Schlessinger, 2010).

6.3.3. Differential regulation of RD and non-RD kinases

The differential impact of *bak1-5* on BRI1-dependent and FLS2/EFR-dependent signalling could also be related to a more general differential regulation of RD versus non-RD kinases. RD kinases carry an arginine (Arg) before the conserved catalytic core Asp, and are in general activated by phosphorylation in the activation loop. The phospho-groups interact with a positively-charged pocket containing the Arg and most likely re-orient residues within the catalytic loop, ATP-binding pocket

and/or facilitate peptide substrate binding (Nolen et al., 2004). In contrast, non-RD kinases do not require phosphorylation of the activation loop to adopt an active confirmation. They are rather regulated by different mechanisms such as relief of auto-inhibition by C-terminal extensions (Kobe et al., 1996), Tyr phosphorylation in the P+1 loop (Mayans et al., 1998), or are constitutively active kinases due to intrinsic structural properties (Nolen et al., 2001).

Interestingly, the RD-kinase BRI1 was far more active *in vitro* in our conditions than the non-RD kinases EFR and FLS2 showing strong auto- and trans-phosphorylation capacities (Figure 6.6, 7, 10). EFR did possess some degree of auto-phosphorylation (Figure 6.6), but no trans-phosphorylation capacity either towards the artificial kinase substrate MBP (Figure 6.6), or towards the physiologically-relevant BAK1 kinase domain (Figure 6.10). Surprisingly, I was unable to detect any *in vitro* kinase activity for FLS2 CD (residues 840 to 1173) neither as N-terminal MBP-tag nor His-tag fusion protein, especially in comparison to the strong BRI1 kinase activity (Figure 6.7). This is in contradiction with previous reports (Gomez-Gomez et al, 2001; Xiang et al., 2008; Lu et al., 2010). Initially, a N-terminal GST-tag fusion of FLS2 (residues 840 to 1173) was reported to be kinase active *in vitro* (Gomez-Gomez et al., 2001; Gohre et al., 2008) and this activity was abolished by a single substitution corresponding to the *fls2-17* mutation leading to the change of a highly conserved Gly into an Arg (G1064R) in the subdomain IX (Gomez-Gomez et al., 2001). This result indicated that FLS2 kinase activity is required for flg22 binding as *fls2-17* mutants showed a reduced flg22-binding capacity (Gomez-Gomez et al. 2001). However, this conclusion was later refuted as no full-length FLS2 protein could be detected in *fls2-17* extracts (Robatzek et al., 2007). Next, *in vitro* kinase activity of a N-terminal His-tag fusion of FLS2 (residues 840 to 1173) was reported (Xiang et al., 2008). Yet, the important control of a kinase inactive variant was omitted, and a recent publication by the same research group reported that recombinant FLS2 possesses only weak kinase activity impeding analysis of trans-phosphorylation events *in vitro* (Zhang et al., 2010). This is in agreement with another recent report showing only residual kinase activity of FLS2 CD (residues 832 to 1173); although once again no control with kinase inactive variant was

presented (Lu et al., 2010). Notably, close sequence analysis of the FLS2 kinase domain revealed a low conservation of the otherwise highly conserved Gly-rich loop [GxGxxG] in subdomain I, which is involved in the correct positioning of the substrate ATP (Bossemeyer 1994). Particularly, the replacement of the second invariant Gly by a Ser (S879) in FLS2 is predicted to lead to a dramatic reduction in kinase activity, as mutation of the corresponding Gly in the model Ser/Thr kinase cAPK reduces the kinase activity by 50-fold (Taylor et al., 1999).

Strikingly, in contrast to the situation with BRI1 and BAK1, no trans-phosphorylation of BAK1 by EFR (or FLS2) could be observed *in vitro* (Figure 6.7, 10, data not shown). Yet, BAK1 is capable of trans-phosphorylating EFR *in vitro* (Figure 6.10). Of course, I cannot exclude that FLS2 and EFR kinase domains are only fully activated *in vivo* after extracellular ligand binding via conformation changes mediated by the trans-membrane domain, which is missing in the *in vitro* system.

Consistently with their low activity in *in vitro* kinase assays, no phosphosites could be identified by mass spectrometry on recombinant EFR or FLS2 CDs (data not shown). Interestingly, even in the case of the well-studied non-RD kinase XA21, all studied phosphorylation sites were initially found by targeted mutagenesis and not by mass spectrometry analysis (Xu et al., 2006; Chen et al., 2010).

Nevertheless, the kinase activities and some potential phosphosites of FLS2 and EFR seem important for downstream signalling. A kinase-dead version of EFR (EFR*) is unable to confer elf18-triggered ROS burst when transiently expressed in *N. benthamiana* (data not shown). A K898M mutation in the FLS2 kinase domain abolished MPK3 and MPK6 activation by flg22 after transient over-expression in *fls2* mutant protoplasts (Asai et al. 2002); however controls for protein expression and kinase activity were missing. Targeted mutagenesis of potential phosphosites in FLS2 revealed that T867, T1040 and T1072 are required for its full functionality (Robatzek et al., 2007). However, it was not investigated if these sites are required for kinase activity, are auto-phosphorylation sites, or whether they represent trans-phophorylation targets of BAK1.

Overall, the striking difference between the kinase activities of the two RD kinases BRI1 and BAK1 compared to the non-RD kinases EFR and FLS2 suggests a different regulatory mechanism between these two kinase classes. Interestingly, a highly conserved Thr residue in the intracellular juxta-membrane domain reveals a differential regulation of the overall kinase activity of RD and non-RD kinase by a single site. Accordingly, T705 of the non-RD kinase XA21 is essential for *in vitro* auto-phosphorylation, interaction with downstream signalling components, and for XA21-mediated resistance (Chen et al., 2010). Similarly, a mutation of the corresponding residue in FLS2 (T867) compromised its function *in planta* (Robatzek et al., 2006). However, in the case of the RD kinase BRI1 the phosphorylation of the corresponding Thr (T880) is not required for its function (Wang et al., 2005).

Another difference between RD and non-RD RK seems to be the requirement of kinase activity for complex formation with the RD-RLK BAK1. We found that the kinase activity of neither interaction partner is required for the ligand-induced interaction of FLS2 or EFR with BAK1 (Milena Roux, unpublished). Optimal ligand-dependent heteromerization could even be induced between double mutant combinations of FLS2* or EFR* with BAK1* (Milena Roux, unpulished). These results obtained after transient over-expression in *N. benthamiana* nicely complement previous pharmalogical studies in *A. thaliana* cell cultures (Schulze et al., 2010). Treatment of cell cultures with the broad-range kinase inhibitor K252a did not block FLS2-BAK1 complex formation, but totally inhibited phosphorylation of either of the interaction partners. Ligand-dependent conformational changes thus seem sufficient to trigger heteromerization between the non-RD kinases EFR and FLS2 with BAK1. Therefore, the interaction of EFR and FLS2 with BAK1 is a requirement for rather than a consequence of detectable phosphorylation. This situation is in stark contrast with the absolute requirement of the BRI1 kinase activity for the ligand-induced complex formation with BAK1 *in planta* (Wang et al., 2008).

Chapter 7: Towards the identification of novel PAMPs inducing BAK1-dependent responses and BAK1-interacting proteins using BAK1-5

7.1. Objectives

Relatively little is know about the immediate downstream events after oligomerization between FLS2/EFR and BAK1. Only recently it was shown that the membrane-associated cytoplasmic kinase BIK1 and related PBL proteins positively regulate PTI-signalling. BIK1 and PBL proteins form constitutive complexes with FLS2 and EFR (Zhang et al., 2010a; Lu et al., 2010). They are phosphorylated within minutes of flg22 or efl18 treatment and released from the complex; both events requiring kinase active BAK1. Whether BAK1 directly interacts with BIK1 is still controversial (Zhang et al., 2010; Lu et al., 2010). Another BAK1-interacting protein is BIR1, a LRR-RLK belonging to the subfamily Xa. Interestingly, *bir1* mutants show constitutive cell death under normal growth conditions suggesting an involvement in *BAK1*-dependent cell-death control (Gao et al., 2009).

Also, the knowledge of the molecular identity of PRRs upstream of BAK1 is scarce. It is known that in *Arabidopsis* the recognition of at least three "orphan" PAMPs, namely HrpZ, lipopolysaccharides and peptidoglycans is BAK1-dependent (Shan et al., 2008). Furthermore, the hyper-susceptibility of *bak1-5 fls2 efr* and *bak1-5 bkk1-1* to bacterial and oomycete pathogens suggests the existence of additional yet unknown PAMPs, which recognition is dependent on *BAK1* and/or *BKK1* (see Chapter 4). Interestingly, BAK1-5 displayed an enhanced interaction with the two known PRRs FLS2 and EFR (see Chapter 6). By extrapolating this knowledge to yet unknown BAK1-dependent PRRs BAK1-5 seems to be the perfect tool to identify new PRRs by MS/MS analysis.

Here, I present recent progresses in identifying novel BAK1/BAK1-5-interacting proteins. First, in a proof of concept experiment I identified FLS2 as a major flg22-dependent BAK1 interaction partner by MS/MS analysis. Furthermore, I show that BAK1 exists in complex with other SERK family members. I also show that BAK1

interacts with close homologs of BIR1, and that BAK1 is involved in the perception of yet unknown PAMPs from bacteria, fungi and oomycetes.

7.2. Results and Discussion

7.2.1. Identification of FLS2 as a BAK1 interactor by MS/MS analysis

BAK1 was initially identified as flg22-dependent FLS2 interaction partner by immunoprecipitation of FLS2 from flg22-treated *Arabidopsis* cell culture followed by MS/MS analysis of co-immunoprecipitated proteins (Heese et al., 2007). Interestingly, BAK1-5 displayed an enhanced interaction capacity with the ligand-binding receptor FLS2 even without ligand addition (see Chapter 6). Therefore I attempted to exploit this intrinsic property of BAK1-5 to identify novel BAK1 interaction proteins especially PRRs. As a proof of concept experiment in collaboration with Frederikke Gro Malinovsky I tested if we were able to identify FLS2 as a BAK1 interaction partner by MS/MS analysis of co-immunoprecipitated proteins, either after flg22 treatment of wild-type BAK1 expressing plants or exploiting the enhanced affinity of BAK1-5 (see Chapter 6). In order to obtain enough protein for MS/MS analysis we performed large-scale immunoprecipitations on 30-45 ml of 3 mg/ml protein using 10-20 g of 2 to 3 week-old seedlings as starting material for total protein extraction. In the initial experimental set-up we used mock treated *bak1-4* seedlings as negative control, seedlings of *bak1-4 pBAK1::BAK1-G*FP T2 lines treated with flg22 or mock treated seedlings of *bak1-4 pBAK1::BAK1-5-GFP* T2 lines. We immunoprecipitated BAK1-GFP or BAK1-5-GFP from total protein extracts using GFP-trap beads. We also incubated total protein from the negative control *bak1-4* with the same amount of GFP-trap in order to control for non-specific interactions. As shown in Figure 7.1 A we were able to immunoprecipitate some BAK1-GFP or BAK1-5-GFP, respectively, under this "large-scale" conditions. However we were not able to deplete all fusion protein from the total protein extract as significant amounts remained in the flow-through (Figure 7.1 A). Next, we investigated the amount of FLS2 in the immunoprecipitates

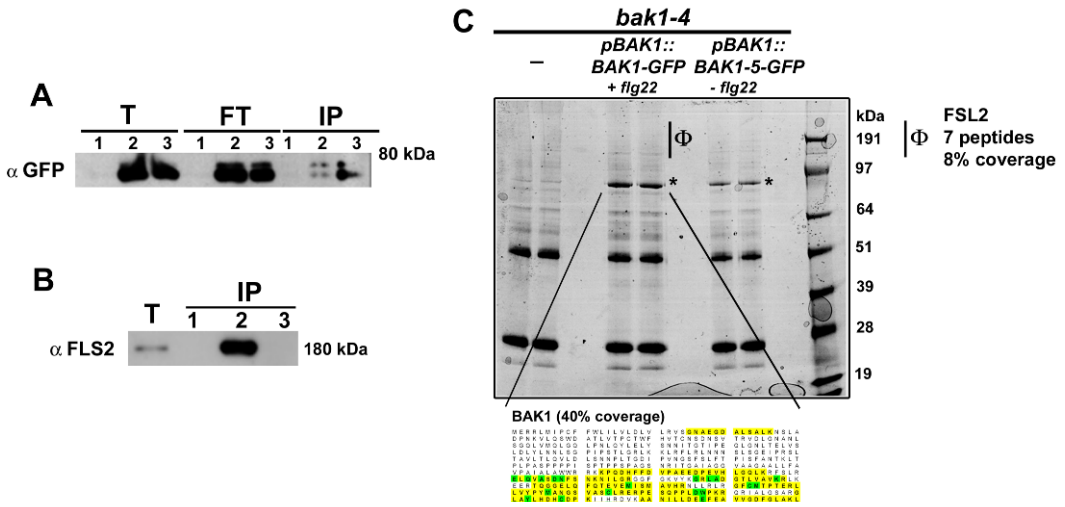

Figure 7.1. Identification of FLS2 as a flg22-dependent BAK1-GFP interacting protein by MS/MS analysis.

A. Partial enrichment of BAK1-GFP or BAK1-5-GFP by large-scale immunoprecipitation. Immunoprecipitation from total protein extracts of *bak1-4* plants (lane 1), *bak1-4 pBAK1::BAK1-GFP* T2 plants treated with 100 nM flg22 for 5 min (lane 2) *or bak1-4 pBAK1::BAK1-5-GFP* T2 plants mock-treated (lane 3) using anti-GFP trap beads. Immunoblot analysis of total protein (T), flow through after immunoprecipitation (FT) and 1/100 of the immunoprecipitate (IP) by anti-GFP antibody.

B. Large-scale co-immunoprecipitation of FLS2 only after flg22-treatment. Immunoprecipitation as described above. Immunoblot analysis of total protein (T) and immunoprecipitate (IP) by anti-FLS2 antibody.

C. Identification of FLS2 as BAK1-GFP interacting protein by MS/MS analysis. Colloidal commasie stain gel of all immunoprecipitated proteins using GFP-trap as described above with graphical depiction of the BAK1 protein sequence coverage obtained by MS/MS analysis. * indicates the band identified as BAK1 or BAK1-5, respectively. Φ indicates the area from where FLS2 peptides were recovered.

by immunoblot analysis using anti-FLS2 antibodies. FLS2 was clearly enriched in the immunoprecipitate of BAK1-GFP but absent in the negative control and the BAK1-5-GFP immunoprecipitate (Figure 7.1 B). The remnant of the immunoprecipitates was separated by SDS-PAGE and proteins visualized using colloidal commassie blue staining (Figure 7.1 C). A protein migrating at similar size to BAK1-GFP and BAK1-5-GFP was clearly enriched in the immunoprecipitates of transgenic plants expressing BAK1-GFP or BAK1-5-GFP, respectively, but absent in the negative control (Figure 7.1 C). No other specific bands could be observed that would be absent in the negative control. As we only wanted to identify FLS2 as a BAK1-interacting protein in this pilot experiment only proteins bigger than 64 kDa were subjected to in-gel tryptic digestion followed by MS/MS analysis. We

Identified Proteins	Accession Number	Identified matching peptides[a]			specific peptides[b]
		plant line/treatment			
		1	2	3	overall
BAK1	AT4G33430.1	0	26	8	8
FLS2	AT5G46330.1	0	7	0	7
LRR-RLK Xa family protein	AT1G27190.1	0	4	0	4
LRR-RLK Xa family protein	AT3G28450.1	0	2	0	2
BIP2	AT5G42020.1	0	16	12	2
IBR3	AT3G06810.1	0	7	0	7
Jacalin lectin family protein	AT3G16460.1	0	6	3	7
RNA binding / nucleic acid binding protein	AT1G33680.1	0	4	0	4
EMB2296	AT2G18020.1	0	2	0	2
ATXYL1	AT1G68560.1	0	2	0	2
ECT4	AT1G55500.1	0	0	3	1
DEAD box RNA helicase	AT2G42520.1	0	0	3	3

Table 7.1 Proteins specifically identified in the immunopreciptates of BAK1-GFP and/or BAK1-5-GFP.

[a] peptides matching the indicated protein and potential other proteins without exclusively matching peptide

[b] number of specific peptides only matching the indicated protein

1 denotes immunoprecipitates of *bak1-4* plants mock treated

2 denotes immunoprecipitates of *bak1-4 pBAK1::BAK1-GFP* plants treated with flg22

3 denotes immunoprecipitates of *bak1-4 pBAK1::BAK1-5-GFP* plants mock treated

identified 26 peptides covering 40% of the BAK1 sequence in the *bak1-4 pBAK1::BAK1-GFP* sample (Figure 7.1 C and Table 7.1). In the case of *bak1-4 pBAK1::BAK1-5-GFP* we were able to identify only 8 peptides covering 19% of the BAK1-5 sequence (Table 7.1). No peptides matching either BAK1 or BAK1-5 were present in the negative control *bak1-4* (Table 7.1). We defined potential BAK1 interacting partners as follows: proteins that are identified by at least two independent peptides with a quality score (Mascot Ion score) greater than 25 and that have no matching peptides identified in immunoprecipitates of the negative

control. The summary of all identified proteins matching these criteria is shown in Table 7.1 and the respective peptides with Mascots scores can be found in the Appendix VII.I.

Interestingly, by applying these criteria we were able to identify FLS2 as an flg22-dependent interaction partner of BAK1 as we recovered 7 peptides in the BAK1-GFP sample covering 8% of the FLS2 sequence (Figure 7.1 C and Table 7.1). However, we were not able to recover any peptides matching FLS2 in the immunoprecipitate of the mock treated BAK1-5-GFP sample. This might be due to the overall low recovery of fusion protein in these large-scale experiments (Figure 7.1 A). Nevertheless, we identified several other specific BAK1/BAK1-5 interacting proteins that will be discussed in more detailed in the following section.

7.2.2. Identification of BAK1/BAK1-5-interacting proteins by MS/MS analysis

In order to obtain more robust data and identify new potential PRRs I performed two additional large-scale immunoprecipitation experiments followed by MS/MS analysis. For each experiment I used different transgenic *bak1-4* lines (*bak1-4 pBAK1::BAK1-HA$_3$* T2, *bak1-4 pBAK1::BAK1-5-HA$_3$* T2, *bak1-4 pBAK1::BAK1-GFP* T2 or *bak1-4 pBAK1::BAK1-5-GFP* T2) expressing either 3xHA or GFP C-terminal epitope tagged fusion proteins. Using two different tags I was able to control for potential tag-specific BAK1-unspecific interaction partners. In the experimental set-up we included the negative control *bak1-4* not expressing any fusion protein, an untreated control and a general crude elicitor extract treatment from different bacterial pathogens. After extracting total proteins I immunoprecipitated C-terminally tagged BAK1 or BAK1-5 using either HA-beads or GFP-trap beads, respectively. The immunoprecipitates were separated by SDS-PAGE and proteins visualized using colloidal commassie blue stain (data not shown). All proteins were subjected to in-gel tryptic digestion followed by MS/MS analysis. The maximal sequence coverage of BAK1 or BAK1-5 in any of these samples was

Identified Proteins	Accession Number	Identified matching peptides[a]						specific peptides[b]
		control		un-treated		treated		overall
		1	2	1	2	1	2	
BAK1	AT4G33430.1	0	0	9	15	10	14	13
SERK1	AT1G71830.1	0	0	8	9	8	9	2
SERK4	AT2G13790.1	0	0	6	3	4	4	4
LRR-RLK Xa family protein	AT1G27190.1	0	0	1	4	1	3	5
Dihydrolipoamide S-acetyltransferase	AT3G13930.1	0	0	9	2	13	1	10
ROF1	AT3G25230.1	0	0	8	2	2	5	10
ASP5	AT4G31990.1	0	0	3	5	3	2	10
VACUOLAR ATP SYNTHASE SUBUNIT B3	AT1G20260.1	0	0	1	2	2	1	2
Phosphoglucomutase	AT1G23190.1	0	0	3	2	2	3	3
ATNAP6	AT1G32500.1	0	0	3	1	1	0	3
MPPBETA	AT3G02090.1	0	0	3	2	3	3	6
MTO3	AT3G17390.1	0	0	2	2	2	4	5
ALDH2B4	AT3G48000.1	0	0	0	3	3	0	5
Arginase	AT4G08900.1	0	0	5	1	4	3	8
SHD	AT4G24190.1	0	0	2	3	0	2	5
EDA9	AT4G34200.1	0	0	3	3	3	3	5
PDX1	AT5G01410.1	0	0	6	1	3	2	4
GSA1	AT5G63570.1	0	0	1	2	2	2	5

Table 7.2 Proteins specifically identified in the immunoprecipitates of BAK1-GFP, BAK1-5-GFP, BAK1-HA_3 and BAK1-5-HA_3.

[a] peptides matching the indicated protein and potential other proteins without unique matching peptide

[b] number of specific peptides

1 denotes first repeat using *bak1-4 pBAK1::BAK1- HA_3* or *bak1-4 pBAK1::BAK1-5-HA_3* plants

2 denotes second repeat using *bak1-4 pBAK1::BAK1-GFP* or *bak1-4 pBAK1::BAK1-5-GFP* plants

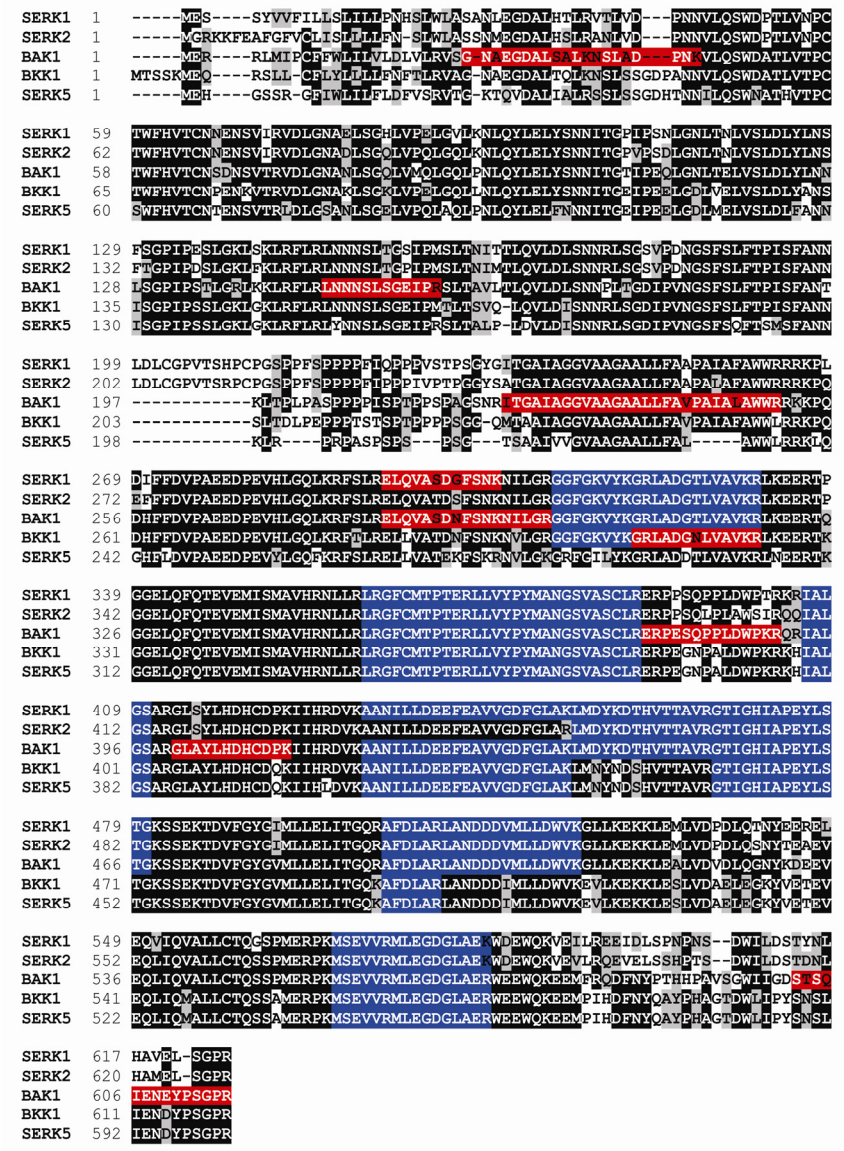

Figure 7.2. Identification of SERK1 and BKK1 as BAK1 interacting proteins by MS/MS analysis.
Alignment of SERK-family members. Blue or red indicates non-specific or specific, respectively, amino acid sequences identified by the MS/MS analysis. See text for experimental details.

20%. I could not observe any difference in the identified proteins between BAK1 and BAK1-5 and therefore summarized all potential interacting proteins as BAK1/BAK1-5 interactors in Table 7.2. Respective peptides and Mascot Ion Score can be found in the Appendix VII.II. When considering all three independent experiments I was able to identify 26 potential BAK1/BAK1-5 interacting proteins (Table 7.1 and 7.2). I identified two chaperones, the HSP90 protein shepherd (SHD) and the HSP70 protein luminal binding protein 2 (BiP2), that are most likely

involved in the proper folding of BAK1 (Saijo, 2010). In addition, I identified several RLKs that were of great interest for us.

The SERK-family members are highly similar at the amino acid level reaching from 66% to 89% identity in a pair-wise comparison (Hecht et. al., 2001; Albrecht et al., 2005) making it very difficult to obtain specific peptides (Figure 7.2). Nevertheless careful peptide sequence analysis identified SERK1 and BKK1 as interaction partners of BAK1. I obtained one specific peptide for SERK1 and one peptide matching either SERK1 or SERK2, which is allocated to SERK1 in the absence of specific peptides for SERK2 (Table 7.2 and Figure 7.2). In the case of BKK1 I found four specific peptides representing different trypsin cleavage products of the same amino acid sequence (Table 7.2 and Figure 7.2). This suggests that SERK-family members form oligomeric complexes and do not function in isolation. Recent findings of cooperative functional interactions of SERK-family members in BR- and PTI signalling support this hypothesis (Chinchilla et al., 2009; Roux et al. *submitted*).

I also identified two LRR-RLKs from the subfamily Xa as BAK1 interaction partners (Table 7.1 and 7.2). Phylogenetic analysis showed that they form an out-group within subfamily Xa containing the known BAK1-interacting protein BIR1 (Figure 7.3 A) (Goa et al., 2008). I identified two specific peptides matching At3g28450.1 the closest homologe of BIR1 (Table 7.1, 2 and Figure 7.3 B). Furthermore, I identified eight specific peptides for the third member of the out-group At1g27190.1 and one additional peptide being shared with its closest homolog At1g69990.1 (Table 7.1, 2 and Figure 7.3 B). I did not identify any BIR1-specific peptides in any of the three repeats suggesting that other family members of this out-group are the main BAK1 interaction partners in my experimental conditions.

In addition I identified several metabolism-related enzymes as potential BAK1 interaction partner (Table 7.1 and 7.2). However, I was unable to identify any peptides matching BRI1 which is in agreement with results from other laboratories (R. Karlova and S. de Vries, personal communication). Consistently, I did not identify proteins displaying the expected topology of potential PRRs.

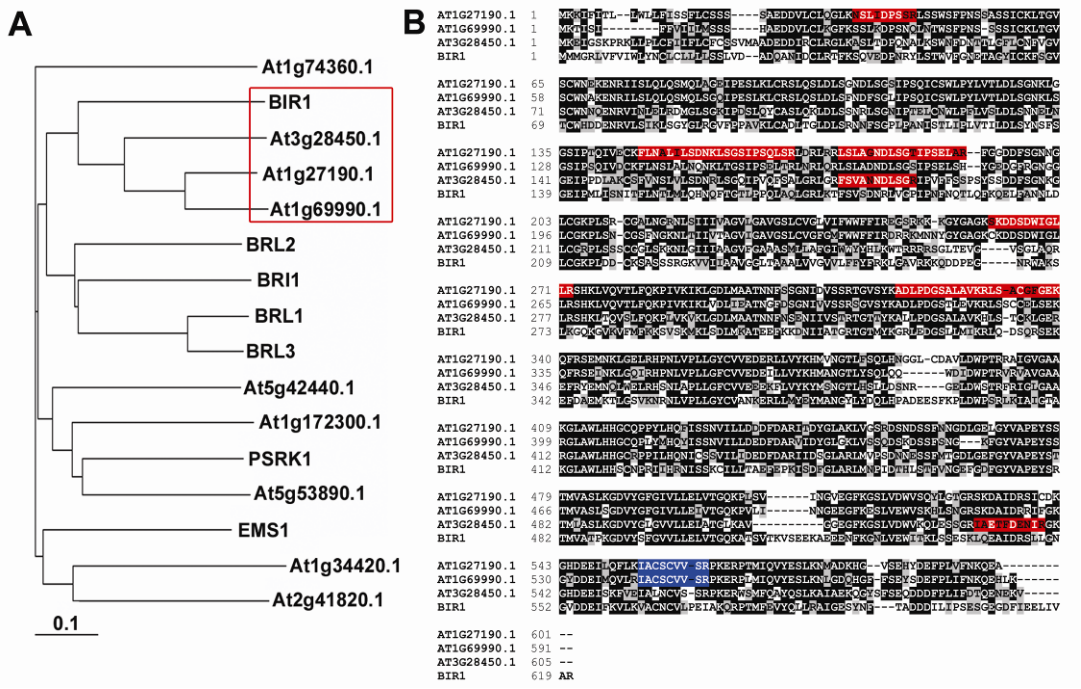

Figure 7.3. Identification of BIR1 homologs as BAK1 interacting proteins by MS/MS analysis.

A. The identified BAK1-interactors are members of LRR-RLK subfamily Xa and form a sub-clade containing BIR1 (boxed). Phylogenetic tree of LRR-RLK sub-family Xa.

B. Alignment of BIR1 and its three closest homologs. Blue or red indicates non-specific or specific, respectively, amino acid sequences identified in the MS/MS analysis. See text for experimental details.

7.2.3. Progress on the identification of PAMPs inducing BAK1/BKK1-dependent responses

I previously showed that *bak1-5* plants are hyper-susceptible to bacterial pathogens and that leaves of *fls2 efr bak1-5* and *bak1-5 bkk1-1* support even more bacterial growth than leaves of *fls2 efr* (see Chapter 4). In addition, seedlings of *bak1-5 bkk1-1* are hyper-suceptible to oomycete pathogens (see Chapter 4). This suggests that BAK1 and/or BKK1 are required for the perception of unknown PAMPs by yet unidentified PRRs. Therefore, in collaboration with Fredderikke Gro Malinovsky I tested if *fls2 efr bak1-5* and/or *bak1-5 bkk1-1* plants are impaired in the perception of PAMPs present in crude elicitor extracts from individual pathogens available at The Sainsbury Laboratory. Initially, we screened for a reduction in the elicitor-induced

ROS-burst as readily recordable read-out. Applying crude elicitor extracts from the bacterial pathogens *Pto* DC3000, *Pta* 6605, the oomycete pathogens *Albugo laibachii Alem1, A. candida 20DD5, Hpa* Emoy2 and two fungal pathogens *Botrytis cinerea* and *A. brassicicola* on Col-0 leaf discs we only obtained reproducible ROS-burst production with extract from *Pta 6605* (Figure 7.4 A, data not shown). Most of the measurable ROS-burst was dependent on FLS2 and EFR as ROS production was markedly reduced in the *fls2 efr* double mutant leaves (Figure 7.4 A). However, it was even further decreased in leaves of *fls2 efr bak1-5* and *bak1-5 bkk1-1* plants (Figure 7.4 A and B).

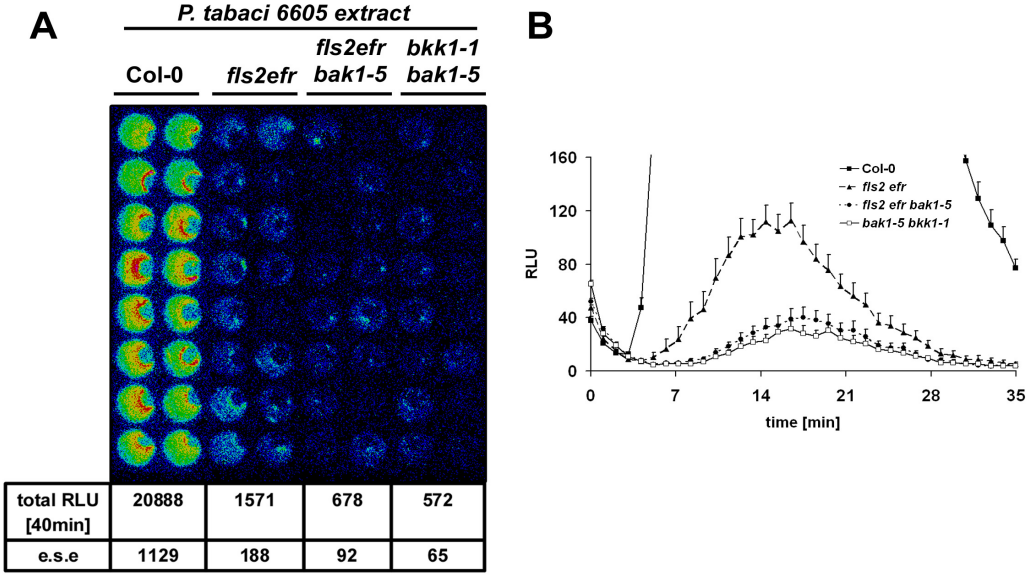

total RLU [40min]	20888	1571	678	572
e.s.e	1129	188	92	65

Figure 7.4. Identification of (potentially) novel BAK1-dependent PAMP (extracts) from *P. tabaci* 6605.

A. *BAK1* and *BKK1* are involved in the perception of *FLS2*- and *EFR*-independent PAMP(s). Graphical depiction of *P. tabaci* crude elicitor extract-triggered ROS-burst in leaves of Col-0, *fls2 efr, fls2 efr bak1-5* and *bak1-5 bkk1-1* plants. Table summarizing total ROS-burst production after 40 min in RLU ± s.e. (n=16).

B. Reduced and delayed *Pta* 6605crude elicitor extract-triggered ROS-burst in *bak1-5 bkk1-1* leaves. Kinetics of *P. tabaci* crude elicitor extract-triggered ROS-burst in leaves of Col-0, *fls2 efr, fls2 efr bak1-5* and *bak1-5 bkk1-1* plants. Results are given as average ± s.e. (n=16)

As several crude elicitor extracts did not induce any reproducible ROS-burst we used a subset of these to test for PTI-gene induction by qPCR in a series of preliminary experiments. We treated Col-0 or *bak1-5* seedling for 30 or 180 min with crude extracts isolated from plants effected with *A. laibachii Alem1, A. candida*

20DD5 or *Hpa* Emoy2 or from *A. brassicicola* grown on V8 plates. As shown in Figure 7.5 all extracts induced the expression of the PTI marker gene *At2g17780* after 30 min in Col-0 and *bak1-5*. The gene induction was transient and the expression level was reduced already after 180 min for some of the extracts (Figure 7.5). Nevertheless, the expression level of *At2g17780* at 30 min was always lower in *bak1-5* seedlings compared to wild-type (Figure 7.5 A). To confirm these initial results in collaboration with Milena Roux I focused on extracts from *Hpa* Emoy2 as *bak1-5 bkk1* are hyper-susceptible to this pathogen (see Chapter 4). In the new experimental set-up we included extracts from non-infected plants as non pathogen related control. We treated seedlings of Col-0, *bak1-5*, *bkk1-1* and *bak1-5 bkk1-1* with extracts from mock or *Hpa* Emoy2-inoculated plants for 30 or 180 min. We did not observe any significant difference in the expression level of the PTI marker gene *At1g51890* after 30 min between the mock control and treatment (Figure 7.5 B). However, the expression of *At1g51890* was markedly induced after 180 min only in samples from seedling treated with Emoy2 crude elicitor extract (Figure 7. 5 B). This induction clearly required functional BAK1 and BKK1 as the expression level of *At1g51890* was reduced in the single mutants *bak1-5* and *bkk1-1* and even lower in the double mutant *bak1-5 bkk1-1* (Figure 7.5B).

All together, this demonstrates the presence of yet unknown PAMPs which are perceived by BAK1- and/or BKK1-dependent PRRs.

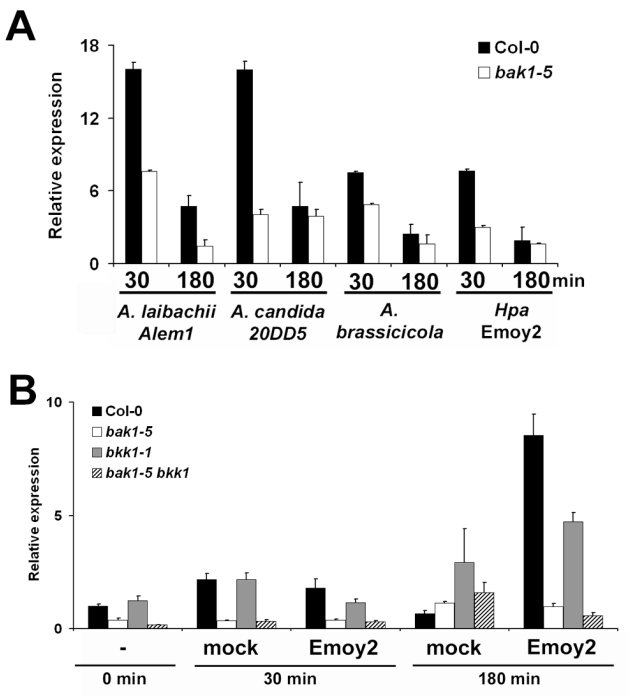

Figure 7.5. BAK1 and BKK1 play a partial redundant role in the recognition of several crude elicitor extracts of non-bacterial pathogens.

A. Identification of *BAK1*-dependent crude elicitor extracts of non-bacterial pathogens. Expression analysis of *At2g17780* by qPCR in Col-0 and *bak1-5* seedlings treated with crude elicitor extracts of *A. laibachii Alem1, A. candida 20DD5, A. brassicicola* or *Hpa* Emoy2 for 30 or 180 min, respectively. Results are average ± s.e. (n=3).

B. Partially redundant roles of BAK1 and BKK1 in the recognition of yet unidentified PAMP(s) from *Hpa* Emoy2. Expression analysis of *At1g51890* by qPCR analysis in seedlings of Col-0, *bak1-5*, *bkk1-1* and *bak1-5 bkk1-1* not treated, mock treated or treated with *Hpa* Emoy2 crude elicitor extract for 30 or 180 min. Results are average ± s.e. (n=3)

7.2.4. Progress on the identification of BAK1/BKK1-dependent PRRs

Next, in collaboration with Yasuhiro Kadota I wanted to identify the corresponding *BAK1*- and/or *BKK1*-dependent PRR(s) responsible for perception of PAMPs present in the crude elicitor preparations tested as shown in Figure 7.4 and 7.5. We focused our initial efforts on the crude elicitor extract of *Pta* 6605. Firstly it induced a reproducible lower ROS-burst in leaves of *fls2 efr bak1-5* and *bak1-5 bkk1-1* compared to *fls2 efr* (Figure 7.4). Secondly, this extract was readily available in large quantities needed for elicitation of sufficient amount of seedlings. As most of the recognition of the *P. tabaci* 6605 crude elicitor extract was dependent either on

FLS2 or EFR (Figure 7.4) we used the *fls2 efr bak1-5* triple mutant plants in order to avoid identifying only FLS2 or EFR as inducible BAK1-5 interaction partners. For the identification of potential novel PRRs we treated *fls2 efr bak1-5* seedlings either with water or with *Pta* 6605 crude elicitor extract for 5 min at the same concentration used in ROS-burst experiments (Figure 7.4). As we performed immunoprecipitation experiments with the newly available anti-BAK1 antibodies (Schulze et al. 2010), we also included *bak1-4* as a negative control. We incubated total protein extracts with anti-BAK1 antibodies and anti-rabbit IgG beads. Immunoprecipitated proteins were separated by SDS-PAGE, visualized by colloidal commasie blue stain, and subjected to in-gel trypsin digestion followed by MS/MS analysis. Unfortunately, we only obtained a maximal sequence coverage of 8% of BAK1-5 including only two specific peptides (Table 7.3). This relatively low recovery rate of BAK1-5 made it difficult to evaluate the identified co-immunoprecipitated proteins (Table 7.3 and Appendix VII.III). Additional experiments are needed to investigate the low recovery rate and to evaluate the significance of the identified proteins.

Interestingly, we recovered two BKK1 specific peptides in the *bak1-4* sample proving that the anti-BAK1 antibody also recognizes BKK1 *in planta* as previously suggested by peptide competition experiments on immunoblots (Schulze et al. 2010).

Identified Proteins	Accession Number	Identified matching peptides[a]			specific peptides[b]
		plant line/treatment			
		1	2	3	overall
BAK1	AT4G33430.1	0	2	4	2
BKK1	AT2G13790.1	2	2	2	2
WD40-containing protein	AT3G50590.1	0	3	0	3
DWF1	AT3G19820.1	0	0	2	2
ATWHY3	AT2G02740.1	0	1	3	3
nucleic acid binding	AT5G06450.1	0	1	2	3
WD40-containing protein	AT5G24710.1	0	2	0	2

Table 7.3. Proteins immunoprecipitated using anti-BAK1/BKK1 antibodies.

[a] peptides matching the indicated protein and potential others without unique matching peptide

[b] number of specific peptides

1 denotes immunoprecipitates of *bak1-4* plants mock treated

2 denotes immunoprecipitates of *fls2 efr bak1-5* plants mock treated

3 denotes immunoprecipitates of *fls2 efr bak1-5* plants treated with *P.tabac*crude elicitor extract

Chapter 8: Conclusion and Outlook

8.1. A novel model of action for BAK1 in PTI-signalling

In contrast to previous models, I found that BAK1 is able to dictate specificity of downstream signalling as the kinase hypo-active BAK1-5 nearly totally blocked FLS2- and EFR-mediated PTI signalling but hardly influenced BRI1-mediated BR signalling, as well as cell death control. Based on these results and the recent work from Chinchilla and colleagues (Schulze et al., 2010), I propose a model for the mechanisms underlying EFR/FLS2 heteromerization with BAK1, and the role of BAK1 in the establishment of PTI signalling. EFR and FLS2 most likely exist in close proximity with BAK1 at the plasma membrane in loose preformed complexes. Conformational changes triggered by ligand-binding lead to the stabilization of the complex. This interaction is kinase-independent, but may lead to the activation of the EFR/FLS2 kinase activity by BAK1 via trans-phosphorylation events. Phosphorylation of specific residues on EFR/FLS2 and/or BAK1 leads to the recruitment of downstream signalling components that dictate the specificity of the signalling output. In this model, BAK1 is not a simple enhancer of the kinase activity of the ligand-binding RKs, but is an integral part of the signalling pathway.
Future studies need to carefully address the role of kinase activity of non-RD kinases for PTI signalling and final defence outcomes. Therefore, careful qualitative and quantitative analyses guided by mass-spectrometry of the phosphorylation status of BAK1, BAK1-5, FLS2 and EFR *in vitro* and *in vivo* will shed more light onto the complex regulatory mechanisms of these two model non-RD kinases by the regulatory RLK BAK1. These studies are however technically challenging, as unlike BRI1, the kinase activity of EFR is very weak and that of FLS2 is practically negligible at least *in vitro*. In addition, the analysis by quantitative proteomics of EFR/FLS2-BAK1 complexes in *bak1-5* compared to wild-type, combined with *bak1-5* and *bak1-5 bkk1-1* suppressor screens will help to identify novel key regulators of PTI. Such approaches are currently undertaken in the laboratory.

8.2. Discovering new PRRs and enhancing plant disease resistance

The identification of BAK1 as a PTI-signalling component could become a seminal discovery in plant science. It was recently shown that the interfamily heterologous expression of EFR in solanaceous plants leads to broad-spectrum disease resistance against bacteria (Lacombe et al., 2010). It is conceivable that this might represent a novel strategy to contain plant diseases in the field, especially if several different PRRs are stacked within the same plant. Stacking of a combination of R-proteins and PRRs might even further enhance disease resistance. However, the number of currently known PRRs is limited. Nonetheless, many orphan PAMPs are known. Several of these orphan PAMPs are perceived by BAK1-dependent PRRs. Importantly, this observation is not restricted to model plants such as *Arabidopsis* and *N. benthamiana* (Chinchilla et al., 2009), but has been recently reported in the case of Ax21-perception in rice also (Pamela Ronald, personal communication). Therefore, the requirement of BAK1 and orthologous proteins for signalling in response to PAMP perception seems to be evolutionary conserved. A concise strategy to identify novel BAK1-interacting proteins in several plant species and/or cultivars using either yeast-two hybrid or proteomic approaches might lead to the identification of novel PRRs. Those could be used for PRR stacking and crop improvement.

A complementary approach is to manipulate currently known PRRs. For example, random mutagenesis of the extracellular domain might generate novel or more efficient PAMP binding sites. Alternatively, the manipulation of the intracellular kinase domain might be suited to create more responsive and/or efficient PRRs. The close examination of oncogenic mutations in mammalian RKs or kinases in general will aid the structure function analysis as cancer is often caused by deregulated or hyper-active growth-promoting kinases.

8.3. From the idea of linear signal transduction pathways to the idea of cytoplasmic states

Signal transduction is often perceived as a linear signal cascade. Ligand binding to the extracellular domain of a RK activates the intracellular kinase domain, phosphorylation and other post-translational modifications relay the signal to the nucleus and thereby induce an appropriate transcriptional reprogramming. The activation of de-activating enzymes such as phosphatases leads to the down-regulation of signalling. This sequential and binary view of signal transduction is a clear over-simplification. For example, it is apparent that PTI is under constant negative regulation by phosphatases and protein degradation mechanisms as treatment with either calyculin A or CHX induces responses reminiscent of PAMP treatment (Felix et al., 1994; Navarro et al., 2004). This means that kinases involved in PTI signalling possess a residual basal kinase activity that has to be controlled by constant de-phosphorylation. Both processes happen within a single cell at the same time. Therefore, ligand binding does not simply lead to the activation of the intracellular kinase domain, but changes the cytoplasmic state (Dehmelt and Bastiaens, 2010). This concept integrates the idea that "protein network reaction states are maintained by dynamic processes, and information transfer occurs by switching from one dynamically maintained state to another" (Dehmelt and Bastiaens, 2010). This means that not only activity of a signalling component defines the final signalling outcome but also its location and interactions. For example, it is known that mammalian RKs are endocytosed and are able to signal from the endosomes (Murphy et al., 2009). Even though endosmal signalling involves RKs with the same activity as plasma membrane-localized RKs, endosomal localized RKs are able to initiate a different set of responses via the interaction with a different set of signal transduction components (Murphy et al., 2009). BAK1-5 might not simply switch on or off a certain signalling pathway but rather influence several cytoplasmic states and interactions of signalling networks, giving rise to the complex phenotypical traits associated with *bak1-5*. Future studies need to address these complexities and ideally lead to the development of tools that not only identify

the activity but also localization and interactions of a single protein at a given moment within an individual cell.

Appendices

Appendix I: Phospho-peptide spectra

Appendix I.I: BAK1(T450A)

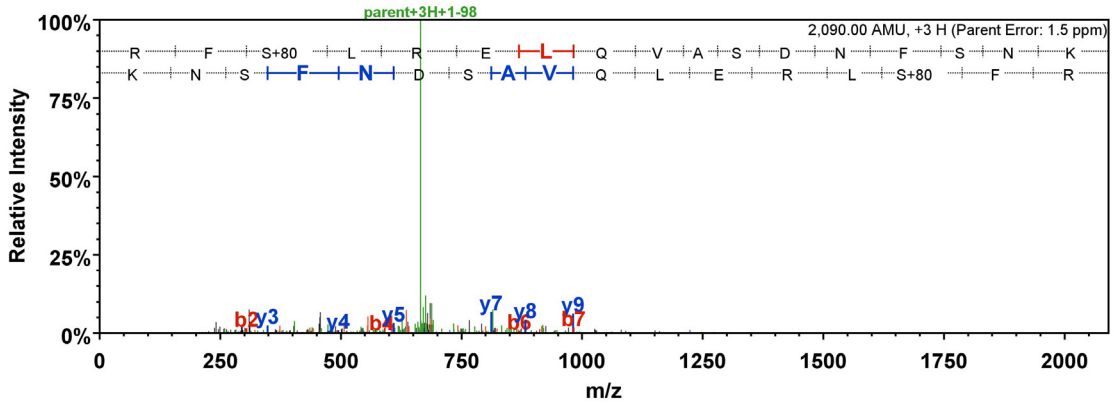

pS286: ELQVApSDNFSNK

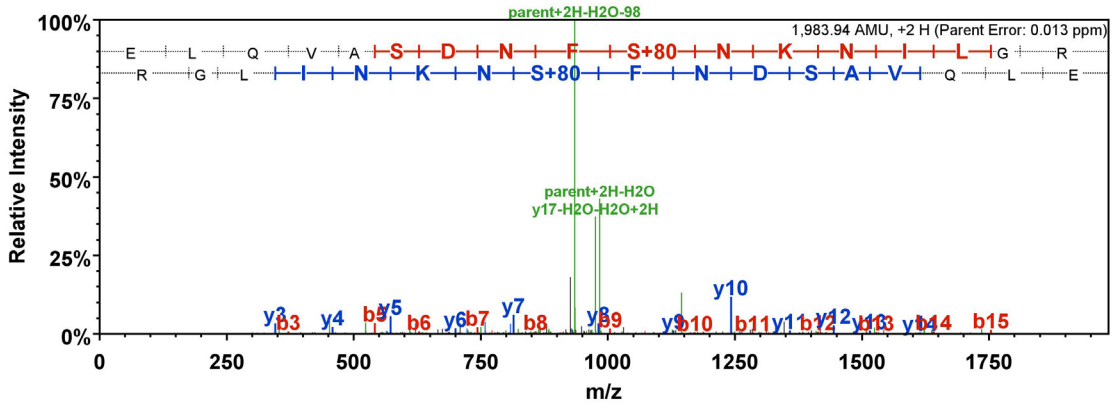

pS290: ELQVASDNFpSNKNILGR

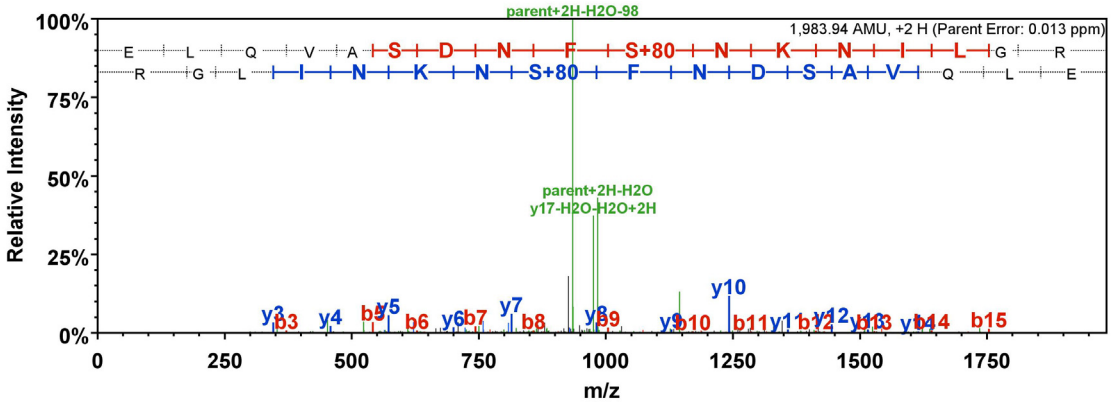

pT312: LADGpTLVAVKR

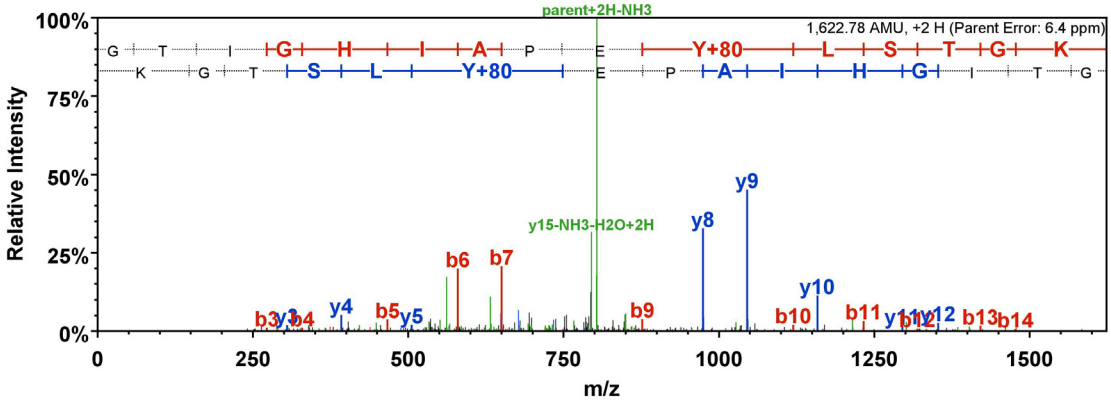

pY463: GTIGHIAPEpYLSTGK

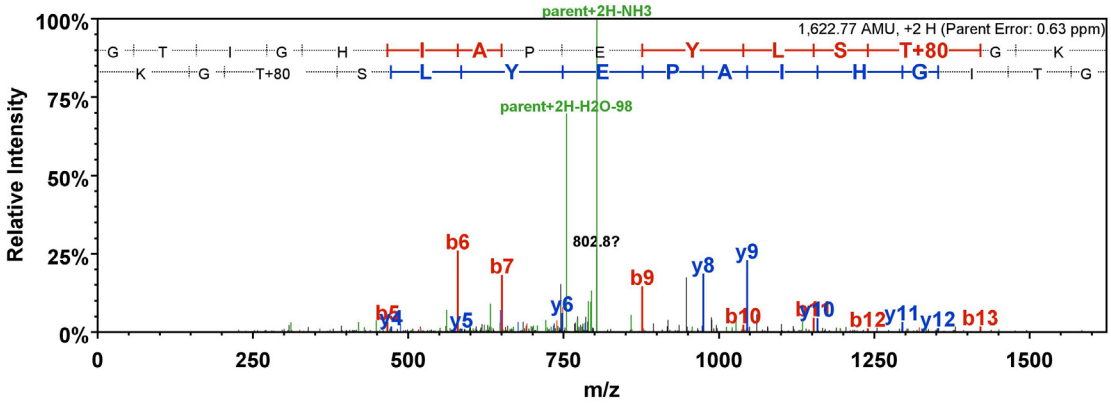

pT466: GTIGHIAPEYLSpTGK

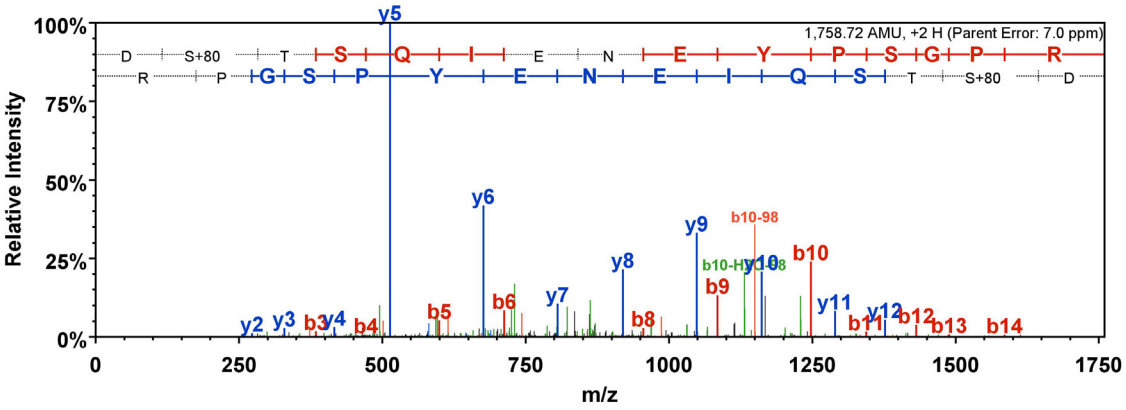

pS602: DpSTSQIENEYPSGPR

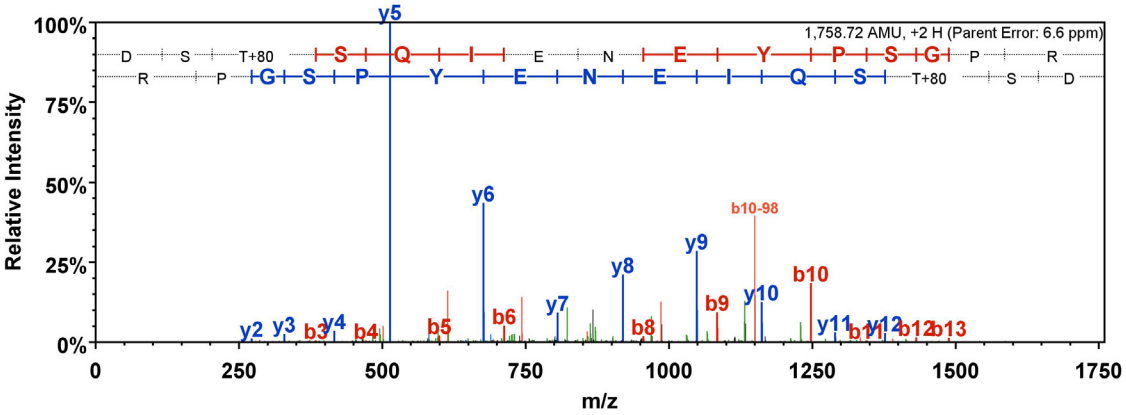

pT603: DSpTSQIENEYPSGPR

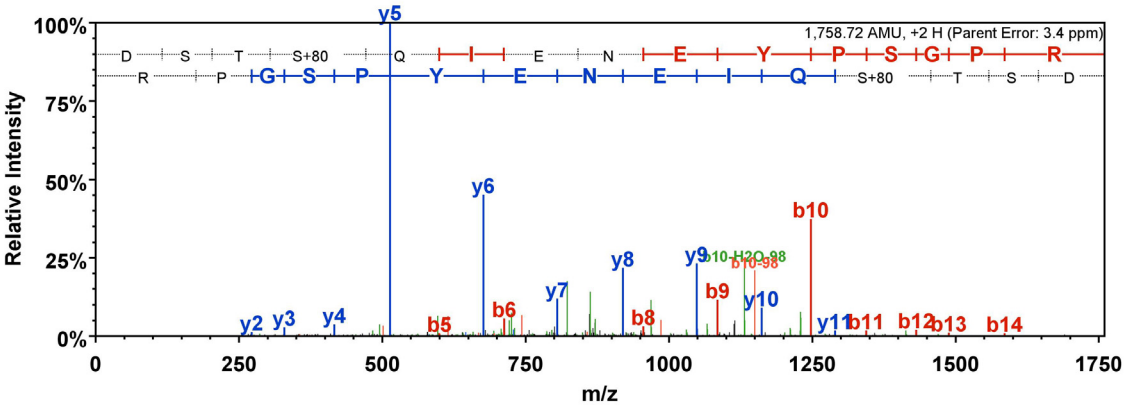

pS604: DSTpSQIENEYPSGPR

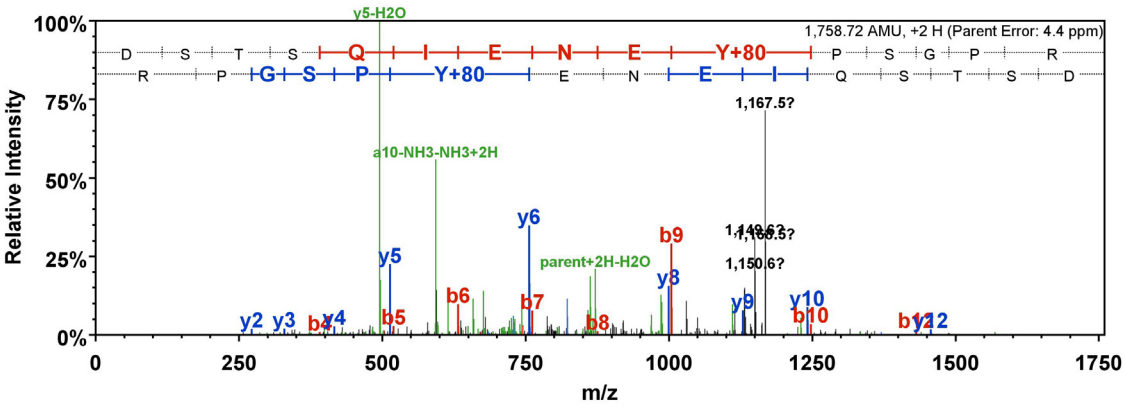

pY610: DSTSQIENEpYPSGPR

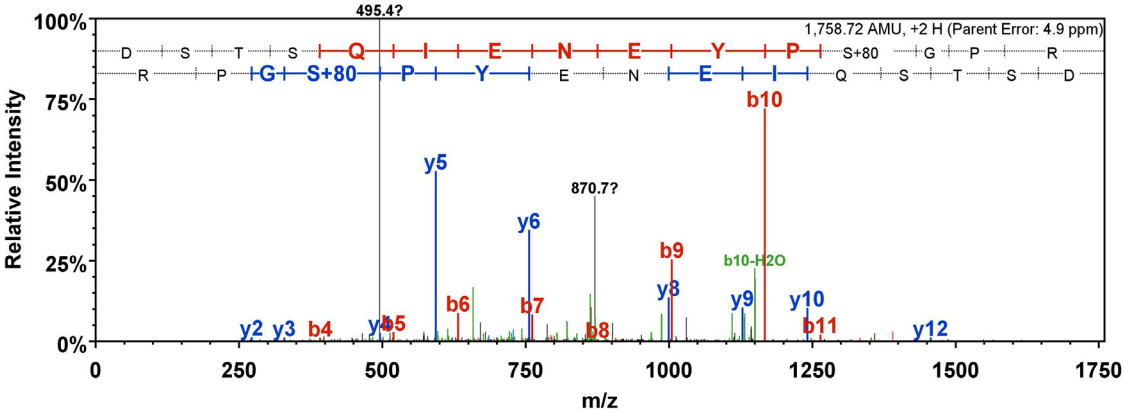

pS612: DSTSQIENEYPpSGPR

Appendix I.II: BAK1-5

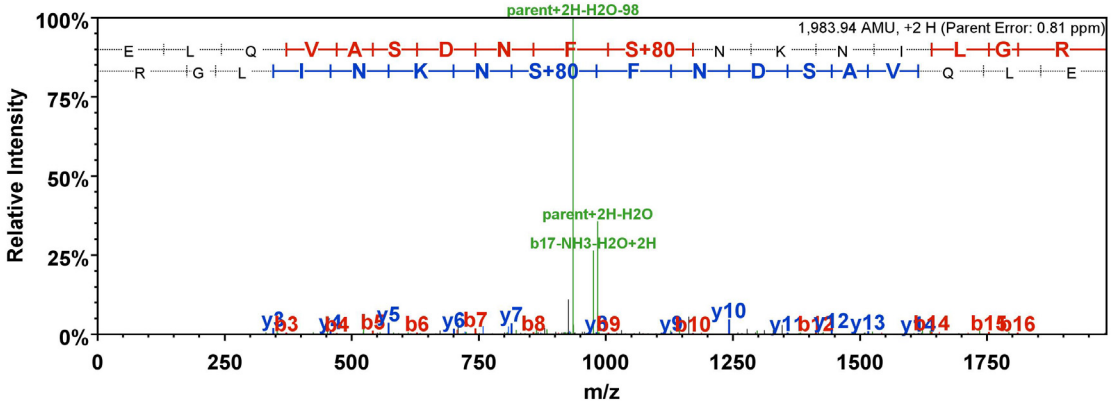

pS286: ELQVApSDNFSNKNILGR

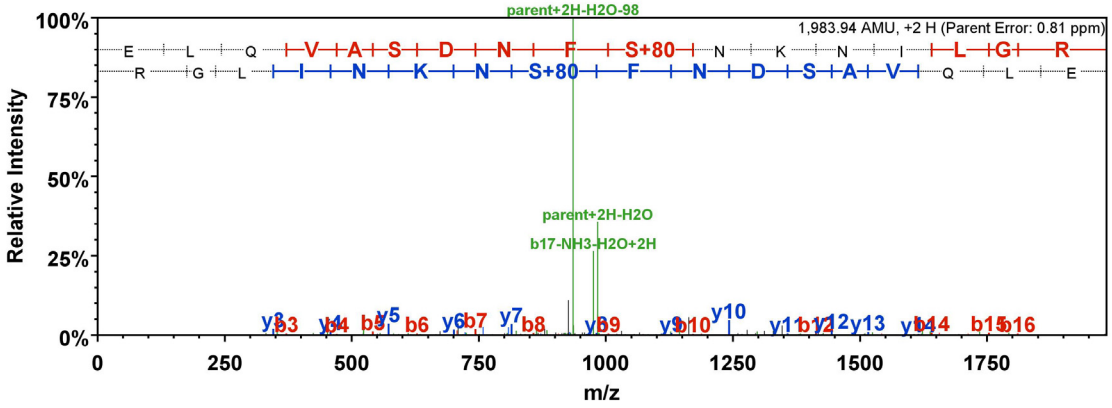

pS290: ELQVASDNFpSNKNILGR

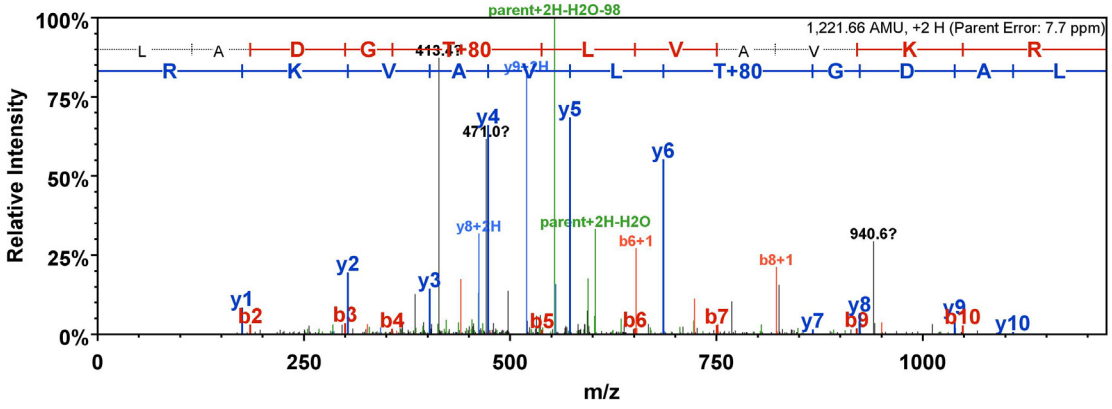

pT312: .LADGpTLVAVKR

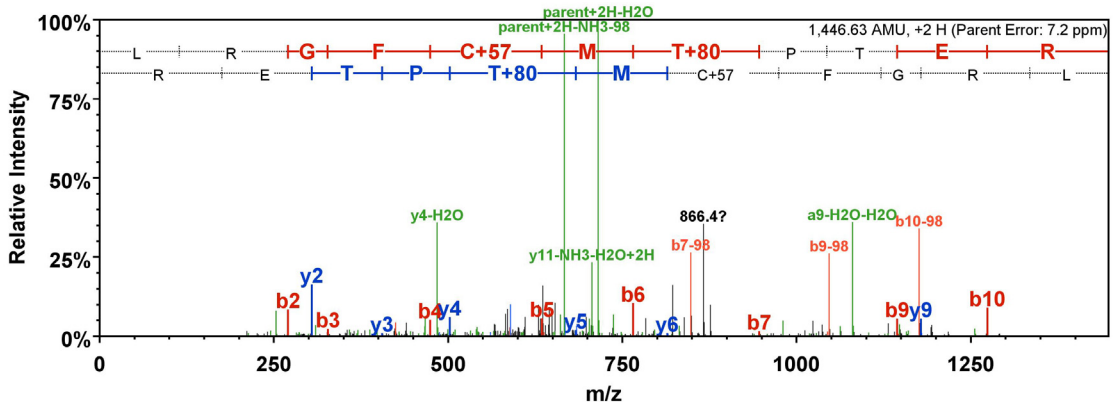

pT355: LRGFcCMpTPTER

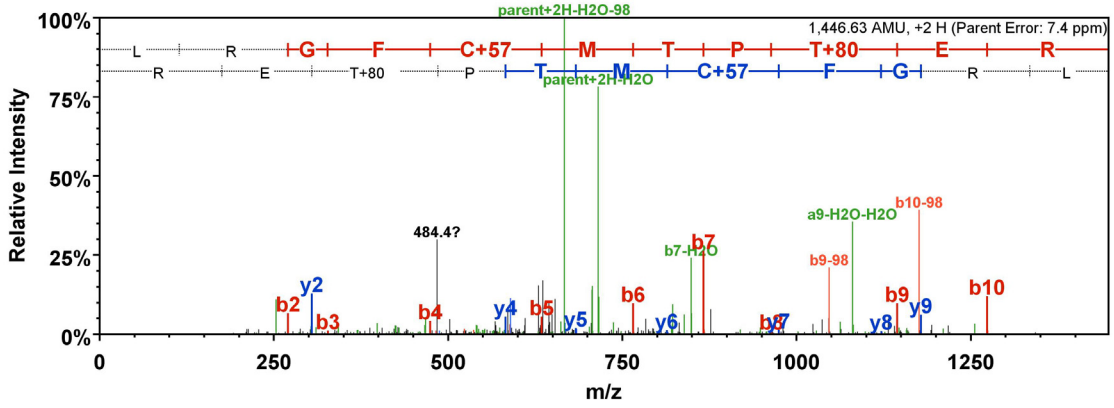

pT357: LRGFcCMTPpTER

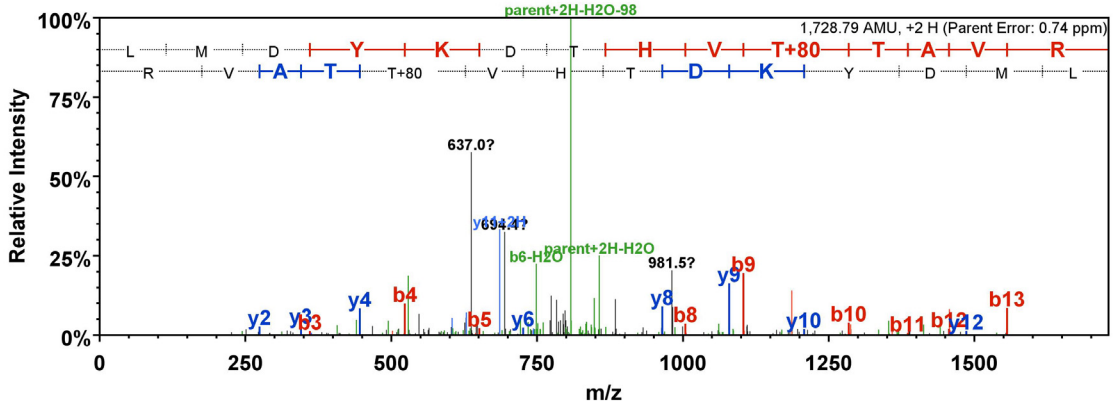

pT449: LMDYKDpTHVTTAVR

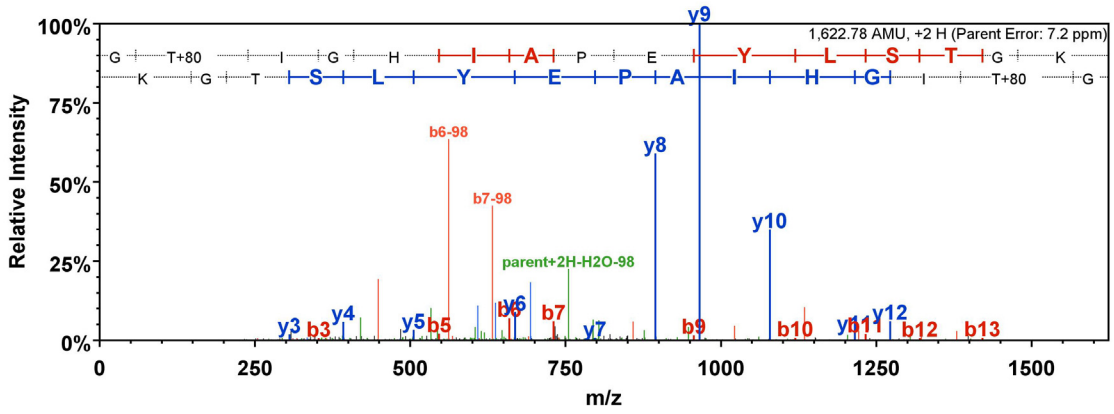

pT455: GpTIGHIAPEYLSTGK

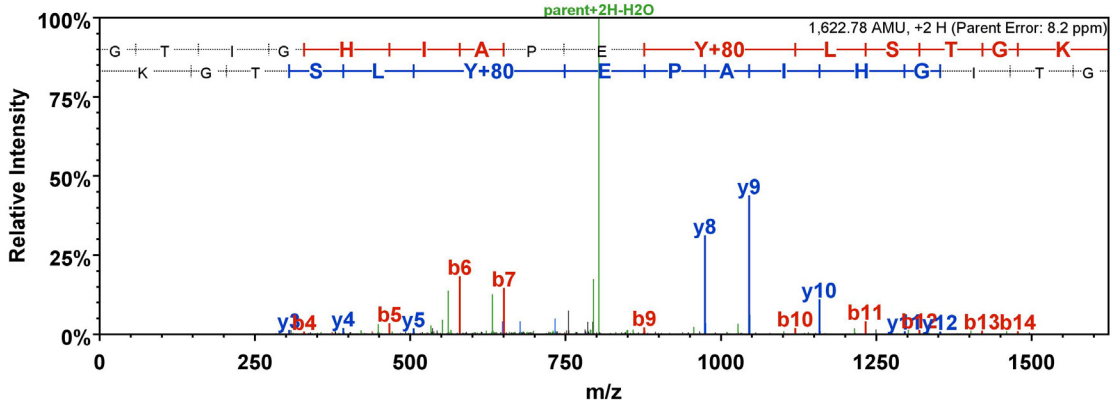

pY463: GTIGHIAPEpYLSTGK

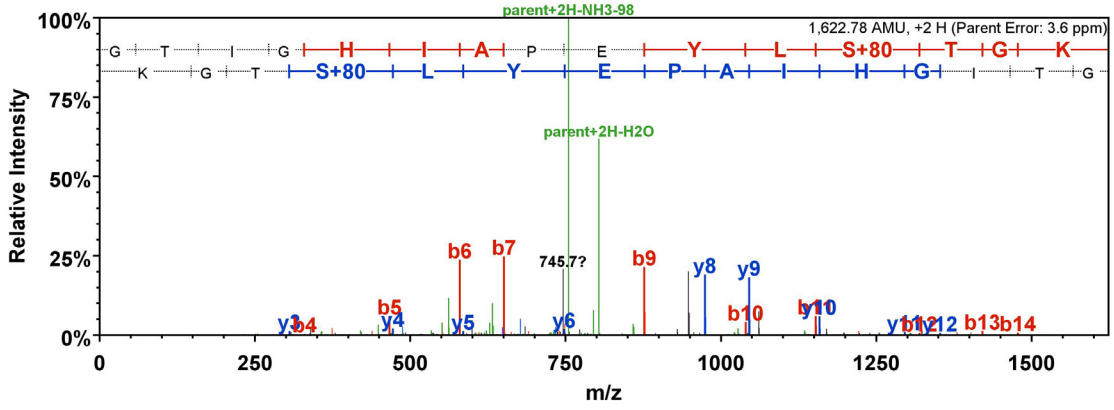

pS465: GTIGHIAPEYLpSTGK

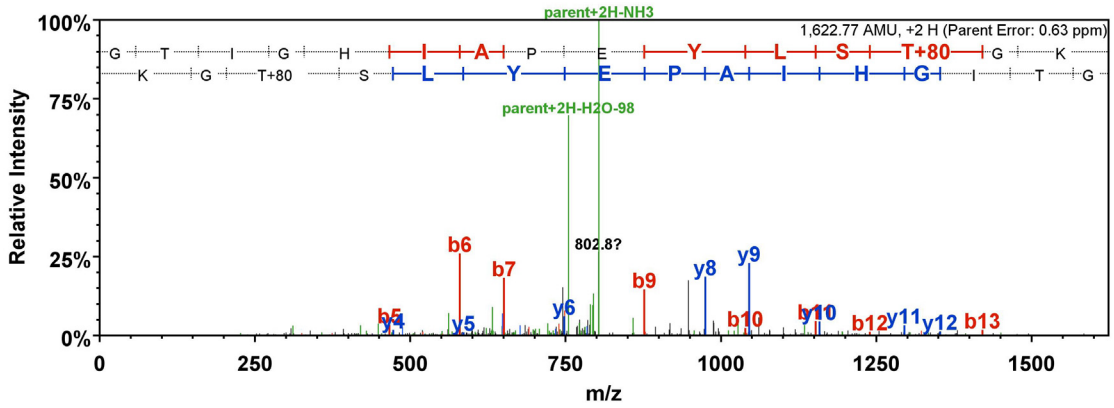

pT466: GTIGHIAPEYLSpTGK

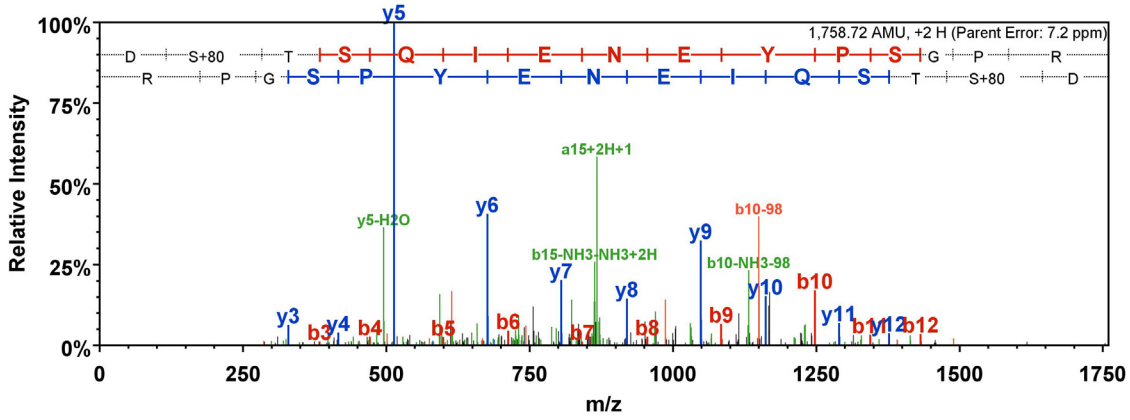

pS602: DpSTSQIENEYPSGPR

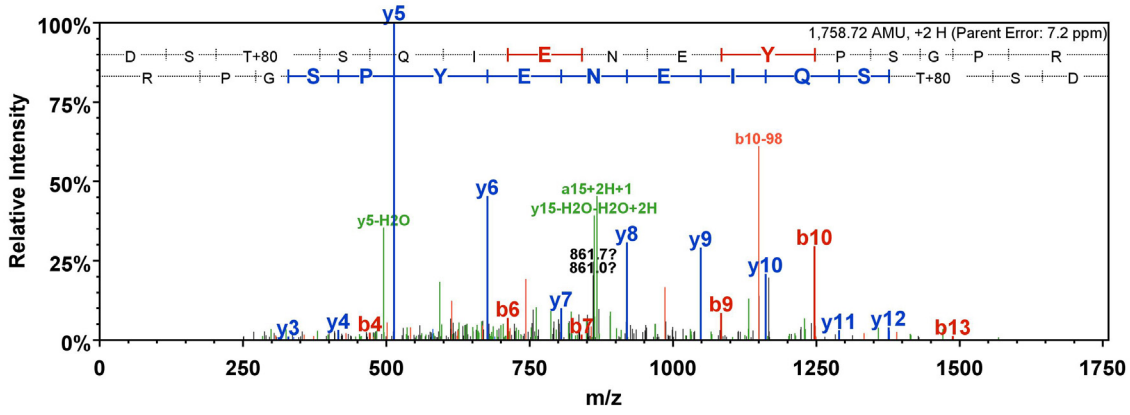

pS603: DSpTSQIENEYPSGPR

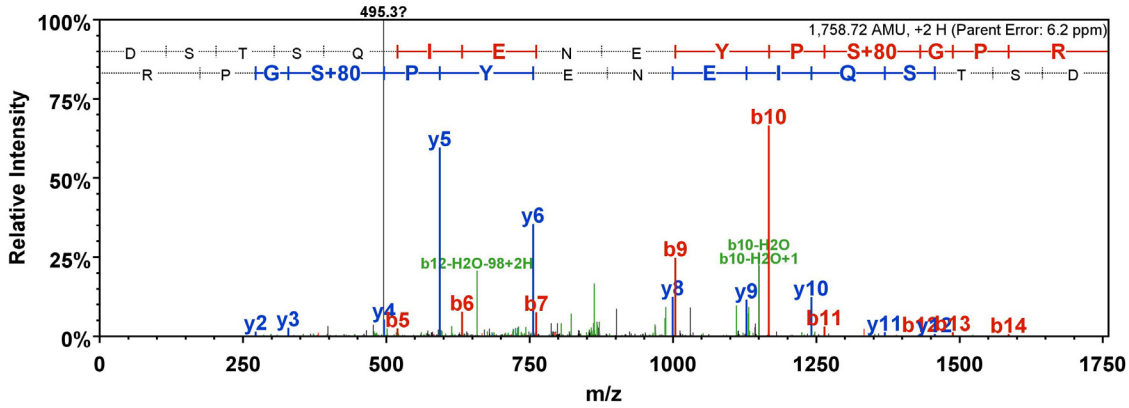

pS612: DSTSQIENEYPpSGPR

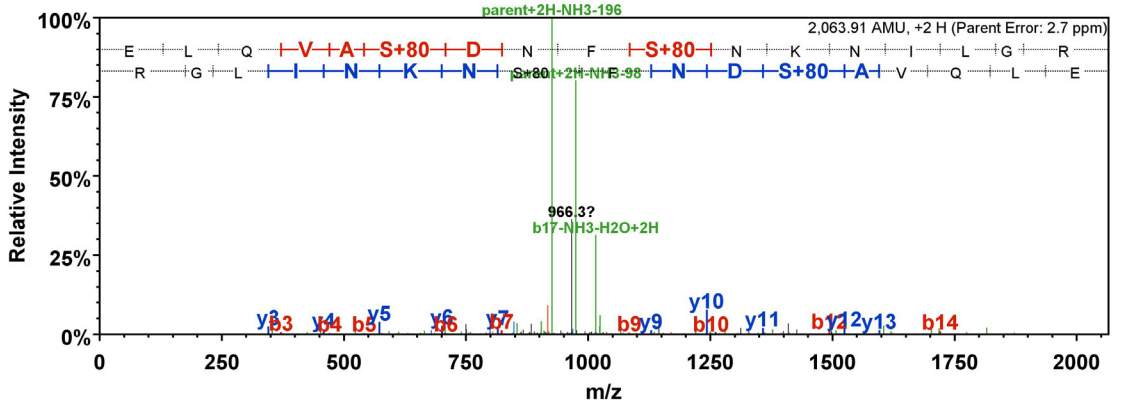

pS286/pS290: ELQVApSDNFpSNKNILGR

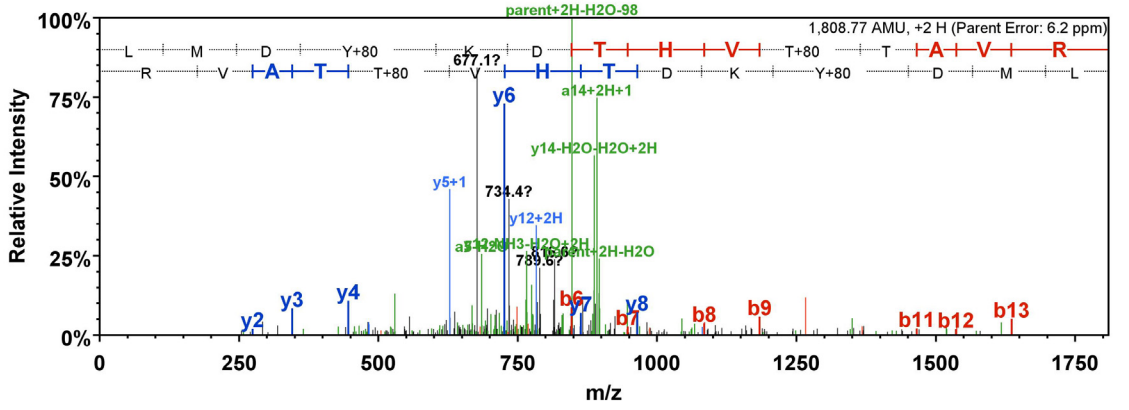

pY443/pT449: LMDpYKDTHVpTTAVR

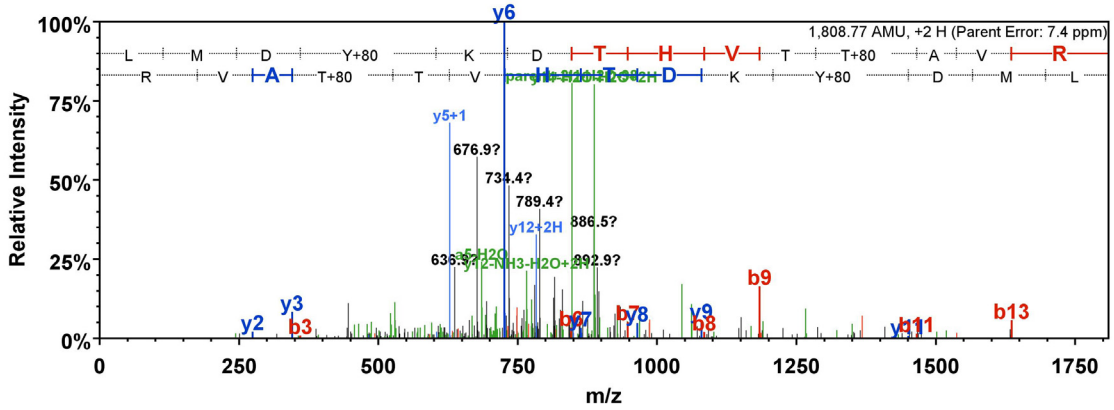

pY443/pT450: LMDpYKDTHVTpTAVR

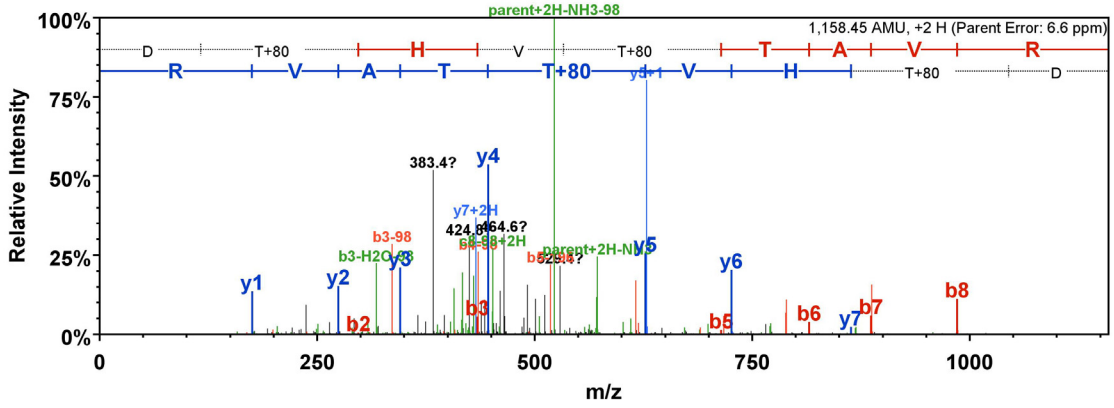

pT446/pT449: DpTHVpTTAVR

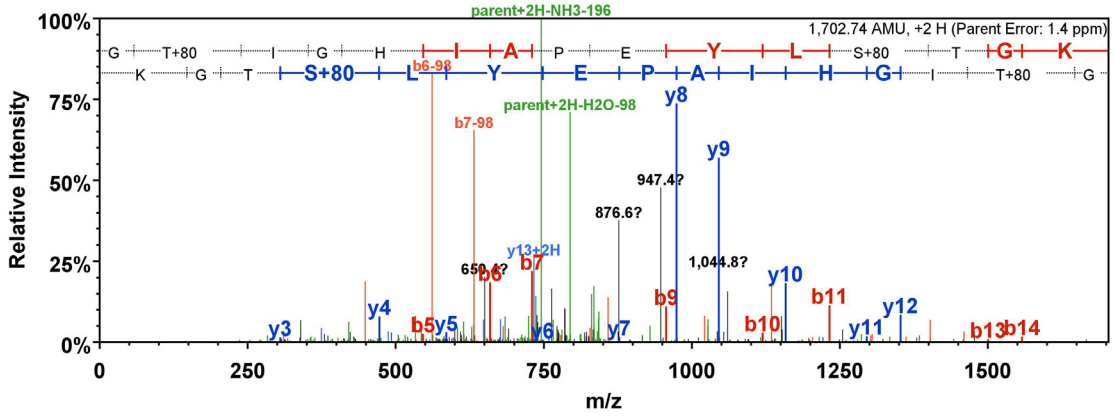

pT455/pS465: GpTIGHIAPEYLpSTGK

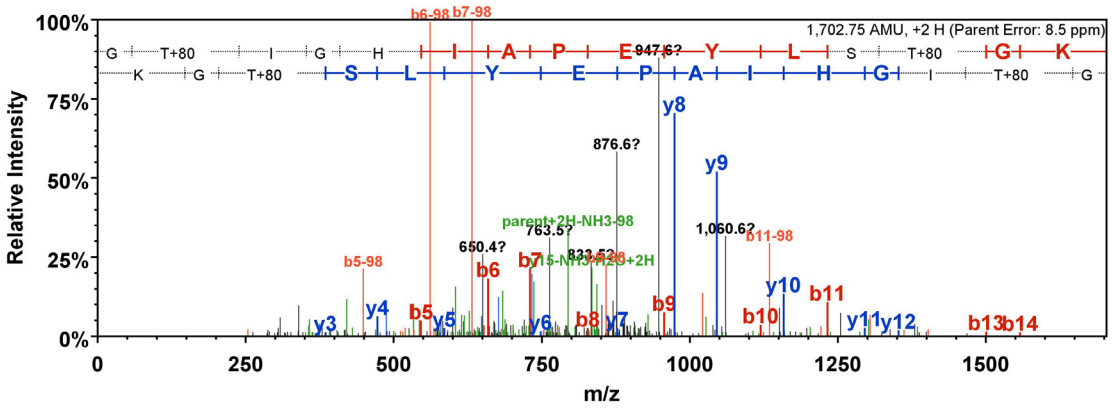

pT455/pT466: GpTIGHIAPEYLSpTGK

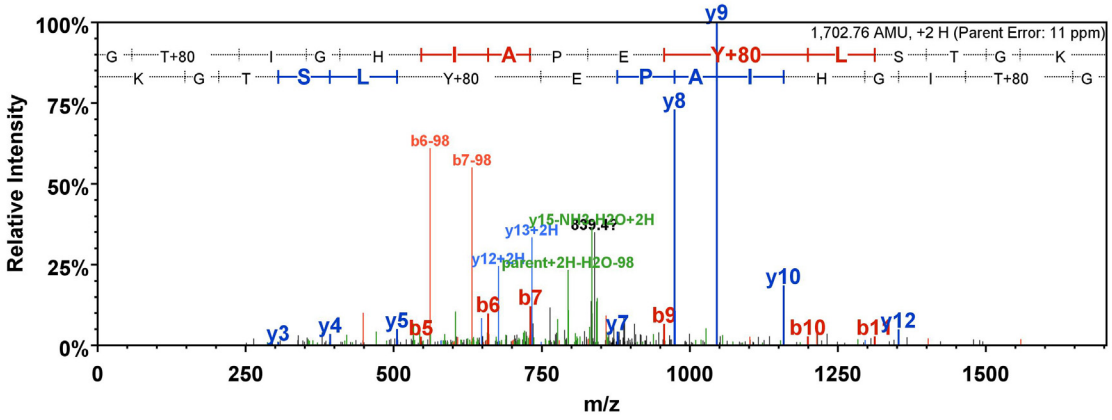

pT455/pY463: GpTIGHIAPEpYLSTGK

Appendix II: Peptides and mascot ion scores of BAK1-interacting proteins

Appendix II.I.

AT4G33430.1	
Peptide sequence	Best Mascot Ion score
AANILLDEEFEAVVGDFGLAK	76.9
DYKDTHVTTAVR	54.5
ELQVASDNFSNK	66.9
ELQVASDNFSNKNILGR	67.1
ERPESQPPLDWPK	39.3
ERPESQPPLDWPKR	50.9
GFCMTPTER	37.5
GLAYLHDH	33.6
GLAYLHDHCDPK	52.7
GNAEGDALSALK	30.5
GRLADGTLVAVK	35.2
GRLADGTLVAVKR	59.6
GTIGHIAPEYLSTGK	63.6
IAPEYLSTGK	46.3
LADGTLVAVK	63.7
LADGTLVAVKR	74.7
LANDDDVMLLDWVK	74.4
LLVYPYMANGSVASCLR	n.d.
LMDYKDTHVTTAVR	107
MLEGDGLAER	64.5
NAEGDALSALK	68

RLADGTLVAVK	47.1
STSQIENEYPSGPR	54.7
Overall	107

AT5G46330.1	
Peptide sequence	Best Mascot Ion score
FSGQIPALFSK	37.5
GQLEDGTVIAVK	60.6
IENSSESSLPDLDSALK	82.2
ILGFAWESGK	33.2
IPAELGNLVQLQALR	75.3
LESLTYLSLQGNK	n.d.
LLSVLDLSNNK	n.d.
Overall	82.2

AT1G27190.1	
Peptide sequence	Best Mascot Ion score
FLNALILSDNK	57.5
LSGSIPSQLSR	35.4
LSLAGNDLSGTIPSELAR	n.d.
SKDDSDWIGLLR	78.4
Overall	78.4

AT3G28450.1	
Peptide sequence	Best Mascot Ion score
FSVANNDLSGR	63.1

IAETFDENIR	27.5
Overall	82.2

AT5G42020.1	
Peptide sequence	Best Mascot Ion score
ARFEELNNDLFR	n.d.
EAEEFAEEDKKVK	47.2
EALEWLDENQNSEKEEYDEK	62.8
FEELNNDLFR	55.6
GRLSQEEIDR	33.9
IINEPTAAAIAYGLDK	90.1
IINEPTAAAIAYGLDKK	74.4
ITPSWVGFTDSER	n.d.
KFEDKEVQKDR	n.d.
KLVPYQIVNK	31.8
LADKLEGDEKEKIEAATK	n.d.
LSQEEIDR	64.5
MKETAEAYLGK	66.4
MKETAEAYLGKK	42.5
NGHVEIIANDQGNR	75.6
RALSSQHQVR	31.5
SGGAPGAGGESSTEEEDESHDEL	89.1
TVFDVKR	29.7
VEIESLFDGVDLSEPLTR	n.d.
VEIIANDQGNR	61.9
Overall	90.1

AT3G06810.1	
Peptide sequence	Best Mascot Ion score
AASIYTGVYSR	39.2
FAADNVSGFPTNPSQFK	n.d.
IADGPDEVHLGTIGK	25.2
IDNLVFHPSEDR	44.6
LLVLEAADHLDK	52.7
LPNVAPER	28.1
RELAATENKHNLSGK	33.3
Overall	52.7

AT3G16460.1	
Peptide sequence	Best Mascot Ion score
LEGAGSEAGTLWDDGAFDGVR	n.d.
LTAEGGETGAVWDDGSHDDVKK	65.4
NGSQVVFGDER	39.8
SGFQISAPEATGK	73.5
SLSTQEVITALTFTTNK	n.d.
SSTTPVPSTPLK	51.7
VYVGQGQDGVAAVK	80.4
Overall	80.4

AT1G33680.1	
Peptide sequence	Best Mascot Ion score
AEEEVIAIPVQPSDHKR	44.2
EVNGSVSHDEIGDESK	60.4

EVNISGSQNEGEDDSKETNDVVAQK	49.6
IQLIPQNEGDASK	25.1
Overall	60.4

AT2G18020.1	
Peptide sequence	Best Mascot Ion score
ASGDYAIVIAHNPDSDTTR	36.8
GVVTEIIHDPGR	50.9
Overall	50.9

AT1G68560.1	
Peptide sequence	Best Mascot Ion score
IYGSDITTLR	35.5
TIATSATHYNGVR	58.3
Overall	58.3

AT1G5550.1	
Peptide sequence	Best Mascot Ion score
DTQEVKLEQGLK	59.7
SVSGSGVASSYSK	69.5
YNVWASTPNGNKK	44.4
Overall	69.5

AT2G42520.1	
Peptide sequence	Best Mascot Ion score
ELASQIHDEAK	46.9
VGSSTDLIVQR	54.2
VGYGGPPSGSR	46.9
Overall	54.2

Appendix II.II.

AT4G33430.1	
Peptide sequence	Best Mascot Ion score
AANILLDEEFEAVVGDFGLAK	37.9
ADGTLVAVKR	35.8
DTHVTTAVR	41.3
ELQVASDNFSNK	74.6
ELQVASDNFSNKNILGR	78.1
ERPESQPPLDWPK	53.8
ERPESQPPLDWPKR	33.5
GFCMTPTER	49.5
GGFGKVYK	38.7
GLAYLHDHCDPK	45.8
GRLADGTLVAVK	52.6
GRLADGTLVAVKR	53.6
GTIGHIAPEYLSTGK	77.2
IENEYPSGPR	52.8
ITGAIAGGVAAGAALLFAVPAIALAWWR	28
LADGTLVAVK	84.7
LADGTLVAVKR	86.5
LMDYKDTHVTTAVR	84.6
LNNNSLSGEIPR	48.4
MLEGDGLAER	52.1
MSEVVR	37.4
NAEGDALSALK	83.6
NSLADPNK	29.7
Overall	86.5

AT1G71830.1	
Peptide sequence	Best Mascot Ion score
AANILLDEEFEAVVGDFGLAK	37.9
ADGTLVAVKR	35.8
AFDLAR	24.5
DTHVTTAVR	41.3
ELQVASDGFSNK	68.2
GFCMTPTER	49.5
GGFGKVYK	38.7
GRLADGTLVAVK	52.6
GRLADGTLVAVKR	53.6
GTIGHIAPEYLSTGK	77.2
LADGTLVAVK	84.7
LADGTLVAVKR	86.5
LMDYKDTHVTTAVR	84.6
LRGFCMTPTER	22.2
MLEGDGLAEK	57.5
MSEVVR	37.4
Overall	86.5

AT2G13790.1	
Peptide sequence	Best Mascot Ion score
AANILLDEEFEAVVGDFGLAK	37.9
GFCMTPTER	49.5
GGFGKVYK	38.7
GRLADGNLVAVK	33

GRLADGNLVAVKR	53.6
GTIGHIAPEYLSTGK	77.2
LADGNLVAVK	84.7
LADGNLVAVKR	86.5
LANDDDIMLLDWVK	73.4
LRGFCMTPTER	22.2
MLEGDGLAER	52.1
MSEVVR	37.4
Overall	86.5

AT1G27190.1	
Peptide sequence	Best Mascot Ion score
ADLPDGSALAVK	42.6
ADLPDGSALAVKR	35.8
IACSCVVSRPK	66.3
NSLIDPSSR	34.6
RLSACGFGEK	36.2
Overall	66.3

AT3G13930.1	
Peptide sequence	Best Mascot Ion score
AAALALR	25.3
ADVEDFLASGSK	89.6
DYTPSSDTGPAAPEAK	72.4
GLSTIGEEVR	48.8
GYIETPESMLL	51.1
IFASPLAR	33.5

ISKPSSAPSEDR	43.3
ISVNDLVIK	60.7
KGLSTIGEEVR	42.2
KLAEDNNVPLSSIK	85.6
LAEDNNVPLSSIK	72
SQLNSFQEASGGK	55.5
SQLNSFQEASGGKR	104
VEKPASAPEAK	40.9
VIDGAIGAEWLK	28.3
Overall	104

AT3G25230.1	
Peptide sequence	Best Mascot Ion score
ALEIDPNNR	29.5
FTLGQGQVIK	32.8
LEDGTVVGK	29.6
LQDGTVFLK	26.6
SDGVEFTVK	27.1
TVSEVTDDNKVVK	63.8
VACNLNDAACK	33.1
VGEEKEIQQGLK	41.2
VGEEKEIQQGLKK	27.8
VLELESTNVK	75.6
Overall	75.6

AT4G31990.1	
Peptide sequence	Best Mascot Ion score
AENLMLER	32
IADVIQEK	35.2
IGAINVVCSSADAATR	69.8
ISLAGLSLAK	47.6
LAAALIER	60.2
NLGLYAER	27.4
QELYDSLVSK	32.4
TEELQPYVLNVVK	81.2
VATIQGLSGTGSLR	38.4
VVISSPTWGNHK	36.9
Overall	81.2

AT1G20260.1	
Peptide sequence	Best Mascot Ion score
FVMQGAYDTR	58
QIYPPINVLPSLSR	31.8
TLDQFYSR	49.6
TPVSLDMLGR	54
TVSGVAGPLVILDK	39.4
Overall	58

AT1G23190.1	
Peptide sequence	Best Mascot Ion score
LSGTGSEGATIR	90.9

SMPTSAALDVVAK	65.5
YDYENVDAGK	32.5
Overall	90.9

AT1G32500.1	
Peptide sequence	Best Mascot Ion score
FAQQTNAGQLTR	46.9
GIDLETAR	34.5
SSQIEPISTQQR	57.5
Overall	57.5

AT3G02090.1	
Peptide sequence	Best Mascot Ion score
HVGSDLTQR	44
IDAVDASTVK	31.8
IDAVDASTVKR	61.7
IPTAELFAR	50.3
TILGPAQNVK	34
VTTLPNGLR	25.2
Overall	61.7

AT3G4800.1	
Peptide sequence	Best Mascot Ion score
FSDVDEVIK	34.1
LAFTGSTDTGK	34.6
TAEQTPLTAFYAGK	56.8

TAFDEGPWPK	32.4
YGLAAGVFTK	41.8
Overall	86.5

AT4G24190.1	
Peptide sequence	Best Mascot Ion score
EESSDDVTDPPKVEEK	34
ELISNASDALDK	48.8
GNLASENVDDVK	29.6
IMQSQTLSDANK	55.8
LADTPCVVVTSK	36.3
Overall	55.8

AT4G34200.1	
Peptide sequence	Best Mascot Ion score
GGVIDEDALVR	47.1
ILNDETFAK	45.6
STGDGSKPTILVAEK	79.4
TLAVLGFGK	55.6
VIAHDPYAPADR	32.2
Overall	79.4

AT5G01410.1	
Peptide sequence	Best Mascot Ion score
GGVIMDVVNAEQAR	67.2
IPFVCGCR	34.6

IREGAAMIR	32.2
LAAPYDLVMQTK	32.1
MSDPQMIKEIK	29.7
NMDDDEVFTFAK	78.7
TKGEAGTGNIIEAVR	87.3
VGLAQMLR	56.4
Overall	87.3

AT5G63570.1	
Peptide sequence	Best Mascot Ion score
AGSGVATLGLPDSPGVPK	37.3
FVNSGTEACMGVLR	60.2
IIGGGLPVGAYGGR	36.5
NLMPGGVNSPVR	41.6
SVGGQPVLIDSVK	52.3
Overall	60.2

Appendix II.III.

AT4G33430.1	
Peptide sequence	Best Mascot Ion score
ELQVASDNFSNK	77.3
ERPESQPPLDWPKR	31.9
GTIGHIAPEYLSTGK	72.6
LADGTLVAVK	74.3
Overall	77.3

AT2G13790.1	
Peptide sequence	Best Mascot Ion score
ELLVATDNFSNK	62.3
ERPEGNPALDWPK	38.9
GTIGHIAPEYLSTGK	72.6
Overall	72.6

AT3G50590.1	
Peptide sequence	Best Mascot Ion score
ILSQQGGEAVYPLPR	37.9
LPLITVVDTK	49.5
LPLITVVDTKDQLK	38.7
Overall	49.5

AT3G19820.1	
Peptide sequence	Best Mascot Ion score
GQFVEYIPTR	32.9
VEPLVNMGQISR	54.8
Overall	54.8

AT2G02740.1	
Peptide sequence	Best Mascot Ion score
APEFVALESGAFK	109
FFNLSVQNK	50.9
YGGDYEWSR	64.6
Overall	109

AT5G06450.1	
Peptide sequence	Best Mascot Ion score
GTLVLEFLGTR	92.8
NLCLFLR	39.3
TSGWSLSSVK	44.3
Overall	92.8

AT5G24710.1	
Peptide sequence	Best Mascot Ion score
ENSAIYILGR	34.7
VSGSAPQLITIGADK	34.3
Overall	34.7

List of References

Aarts, N., Metz, M., Holub, E., Staskawicz, B.J., Daniels, M.J., and Parker, J.E. (1998). Different requirements for EDS1 and NDR1 by disease resistance genes define at least two R gene-mediated signaling pathways in Arabidopsis. Proc Natl Acad Sci U S A **95,** 10306-10311.

Agorio, A., and Vera, P. (2007). ARGONAUTE4 is required for resistance to Pseudomonas syringae in Arabidopsis. Plant Cell **19,** 3778-3790.

Albersheim, P., and Valent, B.S. (1978). Host-pathogen interactions in plants. Plants, when exposed to oligosaccharides of fungal origin, defend themselves by accumulating antibiotics. J Cell Biol **78,** 627-643.

Albrecht, C., Russinova, E., Hecht, V., Baaijens, E., and de Vries, S. (2005). The Arabidopsis thaliana SOMATIC EMBRYOGENESIS RECEPTOR-LIKE KINASES1 and 2 control male sporogenesis. Plant Cell **17,** 3337-3349.

Albrecht, C., Russinova, E., Kemmerling, B., Kwaaitaal, M., and de Vries, S.C. (2008). Arabidopsis SOMATIC EMBRYOGENESIS RECEPTOR KINASE proteins serve brassinosteroid-dependent and -independent signaling pathways. Plant Physiol **148,** 611-619.

Ali, R., Ma, W., Lemtiri-Chlieh, F., Tsaltas, D., Leng, Q., von Bodman, S., and Berkowitz, G.A. (2007). Death don't have no mercy and neither does calcium: Arabidopsis CYCLIC NUCLEOTIDE GATED CHANNEL2 and innate immunity. Plant Cell **19,** 1081-1095.

Anderson, J.C., and Peck, S.C. (2008). A simple and rapid technique for detecting protein phosphorylation using one-dimensional isoelectric focusing gels and immunoblot analysis. Plant J **55,** 881-885.

Apel, K., and Hirt, H. (2004). Reactive oxygen species: metabolism, oxidative stress, and signal transduction. Annu Rev Plant Biol **55,** 373-399.

Asada, K. (1999). THE WATER-WATER CYCLE IN CHLOROPLASTS: Scavenging of Active Oxygens and Dissipation of Excess Photons. Annu Rev Plant Physiol Plant Mol Biol **50,** 601-639.

Asai, S., Ohta, K., and Yoshioka, H. (2008). MAPK signaling regulates nitric oxide and NADPH oxidase-dependent oxidative bursts in Nicotiana benthamiana. Plant Cell **20,** 1390-1406.

Asai, T., Tena, G., Plotnikova, J., Willmann, M.R., Chiu, W.L., Gomez-Gomez, L., Boller, T., Ausubel, F.M., and Sheen, J. (2002). MAP kinase signalling cascade in Arabidopsis innate immunity. Nature **415,** 977-983.

Aslam, S.N., Erbs, G., Morrissey, K.L., Newman, M.A., Chinchilla, D., Boller, T., Molinaro, A., Jackson, R.W., and Cooper, R.M. (2009). Microbe-associated molecular pattern (MAMP) signatures, synergy, size and charge: influences on perception or mobility and host defence responses. Mol Plant Pathol **10,** 375-387.

Aslam, S.N., Newman, M.A., Erbs, G., Morrissey, K.L., Chinchilla, D., Boller, T., Jensen, T.T., De Castro, C., Ierano, T., Molinaro, A., Jackson, R.W., Knight, M.R., and Cooper, R.M. (2008). Bacterial polysaccharides suppress induced innate immunity by calcium chelation. Curr Biol **18,** 1078-1083.

Austin, M.J., Muskett, P., Kahn, K., Feys, B.J., Jones, J.D., and Parker, J.E. (2002). Regulatory role of SGT1 in early R gene-mediated plant defenses. Science **295,** 2077-2080.

Ausubel, F.M. (2005). Are innate immune signaling pathways in plants and animals conserved? Nat Immunol **6,** 973-979.

Axtell, M.J., and Staskawicz, B.J. (2003). Initiation of RPS2-specified disease resistance in Arabidopsis is coupled to the AvrRpt2-directed elimination of RIN4. Cell **112,** 369-377.

Ayers, A.R., Ebel, J., Valent, B., and Albersheim, P. (1976). Host-Pathogen Interactions: X. Fractionation and Biological Activity of an Elicitor Isolated from the Mycelial Walls of Phytophthora megasperma var. sojae. Plant Physiol **57,** 760-765.

Azevedo, C., Sadanandom, A., Kitagawa, K., Freialdenhoven, A., Shirasu, K., and Schulze-Lefert, P. (2002). The RAR1 interactor SGT1, an essential component of R gene-triggered disease resistance. Science **295,** 2073-2076.

Bar, M., and Avni, A. (2009a). EHD2 inhibits ligand-induced endocytosis and signaling of the leucine-rich repeat receptor-like protein LeEix2. Plant J **59,** 600-611.

Bar, M., and Avni, A. (2009b). EHD2 inhibits signaling of leucine rich repeat receptor-like proteins. Plant Signal Behav **4,** 682-684.

Bar, M., Sharfman, M., Ron, M., and Avni, A. (2010). BAK1 is required for the attenuation of Eix-induced defense responses by the decoy receptor LeEix1. Plant J.

Bartels, S., Besteiro, M.A., Lang, D., and Ulm, R. (2010). Emerging functions for plant MAP kinase phosphatases. Trends Plant Sci **15,** 322-329.

Bartels, S., Anderson, J.C., Gonzalez Besteiro, M.A., Carreri, A., Hirt, H., Buchala, A., Metraux, J.P., Peck, S.C., and Ulm, R. (2009). MAP kinase phosphatase1 and protein tyrosine phosphatase1 are repressors of salicylic acid synthesis and SNC1-mediated responses in Arabidopsis. Plant Cell **21,** 2884-2897.

Bednarek, P., Pislewska-Bednarek, M., Svatos, A., Schneider, B., Doubsky, J., Mansurova, M., Humphry, M., Consonni, C., Panstruga, R., Sanchez-Vallet, A., Molina, A., and Schulze-Lefert, P. (2009). A glucosinolate metabolism pathway in living plant cells mediates broad-spectrum antifungal defense. Science **323,** 101-106.

Benschop, J.J., Mohammed, S., O'Flaherty, M., Heck, A.J., Slijper, M., and Menke, F.L. (2007). Quantitative phosphoproteomics of early elicitor signaling in Arabidopsis. Mol Cell Proteomics **6,** 1198-1214.

Berleth, T., Krogan, N.T., and Scarpella, E. (2004). Auxin signals--turning genes on and turning cells around. Curr Opin Plant Biol **7,** 553-563.

Bi, D., Cheng, Y.T., Li, X., and Zhang, Y. (2010). Activation of plant immune responses by a gain-of-function mutation in an atypical receptor-like kinase. Plant Physiol **153,** 1771-1779.

Boller, T. (1995). Chemoperception of Microbial Signals in Plant Cells. Annual Review of Plant Physiology and Plant Molecular Biology **46,** 189-214.

Boller, T., and Felix, G. (2009). A renaissance of elicitors: perception of microbe-associated molecular patterns and danger signals by pattern-recognition receptors. Annu Rev Plant Biol **60,** 379-406.

Borner, G.H., Sherrier, D.J., Weimar, T., Michaelson, L.V., Hawkins, N.D., Macaskill, A., Napier, J.A., Beale, M.H., Lilley, K.S., and Dupree, P. (2005). Analysis of detergent-resistant membranes in Arabidopsis. Evidence for plasma membrane lipid rafts. Plant Physiol **137,** 104-116.

Bos, J.I., Armstrong, M.R., Gilroy, E.M., Boevink, P.C., Hein, I., Taylor, R.M., Zhendong, T., Engelhardt, S., Vetukuri, R.R., Harrower, B., Dixelius, C., Bryan, G., Sadanandom, A., Whisson, S.C., Kamoun, S., and Birch, P.R. (2010). Phytophthora infestans effector AVR3a is essential for virulence and manipulates plant immunity by stabilizing host E3 ligase CMPG1. Proc Natl Acad Sci U S A **107,** 9909-9914.

Bose, D., Joly, N., Pape, T., Rappas, M., Schumacher, J., Buck, M., and Zhang, X. (2008). Dissecting the ATP hydrolysis pathway of bacterial enhancer-binding proteins. Biochem Soc Trans **36,** 83-88.

Bossemeyer, D. (1994). The glycine-rich sequence of protein kinases: a multifunctional element. Trends Biochem Sci **19,** 201-205.

Boudsocq, M., Willmann, M.R., McCormack, M., Lee, H., Shan, L., He, P., Bush, J., Cheng, S.H., and Sheen, J. (2010). Differential innate immune signalling via Ca(2+) sensor protein kinases. Nature **464,** 418-422.

Boutrot, F., Segonzac, C., Chang, K.N., Qiao, H., Ecker, J.R., Zipfel, C., and Rathjen, J.P. (2010). Direct transcriptional control of the Arabidopsis immune receptor FLS2 by the ethylene-dependent transcription factors EIN3 and EIL1. Proc Natl Acad Sci U S A **107,** 14502-14507.

Brueggeman, R., Rostoks, N., Kudrna, D., Kilian, A., Han, F., Chen, J., Druka, A., Steffenson, B., and Kleinhofs, A. (2002). The barley stem rust-resistance gene Rpg1 is a novel disease-resistance gene with homology to receptor kinases. Proc Natl Acad Sci U S A **99,** 9328-9333.

Brunner, F., Rosahl, S., Lee, J., Rudd, J.J., Geiler, C., Kauppinen, S., Rasmussen, G., Scheel, D., and Nurnberger, T. (2002). Pep-13, a plant defense-inducing pathogen-associated pattern from Phytophthora transglutaminases. Embo J **21,** 6681-6688.

Brutus, A., Sicilia, F., Macone, A., Cervone, F., and De Lorenzo, G. (2010). A domain swap approach reveals a role of the plant wall-associated kinase 1 (WAK1) as a receptor of oligogalacturonides. Proc Natl Acad Sci U S A **107,** 9452-9457.

Burch-Smith, T.M., Schiff, M., Caplan, J.L., Tsao, J., Czymmek, K., and Dinesh-Kumar, S.P. (2007). A Novel Role for the TIR Domain in Association with Pathogen-Derived Elicitors. PLoS Biol **5,** e68.

Cabrera, J.C., Boland, A., Messiaen, J., Cambier, P., and Van Cutsem, P. (2008). Egg box conformation of oligogalacturonides: the time-dependent stabilization of the elicitor-active conformation increases its biological activity. Glycobiology **18,** 473-482.

Caplan, J.L., Mamillapalli, P., Burch-Smith, T.M., Czymmek, K., and Dinesh-Kumar, S.P. (2008). Chloroplastic protein NRIP1 mediates innate immune receptor recognition of a viral effector. Cell **132,** 449-462.

Century, K.S., Holub, E.B., and Staskawicz, B.J. (1995). NDR1, a locus of Arabidopsis thaliana that is required for disease resistance to both a bacterial and a fungal pathogen. Proc Natl Acad Sci U S A **92,** 6597-6601.

Century, K.S., Shapiro, A.D., Repetti, P.P., Dahlbeck, D., Holub, E., and Staskawicz, B.J. (1997). NDR1, a pathogen-induced component required for Arabidopsis disease resistance. Science **278,** 1963-1965.

Chen, H., Zhang, D., Guo, J., Wu, H., Jin, M., Lu, Q., Lu, C., and Zhang, L. (2006). A Psb27 homologue in Arabidopsis thaliana is required for efficient repair of photodamaged photosystem II. Plant Mol Biol **61,** 567-575.

Chen, H., Xue, L., Chintamanani, S., Germain, H., Lin, H., Cui, H., Cai, R., Zuo, J., Tang, X., Li, X., Guo, H., and Zhou, J.M. (2009). ETHYLENE INSENSITIVE3 and ETHYLENE INSENSITIVE3-LIKE1 repress SALICYLIC ACID INDUCTION DEFICIENT2 expression to negatively regulate plant innate immunity in Arabidopsis. Plant Cell **21,** 2527-2540.

Chen, X., Chern, M., Canlas, P.E., Ruan, D., Jiang, C., and Ronald, P.C. (2010). An ATPase promotes autophosphorylation of the pattern recognition receptor XA21 and inhibits XA21-mediated immunity. Proc Natl Acad Sci U S A **107,** 8029-8034.

Chinchilla, D., Zipfel, C., Robatzek, S., Kemmerling, B., Nurnberger, T., Jones, J.D., Felix, G., and Boller, T. (2007). A flagellin-induced complex of the receptor FLS2 and BAK1 initiates plant defence. Nature **448,** 497-500.

Chini, A., Fonseca, S., Fernandez, G., Adie, B., Chico, J.M., Lorenzo, O., Garcia-Casado, G., Lopez-Vidriero, I., Lozano, F.M., Ponce, M.R., Micol, J.L., and Solano, R. (2007). The JAZ family of repressors is the missing link in jasmonate signalling. Nature **448,** 666-671.

Chisholm, S.T., Coaker, G., Day, B., and Staskawicz, B.J. (2006). Host-microbe interactions: shaping the evolution of the plant immune response. Cell **124,** 803-814.

Choi, J., Huh, S.U., Kojima, M., Sakakibara, H., Paek, K.H., and Hwang, I. (2010). The cytokinin-activated transcription factor ARR2 promotes plant immunity via TGA3/NPR1-dependent salicylic acid signaling in Arabidopsis. Dev Cell **19,** 284-295.

Chuck, G., and O'Connor, D. (2010). Small RNAs going the distance during plant development. Curr Opin Plant Biol **13,** 40-45.

Clay, N.K., Adio, A.M., Denoux, C., Jander, G., and Ausubel, F.M. (2009). Glucosinolate metabolites required for an Arabidopsis innate immune response. Science **323,** 95-101.

Clough, S.J., and Bent, A.F. (1998). Floral dip: a simplified method for Agrobacterium-mediated transformation of Arabidopsis thaliana. Plant J **16,** 735-743.

Clouse, S.D. (2002). Brassinosteroid signal transduction: clarifying the pathway from ligand perception to gene expression. Mol Cell **10,** 973-982.

Clouse, S.D., and Sasse, J.M. (1998). BRASSINOSTEROIDS: Essential Regulators of Plant Growth and Development. Annu Rev Plant Physiol Plant Mol Biol **49,** 427-451.

Coca, M., and San Segundo, B. (2010). AtCPK1 calcium-dependent protein kinase mediates pathogen resistance in Arabidopsis. Plant J.

Colcombet, J., Boisson-Dernier, A., Ros-Palau, R., Vera, C.E., and Schroeder, J.I. (2005). Arabidopsis SOMATIC EMBRYOGENESIS RECEPTOR KINASES1 and 2 are essential for tapetum development and microspore maturation. Plant Cell **17,** 3350-3361.

Collier, S.M., and Moffett, P. (2009). NB-LRRs work a "bait and switch" on pathogens. Trends Plant Sci **14,** 521-529.

Conti, L., Price, G., O'Donnell, E., Schwessinger, B., Dominy, P., and Sadanandom, A. (2008). Small ubiquitin-like modifier proteases OVERLY TOLERANT TO SALT1 and -2 regulate salt stress responses in Arabidopsis. Plant Cell **20,** 2894-2908.

Coppinger, P., Repetti, P.P., Day, B., Dahlbeck, D., Mehlert, A., and Staskawicz, B.J. (2004). Overexpression of the plasma membrane-localized NDR1 protein results in enhanced bacterial disease resistance in Arabidopsis thaliana. Plant J **40,** 225-237.

Cui, H., Wang, Y., Xue, L., Chu, J., Yan, C., Fu, J., Chen, M., Innes, R.W., and Zhou, J.M. (2010). Pseudomonas syringae effector protein AvrB perturbs Arabidopsis hormone signaling by activating MAP kinase 4. Cell Host Microbe **7,** 164-175.

Dardick, C., and Ronald, P. (2006). Plant and animal pathogen recognition receptors signal through non-RD kinases. PLoS Pathog **2,** e2.

de Jonge, R., van Esse, H.P., Kombrink, A., Shinya, T., Desaki, Y., Bours, R., van der Krol, S., Shibuya, N., Joosten, M.H., and Thomma, B.P. (2010). Conserved fungal LysM effector Ecp6 prevents chitin-triggered immunity in plants. Science **329,** 953-955.

de Torres-Zabala, M., Truman, W., Bennett, M.H., Lafforgue, G., Mansfield, J.W., Rodriguez Egea, P., Bogre, L., and Grant, M. (2007). Pseudomonas syringae pv. tomato hijacks the Arabidopsis abscisic acid signalling pathway to cause disease. Embo J **26,** 1434-1443.

de Torres, M., Mansfield, J.W., Grabov, N., Brown, I.R., Ammouneh, H., Tsiamis, G., Forsyth, A., Robatzek, S., Grant, M., and Boch, J. (2006). Pseudomonas syringae effector AvrPtoB suppresses basal defence in Arabidopsis. Plant J **47,** 368-382.

Dehmelt, L., and Bastiaens, P.I. (2010). Spatial organization of intracellular communication: insights from imaging. Nat Rev Mol Cell Biol **11,** 440-452.

DeYoung, B.J., and Innes, R.W. (2006). Plant NBS-LRR proteins in pathogen sensing and host defense. Nat Immunol **7,** 1243-1249.

Dibb, N.J., Dilworth, S.M., and Mol, C.D. (2004). Switching on kinases: oncogenic activation of BRAF and the PDGFR family. Nat Rev Cancer **4,** 718-727.

Ding, Z., Wang, H., Liang, X., Morris, E.R., Gallazzi, F., Pandit, S., Skolnick, J., Walker, J.C., and Van Doren, S.R. (2007). Phosphoprotein and

phosphopeptide interactions with the FHA domain from Arabidopsis kinase-associated protein phosphatase. Biochemistry **46,** 2684-2696.

Djonovic, S., Pozo, M.J., Dangott, L.J., Howell, C.R., and Kenerley, C.M. (2006). Sm1, a proteinaceous elicitor secreted by the biocontrol fungus Trichoderma virens induces plant defense responses and systemic resistance. Mol Plant Microbe Interact **19,** 838-853.

Dodd, A.N., Kudla, J., and Sanders, D. (2010). The language of calcium signaling. Annu Rev Plant Biol **61,** 593-620.

Dodds, P.N., and Rathjen, J.P. (2010). Plant immunity: towards an integrated view of plant-pathogen interactions. Nat Rev Genet **11,** 539-548.

Dodds, P.N., Lawrence, G.J., Catanzariti, A.M., Teh, T., Wang, C.I., Ayliffe, M.A., Kobe, B., and Ellis, J.G. (2006). Direct protein interaction underlies gene-for-gene specificity and coevolution of the flax resistance genes and flax rust avirulence genes. Proc Natl Acad Sci U S A **103,** 8888-8893.

Domagalska, M.A., Schomburg, F.M., Amasino, R.M., Vierstra, R.D., Nagy, F., and Davis, S.J. (2007). Attenuation of brassinosteroid signaling enhances FLC expression and delays flowering. Development **134,** 2841-2850.

Dong, J., Xiao, F., Fan, F., Gu, L., Cang, H., Martin, G.B., and Chai, J. (2009). Crystal structure of the complex between Pseudomonas effector AvrPtoB and the tomato Pto kinase reveals both a shared and a unique interface compared with AvrPto-Pto. Plant Cell **21,** 1846-1859.

Dunning, F.M., Sun, W., Jansen, K.L., Helft, L., and Bent, A.F. (2007). Identification and Mutational Analysis of Arabidopsis FLS2 Leucine-Rich Repeat Domain Residues That Contribute to Flagellin Perception. Plant Cell **19,** 3297-3313.

Durrant, W.E., and Dong, X. (2004). Systemic acquired resistance. Annu Rev Phytopathol **42,** 185-209.

Earley, K.W., Haag, J.R., Pontes, O., Opper, K., Juehne, T., Song, K., and Pikaard, C.S. (2006). Gateway-compatible vectors for plant functional genomics and proteomics. Plant J **45,** 616-629.

Ellis, J.G., Rafiqi, M., Gan, P., Chakrabarti, A., and Dodds, P.N. (2009). Recent progress in discovery and functional analysis of effector proteins of fungal and oomycete plant pathogens. Curr Opin Plant Biol **12,** 399-405.

Eng, J.K., McCormack, A.L., and Yates Iii, J.R. (1994). An approach to correlate tandem mass spectral data of peptides with amino acid sequences in a protein database. Journal of the American Society for Mass Spectrometry **5,** 976-989.

Escobar-Restrepo, J.M., Huck, N., Kessler, S., Gagliardini, V., Gheyselinck, J., Yang, W.C., and Grossniklaus, U. (2007). The FERONIA receptor-like kinase mediates male-female interactions during pollen tube reception. Science **317,** 656-660.

Fan, J., Hill, L., Crooks, C., Doerner, P., and Lamb, C. (2009). Abscisic acid has a key role in modulating diverse plant-pathogen interactions. Plant Physiol **150,** 1750-1761.

Felix, G., and Boller, T. (2003). Molecular sensing of bacteria in plants. The highly conserved RNA-binding motif RNP-1 of bacterial cold shock proteins is recognized as an elicitor signal in tobacco. J Biol Chem **278,** 6201-6208.

Felix, G., Regenass, M., Spanu, P., and Boller, T. (1994). The protein phosphatase inhibitor calyculin A mimics elicitor action in plant cells and induces rapid hyperphosphorylation of specific proteins as revealed by pulse labeling with [33P]phosphate. Proc Natl Acad Sci U S A **91,** 952-956.

Felix, G., Duran, J.D., Volko, S., and Boller, T. (1999). Plants have a sensitive perception system for the most conserved domain of bacterial flagellin. Plant J **18,** 265-276.

Feys, B.J., Moisan, L.J., Newman, M.A., and Parker, J.E. (2001). Direct interaction between the Arabidopsis disease resistance signaling proteins, EDS1 and PAD4. Embo J **20,** 5400-5411.

Feys, B.J., Wiermer, M., Bhat, R.A., Moisan, L.J., Medina-Escobar, N., Neu, C., Cabral, A., and Parker, J.E. (2005). Arabidopsis SENESCENCE-ASSOCIATED GENE101 stabilizes and signals within an ENHANCED DISEASE SUSCEPTIBILITY1 complex in plant innate immunity. Plant Cell **17,** 2601-2613.

Fiil, B.K., Petersen, K., Petersen, M., and Mundy, J. (2009). Gene regulation by MAP kinase cascades. Curr Opin Plant Biol **12,** 615-621.

Flor, H.H. (1971). Current Status of the Gene-For-Gene Concept. Annual Review of Phytopathology **9,** 275-296.

Friedrichsen, D.M., Joazeiro, C.A., Li, J., Hunter, T., and Chory, J. (2000). Brassinosteroid-insensitive-1 is a ubiquitously expressed leucine-rich repeat receptor serine/threonine kinase. Plant Physiol **123,** 1247-1256.

Friedrichsen, D.M., Nemhauser, J., Muramitsu, T., Maloof, J.N., Alonso, J., Ecker, J.R., Furuya, M., and Chory, J. (2002). Three redundant brassinosteroid early response genes encode putative bHLH transcription factors required for normal growth. Genetics **162,** 1445-1456.

Fu, Z.Q., Guo, M., Jeong, B.R., Tian, F., Elthon, T.E., Cerny, R.L., Staiger, D., and Alfano, J.R. (2007). A type III effector ADP-ribosylates RNA-binding proteins and quells plant immunity. Nature **447,** 284-288.

Fujiwara, M., Hamada, S., Hiratsuka, M., Fukao, Y., Kawasaki, T., and Shimamoto, K. (2009). Proteome analysis of detergent-resistant membranes (DRMs) associated with OsRac1-mediated innate immunity in rice. Plant & cell physiology **50,** 1191-1200.

Fujiwara, S., Tanaka, N., Kaneda, T., Takayama, S., Isogai, A., and Che, F.S. (2004). Rice cDNA microarray-based gene expression profiling of the response to flagellin perception in cultured rice cells. Mol Plant Microbe Interact **17,** 986-998.

Galletti, R., Denoux, C., Gambetta, S., Dewdney, J., Ausubel, F.M., De Lorenzo, G., and Ferrari, S. (2008). The AtrbohD-mediated oxidative burst elicited by oligogalacturonides in Arabidopsis is dispensable for the activation of defense responses effective against Botrytis cinerea. Plant Physiol **148,** 1695-1706.

Gassmann, W., Hinsch, M.E., and Staskawicz, B.J. (1999). The Arabidopsis RPS4 bacterial-resistance gene is a member of the TIR-NBS-LRR family of disease-resistance genes. Plant J **20,** 265-277.

Geldner, N., Hyman, D.L., Wang, X., Schumacher, K., and Chory, J. (2007). Endosomal signaling of plant steroid receptor kinase BRI1. Genes Dev **21,** 1598-1602.

George, R.E., Sanda, T., Hanna, M., Frohling, S., Luther, W., 2nd, Zhang, J., Ahn, Y., Zhou, W., London, W.B., McGrady, P., Xue, L., Zozulya, S., Gregor, V.E., Webb, T.R., Gray, N.S., Gilliland, D.G., Diller, L., Greulich, H., Morris, S.W., Meyerson, M., and Look, A.T. (2008). Activating mutations in ALK provide a therapeutic target in neuroblastoma. Nature **455,** 975-978.

Gimenez-Ibanez, S., Ntoukakis, V., and Rathjen, J.P. (2009a). The LysM receptor kinase CERK1 mediates bacterial perception in Arabidopsis. Plant Signal Behav **4,** 539-541.

Gimenez-Ibanez, S., Hann, D.R., Ntoukakis, V., Petutschnig, E., Lipka, V., and Rathjen, J.P. (2009b). AvrPtoB targets the LysM receptor kinase CERK1 to promote bacterial virulence on plants. Curr Biol **19,** 423-429.

Glazebrook, J. (2005). Contrasting mechanisms of defense against biotrophic and necrotrophic pathogens. Annu Rev Phytopathol **43,** 205-227.

Goda, H., Sawa, S., Asami, T., Fujioka, S., Shimada, Y., and Yoshida, S. (2004). Comprehensive comparison of auxin-regulated and brassinosteroid-regulated genes in Arabidopsis. Plant Physiol **134,** 1555-1573.

Gohre, V., Spallek, T., Haweker, H., Mersmann, S., Mentzel, T., Boller, T., de Torres, M., Mansfield, J.W., and Robatzek, S. (2008). Plant pattern-recognition receptor FLS2 is directed for degradation by the bacterial ubiquitin ligase AvrPtoB. Curr Biol **18,** 1824-1832.

Gomez-Gomez, L., and Boller, T. (2000). FLS2: an LRR receptor-like kinase involved in the perception of the bacterial elicitor flagellin in Arabidopsis. Mol Cell **5,** 1003-1011.

Gomez-Gomez, L., Bauer, Z., and Boller, T. (2001). Both the extracellular leucine-rich repeat domain and the kinase activity of FSL2 are required for flagellin binding and signaling in Arabidopsis. Plant Cell **13,** 1155-1163.

Goodin, M.M., Zaitlin, D., Naidu, R.A., and Lommel, S.A. (2008). Nicotiana benthamiana: its history and future as a model for plant-pathogen interactions. Mol Plant Microbe Interact **21,** 1015-1026.

Granado, J., Felix, G., and Boller, T. (1995). Perception of Fungal Sterols in Plants (Subnanomolar Concentrations of Ergosterol Elicit Extracellular Alkalinization in Tomato Cells). Plant Physiol **107,** 485-490.

Gudesblat, G.E., Torres, P.S., and Vojnov, A.A. (2009a). Stomata and pathogens: Warfare at the gates. Plant Signal Behav **4,** 1114-1116.

Gudesblat, G.E., Torres, P.S., and Vojnov, A.A. (2009b). Xanthomonas campestris overcomes Arabidopsis stomatal innate immunity through a DSF cell-to-cell signal-regulated virulence factor. Plant Physiol **149,** 1017-1027.

Guo, H., Li, L., Ye, H., Yu, X., Algreen, A., and Yin, Y. (2009a). Three related receptor-like kinases are required for optimal cell elongation in Arabidopsis thaliana. Proc Natl Acad Sci U S A **106,** 7648-7653.

Guo, M., Tian, F., Wamboldt, Y., and Alfano, J.R. (2009b). The majority of the type III effector inventory of Pseudomonas syringae pv. tomato DC3000 can suppress plant immunity. Mol Plant Microbe Interact **22,** 1069-1080.

Gust, A.A., Biswas, R., Lenz, H.D., Rauhut, T., Ranf, S., Kemmerling, B., Gotz, F., Glawischnig, E., Lee, J., Felix, G., and Nurnberger, T. (2007). Bacteria-derived peptidoglycans constitute pathogen-associated molecular patterns triggering innate immunity in Arabidopsis. J Biol Chem.

Gutierrez, J.R., Balmuth, A.L., Ntoukakis, V., Mucyn, T.S., Gimenez-Ibanez, S., Jones, A.M., and Rathjen, J.P. (2010). Prf immune complexes of tomato are oligomeric and contain multiple Pto-like kinases that diversify effector recognition. Plant J **61,** 507-518.

Ham, J.H., Kim, M.G., Lee, S.Y., and Mackey, D. (2007). Layered basal defenses underlie non-host resistance of Arabidopsis to Pseudomonas syringae pv. phaseolicola. Plant J **51,** 604-616.

Hann, D.R., and Rathjen, J.P. (2007). Early events in the pathogenicity of Pseudomonas syringae on Nicotiana benthamiana. Plant J **49,** 607-618.

Haweker, H., Rips, S., Koiwa, H., Salomon, S., Saijo, Y., Chinchilla, D., Robatzek, S., and von Schaewen, A. (2010). Pattern recognition receptors require N-glycosylation to mediate plant immunity. J Biol Chem **285,** 4629-4636.

He, J.X., Gendron, J.M., Yang, Y., Li, J., and Wang, Z.Y. (2002). The GSK3-like kinase BIN2 phosphorylates and destabilizes BZR1, a positive regulator of the brassinosteroid signaling pathway in Arabidopsis. Proc Natl Acad Sci U S A **99,** 10185-10190.

He, J.X., Gendron, J.M., Sun, Y., Gampala, S.S., Gendron, N., Sun, C.Q., and Wang, Z.Y. (2005). BZR1 is a transcriptional repressor with dual roles in brassinosteroid homeostasis and growth responses. Science **307,** 1634-1638.

He, K., Gou, X., Yuan, T., Lin, H., Asami, T., Yoshida, S., Russell, S.D., and Li, J. (2007). BAK1 and BKK1 regulate brassinosteroid-dependent growth and brassinosteroid-independent cell-death pathways. Curr Biol **17,** 1109-1115.

He, P., Shan, L., Lin, N.C., Martin, G.B., Kemmerling, B., Nurnberger, T., and Sheen, J. (2006). Specific bacterial suppressors of MAMP signaling upstream of MAPKKK in Arabidopsis innate immunity. Cell **125,** 563-575.

He, Z., Wang, Z.Y., Li, J., Zhu, Q., Lamb, C., Ronald, P., and Chory, J. (2000). Perception of brassinosteroids by the extracellular domain of the receptor kinase BRI1. Science **288,** 2360-2363.

Hecht, V., Vielle-Calzada, J.-P., Hartog, M.V., Schmidt, E.D.L., Boutilier, K., Grossniklaus, U., and de Vries, S.C. (2001). The Arabidopsis Somatic Embryogenesis Receptor Kinase 1 Gene Is Expressed in Developing Ovules and Embryos and Enhances Embryogenic Competence in Culture. Plant Physiol. **127,** 803-816.

Heese, A., Hann, D.R., Gimenez-Ibanez, S., Jones, A.M., He, K., Li, J., Schroeder, J.I., Peck, S.C., and Rathjen, J.P. (2007). The receptor-like kinase SERK3/BAK1 is a central regulator of innate immunity in plants. Proc Natl Acad Sci U S A **104,** 12217-12222.

Holub, E.B. (2007). Natural variation in innate immunity of a pioneer species. Curr Opin Plant Biol **10,** 415-424.

Holub, E.B., and Cooper, A. (2004). Matrix, reinvention in plants: how genetics is unveiling secrets of non-host disease resistance. Trends Plant Sci **9,** 211-214.

Hu, H., Xiong, L., and Yang, Y. (2005). Rice SERK1 gene positively regulates somatic embryogenesis of cultured cell and host defense response against fungal infection. Planta **222,** 107-117.

Hubbard, S.R. (2004). Juxtamembrane autoinhibition in receptor tyrosine kinases. Nat Rev Mol Cell Biol **5,** 464-471.

Huffaker, A., and Ryan, C.A. (2007). Endogenous peptide defense signals in Arabidopsis differentially amplify signaling for the innate immune response. Proc Natl Acad Sci U S A **104,** 10732-10736.

Huffaker, A., Pearce, G., and Ryan, C.A. (2006). An endogenous peptide signal in Arabidopsis activates components of the innate immune response. Proc Natl Acad Sci U S A **103,** 10098-10103.

Ibanes, M., Fabregas, N., Chory, J., and Cano-Delgado, A.I. (2009). Brassinosteroid signaling and auxin transport are required to establish the periodic pattern of Arabidopsis shoot vascular bundles. Proc Natl Acad Sci U S A **106,** 13630-13635.

Ichikawa, T., Nakazawa, M., Kawashima, M., Iizumi, H., Kuroda, H., Kondou, Y., Tsuhara, Y., Suzuki, K., Ishikawa, A., Seki, M., Fujita, M., Motohashi, R., Nagata, N., Takagi, T., Shinozaki, K., and Matsui, M. (2006). The FOX hunting system: an alternative gain-of-function gene hunting technique. Plant J **48,** 974-985.

Ichimura, K., Casais, C., Peck, S.C., Shinozaki, K., and Shirasu, K. (2006). MEKK1 is required for MPK4 activation and regulates tissue-specific and temperature-dependent cell death in Arabidopsis. J Biol Chem **281,** 36969-36976.

Iizasa, E.I., Mitsutomi, M., and Nagano, Y. (2009). Direct binding of a plant LysM receptor-like kinase, LysM RLK1/CERK1, to Chitin in vitro. J Biol Chem.

Janeway, C.A., Jr., and Medzhitov, R. (2002). Innate immune recognition. Annu Rev Immunol **20,** 197-216.

Janjusevic, R., Abramovitch, R.B., Martin, G.B., and Stebbins, C.E. (2006). A bacterial inhibitor of host programmed cell death defenses is an E3 ubiquitin ligase. Science **311,** 222-226.

Jeong, Y.J., Shang, Y., Kim, B.H., Kim, S.Y., Song, J.H., Lee, J.S., Lee, M.M., Li, J., and Nam, K.H. (2010). BAK7 displays unequal genetic redundancy with BAK1 in brassinosteroid signaling and early senescence in arabidopsis. Mol Cells **29,** 259-266.

Jeworutzki, E., Roelfsema, M.R., Anschutz, U., Krol, E., Elzenga, J.T., Felix, G., Boller, T., Hedrich, R., and Becker, D. (2010). Early signaling through the Arabidopsis pattern recognition receptors FLS2 and EFR involves Ca-associated opening of plasma membrane anion channels. Plant J **62,** 367-378.

Johnson, L.N., Noble, M.E., and Owen, D.J. (1996). Active and inactive protein kinases: structural basis for regulation. Cell **85,** 149-158.

Jones, J.D., and Dangl, J.L. (2006). The plant immune system. Nature **444,** 323-329.

Journot-Catalino, N., Somssich, I.E., Roby, D., and Kroj, T. (2006). The transcription factors WRKY11 and WRKY17 act as negative regulators of basal resistance in Arabidopsis thaliana. Plant Cell **18,** 3289-3302.

Kaku, H., Nishizawa, Y., Ishii-Minami, N., Akimoto-Tomiyama, C., Dohmae, N., Takio, K., Minami, E., and Shibuya, N. (2006). Plant cells recognize chitin fragments for defense signaling through a plasma membrane receptor. Proc Natl Acad Sci U S A **103,** 11086-11091.

Kale, S.D., Gu, B., Capelluto, D.G., Dou, D., Feldman, E., Rumore, A., Arredondo, F.D., Hanlon, R., Fudal, I., Rouxel, T., Lawrence, C.B., Shan, W., and Tyler, B.M. (2010). External lipid PI3P mediates entry of eukaryotic pathogen effectors into plant and animal host cells. Cell **142,** 284-295.

Kamoun, S., van West, P., de Jong, A.J., de Groot, K.E., Vleeshouwers, V.G., and Govers, F. (1997). A gene encoding a protein elicitor of Phytophthora infestans is down-regulated during infection of potato. Mol Plant Microbe Interact **10,** 13-20.

Kannan, N., and Neuwald, A.F. (2005). Did protein kinase regulatory mechanisms evolve through elaboration of a simple structural component? J Mol Biol **351,** 956-972.

Karlova, R., Boeren, S., Russinova, E., Aker, J., Vervoort, J., and de Vries, S. (2006). The Arabidopsis SOMATIC EMBRYOGENESIS RECEPTOR-LIKE KINASE1 protein complex includes BRASSINOSTEROID-INSENSITIVE1. Plant Cell **18,** 626-638.

Katagiri, F., and Tsuda, K. (2010). Understanding the plant immune system. Mol Plant Microbe Interact.

Katiyar-Agarwal, S., Gao, S., Vivian-Smith, A., and Jin, H. (2007). A novel class of bacteria-induced small RNAs in Arabidopsis. Genes Dev **21,** 3123-3134.

Katsir, L., Schilmiller, A.L., Staswick, P.E., He, S.Y., and Howe, G.A. (2008). COI1 is a critical component of a receptor for jasmonate and the bacterial virulence factor coronatine. Proc Natl Acad Sci U S A **105,** 7100-7105.

Kawai, T., and Akira, S. (2010). The role of pattern-recognition receptors in innate immunity: update on Toll-like receptors. Nat Immunol **11,** 373-384.

Kawchuk, L.M., Hachey, J., Lynch, D.R., Kulcsar, F., van Rooijen, G., Waterer, D.R., Robertson, A., Kokko, E., Byers, R., Howard, R.J., Fischer, R., and Prufer, D. (2001). Tomato Ve disease resistance genes encode cell surface-like receptors. Proc Natl Acad Sci U S A **98,** 6511-6515.

Kazan, K., and Manners, J.M. (2009). Linking development to defense: auxin in plant-pathogen interactions. Trends Plant Sci **14,** 373-382.

Keen, N.T., Partridge, J., and Zaki, A. (1972). Pathogen-produced elicitor of a chemical defense mechanism in soybeans monogenetically resistant to *Phytophthora megasperma* var. *sojae*. Phytopathology **62,** 768.

Keinath, N.F., Kierszniowska, S., Lorek, J., Bourdais, G., Kessler, S.A., Shimosato-Asano, H., Grossniklaus, U., Schulze, W.X., Robatzek, S., and Panstruga, R. (2010). PAMP (pathogen-associated molecular pattern)-

induced changes in plasma membrane compartmentalization reveal novel components of plant immunity. J Biol Chem **285,** 39140-39149.

Kemmerling, B., and Nurnberger, T. (2008). Brassinosteroid-independent functions of the BRI1-associated kinase BAK1/SERK3. Plant Signal Behav **3,** 116-118.

Kemmerling, B., Schwedt, A., Rodriguez, P., Mazzotta, S., Frank, M., Qamar, S.A., Mengiste, T., Betsuyaku, S., Parker, J.E., Mussig, C., Thomma, B.P., Albrecht, C., de Vries, S.C., Hirt, H., and Nurnberger, T. (2007). The BRI1-associated kinase 1, BAK1, has a brassinolide-independent role in plant cell-death control. Curr Biol **17,** 1116-1122.

Kim, C., Meskauskiene, R., Apel, K., and Laloi, C. (2008). No single way to understand singlet oxygen signalling in plants. EMBO Rep **9,** 435-439.

Kim, M.G., da Cunha, L., McFall, A.J., Belkhadir, Y., DebRoy, S., Dangl, J.L., and Mackey, D. (2005). Two Pseudomonas syringae type III effectors inhibit RIN4-regulated basal defense in Arabidopsis. Cell **121,** 749-759.

Kim, T.W., and Wang, Z.Y. (2010). Brassinosteroid signal transduction from receptor kinases to transcription factors. Annu Rev Plant Biol **61,** 681-704.

Kim, T.W., Guan, S., Sun, Y., Deng, Z., Tang, W., Shang, J.X., Burlingame, A.L., and Wang, Z.Y. (2009). Brassinosteroid signal transduction from cell-surface receptor kinases to nuclear transcription factors. Nat Cell Biol **11,** 1254-1260.

Kinoshita, T., Cano-Delgado, A., Seto, H., Hiranuma, S., Fujioka, S., Yoshida, S., and Chory, J. (2005). Binding of brassinosteroids to the extracellular domain of plant receptor kinase BRI1. Nature **433,** 167-171.

Klarzynski, O., Plesse, B., Joubert, J.M., Yvin, J.C., Kopp, M., Kloareg, B., and Fritig, B. (2000). Linear beta-1,3 glucans are elicitors of defense responses in tobacco. Plant Physiol **124,** 1027-1038.

Kobayashi, M., Ohura, I., Kawakita, K., Yokota, N., Fujiwara, M., Shimamoto, K., Doke, N., and Yoshioka, H. (2007). Calcium-dependent protein kinases regulate the production of reactive oxygen species by potato NADPH oxidase. Plant Cell **19,** 1065-1080.

Kobe, B., Heierhorst, J., Feil, S.C., Parker, M.W., Benian, G.M., Weiss, K.R., and Kemp, B.E. (1996). Giant protein kinases: domain interactions and structural basis of autoregulation. Embo J **15,** 6810-6821.

Kohalmi, S.E., and Kunz, B.A. (1988). Role of neighbouring bases and assessment of strand specificity in ethylmethanesulphonate and N-methyl-N'-nitro-N-nitrosoguanidine mutagenesis in the SUP4-o gene of Saccharomyces cerevisiae. J Mol Biol **204,** 561-568.

Kohorn, B.D., Johansen, S., Shishido, A., Todorova, T., Martinez, R., Defeo, E., and Obregon, P. (2009). Pectin activation of MAP kinase and gene expression is WAK2 dependent. Plant J **60,** 974-982.

Kopp, M., Rouster, J., Fritig, B., Darvill, A., and Albersheim, P. (1989). Host-Pathogen Interactions : XXXII. A Fungal Glucan Preparation Protects Nicotianae against Infection by Viruses. Plant Physiol **90,** 208-216.

Korasick, D.A., McMichael, C., Walker, K.A., Anderson, J.C., Bednarek, S.Y., and Heese, A. (2010). Novel functions of Stomatal Cytokinesis-Defective 1

(SCD1) in innate immune responses against bacteria. J Biol Chem **285,** 23342-23350.

Krol, E., Mentzel, T., Chinchilla, D., Boller, T., Felix, G., Kemmerling, B., Postel, S., Arents, M., Jeworutzki, E., Al-Rasheid, K.A., Becker, D., and Hedrich, R. (2010). Perception of the Arabidopsis danger signal peptide 1 involves the pattern recognition receptor AtPEPR1 and its close homologue AtPEPR2. J Biol Chem **285,** 13471-13479.

Kudla, J., Batistic, O., and Hashimoto, K. (2010). Calcium signals: the lead currency of plant information processing. Plant Cell **22,** 541-563.

Kuhn, J.M., Boisson-Dernier, A., Dizon, M.B., Maktabi, M.H., and Schroeder, J.I. (2006). The protein phosphatase AtPP2CA negatively regulates abscisic acid signal transduction in Arabidopsis, and effects of abh1 on AtPP2CA mRNA. Plant Physiol **140,** 127-139.

Kunze, G., Zipfel, C., Robatzek, S., Niehaus, K., Boller, T., and Felix, G. (2004). The N terminus of bacterial elongation factor Tu elicits innate immunity in Arabidopsis plants. Plant Cell **16,** 3496-3507.

Kurusu, T., Hamada, J., Nokajima, H., Kitagawa, Y., Kiyoduka, M., Takahashi, A., Hanamata, S., Ohno, R., Hayashi, T., Okada, K., Koga, J., Hirochika, H., Yamane, H., and Kuchitsu, K. (2010). Regulation of microbe-associated molecular pattern-induced hypersensitive cell death, phytoalexin production, and defense gene expression by calcineurin B-like protein-interacting protein kinases, OsCIPK14/15, in rice cultured cells. Plant Physiol **153,** 678-692.

Lacombe, S., Rougon-Cardoso, A., Sherwood, E., Peeters, N., Dahlbeck, D., van Esse, H.P., Smoker, M., Rallapalli, G., Thomma, B.P., Staskawicz, B., Jones, J.D., and Zipfel, C. (2010). Interfamily transfer of a plant pattern-recognition receptor confers broad-spectrum bacterial resistance. Nat Biotechnol **28,** 365-369.

Laemmli, U.K. (1970). Cleavage of structural proteins during the assembly of the head of bacteriophage T4. Nature **227,** 680-685.

Laloi, C., Stachowiak, M., Pers-Kamczyc, E., Warzych, E., Murgia, I., and Apel, K. (2007). Cross-talk between singlet oxygen- and hydrogen peroxide-dependent signaling of stress responses in Arabidopsis thaliana. Proc Natl Acad Sci U S A **104,** 672-677.

Lee, J.S., and Ellis, B.E. (2007). Arabidopsis MAPK phosphatase 2 (MKP2) positively regulates oxidative stress tolerance and inactivates the MPK3 and MPK6 MAPKs. J Biol Chem **282,** 25020-25029.

Lee, K.P., Kim, C., Landgraf, F., and Apel, K. (2007). EXECUTER1- and EXECUTER2-dependent transfer of stress-related signals from the plastid to the nucleus of Arabidopsis thaliana. Proc Natl Acad Sci U S A **104,** 10270-10275.

Lee, S.W., Han, S.W., Bartley, L.E., and Ronald, P.C. (2006). From the Academy: Colloquium review. Unique characteristics of Xanthomonas oryzae pv. oryzae AvrXa21 and implications for plant innate immunity. Proc Natl Acad Sci U S A **103,** 18395-18400.

Lee, S.W., Han, S.W., Sririyanum, M., Park, C.J., Seo, Y.S., and Ronald, P.C. (2009). A type I-secreted, sulfated peptide triggers XA21-mediated innate immunity. Science **326,** 850-853.

Lemmon, M.A., and Schlessinger, J. (2010). Cell signaling by receptor tyrosine kinases. Cell **141,** 1117-1134.

Leslie, M.E., Lewis, M.W., Youn, J.Y., Daniels, M.J., and Liljegren, S.J. (2010). The EVERSHED receptor-like kinase modulates floral organ shedding in Arabidopsis. Development **137,** 467-476.

Lewis, M.W., Leslie, M.E., Fulcher, E.H., Darnielle, L., Healy, P.N., Youn, J.Y., and Liljegren, S.J. (2010). The SERK1 receptor-like kinase regulates organ separation in Arabidopsis flowers. Plant J **62,** 817-828.

Li, J., and Chory, J. (1997). A putative leucine-rich repeat receptor kinase involved in brassinosteroid signal transduction. Cell **90,** 929-938.

Li, J., and Nam, K.H. (2002). Regulation of brassinosteroid signaling by a GSK3/SHAGGY-like kinase. Science **295,** 1299-1301.

Li, J., Wen, J., Lease, K.A., Doke, J.T., Tax, F.E., and Walker, J.C. (2002). BAK1, an Arabidopsis LRR receptor-like protein kinase, interacts with BRI1 and modulates brassinosteroid signaling. Cell **110,** 213-222.

Li, J., Zhao-Hui, C., Batoux, M., Nekrasov, V., Roux, M., Chinchilla, D., Zipfel, C., and Jones, J.D. (2009). Specific ER quality control components required for biogenesis of the plant innate immune receptor EFR. Proc Natl Acad Sci U S A **106,** 15973-15978.

Li, X., Lin, H., Zhang, W., Zou, Y., Zhang, J., Tang, X., and Zhou, J.M. (2005). Flagellin induces innate immunity in nonhost interactions that is suppressed by Pseudomonas syringae effectors. Proc Natl Acad Sci U S A **102,** 12990-12995.

Li, Y., Zhang, Q., Zhang, J., Wu, L., Qi, Y., and Zhou, J.M. (2010). Identification of microRNAs involved in pathogen-associated molecular pattern-triggered plant innate immunity. Plant Physiol **152,** 2222-2231.

Liew, F.Y., Xu, D., Brint, E.K., and O'Neill, L.A. (2005). Negative regulation of toll-like receptor-mediated immune responses. Nature reviews **5,** 446-458.

Liu, J., Elmore, J.M., Fuglsang, A.T., Palmgren, M.G., Staskawicz, B.J., and Coaker, G. (2009). RIN4 functions with plasma membrane H+-ATPases to regulate stomatal apertures during pathogen attack. PLoS Biol **7,** e1000139.

Liu, Y., Ren, D., Pike, S., Pallardy, S., Gassmann, W., and Zhang, S. (2007). Chloroplast-generated reactive oxygen species are involved in hypersensitive response-like cell death mediated by a mitogen-activated protein kinase cascade. Plant J **51,** 941-954.

Lu, D., Wu, S., Gao, X., Zhang, Y., Shan, L., and He, P. (2010). A receptor-like cytoplasmic kinase, BIK1, associates with a flagellin receptor complex to initiate plant innate immunity. Proc Natl Acad Sci U S A **107,** 496-501.

Lu, X., Tintor, N., Mentzel, T., Kombrink, E., Boller, T., Robatzek, S., Schulze-Lefert, P., and Saijo, Y. (2009). Uncoupling of sustained MAMP receptor signaling from early outputs in an Arabidopsis endoplasmic reticulum glucosidase II allele. Proc Natl Acad Sci U S A **106,** 22522-22527.

Lukasik, E., and Takken, F.L. (2009). STANDing strong, resistance proteins instigators of plant defence. Curr Opin Plant Biol **12,** 427-436.

Lumbreras, V., Vilela, B., Irar, S., Sole, M., Capellades, M., Valls, M., Coca, M., and Pages, M. (2010). MAPK phosphatase MKP2 mediates disease responses in Arabidopsis and functionally interacts with MPK3 and MPK6. Plant J.

Ma, W., and Berkowitz, G.A. (2007). The grateful dead: calcium and cell death in plant innate immunity. Cell Microbiol **9,** 2571-2585.

Mackey, D., and McFall, A.J. (2006). MAMPs and MIMPs: proposed classifications for inducers of innate immunity. Mol Microbiol **61,** 1365-1371.

Mackey, D., Holt, B.F., 3rd, Wiig, A., and Dangl, J.L. (2002). RIN4 interacts with Pseudomonas syringae type III effector molecules and is required for RPM1-mediated resistance in Arabidopsis. Cell **108,** 743-754.

Mayans, O., van der Ven, P.F., Wilm, M., Mues, A., Young, P., Furst, D.O., Wilmanns, M., and Gautel, M. (1998). Structural basis for activation of the titin kinase domain during myofibrillogenesis. Nature **395,** 863-869.

McGurl, B., Pearce, G., Orozco-Cardenas, M., and Ryan, C.A. (1992). Structure, expression, and antisense inhibition of the systemin precursor gene. Science **255,** 1570-1573.

Medzhitov, R., and Janeway, C.A., Jr. (1997). Innate immunity: the virtues of a nonclonal system of recognition. Cell **91,** 295-298.

Melotto, M., Underwood, W., and He, S.Y. (2008). Role of stomata in plant innate immunity and foliar bacterial diseases. Annu Rev Phytopathol **46,** 101-122.

Melotto, M., Underwood, W., Koczan, J., Nomura, K., and He, S.Y. (2006). Plant stomata function in innate immunity against bacterial invasion. Cell **126,** 969-980.

Merlot, S., Mustilli, A.C., Genty, B., North, H., Lefebvre, V., Sotta, B., Vavasseur, A., and Giraudat, J. (2002). Use of infrared thermal imaging to isolate Arabidopsis mutants defective in stomatal regulation. Plant J **30,** 601-609.

Mersmann, S., Bourdais, G., Rietz, S., and Robatzek, S. (2010). Ethylene signalling regulates accumulation of the FLS2 receptor and is required for the oxidative burst contributing to plant immunity. Plant Physiol.

Meszaros, T., Helfer, A., Hatzimasoura, E., Magyar, Z., Serazetdinova, L., Rios, G., Bardoczy, V., Teige, M., Koncz, C., Peck, S., and Bogre, L. (2006). The Arabidopsis MAP kinase kinase MKK1 participates in defence responses to the bacterial elicitor flagellin. Plant J **48,** 485-498.

Mishina, T.E., and Zeier, J. (2007). Pathogen-associated molecular pattern recognition rather than development of tissue necrosis contributes to bacterial induction of systemic acquired resistance in Arabidopsis. Plant J **50,** 500-513.

Mongrand, S., Morel, J., Laroche, J., Claverol, S., Carde, J.P., Hartmann, M.A., Bonneu, M., Simon-Plas, F., Lessire, R., and Bessoule, J.J. (2004). Lipid rafts in higher plant cells: purification and characterization of Triton X-100-

insoluble microdomains from tobacco plasma membrane. J Biol Chem **279,** 36277-36286.

Mora-Garcia, S., Vert, G., Yin, Y., Cano-Delgado, A., Cheong, H., and Chory, J. (2004). Nuclear protein phosphatases with Kelch-repeat domains modulate the response to brassinosteroids in Arabidopsis. Genes Dev **18,** 448-460.

Morel, J., Claverol, S., Mongrand, S., Furt, F., Fromentin, J., Bessoule, J.J., Blein, J.P., and Simon-Plas, F. (2006). Proteomics of plant detergent-resistant membranes. Mol Cell Proteomics **5,** 1396-1411.

Mosse, Y.P., Laudenslager, M., Longo, L., Cole, K.A., Wood, A., Attiyeh, E.F., Laquaglia, M.J., Sennett, R., Lynch, J.E., Perri, P., Laureys, G., Speleman, F., Kim, C., Hou, C., Hakonarson, H., Torkamani, A., Schork, N.J., Brodeur, G.M., Tonini, G.P., Rappaport, E., Devoto, M., and Maris, J.M. (2008). Identification of ALK as a major familial neuroblastoma predisposition gene. Nature **455,** 930-935.

Murphy, J.E., Padilla, B.E., Hasdemir, B., Cottrell, G.S., and Bunnett, N.W. (2009). Endosomes: a legitimate platform for the signaling train. Proc Natl Acad Sci U S A **106,** 17615-17622.

Mussig, C., Lisso, J., Coll-Garcia, D., and Altmann, T. (2006). Molecular analysis of brassinosteroid action. Plant Biol (Stuttg) **8,** 291-296.

Myouga, F., Hosoda, C., Umezawa, T., Iizumi, H., Kuromori, T., Motohashi, R., Shono, Y., Nagata, N., Ikeuchi, M., and Shinozaki, K. (2008). A heterocomplex of iron superoxide dismutases defends chloroplast nucleoids against oxidative stress and is essential for chloroplast development in Arabidopsis. Plant Cell **20,** 3148-3162.

Nagata, N., Asami, T., and Yoshida, S. (2001). Brassinazole, an inhibitor of brassinosteroid biosynthesis, inhibits development of secondary xylem in cress plants (Lepidium sativum). Plant & cell physiology **42,** 1006-1011.

Nakagami, H., Soukupova, H., Schikora, A., Zarsky, V., and Hirt, H. (2006). A Mitogen-activated protein kinase kinase kinase mediates reactive oxygen species homeostasis in Arabidopsis. J Biol Chem **281,** 38697-38704.

Nakagami, H., Sugiyama, N., Mochida, K., Daudi, A., Yoshida, Y., Toyoda, T., Tomita, M., Ishihama, Y., and Shirasu, K. (2010). Large-scale comparative phosphoproteomics identifies conserved phosphorylation sites in plants. Plant Physiol **153,** 1161-1174.

Nakagawa, T., Kurose, T., Hino, T., Tanaka, K., Kawamukai, M., Niwa, Y., Toyooka, K., Matsuoka, K., Jinbo, T., and Kimura, T. (2007). Development of series of gateway binary vectors, pGWBs, for realizing efficient construction of fusion genes for plant transformation. J Biosci Bioeng **104,** 34-41.

Nam, K.H., and Li, J. (2002). BRI1/BAK1, a receptor kinase pair mediating brassinosteroid signaling. Cell **110,** 203-212.

Navarro, L., Jay, F., Nomura, K., He, S.Y., and Voinnet, O. (2008a). Suppression of the microRNA pathway by bacterial effector proteins. Science **321,** 964-967.

Navarro, L., Zipfel, C., Rowland, O., Keller, I., Robatzek, S., Boller, T., and Jones, J.D. (2004). The transcriptional innate immune response to flg22.

Interplay and overlap with Avr gene-dependent defense responses and bacterial pathogenesis. Plant Physiol **135,** 1113-1128.

Navarro, L., Bari, R., Achard, P., Lison, P., Nemri, A., Harberd, N.P., and Jones, J.D. (2008b). DELLAs control plant immune responses by modulating the balance of jasmonic acid and salicylic acid signaling. Curr Biol **18,** 650-655.

Navarro, L., Dunoyer, P., Jay, F., Arnold, B., Dharmasiri, N., Estelle, M., Voinnet, O., and Jones, J.D. (2006). A plant miRNA contributes to antibacterial resistance by repressing auxin signaling. Science **312,** 436-439.

Neff, M.M., Turk, E., and Kalishman, M. (2002). Web-based primer design for single nucleotide polymorphism analysis. Trends Genet **18,** 613-615.

Nekrasov, V., Li, J., Batoux, M., Roux, M., Chu, Z.H., Lacombe, S., Rougon, A., Bittel, P., Kiss-Papp, M., Chinchilla, D., van Esse, H.P., Jorda, L., Schwessinger, B., Nicaise, V., Thomma, B.P., Molina, A., Jones, J.D., and Zipfel, C. (2009). Control of the pattern-recognition receptor EFR by an ER protein complex in plant immunity. Embo J **28,** 3428-3438.

Nemhauser, J.L., Mockler, T.C., and Chory, J. (2004). Interdependency of brassinosteroid and auxin signaling in Arabidopsis. PLoS Biol **2,** E258.

Newman, M.A., Dow, J.M., Molinaro, A., and Parrilli, M. (2007). Priming, induction and modulation of plant defence responses by bacterial lipopolysaccharides. Journal of endotoxin research **13,** 69-84.

Nicaise, V., Roux, M., and Zipfel, C. (2009). Recent advances in PAMP-triggered immunity against bacteria: pattern recognition receptors watch over and raise the alarm. Plant Physiol **150,** 1638-1647.

Nishimura, M.T., Stein, M., Hou, B.H., Vogel, J.P., Edwards, H., and Somerville, S.C. (2003). Loss of a callose synthase results in salicylic acid-dependent disease resistance. Science **301,** 969-972.

Nolen, B., Taylor, S., and Ghosh, G. (2004). Regulation of protein kinases; controlling activity through activation segment conformation. Mol Cell **15,** 661-675.

Nolen, B., Yun, C.Y., Wong, C.F., McCammon, J.A., Fu, X.D., and Ghosh, G. (2001). The structure of Sky1p reveals a novel mechanism for constitutive activity. Nat Struct Biol **8,** 176-183.

Nomura, K., Melotto, M., and He, S.Y. (2005). Suppression of host defense in compatible plant-Pseudomonas syringae interactions. Curr Opin Plant Biol **8,** 361-368.

Nomura, K., Debroy, S., Lee, Y.H., Pumplin, N., Jones, J., and He, S.Y. (2006). A bacterial virulence protein suppresses host innate immunity to cause plant disease. Science **313,** 220-223.

Nothnagel, E.A., McNeil, M., Albersheim, P., and Dell, A. (1983). Host-Pathogen Interactions : XXII. A Galacturonic Acid Oligosaccharide from Plant Cell Walls Elicits Phytoalexins. Plant Physiol **71,** 916-926.

Nowaczyk, M.M., Hebeler, R., Schlodder, E., Meyer, H.E., Warscheid, B., and Rogner, M. (2006). Psb27, a cyanobacterial lipoprotein, is involved in the repair cycle of photosystem II. Plant Cell **18,** 3121-3131.

Ntoukakis, V., Mucyn, T.S., Gimenez-Ibanez, S., Chapman, H.C., Gutierrez, J.R., Balmuth, A.L., Jones, A.M., and Rathjen, J.P. (2009). Host inhibition of a bacterial virulence effector triggers immunity to infection. Science **324,** 784-787.

Nuhse, T.S., Bottrill, A.R., Jones, A.M., and Peck, S.C. (2007). Quantitative phosphoproteomic analysis of plasma membrane proteins reveals regulatory mechanisms of plant innate immune responses. Plant J **51,** 931-940.

Nurnberger, T., Brunner, F., Kemmerling, B., and Piater, L. (2004). Innate immunity in plants and animals: striking similarities and obvious differences. Immunol Rev **198,** 249-266.

Ochsenbein, C., Przybyla, D., Danon, A., Landgraf, F., Gobel, C., Imboden, A., Feussner, I., and Apel, K. (2006). The role of EDS1 (enhanced disease susceptibility) during singlet oxygen-mediated stress responses of Arabidopsis. Plant J **47,** 445-456.

Oh, M.H., Ray, W.K., Huber, S.C., Asara, J.M., Gage, D.A., and Clouse, S.D. (2000). Recombinant brassinosteroid insensitive 1 receptor-like kinase autophosphorylates on serine and threonine residues and phosphorylates a conserved peptide motif in vitro. Plant Physiol **124,** 751-766.

Oh, M.H., Wang, X., Kota, U., Goshe, M.B., Clouse, S.D., and Huber, S.C. (2009). Tyrosine phosphorylation of the BRI1 receptor kinase emerges as a component of brassinosteroid signaling in Arabidopsis. Proc Natl Acad Sci U S A **106,** 658-663.

Oh, M.H., Wang, X., Wu, X., Zhao, Y., Clouse, S.D., and Huber, S.C. (2010). Autophosphorylation of Tyr-610 in the receptor kinase BAK1 plays a role in brassinosteroid signaling and basal defense gene expression. Proc Natl Acad Sci U S A **107,** 17827-17832.

Padmanabhan, M., Cournoyer, P., and Dinesh-Kumar, S.P. (2009). The leucine-rich repeat domain in plant innate immunity: a wealth of possibilities. Cell Microbiol **11,** 191-198.

Paradies, I., Konze, J.R., and Elstner, E.F. (1980). Ethylene: indicator but not inducer of phytoalexin synthesis in soybean. Plant Physiol **66,** 1106-1109.

Park, C.J., Peng, Y., Chen, X., Dardick, C., Ruan, D., Bart, R., Canlas, P.E., and Ronald, P.C. (2008). Rice XB15, a protein phosphatase 2C, negatively regulates cell death and XA21-mediated innate immunity. PLoS Biol **6,** e231.

Pazzagli, L., Cappugi, G., Manao, G., Camici, G., Santini, A., and Scala, A. (1999). Purification, characterization, and amino acid sequence of cerato-platanin, a new phytotoxic protein from Ceratocystis fimbriata f. sp. platani. J Biol Chem **274,** 24959-24964.

Pearce, G., Yamaguchi, Y., Barona, G., and Ryan, C.A. (2010). A subtilisin-like protein from soybean contains an embedded, cryptic signal that activates defense-related genes. Proc Natl Acad Sci U S A **107,** 14921-14925.

Peng, P., Yan, Z., Zhu, Y., and Li, J. (2008). Regulation of the Arabidopsis GSK3-like kinase BRASSINOSTEROID-INSENSITIVE 2 through proteasome-mediated protein degradation. Mol Plant **1,** 338-346.

Perkins, D.N., Pappin, D.J.C., Creasy, D.M., and Cottrell, J.S. (1999). Probability-based protein identification by searching sequence databases using mass spectrometry data. Electrophoresis **20,** 3551-3567.

Petersen, M., Brodersen, P., Naested, H., Andreasson, E., Lindhart, U., Johansen, B., Nielsen, H.B., Lacy, M., Austin, M.J., Parker, J.E., Sharma, S.B., Klessig, D.F., Martienssen, R., Mattsson, O., Jensen, A.B., and Mundy, J. (2000). Arabidopsis map kinase 4 negatively regulates systemic acquired resistance. Cell **103,** 1111-1120.

Petutschnig, E.K., Jones, A.M., Serazetdinova, L., Lipka, U., and Lipka, V. (2010). The LysM-RLK CERK1 is a major chitin binding protein in Arabidopsis thalianaand subject to chitin-induced phosphorylation. J Biol Chem.

Pitzschke, A., Schikora, A., and Hirt, H. (2009a). MAPK cascade signalling networks in plant defence. Curr Opin Plant Biol **12,** 421-426.

Pitzschke, A., Djamei, A., Bitton, F., and Hirt, H. (2009b). A major role of the MEKK1-MKK1/2-MPK4 pathway in ROS signalling. Mol Plant **2,** 120-137.

Postel, S., and Kemmerling, B. (2009). Plant systems for recognition of pathogen-associated molecular patterns. Semin Cell Dev Biol **20,** 1025-1031.

Postel, S., Kufner, I., Beuter, C., Mazzotta, S., Schwedt, A., Borlotti, A., Halter, T., Kemmerling, B., and Nurnberger, T. (2009). The multifunctional leucine-rich repeat receptor kinase BAK1 is implicated in Arabidopsis development and immunity. Eur J Cell Biol.

Qiu, J.L., Zhou, L., Yun, B.W., Nielsen, H.B., Fiil, B.K., Petersen, K., Mackinlay, J., Loake, G.J., Mundy, J., and Morris, P.C. (2008a). Arabidopsis mitogen-activated protein kinase kinases MKK1 and MKK2 have overlapping functions in defense signaling mediated by MEKK1, MPK4, and MKS1. Plant Physiol **148,** 212-222.

Qiu, J.L., Fiil, B.K., Petersen, K., Nielsen, H.B., Botanga, C.J., Thorgrimsen, S., Palma, K., Suarez-Rodriguez, M.C., Sandbech-Clausen, S., Lichota, J., Brodersen, P., Grasser, K.D., Mattsson, O., Glazebrook, J., Mundy, J., and Petersen, M. (2008b). Arabidopsis MAP kinase 4 regulates gene expression through transcription factor release in the nucleus. Embo J **27,** 2214-2221.

Rafiqi, M., Gan, P.H., Ravensdale, M., Lawrence, G.J., Ellis, J.G., Jones, D.A., Hardham, A.R., and Dodds, P.N. (2010). Internalization of flax rust avirulence proteins into flax and tobacco cells can occur in the absence of the pathogen. Plant Cell **22,** 2017-2032.

Raghavendra, A.S., Gonugunta, V.K., Christmann, A., and Grill, E. (2010). ABA perception and signalling. Trends Plant Sci **15,** 395-401.

Rahimi, R.A., and Leof, E.B. (2007). TGF-beta signaling: a tale of two responses. J Cell Biochem **102,** 593-608.

Ramonell, K., Berrocal-Lobo, M., Koh, S., Wan, J., Edwards, H., Stacey, G., and Somerville, S. (2005). Loss-of-function mutations in chitin responsive genes show increased susceptibility to the powdery mildew pathogen Erysiphe cichoracearum. Plant Physiol **138,** 1027-1036.

Ridout, C.J., Skamnioti, P., Porritt, O., Sacristan, S., Jones, J.D., and Brown, J.K. (2006). Multiple avirulence paralogues in cereal powdery mildew fungi may contribute to parasite fitness and defeat of plant resistance. Plant Cell **18,** 2402-2414.

Rigano, L.A., Payette, C., Brouillard, G., Marano, M.R., Abramowicz, L., Torres, P.S., Yun, M., Castagnaro, A.P., Oirdi, M.E., Dufour, V., Malamud, F., Dow, J.M., Bouarab, K., and Vojnov, A.A. (2007). Bacterial cyclic beta-(1,2)-glucan acts in systemic suppression of plant immune responses. Plant Cell **19,** 2077-2089.

Rivas, S., and Thomas, C.M. (2005). Molecular interactions between tomato and the leaf mold pathogen Cladosporium fulvum. Annu Rev Phytopathol **43,** 395-436.

Rizhsky, L., Liang, H., and Mittler, R. (2003). The water-water cycle is essential for chloroplast protection in the absence of stress. J Biol Chem **278,** 38921-38925.

Robatzek, S., Chinchilla, D., and Boller, T. (2006). Ligand-induced endocytosis of the pattern recognition receptor FLS2 in Arabidopsis. Genes Dev **20,** 537-542.

Robatzek, S., Bittel, P., Chinchilla, D., Kochner, P., Felix, G., Shiu, S.H., and Boller, T. (2007). Molecular identification and characterization of the tomato flagellin receptor LeFLS2, an orthologue of Arabidopsis FLS2 exhibiting characteristically different perception specificities. Plant Mol Biol **64,** 539-547.

Robert-Seilaniantz, A., Navarro, L., Bari, R., and Jones, J.D. (2007). Pathological hormone imbalances. Curr Opin Plant Biol **10,** 372-379.

Ron, M., and Avni, A. (2004). The receptor for the fungal elicitor ethylene-inducing xylanase is a member of a resistance-like gene family in tomato. Plant Cell **16,** 1604-1615.

Rooney, H.C., Van't Klooster, J.W., van der Hoorn, R.A., Joosten, M.H., Jones, J.D., and de Wit, P.J. (2005). Cladosporium Avr2 inhibits tomato Rcr3 protease required for Cf-2-dependent disease resistance. Science **308,** 1783-1786.

Rosebrock, T.R., Zeng, L., Brady, J.J., Abramovitch, R.B., Xiao, F., and Martin, G.B. (2007). A bacterial E3 ubiquitin ligase targets a host protein kinase to disrupt plant immunity. Nature **448,** 370-374.

Russinova, E., Borst, J.W., Kwaaitaal, M., Cano-Delgado, A., Yin, Y., Chory, J., and de Vries, S.C. (2004). Heterodimerization and endocytosis of Arabidopsis brassinosteroid receptors BRI1 and AtSERK3 (BAK1). Plant Cell **16,** 3216-3229.

Saijo, Y., Tintor, N., Lu, X., Rauf, P., Pajerowska-Mukhtar, K., Haweker, H., Dong, X., Robatzek, S., and Schulze-Lefert, P. (2009). Receptor quality control in the endoplasmic reticulum for plant innate immunity. Embo J **28,** 3439-3449.

Santos, M.O., Romano, E., Vieira, L.S., Baldoni, A.B., and Aragão, F.J.L. (2009). Suppression of SERK gene expression affects fungus tolerance and somatic embryogenesis in transgenic lettuce. Plant Biology **11,** 83-89.

Sato, M., Tsuda, K., Wang, L., Coller, J., Watanabe, Y., Glazebrook, J., and Katagiri, F. (2010). Network modeling reveals prevalent negative regulatory relationships between signaling sectors in Arabidopsis immune signaling. PLoS Pathog **6,** e1001011.

Sato, M., Mitra, R.M., Coller, J., Wang, D., Spivey, N.W., Dewdney, J., Denoux, C., Glazebrook, J., and Katagiri, F. (2007). A high-performance, small-scale microarray for expression profiling of many samples in Arabidopsis-pathogen studies. Plant J **49,** 565-577.

Schweighofer, A., Kazanaviciute, V., Scheikl, E., Teige, M., Doczi, R., Hirt, H., Schwanninger, M., Kant, M., Schuurink, R., Mauch, F., Buchala, A., Cardinale, F., and Meskiene, I. (2007). The PP2C-Type Phosphatase AP2C1, Which Negatively Regulates MPK4 and MPK6, Modulates Innate Immunity, Jasmonic Acid, and Ethylene Levels in Arabidopsis. Plant Cell **19,** 2213-2224.

Schwessinger, B., and Zipfel, C. (2008). News from the frontline: recent insights into PAMP-triggered immunity in plants. Curr Opin Plant Biol **11,** 389-395.

Shan, L., He, P., Li, J., Heese, A., Peck, S.C., Nurnberger, T., Martin, G.B., and Sheen, J. (2008). Bacterial effectors target the common signaling partner BAK1 to disrupt multiple MAMP receptor-signaling complexes and impede plant immunity. Cell Host Microbe **4,** 17-27.

Shao, F., Golstein, C., Ade, J., Stoutemyer, M., Dixon, J.E., and Innes, R.W. (2003). Cleavage of Arabidopsis PBS1 by a bacterial type III effector. Science **301,** cl1230-1233.

Sharp, J.K., McNeil, M., and Albersheim, P. (1984a). The primary structures of one elicitor-active and seven elicitor-inactive hexa(beta-D-glucopyranosyl)-D-glucitols isolated from the mycelial walls of Phytophthora megasperma f. sp. glycinea. J Biol Chem **259,** 11321-11336.

Sharp, J.K., Albersheim, P., Ossowski, P., Pilotti, A., Garegg, P., and Lindberg, B. (1984b). Comparison of the structures and elicitor activities of a synthetic and a mycelial-wall-derived hexa(beta-D-glucopyranosyl)-D-glucitol. J Biol Chem **259,** 11341-11345.

Shen, Q.H., Saijo, Y., Mauch, S., Biskup, C., Bieri, S., Keller, B., Seki, H., Ulker, B., Somssich, I.E., and Schulze-Lefert, P. (2006). Nuclear Activity of MLA Immune Receptors Links Isolate-Specific and Basal Disease-Resistance Responses. Science.

Shimizu, T., Nakano, T., Takamizawa, D., Desaki, Y., Ishii-Minami, N., Nishizawa, Y., Minami, E., Okada, K., Yamane, H., Kaku, H., and Shibuya, N. (2010). Two LysM receptor molecules, CEBiP and OsCERK1, cooperatively regulate chitin elicitor signaling in rice. The Plant Journal**,** no-no.

Shirasu, K. (2009). The HSP90-SGT1 chaperone complex for NLR immune sensors. Annu Rev Plant Biol **60,** 139-164.

Silipo, A., Erbs, G., Shinya, T., Dow, J.M., Parrilli, M., Lanzetta, R., Shibuya, N., Newman, M.A., and Molinaro, A. (2010). Glyco-conjugates as elicitors or suppressors of plant innate immunity. Glycobiology **20,** 406-419.

Sohn, K.H., Lei, R., Nemri, A., and Jones, J.D. (2007). The downy mildew effector proteins ATR1 and ATR13 promote disease susceptibility in Arabidopsis thaliana. Plant Cell **19,** 4077-4090.

Song, D., Li, G., Song, F., and Zheng, Z. (2008). Molecular characterization and expression analysis of OsBISERK1, a gene encoding a leucine-rich repeat receptor-like kinase, during disease resistance responses in rice. Mol Biol Rep **35,** 275-283.

Song, W.Y., Pi, L.Y., Wang, G.L., Gardner, J., Holsten, T., and Ronald, P.C. (1997). Evolution of the rice Xa21 disease resistance gene family. Plant Cell **9,** 1279-1287.

Song, W.Y., Wang, G.L., Chen, L.L., Kim, H.S., Pi, L.Y., Holsten, T., Gardner, J., Wang, B., Zhai, W.X., Zhu, L.H., Fauquet, C., and Ronald, P. (1995). A receptor kinase-like protein encoded by the rice disease resistance gene, Xa21. Science **270,** 1804-1806.

Stanislas, T., Bouyssie, D., Rossignol, M., Vesa, S., Fromentin, J., Morel, J., Pichereaux, C., Monsarrat, B., and Simon-Plas, F. (2009). Quantitative proteomics reveals a dynamic association of proteins to detergent-resistant membranes upon elicitor signaling in tobacco. Mol Cell Proteomics **8,** 2186-2198.

Stergiopoulos, I., and de Wit, P.J. (2009). Fungal effector proteins. Annu Rev Phytopathol **47,** 233-263.

Straus, M.R., Rietz, S., Ver Loren van Themaat, E., Bartsch, M., and Parker, J.E. (2010). Salicylic acid antagonism of EDS1-driven cell death is important for immune and oxidative stress responses in Arabidopsis. Plant J **62,** 628-640.

Suarez-Rodriguez, M.C., Adams-Phillips, L., Liu, Y., Wang, H., Su, S.H., Jester, P.J., Zhang, S., Bent, A.F., and Krysan, P.J. (2006). MEKK1 Is Required for flg22-induced MPK4 Activation in Arabidopsis Plants. Plant Physiol.

Takahashi, A., Casais, C., Ichimura, K., and Shirasu, K. (2003). HSP90 interacts with RAR1 and SGT1 and is essential for RPS2-mediated disease resistance in Arabidopsis. Proc Natl Acad Sci U S A **100,** 11777-11782.

Tanaka, N., Che, F.S., Watanabe, N., Fujiwara, S., Takayama, S., and Isogai, A. (2003). Flagellin from an incompatible strain of Acidovorax avenae mediates H2O2 generation accompanying hypersensitive cell death and expression of PAL, Cht-1, and PBZ1, but not of Lox in rice. Mol Plant Microbe Interact **16,** 422-428.

Tang, W., Kim, T.W., Oses-Prieto, J.A., Sun, Y., Deng, Z., Zhu, S., Wang, R., Burlingame, A.L., and Wang, Z.Y. (2008). BSKs mediate signal transduction from the receptor kinase BRI1 in Arabidopsis. Science **321,** 557-560.

Taylor, S.S., Radzio-Andzelm, E., Madhusudan, Cheng, X., Ten Eyck, L., and Narayana, N. (1999). Catalytic subunit of cyclic AMP-dependent protein kinase: structure and dynamics of the active site cleft. Pharmacol Ther **82,** 133-141.

Thilmony, R., Underwood, W., and He, S.Y. (2006). Genome-wide transcriptional analysis of the Arabidopsis thaliana interaction with the plant pathogen

Pseudomonas syringae pv. tomato DC3000 and the human pathogen Escherichia coli O157:H7. Plant J **46,** 34-53.

Thompson, M.J., Meudt, W.J., Mandava, N.B., Dutky, S.R., Lusby, W.R., and Spaulding, D.W. (1982). Synthesis of brassinosteroids and relationship of structure to plant growth-promoting effects. Steroids **39,** 89-105.

Thordal-Christensen, H. (2003). Fresh insights into processes of nonhost resistance. Curr Opin Plant Biol **6,** 351-357.

Trujillo, M., and Shirasu, K. (2010). Ubiquitination in plant immunity. Curr Opin Plant Biol **13,** 402-408.

Trujillo, M., Ichimura, K., Casais, C., and Shirasu, K. (2008). Negative regulation of PAMP-triggered immunity by an E3 ubiquitin ligase triplet in Arabidopsis. Curr Biol **18,** 1396-1401.

Truman, W., de Zabala, M.T., and Grant, M. (2006). Type III effectors orchestrate a complex interplay between transcriptional networks to modify basal defence responses during pathogenesis and resistance. Plant J **46,** 14-33.

Tsuda, K., Sato, M., Glazebrook, J., Cohen, J.D., and Katagiri, F. (2008). Interplay between MAMP-triggered and SA-mediated defense responses. Plant J **53,** 763-775.

Tsuda, K., Sato, M., Stoddard, T., Glazebrook, J., and Katagiri, F. (2009). Network properties of robust immunity in plants. PLoS Genet **5,** e1000772.

Underwood, W., Zhang, S., and He, S.Y. (2007). The Pseudomonas syringae type III effector tyrosine phosphatase HopAO1 suppresses innate immunity in Arabidopsis thaliana. Plant J.

van der Hoorn, R.A., and Kamoun, S. (2008). From Guard to Decoy: a new model for perception of plant pathogen effectors. Plant Cell **20,** 2009-2017.

van Esse, H.P., Bolton, M.D., Stergiopoulos, I., de Wit, P.J., and Thomma, B.P. (2007). The chitin-binding Cladosporium fulvum effector protein Avr4 is a virulence factor. Mol Plant Microbe Interact **20,** 1092-1101.

Varnier, A.L., Sanchez, L., Vatsa, P., Boudesocque, L., Garcia-Brugger, A., Rabenoelina, F., Sorokin, A., Renault, J.H., Kauffmann, S., Pugin, A., Clement, C., Baillieul, F., and Dorey, S. (2009). Bacterial rhamnolipids are novel MAMPs conferring resistance to Botrytis cinerea in grapevine. Plant Cell Environ **32,** 178-193.

Veronese, P., Nakagami, H., Bluhm, B., Abuqamar, S., Chen, X., Salmeron, J., Dietrich, R.A., Hirt, H., and Mengiste, T. (2006). The membrane-anchored BOTRYTIS-INDUCED KINASE1 plays distinct roles in Arabidopsis resistance to necrotrophic and biotrophic pathogens. Plant Cell **18,** 257-273.

Vert, G., Nemhauser, J.L., Geldner, N., Hong, F., and Chory, J. (2005). Molecular mechanisms of steroid hormone signaling in plants. Annu Rev Cell Dev Biol **21,** 177-201.

Voinnet, O. (2005). Induction and suppression of RNA silencing: insights from viral infections. Nat Rev Genet **6,** 206-220.

von Numers, N., Survila, M., Aalto, M., Batoux, M., Heino, P., Palva, E.T., and Li, J. (2010). Requirement of a Homolog of Glucosidase II {beta}-Subunit for EFR-Mediated Defense Signaling in Arabidopsis thaliana. Mol Plant **3,** 740-750.

Wan, J., Zhang, X.C., Neece, D., Ramonell, K.M., Clough, S., Kim, S.Y., Stacey, M.G., and Stacey, G. (2008). A LysM receptor-like kinase plays a critical role in chitin signaling and fungal resistance in Arabidopsis. Plant Cell **20,** 471-481.

Wang, D., Pajerowska-Mukhtar, K., Culler, A.H., and Dong, X. (2007). Salicylic acid inhibits pathogen growth in plants through repression of the auxin signaling pathway. Curr Biol **17,** 1784-1790.

Wang, X., Li, X., Meisenhelder, J., Hunter, T., Yoshida, S., Asami, T., and Chory, J. (2005a). Autoregulation and homodimerization are involved in the activation of the plant steroid receptor BRI1. Dev Cell **8,** 855-865.

Wang, X., Kota, U., He, K., Blackburn, K., Li, J., Goshe, M.B., Huber, S.C., and Clouse, S.D. (2008). Sequential transphosphorylation of the BRI1/BAK1 receptor kinase complex impacts early events in brassinosteroid signaling. Dev Cell **15,** 220-235.

Wang, X., Goshe, M.B., Soderblom, E.J., Phinney, B.S., Kuchar, J.A., Li, J., Asami, T., Yoshida, S., Huber, S.C., and Clouse, S.D. (2005b). Identification and functional analysis of in vivo phosphorylation sites of the Arabidopsis BRASSINOSTEROID-INSENSITIVE1 receptor kinase. Plant Cell **17,** 1685-1703.

Wang, Y., Li, J., Hou, S., Wang, X., Li, Y., Ren, D., Chen, S., Tang, X., and Zhou, J.M. (2010). A Pseudomonas syringae ADP-ribosyltransferase inhibits Arabidopsis mitogen-activated protein kinase kinases. Plant Cell **22,** 2033-2044.

Wang, Y.S., Pi, L.Y., Chen, X., Chakrabarty, P.K., Jiang, J., De Leon, A.L., Liu, G.Z., Li, L., Benny, U., Oard, J., Ronald, P.C., and Song, W.Y. (2006). Rice XA21 binding protein 3 is a ubiquitin ligase required for full Xa21-mediated disease resistance. Plant Cell **18,** 3635-3646.

Wang, Z.Y., Nakano, T., Gendron, J., He, J., Chen, M., Vafeados, D., Yang, Y., Fujioka, S., Yoshida, S., Asami, T., and Chory, J. (2002). Nuclear-localized BZR1 mediates brassinosteroid-induced growth and feedback suppression of brassinosteroid biosynthesis. Dev Cell **2,** 505-513.

Wiermer, M., Feys, B.J., and Parker, J.E. (2005). Plant immunity: the EDS1 regulatory node. Curr Opin Plant Biol **8,** 383-389.

Wilton, M., Subramaniam, R., Elmore, J., Felsensteiner, C., Coaker, G., and Desveaux, D. (2010). The type III effector HopF2Pto targets Arabidopsis RIN4 protein to promote Pseudomonas syringae virulence. Proc Natl Acad Sci U S A **107,** 2349-2354.

Wirthmueller, L., Zhang, Y., Jones, J.D., and Parker, J.E. (2007). Nuclear accumulation of the Arabidopsis immune receptor RPS4 is necessary for triggering EDS1-dependent defense. Curr Biol **17,** 2023-2029.

Wulf, J., Pascuzzi, P.E., Fahmy, A., Martin, G.B., and Nicholson, L.K. (2004). The solution structure of type III effector protein AvrPto reveals conformational and dynamic features important for plant pathogenesis. Structure **12,** 1257-1268.

Xiang, T., Zong, N., Zou, Y., Wu, Y., Zhang, J., Xing, W., Li, Y., Tang, X., Zhu, L., Chai, J., and Zhou, J.M. (2008). Pseudomonas syringae effector AvrPto blocks innate immunity by targeting receptor kinases. Curr Biol **18,** 74-80.

Xing, W., Zou, Y., Liu, Q., Liu, J., Luo, X., Huang, Q., Chen, S., Zhu, L., Bi, R., Hao, Q., Wu, J.W., Zhou, J.M., and Chai, J. (2007). The structural basis for activation of plant immunity by bacterial effector protein AvrPto. Nature **449,** 243-247.

Xu, W.H., Wang, Y.S., Liu, G.Z., Chen, X., Tinjuangjun, P., Pi, L.Y., and Song, W.Y. (2006a). The autophosphorylated Ser686, Thr688, and Ser689 residues in the intracellular juxtamembrane domain of XA21 are implicated in stability control of rice receptor-like kinase. Plant J **45,** 740-751.

Xu, X., Chen, C., Fan, B., and Chen, Z. (2006b). Physical and functional interactions between pathogen-induced Arabidopsis WRKY18, WRKY40, and WRKY60 transcription factors. Plant Cell **18,** 1310-1326.

Yakushiji, S., Ishiga, Y., Inagaki, Y., Toyoda, K., Shiraishi, T., and Ichinose, Y. (2009). Bacterial DNA activates immunity in *Arabidopsis thaliana*. Journal of General Plant Pathology **75,** 227-234.

Yamaguchi, Y., Pearce, G., and Ryan, C.A. (2006). The cell surface leucine-rich repeat receptor for AtPep1, an endogenous peptide elicitor in Arabidopsis, is functional in transgenic tobacco cells. Proc Natl Acad Sci U S A **103,** 10104-10109.

Yamaguchi, Y., Huffaker, A., Bryan, A.C., Tax, F.E., and Ryan, C.A. (2010). PEPR2 is a second receptor for the Pep1 and Pep2 peptides and contributes to defense responses in Arabidopsis. Plant Cell **22,** 508-522.

Yin, Y., Wang, Z.Y., Mora-Garcia, S., Li, J., Yoshida, S., Asami, T., and Chory, J. (2002). BES1 accumulates in the nucleus in response to brassinosteroids to regulate gene expression and promote stem elongation. Cell **109,** 181-191.

Zeng, W., and He, S.Y. (2010). A prominent role of the flagellin receptor FLAGELLIN-SENSING2 in mediating stomatal response to Pseudomonas syringae pv tomato DC3000 in Arabidopsis. Plant Physiol **153,** 1188-1198.

Zhang, J., and Zhou, J.M. (2010). Plant Immunity Triggered by Microbial Molecular Signatures. Mol Plant.

Zhang, J., Shao, F., Li, Y., Cui, H., Chen, L., Li, H., Zou, Y., Long, C., Lan, L., Chai, J., Chen, S., Tang, X., and Zhou, J.-M. (2007). A Pseudomonas syringae Effector Inactivates MAPKs to Suppress PAMP-Induced Immunity in Plants. Cell Host & Microbe **1,** 175-185.

Zhang, J., Li, W., Xiang, T., Liu, Z., Laluk, K., Ding, X., Zou, Y., Gao, M., Zhang, X., Chen, S., Mengiste, T., Zhang, Y., and Zhou, J.M. (2010a). Receptor-like cytoplasmic kinases integrate signaling from multiple plant immune receptors and are targeted by a Pseudomonas syringae effector. Cell Host Microbe **7,** 290-301.

Zhang, Y., Yang, Y., Fang, B., Gannon, P., Ding, P., Li, X., and Zhang, Y. (2010b). Arabidopsis snc2-1D Activates Receptor-Like Protein-Mediated Immunity Transduced through WRKY70. Plant Cell**,** tpc.110.074120.

Zipfel, C. (2008). Pattern-recognition receptors in plant innate immunity. Curr Opin Immunol **20,** 10-16.

Zipfel, C. (2009). Early molecular events in PAMP-triggered immunity. Curr Opin Plant Biol **12,** 414-420.

Zipfel, C., and Felix, G. (2005). Plants and animals: a different taste for microbes? Curr Opin Plant Biol **8,** 353-360.

Zipfel, C., Robatzek, S., Navarro, L., Oakeley, E.J., Jones, J.D., Felix, G., and Boller, T. (2004). Bacterial disease resistance in Arabidopsis through flagellin perception. Nature **428,** 764-767.

Zipfel, C., Kunze, G., Chinchilla, D., Caniard, A., Jones, J.D., Boller, T., and Felix, G. (2006). Perception of the bacterial PAMP EF-Tu by the receptor EFR restricts Agrobacterium-mediated transformation. Cell **125,** 749-760.

Zurbriggen, M.D., Carrillo, N., Tognetti, V.B., Melzer, M., Peisker, M., Hause, B., and Hajirezaei, M.R. (2009). Chloroplast-generated reactive oxygen species play a major role in localized cell death during the non-host interaction between tobacco and Xanthomonas campestris pv. vesicatoria. Plant J **60,** 962-973.